PSDF

Power Systems Development Facility

Technical Progress Report Gasification Test Run TC10

November 16, 2002 - December 18, 2002

DOE Cooperative Agreement Number DE-FC21-90MC25140

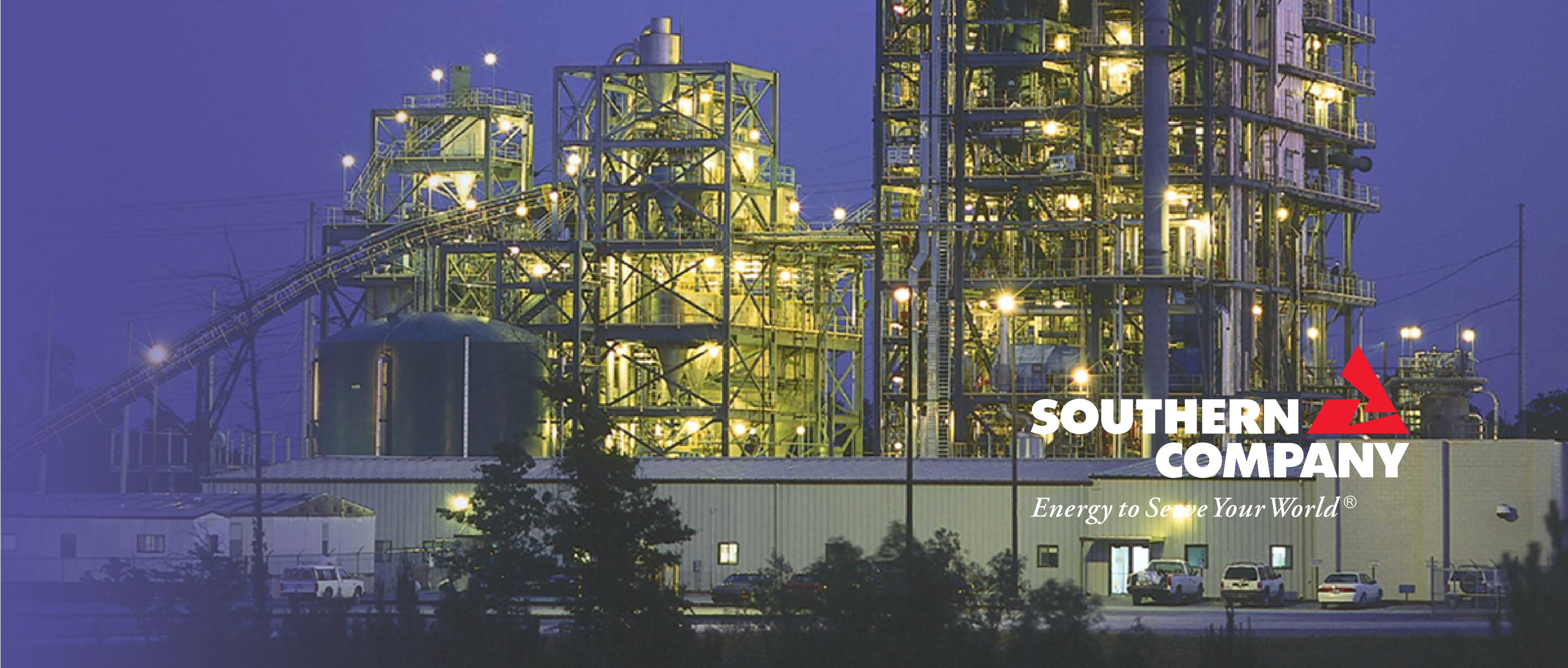

SOUTHERN COMPANY

Energy to Serve Your World®

POWER SYSTEMS DEVELOPMENT FACILITY
TECHNICAL PROGRESS REPORT

GASIFICATION TEST RUN TC10

NOVEMBER 16, 2002 – DECEMBER 18, 2002

DOE Cooperative Agreement Number
DE-FC21-90MC25140

Prepared by:
Southern Company Services, Inc.
Power Systems Development Facility
P.O. Box 1069
Wilsonville, AL 35186
Tel: 205-670-5840
Fax: 205-670-5843
http://psdf.southernco.com

December 2004

POWER SYSTEMS DEVELOPMENT FACILITY

DISCLAIMER

ABSTRACT

This report discusses Test Campaign TC10 of the Kellogg Brown & Root, Inc. (KBR) Transport Gasifier train with a Siemens Westinghouse Power Corporation (Siemens Westinghouse) particle filter system at the Power Systems Development Facility (PSDF) located in Wilsonville, Alabama. The Transport Gasifier is an advanced circulating fluidized-bed gasifier designed to operate as either a combustor or a gasifier in air- or oxygen-blown mode of operation using a particulate control device (PCD). The Transport Gasifier was operated as a pressurized gasifier during TC10 in air- (mainly for transitions and problematic operations) and oxygen-blown mode.

Test Run TC10 was started on November 16, 2002, and completed on December 18, 2002. During oxygen-blown operations, gasifier temperatures varied between 1,675 and 1,825°F at pressures from 150 to 180 psig. After initial adjustments were made to reduce the feed rate, operations with the new fluidized coal feeder were stable with about half of the total coalfeed rate through the new feeder. However, the new fluidized-bed coal feeder proved to be difficult to control at low feed rates. Later the coal mills and original coal feeder experienced difficulties due to a high moisture content in the coal from heavy rains. Additional operational difficulties were experienced when several of the pressure sensing taps in the gasifier plugged. As the run progressed, modifications to the mills (to address processing the wet coal) resulted in a much larger feed size. This eventually resulted in the accumulation of large particles in the circulating solids causing operational instabilities in the standpipe and loop seal. Despite problems with the coal mills, coal feeder, pressure tap nozzles and the standpipe, the gasifier did experience short periods of stability during oxygenblown operations. During these periods, the syngas quality was high. During TC10, the gasifier gasified over 609 tons of Powder River Basin subbituminous coal and accumulated a total of 416 hours of coal feed, over 293 hours of which were in oxygen-blown operation. No sorbent was used during the run.

ACKNOWLEDGMENT

The authors wish to acknowledge the contributions and support provided by various project managers: Jim Longanbach (DOE), Neville Holt (EPRI), Nicola Salazar (KBR), Zal Sanjana (Siemens Westinghouse), and Vann Bush (SRI). Also, the enterprising solutions to problems and the untiring endeavors of many personnel at the site are greatly appreciated. The project was sponsored by the U.S. Department of Energy National Energy Technology Laboratory under contract DE-FC21-90MC25140.

CONTENTS

Listing of Tables

Listing of Figures

1.0 EXECUTIVE SUMMARY

1.1 SUMMARY

This report discusses Test Campaign TC10 of the Kellogg Brown & Root, Inc. (KBR) Transport Gasifier train with a Siemens Westinghouse Power Corporation (Siemens Westinghouse) particle filter system at the Power Systems Development Facility (PSDF) located in Wilsonville, Alabama. The Transport Gasifier is an advanced circulating fluidized-bed gasifier designed to operate as either a combustor or a gasifier in air- or oxygen-blown mode of operation using a particulate control device (PCD). The Transport Gasifier was operated as a pressurized gasifier during TC10 in air- (mainly for transitions and problematic operations) and oxygen-blown mode.

The Transport Gasifier was modified prior to TC07 to operate with enriched air or pure oxygen mixed with superheated steam by adding a lower mixing zone (LMZ). The LMZ operates like a bubbling fast fluidized bed. TC10 was planned as a 500-hour test run to evaluate gasifier and PCD operations during a long-term test with a mixture of three subbituminous coals from the Powder River Basin (PRB) using pure oxygen. The primary test objectives were:

- PRB Oxygen-Blown Operation – Successfully gasify PRB coal using oxygen, while maintaining stable gasifier conditions for long periods of time.
- Operational Stability – Characterize gasifier loop and PCD operations for commercial performance with long-term tests by maintaining a near-constant coal-feed rate, air/coal ratio, riser velocity, solids circulation rate, system pressure, and air/oxygen distribution.
- Fluidized-Bed Coal Feeder Commissioning – Use the new fluidized-bed coal feeder to feed coal into the Transport Gasifier without disturbing the gasifier performance or stability.
- PCD Operation – Continue to demonstrate reliable performance by focusing on controlling pressure drop and eliminating gasification ash (g-ash, formerly known as char) bridging.

Secondary objectives included the continuation of the following gasifier characterizations:

- Process performance – Continue to evaluate the effect of gasifier operating parameters such as steam/coal ratio, solids-circulation rate, and gasifier temperature on CO/CO_2 ratio, carbon conversion, synthesis gas composition, synthesis gas Lower Heating Value (LHV), sulfur and ammonia emissions, and cold and hot gas efficiencies.
- Standpipe Operations – Determine the causes of bubbles and packing in the standpipe and eliminate future occurrences.
- Coal as a Startup Fuel – Test the ability of coal to heat the gasifier at temperatures between 1,200 and 1,650°F without producing tar and develop techniques for preventing tar formation.

- PCD – Continue to evaluate filter element and failsafe material properties and performance.

Test Run TC10 was started on November 16, 2002, and completed on December 18, 2002. During oxygen-blown operations, gasifier temperatures varied between 1,675 and 1,825°F at pressures from 150 to 180 psig. After initial adjustments were made to reduce the feed rate, operations with the new fluidized coal feeder were stable with about half of the total coal feed rate through the new feeder. However, the new fluidized-bed coal feeder proved to be difficult to control at low feed rates. Later the coal mills and original coal feeder experienced difficulties due to a high moisture content in the coal from heavy rains. Additional operational difficulties were experienced when several of the pressure sensing taps in the gasifier plugged. As the run progressed, modifications to the mills (to address processing the wet coal) resulted in a much larger feed size. This eventually resulted in the accumulation of large particles in the circulating solids causing operational instabilities in the standpipe and loop seal. Despite problems with the coal mills, coal feeder, pressure tap nozzles and the standpipe, the gasifier did experience short periods of stability during oxygen-blown operations. During these periods, the syngas quality was high. During TC10, the gasifier gasified over 609 tons of Powder River Basin (PRB) subbituminous coal and accumulated a total of 416 hours of coal feed, over 293 hours of which were in oxygen-blown operation. No sorbent was used during the run.

1.2 PSDF ACCOMPLISHMENTS

The PSDF has achieved over 4,985 hours of operation on coal feed and about 6,470 hours of solids circulation in combustion mode and 4,610 hours of solid circulation and 3,433 hours of coal feed in gasification mode of operation. The major accomplishments in TC10 are summarized below. For combustion-related accomplishments see the technical progress report for the TC05 Test Campaign and for accomplishments in GCT1 through TC09 see the technical progress report for the TC06, TC07, TC08, and TC09 Test Campaign technical progress reports.

1.2.1 Transport Gasifier Train

The major accomplishments and observations in TC10 included the following:

Process

- The Transport Gasifier operated for 416 hours in TC10 using PRB coal, accumulating over 104 hours in air-blown mode, over 18 hours in oxygen-enriched air mode, and around 293 hours in oxygen-blown mode. At the conclusion of TC10, the Transport Gasifier had accumulated over 3,400 total gasification hours.
- The Transport Gasifier operated smoothly at a wide range of operating conditions in both air-blown and oxygen-blown modes. Temperatures ranged from 1,675 to 1,825°F in the gasifier.
- The as-received coal during TC10 contained an extraordinary amount of total moisture, often exceeding 45 percent. Low ambient temperatures and rainy weather made it impossible to dry the soaking wet coal. Since the surface moisture was so high, the coal mills had difficulty grinding the coal, and operations had to remove the 1,200 μ top size screen due to frequent plugging. As a result, 5 to 10 percent of the coal fed to the gasifier has particle sizes between 2,000 and 6,000 μ. The large particle sizes impeded proper operation of the standpipe. At times, the coarse ash removal system was not able to keep up with accumulation in the standpipe and the increasing solids level in the standpipe blocked the smooth flow of solids from the loop seal.
- Since the gasifier interlocks swapped oxygen to nitrogen in the event of a gasifier trip, oxygen breakthrough was minimized after any gasifier trip. During hot restarts using coke breeze or the burner, however, the oxygen concentration in the PCD occasionally exceeded 2 percent. No major thermal excursions accompanied the periods of operation with high oxygen levels in the PCD.
- Due to the many gasifier trips that occurred, the use of subbituminous coal at low feed rates was tested as a startup/restart fuel for the Transport Gasifier, instead of coke breeze. The coal successfully heated the Transport Gasifier from 1,100°F (the maximum temperature obtainable using the start-up burner in a reasonable time period) to 1,800°F without producing tar, provided that the unit was operated at a low coal-feed rate.

- The gasifier experienced many difficulties with standpipe operations, including standpipe packing, slugging, and bubble formation. The new standpipe nuclear density gauge proved useful in determining the problem (packing or bubbles), but due to the type of solids circulating in the gasifier, the standpipe aeration was quite sensitive to its operation.
- The test run consisted of two periods of testing: TC10A and TC10B. TC10A ended after a large deposit formed in the gasifier mixing zone due to problems with the standpipe operation. After operations and maintenance cleared the clinker, the test run resumed as TC10B. TC10B ended a few hours ahead of schedule when the standpipe packed, preventing carbon from entering the lower mixing zone (LMZ). The gasifier tripped on low LMZ temperature.
- Over the course of the run, the gasifier ran at pressures between 150 and 180 psig in the LMZ, the latter being the highest pressure seen to date by the Transport Gasifier during oxygen-blown operations. Currently, the design of the oxygen supply system limits the gasifier pressure during oxygen-blown operations.
- The gasifier maintained high circulation rates and riser densities. These characteristics improved the temperature distribution in both the mixing zone and the riser and resulted in higher coal particle heat-up rates.
- The raw gas dry heating value attained values up to 100 Btu/scf in oxygen-blown mode, resulting in adiabatic nitrogen-corrected values of up to 227 Btu/scf. Based on the corresponding flow of coal, PCD solids, and synthesis gas, the carbon conversion was between 92 and 98 percent during the run.
- Typical riser velocities ranged from 35 to 50 ft/s during oxygen-blown operations. The solids circulation rate was between 200,000 and 600,000 pph, assuming a slip factor of 2.
- The g-ash fines for TC10 were typical, containing carbon contents values varying mostly between 15 and 40 percent. The standpipe solids were also typical, with very low carbon contents—usually less than 0.5 percent, except during coke breeze feed.
- For the first time, operations took solids samples from the new cyclone dipleg sampling system. The LOI data values of the cyclone dipleg fall between those of the PCD solids and the standpipe solids. Since all of the material in the cyclone dipleg goes to the standpipe, the cyclone dipleg LOI indicates that, despite low standpipe LOI values, some g-ash returns to the gasifier. The data also indicate that the disengager removed many more solids than the cyclone during the oxygen-blown portion of TC10.

Equipment

- The FD0210 rotary feeder plugged often due to the high surface moisture present in the feed coal. The exact concentration at which moisture began to pose a problem is still unknown. The average total moisture content was around 25 percent at which the feeder worked fine, but a small batch of ground coal that contained a higher moisture content (due to variability in the mill operation and the large coal inventory) was sufficient to cause plugs. In previous test runs, the feed coal moisture content varied between 18 to 20 percent.

- For the first time, the FD0200 fluidized-bed feeder fed coal to the gasifier. The feeder ran fairly well at high coal-feed rates, but poor at lower feed rates. Modifications should improve the feeder performance at lower feed rates. When the system operated well, the coal-feed rate was steady, with very little fluctuation as indicated by the stability of the gasifier temperatures. Unlike the cycling of the FD0210 feeder, the cycling of the FD0200 feeder did not affect gasifier temperatures.
- Most of the gas analyzers were online for the majority of the test run, presenting good gas composition data. The dry gas compositions added up to between 97 and 98 percent for the oxygen-blown testing.
- During TC10, two ammonia analyzers and one hydrogen cyanide analyzer provided data. In addition to these three gas analyzers, five extractive wet chemistry tests, each lasting 10 minutes, yielded additional data for both ammonia and hydrogen cyanide. For most of the test run, the ammonia concentration in the syngas ranged from 1,500 to 2,500 ppm. The hydrogen cyanide concentration ranged from 25 to 50 ppm.
- During TC10, the sulfator system operated for a total of 620 hours with 121 hours of gasification ash feed. An insufficient quantity of g-ash required 388 hours of diesel fuel feed. Operations were smooth and normal. The bed temperatures for most of the run were between 1,250 and 1,550°F.
- An unusually large number of gasifier pressure taps became plugged during the run, resulting in the loss of much of the gasifier pressure differential pressure data. Studies are underway to examine the cause of the plugging pressure taps and develop recommendations for avoiding plugged taps.

1.2.2 PCD

The highlights of PCD operation for TC10 are listed below.

- The pressure drop in the PCD was controllable throughout TC10. During most of the coal run, the baseline differential pressure was about 40 to 65 inH_2O. During steady-state operations, the inlet temperature was about 750°F, and the face velocity was maintained at about 2.5 to 3 ft/min. Throughout periods of solids feed to the gasifier, a 5-minute back-pulse cycle was used, as well as a back-pulse pressure of 400 psid on the top plenum and 600 psid on the bottom plenum. Filter surface thermocouple response during operations was normal, indicating no permanent buildup of g-ash.
- There were several instances of oxygen breakthrough, usually resulting from coal feeder failures. High oxygen levels were also seen during hot restarts with coal. However, no major thermal excursions occurred in the PCD.

- The fines removal system operated fairly well during normal operations. However, before system operation began for TC10, FD0520 lock vessel spheri valve seal had to be replaced. The seal had to be replaced twice more, and the dispense vessel spheri valve seal required replacement also.
- The PCD outlet loading measurements indicated that the PCD was leak tight during TC10. Although several of the measurements were above the sampling system lower limit of resolution of 0.1 ppmw, close examination of the sampling filters showed contamination by condensed material, and significant particle deposition was not present on the filters. There was no evidence to indicate a PCD leak at any time.
- Failsafe testing with g-ash injection was not performed during the run because the outlet loading measurements, the most reliable method of evaluating failsafe performance, were not consistently below 0.1 ppmw throughout the run due to the contamination.
- Upon preliminary inspection, no problems were observed, i.e., there were no g-ash bridging nor apparent filter failures. The seven Westinghouse filter cans with inverted filters did not appear to be plugged.

2.0 INTRODUCTION

This report provides an account of the TC10 test campaign with the Kellogg Brown & Root, Inc. (KBR) Transport Gasifier and the Siemens Westinghouse Power Corporation (Siemens Westinghouse) filter vessel at the Power Systems Development Facility (PSDF) located in Wilsonville, Alabama, 40 miles southeast of Birmingham. The PSDF is sponsored by the U. S. Department of Energy (DOE) and is an engineering-scale demonstration of advanced coal-fired power systems. In addition to DOE, Southern Company Services, Inc., (SCS), Electric Power Research Institute (EPRI), and Peabody Energy are cofunders. Other cofunding participants supplying services or equipment currently include KBR and Siemens Westinghouse. SCS is responsible for constructing, commissioning, and operating the PSDF.

2.1 THE POWER SYSTEMS DEVELOPMENT FACILITY

SCS entered into an agreement with DOE/National Energy Technology Laboratory (NETL) for the design, construction, and operation of a hot gas clean-up test facility for pressurized gasification and combustion. The purpose of the PSDF is to provide a flexible test facility that can be used to develop advanced power system components and assess the integration and control issues of these advanced power systems. The facility also supports Vision 21 programs to eliminate environmental concerns associated with using fossil fuels for producing electricity, chemicals, and transportation fuels. The facility was designed as a resource for rigorous, long-term testing and performance assessment of hot stream clean-up devices and other components in an integrated environment.

The PSDF now consists of the following modules for systems and component testing:

- A Transport Reactor module.
- A hot gas clean-up module.
- A compressor/turbine module.

The Transport Reactor module includes KBR Transport Reactor technology for pressurized combustion and gasification to provide either an oxidizing or reducing gas for parametric testing of hot particulate control devices. The Transport Gasifier can be operated in either air- or oxygen-blown modes. Oxygen-blown operations are primarily focused on testing and developing various Vision 21 programs to benefit gasification technologies in general. The hot gas clean-up filter system tested to date at the PSDF is the particulate control device (PCD) supplied by Siemens Westinghouse. The gas turbine is an Allison Model 501-KM gas turbine, which drives a synchronous generator through a speed reducing gearbox. The Model 501-KM engine was designed as a modification of the Allison Model 501-KB5 engine to provide operational flexibility. Design considerations include a large, close-coupled external combustor to burn a wide variety of fuels and a fuel delivery system that is much larger than standard.

2.2 TRANSPORT GASIFIER SYSTEM DESCRIPTION

The Transport Gasifier is an advanced circulating fluidized-bed reactor operating in air- or oxygen-blown mode, using a hot gas clean-up filter technology (PCDs) at a component size readily scaleable to commercial systems. The Transport Gasifier train is shown schematically in Figure 2.2-1. A taglist of all major equipment in the process train and associated balance-of-plant is provided in Tables 2.2-1 and -2.

The Transport Gasifier consists of a mixing zone, a riser, a disengager, a cyclone, a standpipe, a loopseal, and J-legs. Steam and air or oxygen are mixed together and introduced in the lower mixing zone (LMZ) while the fuel, sorbent, and additional air and steam (if needed) are added in the upper mixing zone (UMZ). The steam and air or oxygen along with the fuel, sorbent and solids from the standpipe are mixed together in the UMZ. The mixing zone, located below the riser, has a slightly larger diameter than the riser. The gas and solids move up the riser together, make two turns and enter the disengager. The disengager removes larger particles by gravity separation. The gas and remaining solids then move to the cyclone, which removes most of the particles not collected by the disengager. The gas then exits the Transport Gasifier and goes to the primary gas cooler and the PCD for final particulate cleanup. The solids collected by the disengager and cyclone are recycled back to the gasifier mixing zone through the standpipe and a J-leg. The nominal Transport Gasifier operating temperature is 1,800°F. The gasifier system is designed to have a maximum operation pressure of 294 psig with a thermal capacity of about 41 MBtu/hr. Due to a lower oxygen supply pressure, the maximum operation pressure is about 180 psi in oxygen-blown mode.

For startup purposes, a burner (BR0201) is provided at the gasifier mixing zone. Liquefied propane gas (LPG) is used as start-up fuel. The fuel and sorbent are separately fed into the Transport Gasifier through lockhoppers. Coal is ground to a nominal average particle diameter of between 250 to 400 μ. Sorbent is ground to a nominal average particle diameter of 10 to 30 μ. Limestone or dolomitic sorbents are fed into the gasifier for sulfur capture. The gas leaves the Transport Gasifier cyclone and goes to the primary gas cooler, which cools the gas prior to entering the Siemens Westinghouse PCD barrier filter. The PCD uses ceramic or metal elements to filter out dust from the gasifier. The filters remove almost all the dust from the gas stream to prevent erosion of a downstream gas turbine in a commercial plant. The operating temperature of the PCD is controlled both by the gasifier temperature and by an upstream gas cooler. For test purposes, 0 to 100 percent of the gas from the Transport Gasifier can flow through the gas cooler. The PCD gas temperature can range from 700 to 1,600°F. The filter elements are back-pulsed by high-pressure nitrogen in a desired time interval or at a given maximum pressure difference across the elements. There is a secondary gas cooler after the filter vessel to cool the gas before discharging to the stack or atmospheric syngas combustor (thermal oxidizer). In a commercial process, the gas from the PCD would be sent to a gas turbine in a combined-cycle package. The fuel gas is sampled for on-line analysis after traveling through the secondary gas cooler.

After exiting the secondary gas cooler, the gas is then let down to about 2 psig through a pressure control valve. The fuel gas is then sent to the atmospheric syngas burner to burn the gas and oxidize all reduced sulfur compounds (H_2S, COS, and CS_2) and reduced nitrogen compounds

(NH_3 and HCN). The atmospheric syngas burner uses propane as a supplemental fuel. The gas from the atmospheric syngas burner goes to the baghouse and then to the stack.

The Transport Gasifier produces both fine ash collected by the PCD and coarse ash extracted from the Transport Gasifier standpipe. The two solid streams are cooled using screw coolers, reduced in pressure in lock hoppers and then combined together. Any fuel sulfur captured by sorbent should be present as calcium sulfide (CaS). The g-ash is processed in the atmospheric fluidized-bed combustor (sulfator) to oxidize the CaS to calcium sulfate ($CaSO_4$) and burn any residual carbon on the ash. The waste solids are then suitable for commercial use or disposal.

Table 2.2-1

Major Equipment in the Transport Reactor Train

TAG NAME	DESCRIPTION
BR0201	Reactor Start-Up Burner
BR0401	Syngas Combustor (Thermal Oxidizer)
BR0602	AFBC Start-Up/PCD Preheat Burner
CO0201	Main Air Compressor
CO0401	Recycle Gas Booster Compressor
CO0601	AFBC Air Compressor
CY0201	Primary Cyclone in the Reactor Loop
CY0207	Disengager in the Reactor Loop
CY0601	AFBC Cyclone
DR0402	Steam Drum
DY0201	Feeder System Air Dryer
FD0206	Spent Solids Screw Cooler
FD0210	Coal Feeder System
FD0220	Sorbent Feeder System
FD0502	Fines Screw Cooler
FD0510	Spent Solids Transporter System
FD0520	Fines Transporter System
FD0530	Spent Solids Feeder System
FD0602	AFBC Solids Screw Cooler
FD0610	AFBC Sorbent Feeder System
FL0301	PCD — Siemens Westinghouse
FL0302	PCD — Combustion Power
FL0401	Compressor Intake Filter
HX0202	Primary Gas Cooler
HX0203	Combustor Heat Exchanger
HX0204	Transport Air Cooler
HX0402	Secondary Gas Cooler
HX0405	Compressor Feed Cooler
HX0601	AFBC Heat Recovery Exchanger
ME0540	Heat Transfer Fluid System
RX0201	Transport Reactor
SI0602	Spent Solids Silo
SU0601	Atmospheric Fluidized Bed Combustor-AFBC (Sulfator)

Table 2.2-2 (Page 1 of 3)

Major Equipment in the Balance-of-Plant

TAG NAME	DESCRIPTION
BO2920	Auxiliary Boiler
BO2921	Auxiliary Boiler – Superheater
CL2100	Cooling Tower
CO2201A-D	Service Air Compressor A-D
CO2202	Air-Cooled Service Air Compressor
CO2203	High-Pressure Air Compressor
CO2601A-C	Reciprocating N_2 Compressor A-C
CR0104	Coal and Sorbent Crusher
CV0100	Crushed Feed Conveyor
CV0101	Crushed Material Conveyor
DP2301	Baghouse Bypass Damper
DP2303	Inlet Damper on Dilution Air Blower
DP2304	Outlet Damper on Dilution Air Blower
DY2201A-D	Service Air Dryer A-D
DY2202	Air-Cooled Service Air Compressor Air Dryer
DY2203	High-Pressure Air Compressor Air Dryer
FD0104	MWK Coal Transport System
FD0111	MWK Coal Mill Feeder
FD0113	Sorbent Mill Feeder
FD0140	Coke Breeze and Bed Material Transport System
FD0154	MWK Limestone Transport System
FD0810	Ash Unloading System
FD0820	Baghouse Ash Transport System
FL0700	Baghouse
FN0700	Dilution Air Blower
HO0100	Reclaim Hopper
HO0105	Crushed Material Surge Hopper
HO0252	Coal Surge Hopper
HO0253	Sorbent Surge Hopper
HT2101	MWK Equipment Cooling Water Head Tank
HT2103	SCS Equipment Cooling Water Head Tank
HT0399	60-Ton Bridge Crane
HX2002	MWK Steam Condenser
HX2003	MWK Feed Water Heater

Table 2.2-2 (Page 2 of 3)

Major Equipment in the Balance-of-Plant

TAG NAME	DESCRIPTION
HX2004	MWK Subcooler
HX2103A	SCS Cooling Water Heat Exchanger
HX2103C	MWK Cooling Water Heat Exchanger
LF0300	Propane Vaporizer
MC3001-3017	MCCs for Various Equipment
ME0700	MWK Stack
ME0701	Flare
ME0814	Dry Ash Unloader for MWK Train
ML0111	Coal Mill for MWK Train
ML0113	Sorbent Mill for Both Trains
PG0011	Oxygen Plant
PG2600	Nitrogen Plant
PU2000A-B	MWK Feed Water Pump A-B
PU2100A-B	Raw Water Pump A-B
PU2101A-B	Service Water Pump A-B
PU2102A-B	Cooling Tower Make-Up Pump A-B
PU2103A-D	Circulating Water Pump A-D
PU2107	SCS Cooling Water Make-Up Pump
PU2109A-B	SCS Cooling Water Pump A-B
PU2111A-B	MWK Cooling Water Pump A-B
PU2300	Propane Pump
PU2301	Diesel Rolling Stock Pump
PU2302	Diesel Generator Transfer Pump
PU2303	Diesel Tank Sump Pump
PU2400	Fire Protection Jockey Pump
PU2401	Diesel Fire Water Pump #1
PU2402	Diesel Fire Water Pump #2
PU2504A-B	Waste Water Sump Pump A-B
PU2507	Coal and Limestone Storage Sump Pump
PU2700A-B	Demineralizer Forwarding Pump A-B

Table 2.2-2 (Page 3 of 3)

Major Equipment in the Balance-of-Plant

TAG NAME	DESCRIPTION
PU2920A-B	Auxiliary Boiler Feed Water Pump A-B
SB3001	125-V DC Station Battery
SB3002	UPS
SC0700	Baghouse Screw Conveyor
SG3000-3005	4160-V, 480-V Switchgear Buses
SI0101	MWK Crushed Coal Storage Silo
SI0103	Crushed Sorbent Storage Silo
SI0111	MWK Pulverized Coal Storage Silo
SI0113	MWK Limestone Silo
SI0114	FW Limestone Silo
SI0810	Ash Silo
ST2601	N_2 Storage Tube Bank
TK2000	MWK Condensate Storage Tank
TK2001	FW Condensate Tank
TK2100	Raw Water Storage Tank
TK2300A-D	Propane Storage Tank A-D
TK2301	Diesel Storage Tank
TK2401	Fire Water Tank
XF3000A	230/4.16-kV Main Power Transformer
XF3001B-5B	4160/480-V Station Service Transformer No. 1-5
XF3001G	480/120-V Miscellaneous Transformer
XF3010G	120/208 Distribution Transformer
XF3012G	UPS Isolation Transformer
VS2203	High-Pressure Air Receiver

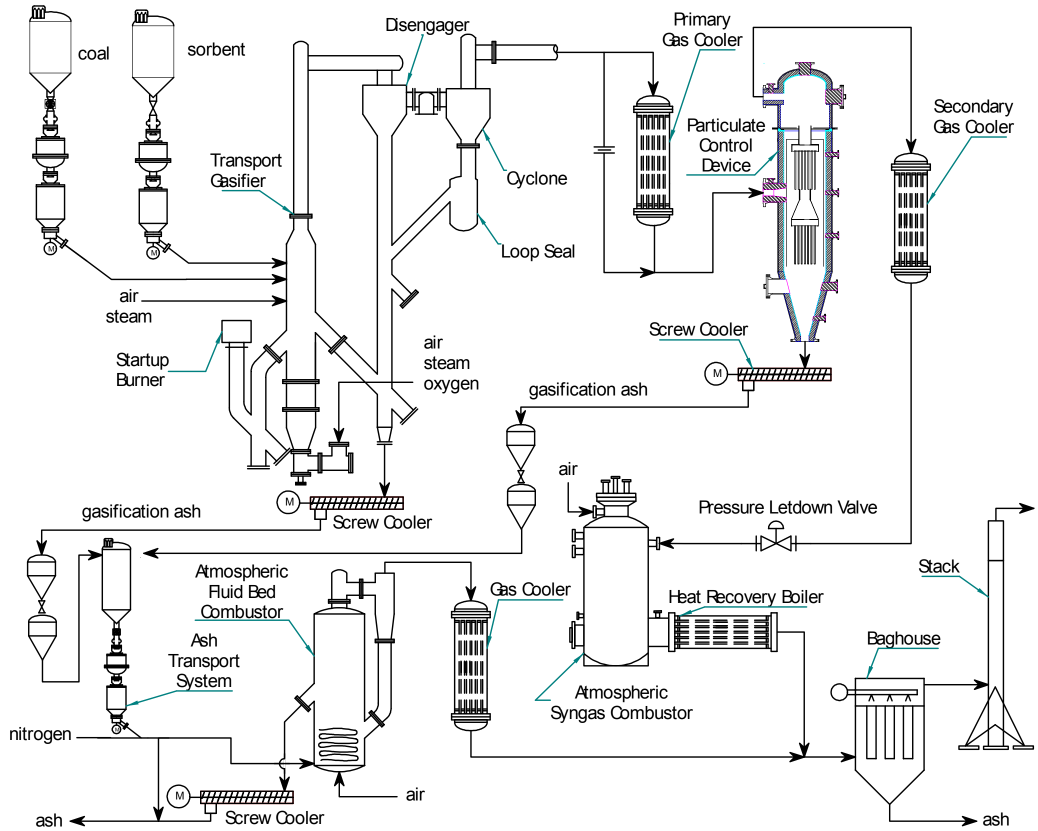

Figure 2.2-1 Flow Diagram of the Transport Gasifier Train

2.3 SIEMENS WESTINGHOUSE PARTICULATE CONTROL DEVICE

Different PCDs will be evaluated on the Transport Reactor train. The first PCD that was commissioned in 1996 and has been used in all of the testing to date was the filter system designed by Siemens Westinghouse. The dirty gas enters the PCD below the tube sheet, flows through the filter elements, and the ash collects on the outside of the filter. The clean gas passes from the plenum/filter element assembly through the plenum pipe to the outlet pipe. As the ash collects on the outside surface of the filter elements, the pressure drop across the filter system gradually increases. The filter cake is periodically dislodged by injecting a high-pressure gas pulse to the clean side of the filter elements. The cake then falls to the discharge hopper.

Until the first gasification run in late 1999, the Transport Reactor had been operated only in the combustion mode. Initially, high-pressure air was used as the pulse gas for the PCD, however, the pulse gas was changed to nitrogen early in 1997. The pulse gas was routed individually to the two-plenum/filter element assemblies via injection tubes mounted on the top head of the PCD vessel. The pulse duration was typically 0.1 to 0.5 seconds.

A sketch of the Siemens Westinghouse PCD is shown in Figure 2.3-1.

Siemens Westinghouse PCD FL0301

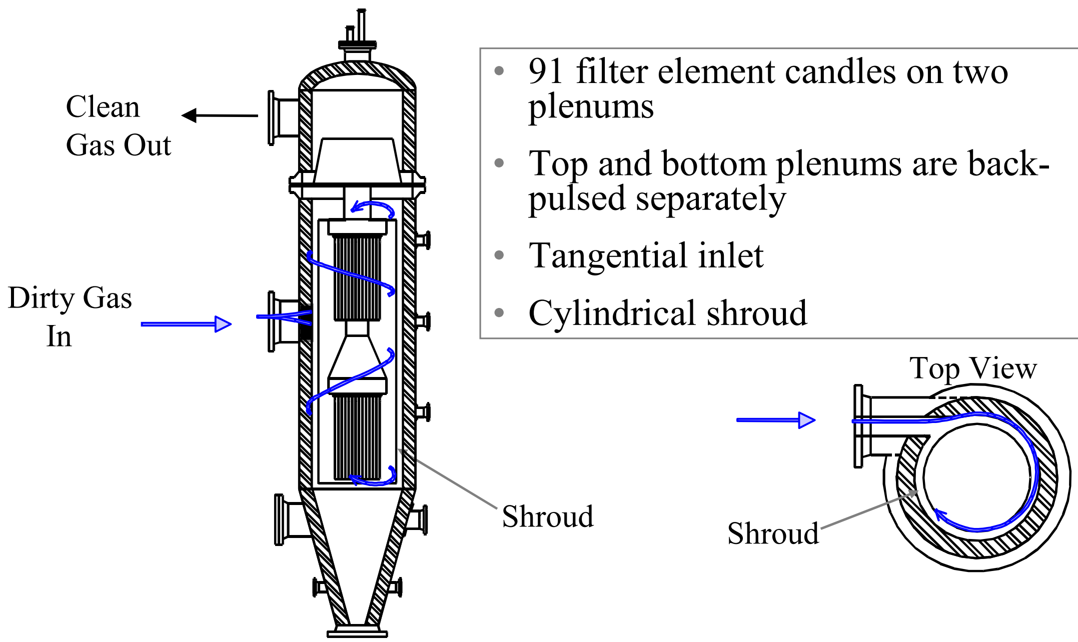

- 91 filter element candles on two plenums
- Top and bottom plenums are back-pulsed separately
- Tangential inlet
- Cylindrical shroud

Figure 2.3-1 Siemens Westinghouse PCD

2.4 OPERATION HISTORY

Conversion of the Transport Reactor train to gasification mode of operation was performed from May to September 1999. The first gasification test run, GCT1, was planned as a 250-hour test run to commission the Transport Gasifier and to characterize the limits of operational parameter variations. GCT1 was started on September 9, 1999, with the first part completed on September 15, 1999 (GCT1A). The second part of GCT1 was started on December 7, 1999, and completed on December 15, 1999 (GCT1B-D). This test run provided the data necessary for preliminary analysis of gasifier operations and for identification of necessary modifications to improve equipment and process performance. Five different feed combinations of coal and sorbent were tested to gain a better understanding of the gasifier solids collection system efficiency.

GCT2, planned as a 250-hour characterization test run, was started on April 10, 2000, and completed on April 27, 2000. Additional data was taken to analyze effect of different operating conditions on gasifier performance and operability. A blend of several Powder River Basin (PRB) coals was used with Longview limestone from Alabama. In the outage following GCT2, the Transport Gasifier underwent a major modification to improve the operation and performance of the gasifier solids collection system. The most fundamental change was the addition of the loop seal underneath the primary cyclone.

GCT3 was planned as a 250-hour characterization with the primary objective to commission the loop seal. A hot solids circulation test (GCT3A) was started on December 1, 2000, and completed December 15, 2000. After a 1-month outage to address maintenance issues with the main air compressor, GCT3 was continued. The second part of GCT3 (GCT3B) was started on January 20, 2001, and completed on February 1, 2001. During GCT3B, a blend of several PRB coals was used with Bucyrus limestone from Ohio. The loop seal performed well needing little attention and promoting much higher solids circulation rates and higher coal-feed rates that resulted in lower relative solids loading to the PCD and higher g-ash retention in the gasifier.

GCT4, planned as a 250-hour characterization test run, was started on March 7, 2001, and completed on March 30, 2001. A blend of several PRB coals with Bucyrus limestone from Ohio was used. More experience was gained with the loop seal operations and additional data was collected to better understand gasifier performance.

TC06, planned as a 1,000-hour test campaign, was started on July 4, 2001, and completed on September 24, 2001. A blend of several PRB coals with Bucyrus limestone from Ohio was used. Both gasifier and PCD operations were stable during the test run with a stable baseline pressure drop. Due to its length and stability, the TC06 test run provided valuable data necessary to analyze long-term gasifier operations and to identify necessary modifications to improve equipment and process performance as well as progressing the goal of many thousands of hours of candle exposure.

TC07, planned as a 500-hour test campaign, was started on December 11, 2001, and completed on April 5, 2002. A blend of several PRB coals and a bituminous coal from the

Calumet mine in Alabama were tested with Bucyrus limestone from Ohio. Due to operational difficulties with the gasifier (stemming from instrumentation problems) the unit was taken offline several times. PCD operations were relatively stable considering the numerous gasifier upsets.

TC08, planned as a 250-hour test campaign to commission the gasifier in oxygen-blown mode of operation, was started on June 9, 2002, and completed on June 29, 2002. A blend of several PRB coals was tested in air-blown, enriched air- and oxygen-blown modes of operation. The transition from different modes of operation was smooth and it was demonstrated that the full transition could be made within 15 minutes. Both gasifier and PCD operations were stable during the test run, with a stable baseline pressure drop.

TC09 was planned as a 250-hour test campaign to characterize the gasifier and PCD operations in air- and oxygen-blown mode of operations using a bituminous coal. TC09 was started on September 3, 2002, and completed on September 26, 2002. A bituminous coal from the Sufco mine in Utah was successfully tested in air- and oxygen-blown modes of operation. Both gasifier and PCD operations were stable during the test run.

TC10, was planned as a 500-hour test campaign to conduct long-term tests to evaluate the gasifier and PCD operations in oxygen-blown mode of operations using a blend of several PRB coals. TC10 was started on November 16, 2002, and completed on December 18, 2002. Despite problems with the coal mills, coal feeder, pressure tap nozzles, and the standpipe, the gasifier did experience short periods of stability during oxygen-blown operations. During these periods, the syngas quality was high. During TC10, over 609 tons of PRB subbituminous coal were gasified.

Figure 2.4-1 gives a summary of operating test hours achieved with the Transport Reactor at the PSDF.

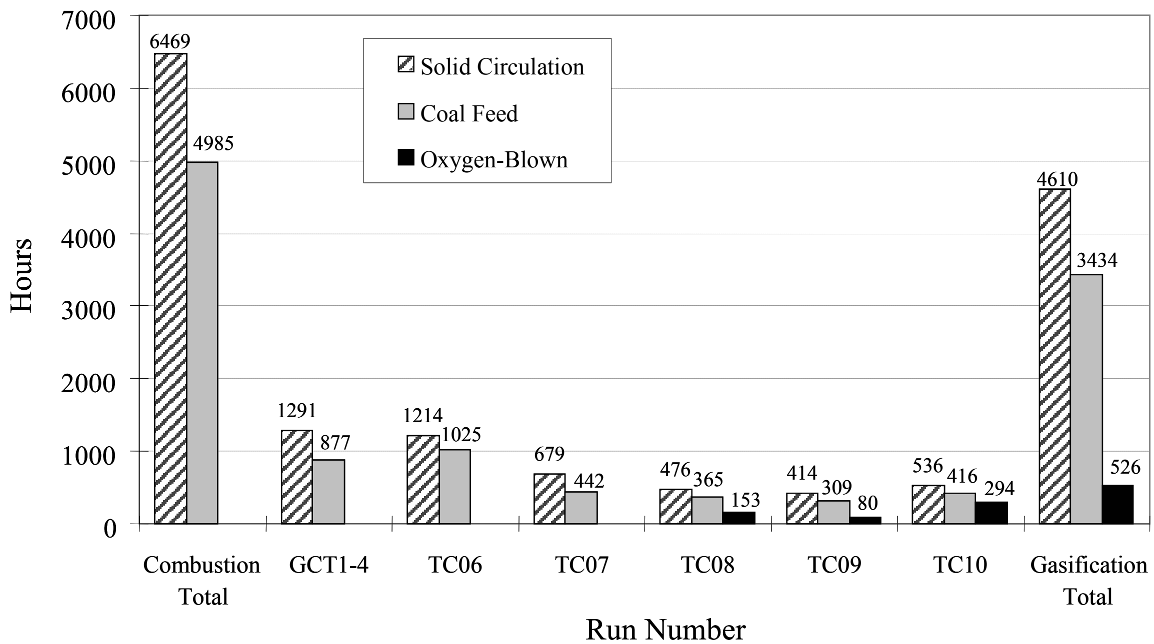

Figure 2.4-1 Operating Hours Summary for the Transport Reactor Train

3.0 TRANSPORT GASIFIER OPERATIONS

3.1 TC10 RUN SUMMARY

Test Run TC10 began on November 16, 2002, with the startup of main air compressor and lighting of the gasifier startup burner. The Transport Gasifier operated until November 26, 2002, when a large deposit formed in the mixing zone, forcing operations to shut the gasifier down and remove the restriction. On December 5, 2002, the test run resumed and continued until a standpipe bubble stopped solids circulation and tripped the gasifier on December 18, 2002. Over the course of the entire test run, gasifier temperatures varied between 1,675 and 1,825°F at pressures from 150 to 180 psig during oxygen-blown operations.

During TC10, the gasifier processed over 609 tons of Powder River Basin (PRB) subbituminous coal and accumulated a total of 416 hours of coal feed, over 293 hours of which were in oxygen-blown operation. No sorbent was used during the run.

The primary objectives of test run TC10 were as follows:

- PRB Oxygen-Blown Operation – Successfully gasify PRB coal using pure oxygen as an oxidant, while maintaining stable gasifier conditions for long periods of time.
- Operational Stability – Characterize gasifier loop and PCD operations for commercial performance with long-term testing by maintaining a near-constant coal-feed rate, air/coal ratio, riser velocity, solids-circulation rate, system pressure, and air distribution.
- Fluidized-Bed Coal Feeder Commissioning – Use the new fluidized-bed coal feeder to feed coal into the Transport Gasifier without disturbing gasifier performance or stability.

Secondary objectives included the continuation of the following gasifier characterizations:

- Gasifier Operations – Study the devolatilization and tar cracking effects from transient conditions during the transition from start-up burner to coke breeze to coal. Evaluate the effect of process operations on heat release, heat transfer, and accelerated fuel particle heat-up rates. Study the effect of changes in gasifier conditions on transient temperature profiles, pressure balance, and product gas composition. Observe performance of new gasifier temperature and coal-feed rate controllers.
- Effects of Gasifier Conditions on Syngas Composition – Evaluate the effect of air distribution, steam/coal ratio, solids-circulation rate, and gasifier temperature on CO/CO_2 ratio, carbon conversion, and cold and hot gas efficiencies.
- Standpipe Operations – Determine the causes of standpipe bubbles or packing in the standpipe and eliminate future occurrences.

- Coal as a Start-Up Fuel – Test the ability of coal to heat the gasifier at temperatures between 1,200 and 1,650°F without producing tar. Develop techniques for preventing tar formation.

The activities that occurred during the outage preceding test run TC10 included 32 equipment revisions. Those revisions that most affected the process are listed below:

- New gas analyzers, including continuous hydrogen chloride, carbonyl sulfide, and naphthalene measurements were added.
- A new sampling system for collecting solids from the cyclone dipleg was installed.
- The gasifier interlocks were modified to allow the new fluidized-bed coal feeder to safely feed coal at the same time as the original coal feeder.
- A new gauge measuring the differential pressure across the primary gas cooler was installed to assist detection of problems with the cooler.

The following paragraphs summarize the events that occurred during TC10.

The main air compressor was started and the gasifier start-up burner was lit on November 16, 2002, beginning test run TC10. While the burner heated the gasifier and the sorbent feeder added sand to the gasifier, a hole developed in the sorbent feeder conveying line. Since the rupture was downstream of the line isolation valves, a gasifier shutdown was necessary. Once the hole was repaired, the start-up burner was lit again and resumed heating the gasifier according to the refractory curing procedure. Early on November 18, 2002, once the gasifier had achieved 1,250°F, coke breeze feed began. By that afternoon, after the gasifier temperature exceeded 1,600°F, coal feed began, and operations shut down the gasifier start-up burner and the coke breeze feeder.

Shortly after starting the original coal feeder, operations began feeding coal through the new fluidized-bed coal feeder designed by Southern Company Services (SCS). Initially, the feeder fed coal at a high rate, forcing the gasifier temperatures to drop. Eventually, the system steadied and the new coal feeder ran well for a few hours before the coal-feed rate became unstable. Shortly thereafter, the original coal feeder developed a leak on one of its lock vessel flanges. Both feeders were stopped and coke breeze was fed to keep the gasifier temperatures constant while maintenance repaired the original coal feeder. Once the repairs were complete, both coal feeders were restarted and the coke breeze feeder was stopped.

The new fluidized-bed coal feeder proved to be difficult to control at low feed rates and plugged often. Whenever the feeder plugged, the coal-feed rate was increased from the original coal feeder, while clearing the plugged areas in the new feeder. For the most part, the total coal-feed rate was around 3,500 pph, about 800 pph coming from the new feeder.

On the evening of November 19, 2002, the gasifier pressure was lowered and the steam-flow rate was increased in preparation of transitioning to oxygen-blown operations. The transition was fairly smooth and took place in just over 1 hour. The gasifier continued to operate well with the exception of the erratic performance of the new coal feeder, which continued to plug. Late the next morning, the varying coal-feed rate (and the resulting temperature swings) caused the steam drum level to fall. The low drum level tripped the gasifier, the atmospheric syngas burner, and redirected the syngas flow to the flare. Within a few hours, once the level in the steam drum had returned to normal, coal feed through both feeders was resumed and then the gasifier was transitioned from air-blown operations to oxygen-blown mode.

Gasifier operations remained unstable, however, since the new coal feeder continued to both plug and experience coal-feed surges. In the early morning of November 21, 2002, the new coal feeder was stopped and the feed rate through the original coal feeder was increased to ensure stable operations for the environmental tests scheduled later that day. The gasifier operated steadily through the testing periods. After the testing was complete, operations tried to restart the new coal feeder, but it continued to have operational issues, forcing the abandonment of the feeder for the rest of the test run.

Over the next few days, the original coal feeder also experienced difficulties with wet coal. The wet coal was very difficult to feed, and it caused many coal feeder trips due to the material plugging the conveying line. The first coal feeder trip took place early on November 22, 2002. Operations tried to start the coke breeze feeder and the new coal feeder, but neither was functioning. When depressurizing the gasifier, in preparation for lighting the start-up burner, the gasifier standpipe became unstable. Later that morning, after the gasifier stabilized, sand was added to the gasifier, and the system was heated using coke breeze. Then, coal-feed and oxygen-blown operations resumed.

Over the next 3 days, the coal feeder experienced seven trips and several periods of unsteady operation. On November 24, 2002, the gasifier returned to coke breeze operations to allow the coal feeder system to be dismantled and cleaned out. However, the feeder continued to trip periodically due to the wet nature of the coal after it was put back in service. Each time the feeder tripped, the line was quickly cleared, the feeder was restarted, and the gasifier was transitioned back to oxygen-blown operations.

Another problem the gasifier experienced during most of the test run was the plugging of pressure taps. The plugged taps caused the loss of much of the differential pressure data for the gasifier in TC10. At several points during the run, almost every pressure tap in the mixing zone and standpipe was plugged, making it difficult to evaluate the gasifier performance.

Despite the coal feeder and nozzle difficulties, the gasifier did experience short periods of stability. During these periods, syngas quality was high. Figures 3.1-1, -2 and -3 illustrate conditions typical of normal oxygen-blown gasification in TC10.

In the early morning of November 26, 2002, the gasifier temperature profile became distorted. The lower mixing zone (LMZ) and riser temperatures plummeted, while the mixing zone temperatures soared to values as high as 1,940°F. The low LMZ temperature interlock tripped the gasifier. Unfortunately, the exact cause of the temperature distortion is unknown, but poor solids circulation due to standpipe packing seems to be a possible reason. Upon restoring coal feed to the gasifier, the air flow through the mixing zone air nozzles was restricted. Later that morning, temperatures in the mixing zone and LMZ increased to around 2,000°F, tripping the gasifier. At that point, solids circulation completely stopped, indicating that a deposit had formed in the mixing zone. The gasifier was shutdown to open the gasifier and clear the deposit.

Upon removing the LMZ portion of the gasifier, a deposit was found in the mixing zone preventing solids from entering the mixing zone from the gasifier J-leg. After the deposit was dislodged and the gasifier was resealed, the start-up burner was lit and the test run continued on December 5, 2002.

After a short time period of heating the gasifier using coke breeze, coal feed resumed on the afternoon of December 6, 2002. Most of the gasifier pressure taps plugged almost immediately thereafter, making it difficult to determine the gasifier circulation rate and the standpipe solids level. Although numerous attempts were made to clear the nozzles, the majority remained plugged throughout the remainder of the test run.

The transition to oxygen-blown operations began shortly after the establishment of coal feed. To avoid generating deposits, the transition was performed slowly, taking over 2 hours. As soon as the gasifier achieved oxygen-blown operations, however, the gasifier tripped when material plugged the coal conveying line. Coke breeze was fed briefly to maintain gasifier temperatures. Once the coal conveying line was clear, the coal feeder was restarted and the gasifier was transitioned back to oxygen-blown mode.

Steady operations again proved to be short-lived. The nitrogen system loading pumps failed a few hours after resuming oxygen-blown operations. The broken pumps made filling the liquid nitrogen tanks impossible. When the tank levels became too low to safely operate the gasifier, coal and oxygen feed to the gasifier was stopped until the contractor responsible for the nitrogen system finished repairing the pumps. Once the pumps were operational, the gasifier temperature had cooled below 1,100°F, a temperature low enough to require heating via the start-up burner.

The start-up burner was lit and began to heat the gasifier, but faulty heat tracing on the propane system allowed condensate to enter the propane pressure transmitter, which caused the pressure to incorrectly read high and forced the pressure control valve to close. The resulting loss of propane flow tripped the main start-up burner and the atmospheric syngas burner. Eventually, the problem was corrected and the start-up burner was relit by midmorning on December 7, 2002.

The gasifier was heated to over 1,200°F, the maximum temperature obtainable using the start-up burner. When coke breeze feed began, however, the material did not ignite. Therefore, coal was fed at a very low feed rate to increase gasifier temperatures. Within a few hours, when the gasifier temperature approached 1,420°F, the coke breeze ignited, and the coal feeder was stopped until the gasifier reached 1,650°F, whereupon coal feed resumed. The gasifier was then transitioned back to oxygen-blown mode.

The coal feeder continued to experience problems conveying the wet coal, and it tripped twice more the next morning. Both times the feeder was restored within a few minutes. By midmorning the coal feeder was operating steadily, and, with the exception of the continuously plugging gasifier pressure taps, the gasifier performed well.

Early the next morning, on December 9, 2002, the oxygen tank level became low. Dispatching problems prevented the oxygen supply truck from arriving at the plant site until after the oxygen tank had emptied. The lack of oxygen forced the transition back to air-blown mode. Once the oxygen truck had filled the tanks, operations placed the gasifier back in oxygen-blown mode and continued the test run.

The gasifier ran smoothly for several hours until the coal feeder plugged again. In an attempt to prevent future plugging, coke breeze feed was started to the gasifier while emptying the coal feeder dispense vessel. Then, the bottom of the coal feeder was removed to check for potential problems. No plugged material was found but some of the feeder internals were bent. After the repairs to the feeder internals were complete, the feeder was reinstalled, and the gasifier was restored to oxygen-blown coal gasification.

During the next day, the gasifier operated in a fairly stable manner with a temperature of around 1,750°F in the mixing zone. Although the coal feeder began experiencing difficulty transferring coal from its surge bin through the lock hopper to the dispense vessel, it did not trip. The nitrogen flow in the lock vessel was increased to aid the transferring, and the feeder performance improved.

On December 11, 2002, the coal silo transport system stopped working, which caused the coal surge bin to run out of coal and forced the return to coke breeze feed and air-blown operations for a short period of time. Once the transport system was operational, coal feed and oxygen-blown operations resumed. The coal feeder performance improved marginally, and with a coal-feed rate of around 3,800 pph, the gasifier generated syngas with a corrected lower heating value (LHV) of around 225 Btu/scf.

The next day, standpipe operations became erratic. Many times the standpipe began to pack with solids. At other times bubbles formed in the standpipe. To avoid a loss of standpipe solids to the particulate control device (PCD) during full oxygen-blown conditions, the coal-feed rate and oxygen-flow rates were reduced. After several hours, when the standpipe conditions returned to normal, the coal-feed and oxygen-flow rates were restored.

Gasifier operations continued in much the same way for the next few days. Occasionally the standpipe experienced problems, at which point operations often placed the gasifier back in air-blown mode to avoid a gasifier upset during oxygen-blown conditions. The coal feeder continued to plug often, tripping the entire system whenever it did. Each time either a standpipe upset or coal feeder trip cleared, the gasifier was restored to oxygen-blown operations, heating the gasifier with coke breeze or coal, as necessary.

In the morning on December 15, 2002, the coal feeder tripped on a motor inverter fault. A restart was attempted but the feeder plugged almost immediately. At the same time, a bubble formed in the standpipe. The coal feeder was restarted and the gasifier remained in air-blown mode. Except for a brief period that afternoon, the gasifier did not return to full oxygen-blown operations for almost 2 days due to the instability of the coal feeder and the standpipe.

Full oxygen-blown operations resumed at 09:23 on December 17, 2002. Gasifier conditions were comparatively steady, but the plugged gasifier pressure taps continued to hinder gasifier analysis. Late that night, the g-ash feeder (FD0520) experienced operational difficulties. Since the gearbox could not be repaired, FD0530 was piped directly to the ash silo. Operations ran the feeder as a blower and used it to fill the ash silo. Although the coal feeder performance improved, standpipe operations worsened over the night. Eventually, the standpipe packed, preventing carbon from returning to the mixing zone, and the gasifier tripped on low LMZ temperatures at 12:28 on December 18, 2002. Since the test run was originally scheduled to end a few hours later, the decision was made to terminate the run, resulting in over 416 hours of coal feed and 293 hours of oxygen-blown operations.

After the run, the gasifier was inspected visually and with a borescope. The inspections revealed no major problems and the gasifier was essentially clean. Minor deposits were found on the walls in a few places. The primary cyclone had a few very small deposits on the walls. The riser walls were coated in dark, tarry material in one section. The mixing zone had a few minor deposits on the walls scattered over most of its length. The crossover, standpipe, and J-legs appeared completely clean.

Several parameters that affect gasifier performance were looked at after the run. The circulation rate is one of the more important parameters that affects the gasifier. The circulation rate, with some corrections due to specific conditions, is proportional to the riser differential pressure. The two main contributors to the circulation rate are generally taken to be the standpipe level and the J-leg aeration rate. In Figure 3.1-4, the riser differential pressure and the standpipe differential pressure are plotted against one another. A strong correlation between the two values can be seen, even when looking at data from different operating conditions. In contrast, Figure 3.1-5 shows the effect of the J-leg aeration rate on the riser differential pressure. In this case, there does not seem to be any relation between the two. The data is from a narrow range of standpipe levels measuring between 200 and 215 in H_2O on LI339. In other words, the standpipe level is the only controllable parameter to have a measurable effect on the circulation rate.

The circulation rate affects other gasifier parameters. One obvious effect (see Figure 3.1-6) is that the variation in gasifier temperatures decreases as the circulation rate increases because of the greater amount of solids to act as a heat sink. An important follow-on issue is the effect of the circulation rate on gas quality, shown in Figure 3.1-7. The effect on circulation rate on gas quality seems small, though there appears to be a slight increase in gas quality with increasing circulation rate during oxygen-blown testing. A related issue is the effect of riser temperature on gas quality, shown in Figure 3.1-8. The effect again seems slight, though there is a bit of an increase in gas quality with increasing temperature in oxygen-blown operations.

Table 3.1-1 gives general operating conditions for the gasifier operations in TC10. The coal analysis data are given in Table 3.1-2. The following steady-state test periods were selected and are shown in Table 3.1-3 with details of operating conditions:

TC10A-1	First period (air-blown with FD0200).
TC10A-2	FD0200 feeding in oxygen mode.
TC10A-3	Recovery after steam drum trip.
TC10A-4	Increased coal feed, reduced steam.
TC10A-5	Recovery after coal feeder trip.
TC10A-6	Increased pressure and circulation rate.
TC10A-7	Air-blown after trip.
TC10A-8	High coal-feed rate.
TC10A-9	Reduced steam-flow rate.
TC10B-1	First period after outage.
TC10B-2	Reduced temperatures.
TC10B-3	Increased coal feed.
TC10B-4	Reduced circulation rate. Increased pressure.
TC10B-5	Reduced temperatures.
TC10B-6	Increased temperatures.
TC10B-7	Recovery after coal feeder problems.
TC10B-8	Recovery after coal feeder trip.
TC10B-9	Reduced coal-feed rate.
TC10B-10	Increased coal feed.

Table 3.1-1

TC10 Operating Conditions for Transport Gasifier

Start-Up Bed Material	Sand, ~120 μm
Start-Up Fuel	Coke Breeze
Fuel Type	Powder River Basin
Fuel Particle Size (mmd)	280 to 500 μm
Average Fuel-Feed Rate, pph	3,100 – 4,100
Sorbent Type	None
Sorbent Particle Size (mmd)	N/A
Sorbent-Feed Rate	N/A
Gasifier Temperature, °F	1,675 – 1,825
Gasifier Pressure, psig	150-180
Riser Gas Velocity, fps	35 – 50
Riser Mass Flux, $lb/s \cdot ft^2$	350 - 450 (average slip ratio = 2)
Standpipe Level, InH_2O (LI339)	150 - 250
Primary Gas Cooler Bypass	0%
PCD Temperature, °F	700 – 800
Total Gas Flowrate, pph	14,000 - 24,000
Oxygen/Coal Mass Ratio, lb/lb	0.6 – 0.7 (O_2) 0.8 (air)
Oxygen/Steam Mass Ratio, lb/lb	0.8-1.6, as needed to control gasifier temperature
Steam/Coal Mass Ratio, lb/lb	0.3 to 0.85

Table 3.1-2

PRB Coal Analyses as Fed

	Weight Percent
Moisture	22.64
Ash	5.92
Sulfur	0.28
C	53.73
H	3.53
N	0.71
O	13.19
Vol	32.27
Fix C	39.17
Higher Heating Value (Btu/lb)	9,088

Table 3.1-3

Operating Periods

	Start	End	MZ Temp °F	Rsr Temp °F	Pres (psig)	Coal-Feed Rate[1] (lb/hr)	Air Flow (lb/hr)	Oxygen Flow (lb/hr)	Steam Flow[2] (lb/hr)	Steam/ Coal
TC10A-1	11/19/2002 07:15	11/19/2002 15:15	1,672	1,704	180	3,356	12,489	0	810	0.24
TC10A-2	11/19/2002 20:00	11/20/2002 07:00	1,652	1,671	146	2,883	0	2,190	2,668	0.93
TC10A-3	11/21/2002 00:15	11/21/2002 06:30	1,701	1,704	146	2,712	0	2,070	1,958	0.72
TC10A-4	11/21/2002 07:45	11/21/2002 18:00	1,754	1,700	146	3,236	0	2,319	1,424	0.44
TC10A-5	11/21/2002 18:30	11/22/2002 02:00	1,741	1,674	146	2,997	0	2,273	1,498	0.50
TC10A-6	11/22/2002 14:00	11/23/2002 13:45	1,737	1,708	152	2,653	0	2,309	1,594	0.60
TC10A-7	11/24/2002 02:15	11/24/2002 06:15	1,727	1,712	152	2,355	11,129	0	0	0.00
TC10A-8	11/25/2002 03:15	11/25/2002 07:15	1,769	1,678	152	3,422	0	2,457	2,333	0.68
TC10A-9	11/25/2002 16:30	11/25/2002 22:00	1,744	1,723	152	2,860	0	2,302	1,182	0.41
TC10B-1	12/7/2002 22:15	12/8/2002 05:00	1,703	1,777	150	2,610	0	2,207	1,579	0.60
TC10B-2	12/8/2002 07:00	12/9/2002 01:30	1,699	1,740	150	2,448	0	2,277	1,298	0.53
TC10B-3	12/9/2002 07:00	12/9/2002 14:45	1,713	1,729	150	2,858	0	2,395	1,295	0.45
TC10B-4	12/10/2002 05:30	12/11/2002 08:00	1,704	1,734	160	2,778	0	2,199	1,226	0.44
TC10B-5	12/11/2002 23:15	12/12/2002 06:00	1,680	1,721	160	2,909	0	2,243	881	0.30
TC10B-6	12/12/2002 16:30	12/13/2002 05:15	1,709	1,741	158	3,430	0	2,185	1,131	0.33
TC10B-7	12/13/2002 16:15	12/13/2002 23:45	1,722	1,740	158	3,435	0	2,325	1,176	0.34
TC10B-8	12/14/2002 02:00	12/14/2002 06:30	1,708	1,726	158	3,282	0	2,253	1,143	0.35
TC10B-9	12/14/2002 09:15	12/14/2002 13:15	1,654	1,739	158	2,912	0	2,166	1,255	0.43
TC10B-10	12/14/2002 15:45	12/14/2002 20:15	1,709	1,753	158	3,581	0	2,365	1,191	0.33

Notes:

1. Coal-feed rate by nuclear density gauges.
2. Steam rate as measured by the sum of the flow indicators.

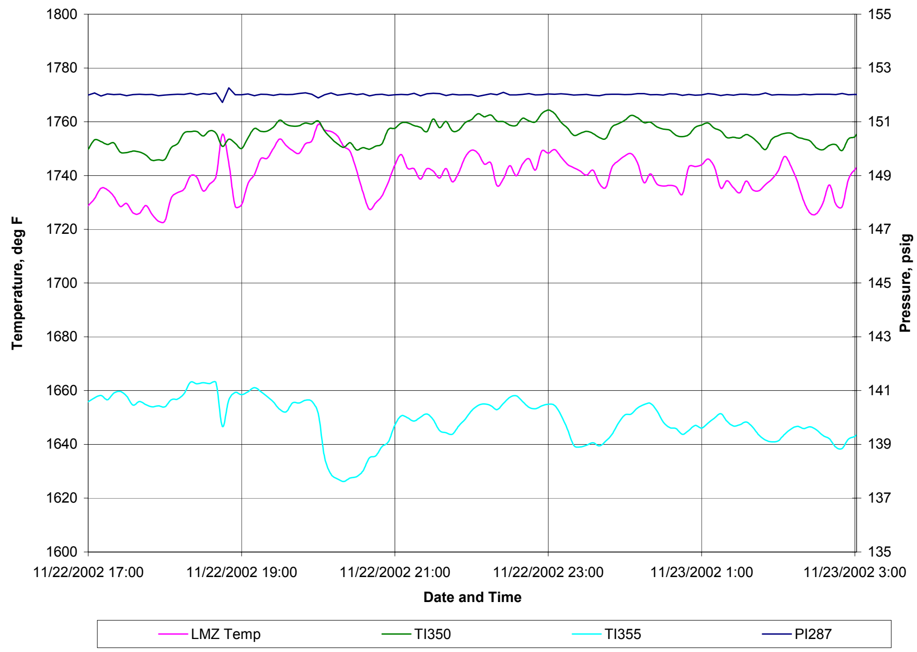

Figure 3.1-1 Typical Gasifier Temperature and Pressure Conditions During Stable Gasification in TC10

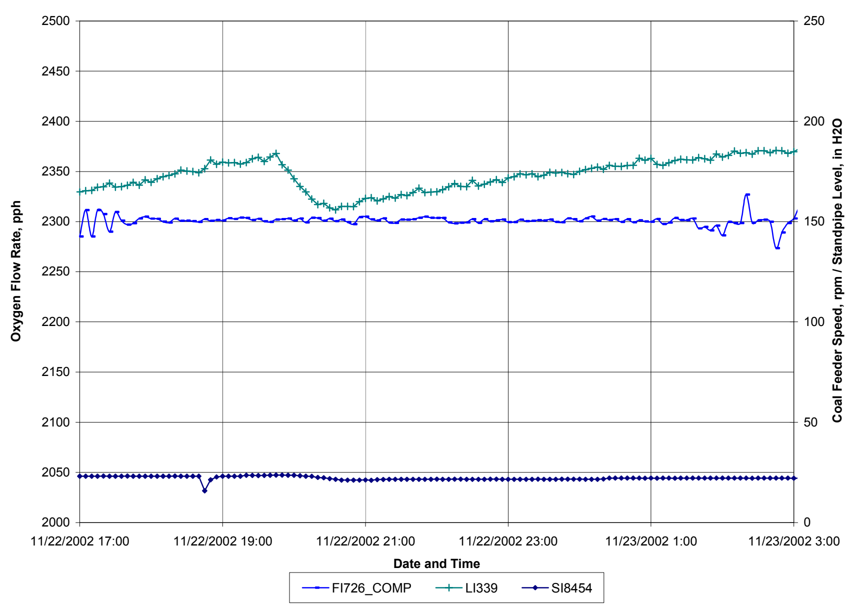

Figure 3.1-2 Typical Standpipe Level, Coal Feeder Speed, and Oxygen-Flow Rate During Stable Gasification in TC10

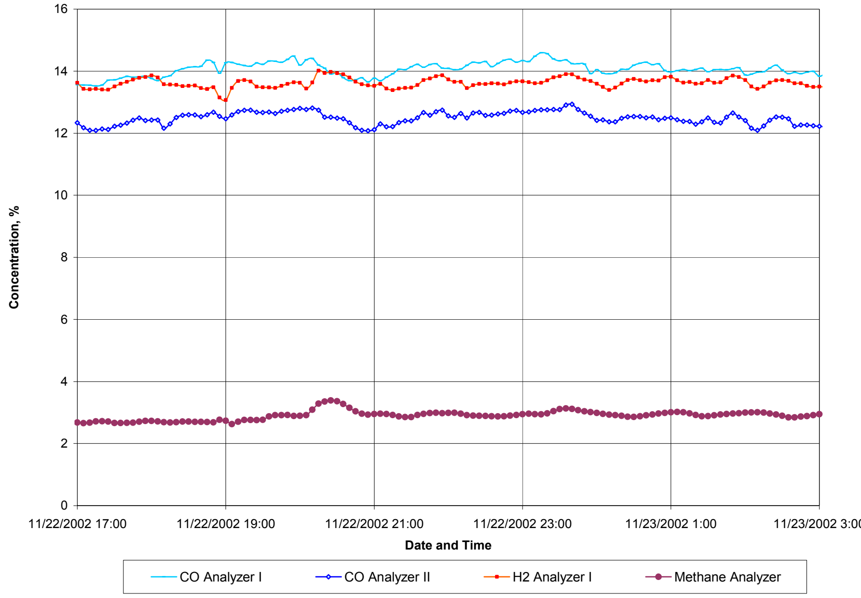

Figure 3.1-3 Typical Gas Analysis Data During Stable Gasification in TC10

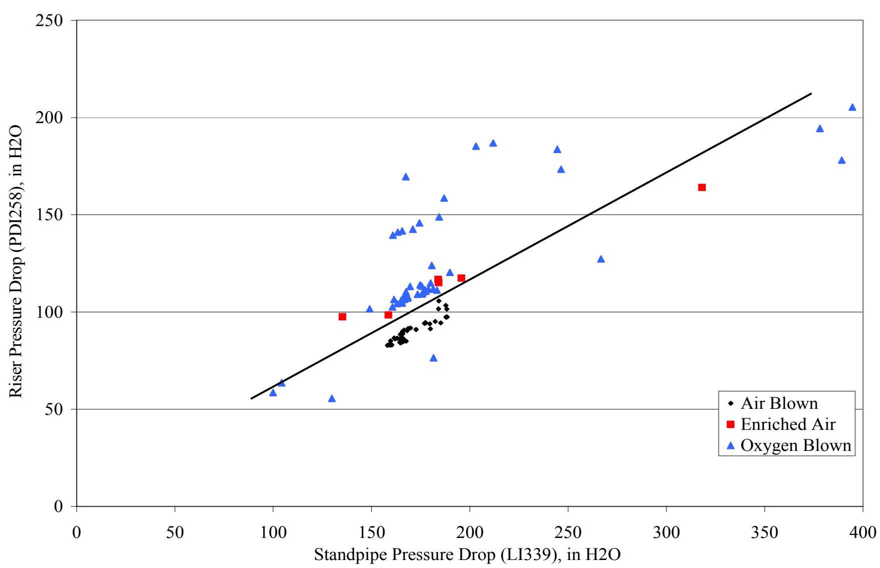

Figure 3.1-4 Effect of Standpipe Level on Circulation Rate

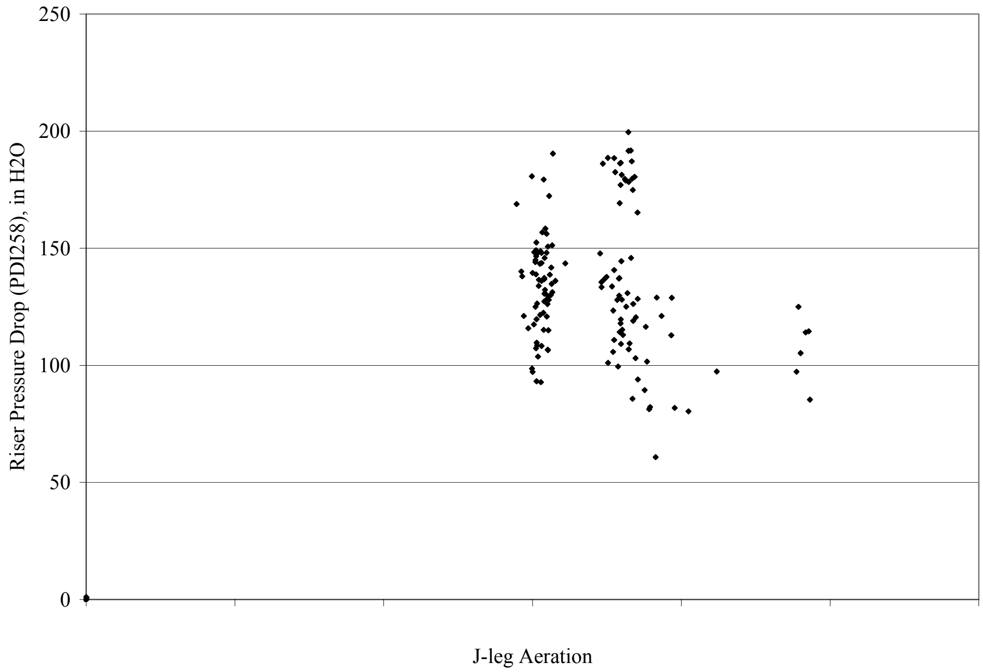

Figure 3.1-5 Effect of J-leg Aeration on Circulation Rate at Given Standpipe Level

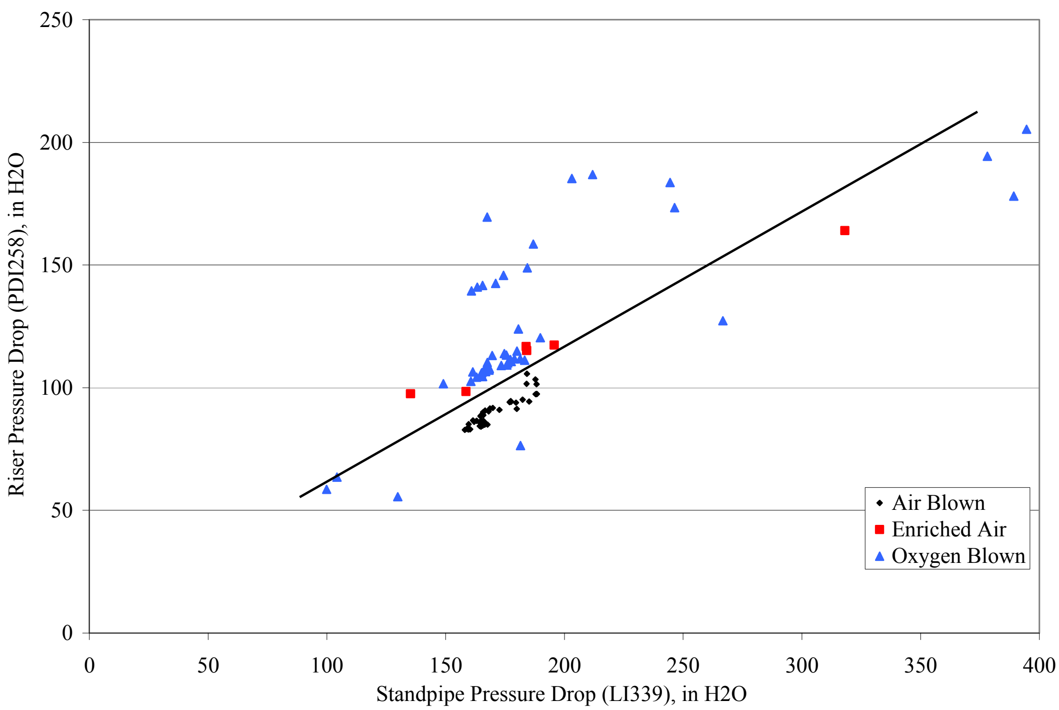

Figure 3.1-6 Change in Gasifier Temperature Differences With Increasing Circulation Rate

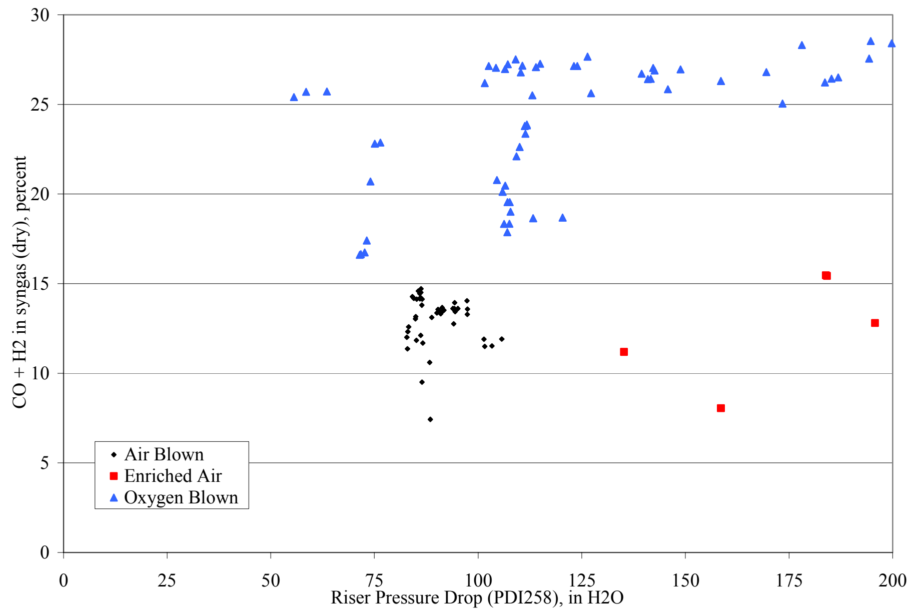

Figure 3.1-7 Effect of Circulation Rate on Gas Quality

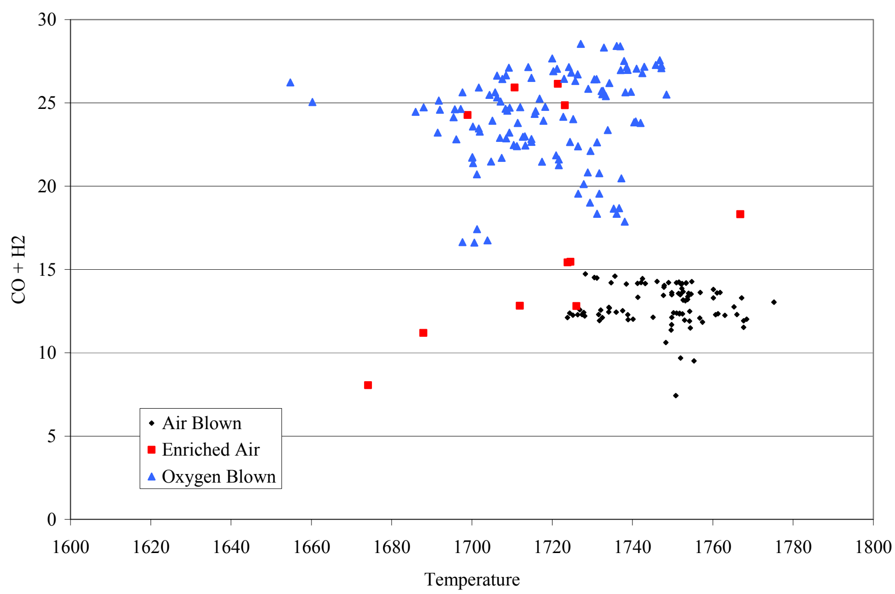

Figure 3.1-8 Effect of Temperature on Gas Quality

3.2 GASIFIER TEMPERATURE PROFILES

Section 3.2 describes the temperature profiles in TC10. A schematic of the gasifier with relative thermocouple locations is given in Figure 3.2-1. The gasifier was predominantly operated in oxygen-blown mode during TC10. In this section the temperature profile for TC10 is compared to TC08 and the effect of a lower coal-feed rate and a higher steam-flow rate on the temperature profile is evaluated.

Figure 3.2-2 compares the temperature profile for oxygen-blown operations in TC08 (PRB coal) and TC10. The steady-state periods used for analysis for TC08 and TC10 are TC08-25 and TC10A-4, respectively. The temperature profile for TC08 and TC10 are similar with TC10 operating at a slightly higher temperature. For both steady-state periods, the lower mixing zone (LMZ) temperature, T1-T4, increased quickly as the heat released from char combustion heated the oxygen, steam, and solids in the LMZ. The temperature then decreased as cooler solids from the J-leg, T11, entered the upper mixing zone (UMZ), T5. Excess oxygen from the LMZ combusts the g-ash in circulating solids and again the temperature, T6 and T7, rises. When all of the oxygen is consumed, the temperature begins to decrease. The temperature decreases further through the riser, T8, due to the coal and conveying gas heat-up, coal devolatilization, endothermic gasification reactions, and heat losses. The solids removed by the disengager and cyclone cool as they flow down the standpipe, T9-T11.

Several operating parameters influence the temperature profile: coal-feed rate, amount of carbon in circulating solids, solids circulation rate, and oxygen and steam flow rates and distribution. The temperature profile for a steady-state period with low carbon content in circulating solids and higher steam flow rate (TC10A-3) is shown in Figure 3.2-3. Since there is little carbon and a higher steam flow rate in the lower mixing zone (LMZ), the temperature in the LMZ is relatively low. The moderate increase in temperature is due to mixing with the hot solids from the J-leg. The solids returning from the J-leg are at a higher temperature, T11, than the gas and solids coming from the LMZ, T4. Thus, the J-leg solids are cooled further as they enter the UMZ, T5. The carbon in circulating solids from the J-leg is consumed and the temperature, T6 and T7, increases. The temperature continues to increase around the coal-feed nozzle and throughout the riser as the oxygen is consumed by the coal.

In comparison, the temperature profile for a higher carbon content and lower steam flow rate period (TC10A-4) is also shown in Figure 3.2-2. Due to the higher carbon content in the circulating solids and lower steam flow rate in the LMZ, the LMZ temperature, T1-T4, increases quickly. As cooler solids from the J-leg, T11, enter the UMZ the temperature, T5, decreases. The carbon in circulating solids from the J-leg is consumed and the temperature, T6 and T7, increases. Coal and conveying gas heat-up, coal devolatilization and endothermic gasification reactions combined with heat losses decrease the temperature, T8, further as the gas and solids flow up through the riser.

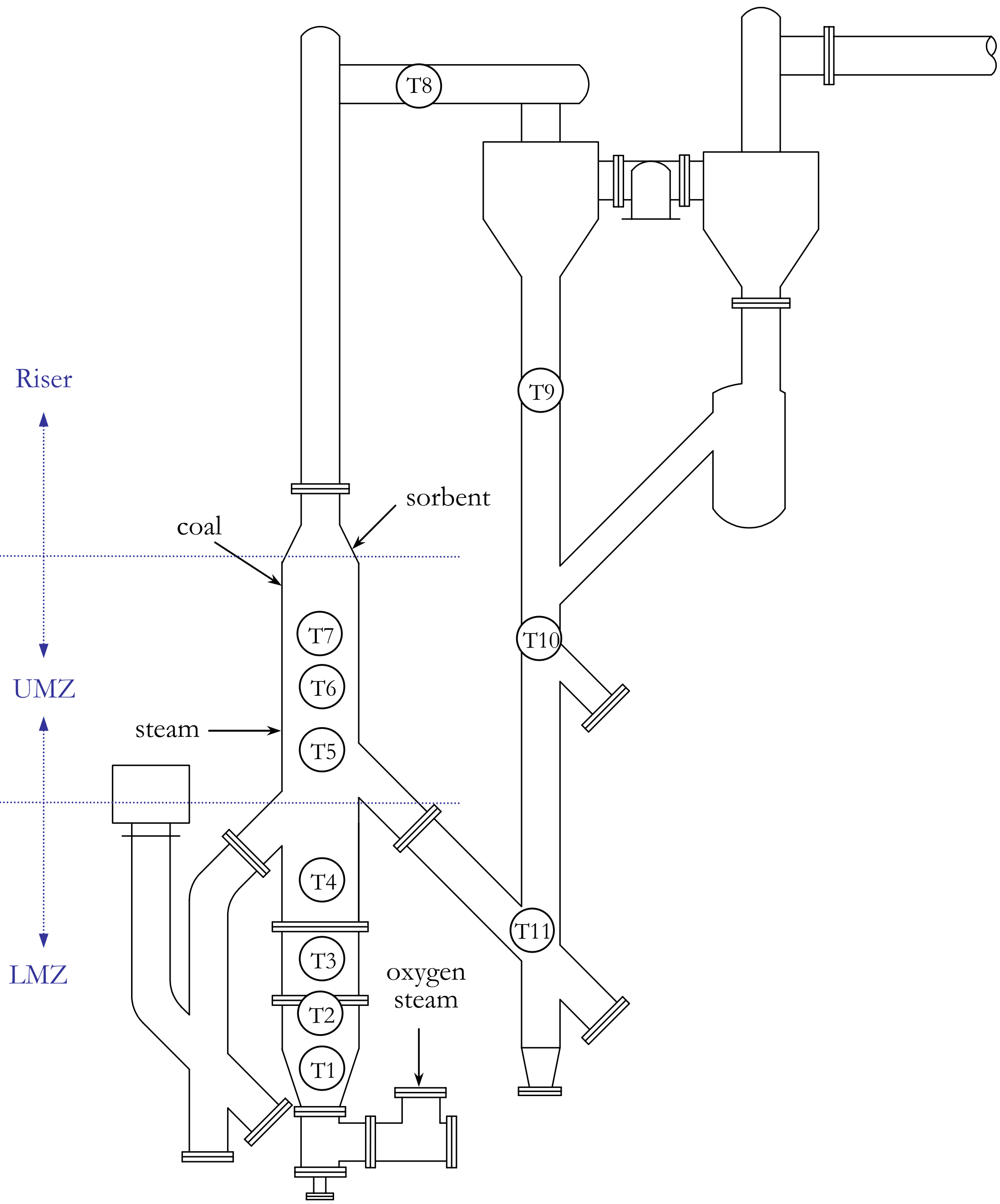

Figure 3.2-1 Transport Gasifier Schematic

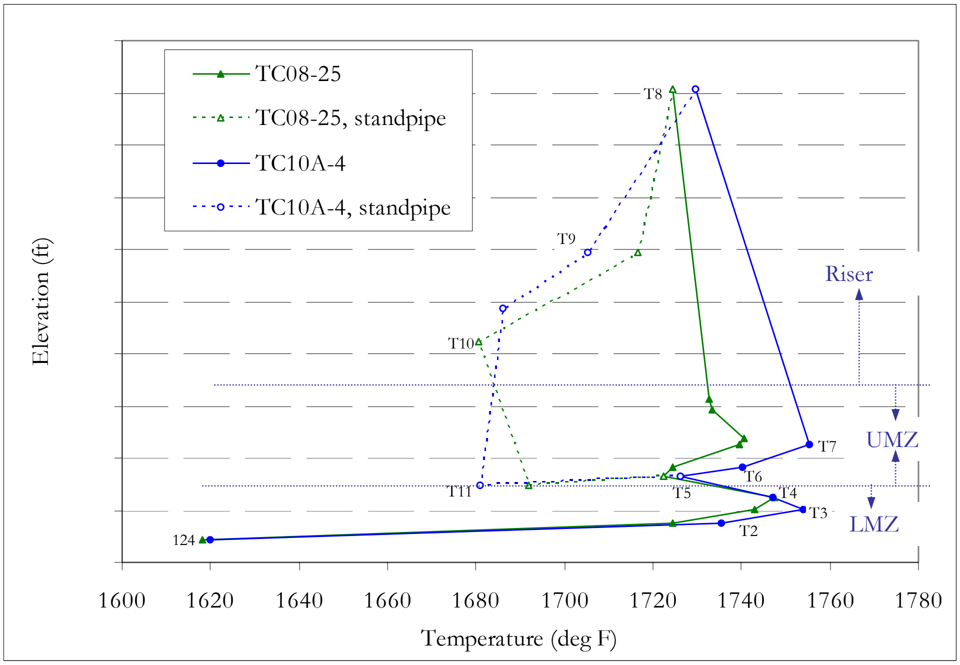

Figure 3.2-2 Temperature Profile in Oxygen-Blown Mode in TC08 (TC08-25) and TC10 (TC10A-4)

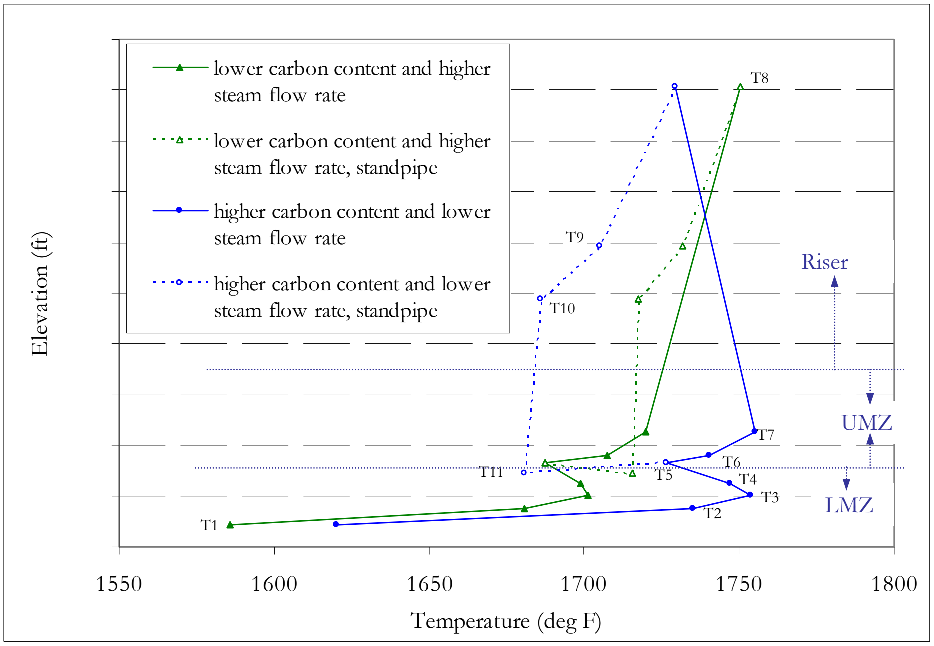

Figure 3.2-3 Comparison of Temperature Profiles for Low and Higher Carbon Content in Circulating Solids (TC10A-3 and A-4)

3.3 GAS ANALYSIS

3.3.1 Summary and Conclusions

- The raw synthesis gas lower heating values (LHV) were between 46 and 52 Btu/scf for air-blown operation and between 57 and 100 Btu/scf for oxygen-blown operation.
- The LHV for all modes of operation were strong functions of the relative amount of oxygen fed to the Transport Gasifier.
- The nitrogen-corrected, adiabatic synthesis gas LHV was between 94 and 106 Btu/scf for air-blown operation and between 121 and 222 Btu/scf for oxygen-blown operation.
- Total reduced sulfur (TRS, mostly H_2S) emissions were between 311 and 540 ppm.
- Synthesis gas analyzer data for CO was excellent, with four of six analyzers in agreement with each other for most of the run.
- Synthesis gas analyzer data for H_2 was good with both gas chromatographic analyzers within a few percent, but AI419 was only available for about 20 percent of TC10.
- Synthesis gas analyzer data for CH_4 was good in that the both GC analzyers (AI464 & AI419) agreed very well when AI419 was in service (about 20 percent of TC10). The Procal analyzer, AI475, gave 2 percent higher CH_4 values than AI464.
- Synthesis gas analyzer data for C_2^+ was poor in that the AI419 was unavailable for most of the test run and AI464 read erratically, except for the last 40 hours of TC10.
- Synthesis gas analyzer data for CO_2 was good in that AI464 and AI434 agreed for the entire run, and AI419 agreed whenever it was in service (about 20 percent of TC10). The moisture-corrected AI475 data read about twice the values of the other analyzers.
- Synthesis gas analyzer data for N_2 was good in that AI464 read reasonably and agreed with AI419 when AI419 was in service.
- AI475H gas analyzer data for H_2O agreed with two out of the nine in situ H_2O measurements. AI479H agreed for four out of the nine measurements. The synthesis gas moisture was calculated using the thermodynamic equilibrium of the water-gas shift reaction at the mixing zone temperature.
- The sums of the dry gas analyzer concentrations were between 97 and 101 percent, a slightly low bias.
- The syngas H_2S analyzer was out of service for the majority of the test run.
- The NH_3 data were occasionally above the high range of the analyzers. AI480Q data corresponded well with three of the five extractive samples.
- The CO/CO_2 ratio was between 0.4 and 0.9.
- The water-gas shift constant using the in situ H_2O measurements were between 0.65 and 0.84, with one outlier at 0.97, despite large variations in H_2O, H_2, CO, and CO_2 concentrations.

- The synthesis gas molecular weight was 27.0 pounds/mole (during an air-blown operating period) and 25.2 pounds/mole (during an oxygen-blown operating period).
- The synthesis gas combustor oxygen balance was excellent.
- The synthesis gas combustor hydrogen balance was excellent.
- The synthesis gas combustor carbon balance was good, after correcting for analyzer error.

3.3.2 Introduction

The major goal for TC10 was the demonstration of the Transport Gasifier in oxygen mode with Powder River Basin (PRB) coal. PRB coal feed was established with air on November 18, 2002. The transition to oxygen-blown operations took place the next day. An unscheduled outage began on November 26, 2002, when a large deposit formed in the gasifier mixing zone. Coal feed resumed on December 6, 2002, and continued until December 18, 2002.

Over the course of the test run, the Transport Gasifier operated on coal feed for 416 hours, 293 hours of which were in oxygen-blown mode. The gasifier experienced several trips due to wet coal plugging the coal conveying line. After each trip the gasifier was briefly returned to air-blown operation prior to the resumption of oxygen-blown operation.

There were nine steady periods of operation between November 18 and 26 and 10 steady-state periods between December 6 and 18. The only fuel used during the steady periods of TC10 was PRB coal, which is a mixture of four different coals. Table 3.3-1 shows the steady periods of operation used for gas analysis. Some periods, including the second parts of TC10A-4 and TC10B-2, the first part of TC10B-3, and the entirety of TC10B-6 did not have adequate gas analyzer data. Thus, they are absent from Table 3.3-1. Also, two periods (TC10A-6 and TC10B-4) were longer than 16 hours and were split into periods of about 8 hours each, resulting in 22 operating periods useful for gas analysis and material balances.

Sorbent was not injected into the Transport Gasifier during TC10; all sulfur removal was from the alkali contained in the PRB coal. Small amounts of coke breeze were added to the Transport Gasifier as a pilot fuel during TC10A-7 in case the coal feeder tripped and the coke breeze feeder would not start.

Table 3.3-2 lists some of the operating conditions for TC10, including mixing zone temperatures, pressure control valve pressures, PCD inlet temperatures, air rate, oxygen rate, syngas rate, steam rate, and nitrogen rate. The system pressure was decreased prior to the first oxygen-blown period of operation at hour 37 (TC10A-2) from 180 psig to 146 psig to prepare for the lower pressure oxygen-blown testing. The steam rate was increased during the oxygen-blown testing.

3.3.3 Raw Gas Analyzer Data

During TC10, the Transport Gasifier and synthesis gas combustor outlet gas analyzers were continuously monitored and recorded by the Plant Information System (PI). Several in situ grab samples of synthesis gas moisture content were measured during PCD outlet loading sampling.

The gas analyzer system analyzed synthesis gas for the following gases during TC10 using the associated analyzers:

CO	AI425, AI434B, AI453G, AI464C, AI419C, AI475C
CO_2	AI434C, AI464D, AI419D, AI475D
CH_4	AI464E, AI419E, AI475E
C_2^+	AI464F, AI419F
H_2	AI464G, AI419G
H_2O	AI419H, AI475H, AI479H, AI480H
N_2	AI464B, AI419B
NH_3	AI475Q, AI480Q
H_2S	AI419J, AI480J
$C_{10}H_8$	AI480X
COS	AI480V
HCl	AI479R
HCN	AI479S

The AI464 and AI419 analyzers use a gas chromatograph and typically have about a 6-minute delay. The other four CO analyzers (AI425, AI434B, AI453B, and AI475C) and two CO_2 analyzers (AI434C and AI475C) are IR based and give more real-time measurements. All analyzers, except for AI475, AI479, and AI480, require that the gas sample be conditioned to remove water vapor. Therefore, all the analyzers except for AI475, AI479, and AI480 report gas compositions on a dry basis. Analyzers AI475, AI479, and AI480 are in situ gas analyzers and hence all readings include moisture (wet). The AI475 analyzer bank provides backup CO, CO_2, and CH_4 measurements.

The locations of the synthesis gas analyzers are shown on Figure 3.3-1. The gas analyzers obtain synthesis gas samples from three different locations:

- Between the PCD and the secondary gas cooler (HX0402).
- Between the secondary gas cooler and the pressure letdown valve (PV287).
- Between the pressure letdown valve and the syngas combustor (BR0401).

The six CO analyzers provide a measure of self-consistency when all or several of the six analyzers read the same value. An analyzer must be selected for use if all the analyzers do not agree. The TC10 hourly averages for the six CO analyzers are given in Figure 3.3-2. For most of TC10, analyzers AI434B, AI453G, AI464C, and AI425 were in good agreement. Analyzer AI419C was only in agreement with the other four CO analyzers at the beginning and end of the test run; it was out of service for the rest of TC10. The dry equivalent reading of AI475C (using

H_2O analyzer AI475H) is plotted in Figure 3.3-2 rather than the actual reading in order to be consistent with the other analyzers.

Analyzer AI475C (dry) ran slightly higher than the other analyzers at the beginning of the test run and slightly lower at the end. Either AI453 or AI425 was used as CO data for further analysis. The analyzer choice for each operating period is given in Table 3.3-3. The good agreement between the CO analyzers gives confidence to the accuracy of the CO data. The low CO measurements are either periods when the gas analyzers were being calibrated or analyzer measurements made during coal feeder trips. The CO data used in calculations were interpolated for times when the gas analyzers were being calibrated.

The unit trips are shown on Figure 3.3-2 as sharp decreases in CO concentration. Each trip was restarted on air, and then transitioned to enriched air for a brief period before the oxygen-blown operation was resumed. Shown on Figure 3.3-2 are the major gasifier trips at hours 85, 112, 126, 160, 170, 223, 367, and 379. A deposit formed in the gasifier at hour 160, forcing an unscheduled outage to allow maintenance to remove it. In addition to the trips shown in the figure, several minor trips occurred at hours 10, 47, 116, 123, 131, 139, 165, and 175.

TC10 hourly averaged data for the hydrogen analyzers are shown on Figure 3.3-3. Analyzer AI464G gave reasonable results for the entire run. Due to a problem with the second bank of GC analyzers, Analyzer AI419G was out of service from hours 13 to 372, but agreed well with AI464G during the brief time it was in operation. Gas analyzer AI464G was used for all of the operating periods.

Figure 3.3-4 gives the TC10 hourly average gas analyzer data for CH_4. The AI475E data are measured wet and presented dry on Figure 3.3-4 to be consistent with the other two CH_4 analyzers, which measure dry. Due to a problem with the second bank of GC analyzers, AI419E was not available for the time between hours 13 and 372. The data from AI419E agreed well with the data from AI464E when it was in service. Although reasonably close in air-blown operation, analyzer AI475E was not consistent with the other two analyzers for the oxygen-blown part of TC10. Since AI464E gave reasonable results for virtually the entire run, it was used for all of the test periods, except for TC10A-1 when neither analyzer was reading reliably.

The TC10 hourly average gas analyzer data for C_2^+ are given in Figure 3.3-5. At the beginning of the test run, AI464F read only a negligible amount of C_2^+, except for a brief period of time around hour 60. Later, at hour 253, the value increased to 0.3 percent and fluctuated between 0.1 and 0.3 percent for the remainder of the test run. Due to the problem with the second bank of GC analyzers, AI419F was not in service except during the beginning and end of the test run. AI419F indicated values of around 0.2 percent during the brief period of time that it was reading. The AI464F values in TC10 were used whenever they seemed reasonable after hour 325. Before hour 325, a value of 0.25 percent C_2^+ was used for further analysis using the operating periods. This value made the syngas combustor balances more consistent (see Section 3.5).

The CO_2 analyzer data are given on Figure 3.3-6. The AI419D analyzer was out of service, along with the other AI419 analyzers, from hour 25 and hour 372. Analyzer AI475D reads wet, while the other analyzers read dry. The AI475D data on Figure 3.3-6 were corrected for moisture to be comparable with the other three CO_2 analyzers. Analyzers AI434C and AI464D agreed with each other very well for the entire test run, with analyzer AI419D agreeing whenever it was in service. The moisture-corrected AI475D data usually read poorly, about 15 percent higher than the other three analyzers. Since it proved to be the most reliable, AI464D was exclusively used for further data analysis.

The nitrogen analyzer data are given in Figure 3.3-7. Like all of the other AI419 analyzers, the AI419B analyzer was only available at the beginning and at the end of the test run. When both analyzers were in service, they agreed almost perfectly. Analyzer AI464B was selected for further analysis for all of the operating periods because of its availability.

Since both GC analyzers, AI419 and AI464, analyze for nearly the entire spectrum of expected gas components, a useful consistency check of each analyzer is to plot the sum of the gases measured by each bank of analyzers to see how close the sum of compositions is to 100 percent. The sum of both of the GC analyzer banks is given on Figure 3.3-8. AI464 was fairly consistent during TC10, usually between 96 and 100 percent. The AI419 data were also good when the AI419 analyzers were in service, also adding up to between 96 and 100 percent. The lack of the AI419 data dictated that AI464 data be used for analysis in TC10. The small variation from 100 percent during TC10 for AI464 gives good credibility to all AI464 data.

The raw H_2S analyzer data are shown on Figure 3.3-9. Like the other AI419 analyzers, the AI419J analyzer was out of service between hour 25 and hour 372. The available AI419 H_2S data, ranging from 100 to 600 ppm, seem reasonable in that they were comparable to data from earlier PRB oxygen-blown test runs. The AI480J analyzer, however, did not provide reliable data for the majority of the test run. In the early part of the run, the AI480J analyzer fluctuated over a wide range of 0 to 800 ppm, before going out of range high. It then read a negative value for the remainder of the test run.

The raw NH_3 analyzer data are shown on Figure 3.3-10. Analyzers AI475Q and AI480Q are in situ analyzers and measure the NH_3 composition without any sample conditioning and hence the compositions are "wet." During the beginning of TC10, AI475Q was over the maximum range (4,000 ppm) of the analyzer. As the run progressed, AI475Q began to read values between 2,000 and 3,000 ppm. The AI480Q analyzer read values of around 1,500 ppm at the beginning of the test run. As the second part of the test run began (at hour 167), the AI480Q analyzer started to read 2,500 ppm, then gradually dropped off to around 500 ppm. A decrease in steam flow rate toward the end of the test run possibly caused the decrease in ammonia concentration based on chemical equilibrium. Along with the gas analysis data, Figure 3.3-10 gives ammonia concentrations for five extractive samples. Although the extractive sample data were much lower than the AI475Q data, they agreed well with the AI480Q data.

Figure 3.3-11 shows the AI479S HCN data for TC10, along with data from five extractive samples taken during the test run. The analyzer data fluctuated over a wide range—mostly from 0 to 250 ppm and occasionally reaching 400 ppm. The extractive samples were each between 17 and 30 ppm. Comparing the samples to the gas analysis data, however, is impractical, since the analyzer data fluctuated over a very large range.

Figure 3.3-12 plots the AI479R HCl data and the AI480W CS_2 data. At the beginning of the test run, the HCl data fluctuated widely between 0 and 400 ppm, until hour 92, when the analyzer dropped to 0 for the remainder of the test run. The CS_2 data appeared to be more reliable, reading between 0 and 35 ppm for the entire test run.

Shown on Figure 3.3-13 are the AI480X $C_{10}H_8$ data and the AI480V COS data. The $C_{10}H_8$ data do not appear to be reliable, since they fluctuated over a wide range for most of the test run. The COS data started the test run in an unstable manner, but steadied out around 350 ppm around hour 160 and remained there until the end of TC10.

The synthesis gas H_2O analyzers data and the in situ H_2O data are plotted on Figure 3.3-14. Nine in situ H_2O measurements were taken during TC10. The in situ H_2O and AI475H data agreed with each other for two out of the nine in situ H_2O data points, while the in situ measurements agreed with the AI479H data for four out of the nine measurements. During the first three measurements AI479H was out of service. During the second and third measurements, AI475H was out of service. Except for the first 85 hours of the test run, AI480H consistently read up to 10 percent higher than the other two gas analyzers. Since the in situ technique has given reliable results in the past, the in situ results will be used for further analysis.

The H_2O analyzer AI419H is part of the AI419 GC. Since AI419 operates dry, and the synthesis gas H_2O is removed prior to analysis, AI419H always read 0.0 percent and will not be discussed further.

3.3.4 Gas Analysis Results

The dry, raw synthesis gas analyzer data was adjusted to produce the best estimate of the actual gas composition in three steps:

1. Choice of CO, H_2, CH_4, N_2, and CO_2 analyzer data to use (see Table 3.3-3).
2. Normalization of dry gas compositions (force to 100-percent total).
3. Conversion of dry compositions to wet compositions.

For the rest of this section, the data analysis will be based on only the TC10 operating periods. The operating period averages of the sum of the dry gas analyses selected are shown on Figure 3.3-15. The majority of the operating periods have the sum of dry gas compositions between 97 and 100 percent, indicating that the data is consistent. The two air-blown operating periods has the highest sum of dry gas compositions. The average of all the operating period sums of dry gas composition is 97.68 percent indicating that there is a slightly low bias in the data. A low bias means that some of the gas compositions are being underestimated by the selected gas analyzers.

In previous gasification runs, the water-gas shift reaction was used to interpolate H_2O measurements between in situ H_2O measurements and to check the consistency of the H_2O analyzers. Since the H_2O analyzers did not always agree well with the in situ H_2O measurements, the water-gas shift (WGS) equilibrium will be used to interpolate H_2O data between in situ H_2O measurements. The water-gas shift equilibrium constant should be a function of a Transport Gasifier mixing zone or riser temperature. Plotted on Figure 3.3-16 are the H_2O concentrations calculated from the water-gas shift equilibrium constant based on the mixing zone temperature TI350 at an approach temperature of -100ºF and using the measured H_2, CO, and CO_2 concentrations. The approach temperature of -100ºF seemed to give the best fit of the in situ data. For comparison, Figure 3.3-16 also presents the AI475H gas analyzer data, as well as the in situ measurement data. The WGS H_2O data will be used for further data analyses.

The water-gas shift reaction and equilibrium constant are given below:

$$CO + H_2O \leftrightarrow H_2 + CO_2 \qquad (1)$$

$$Kp = \frac{(H_2)(CO_2)}{(H_2O)(CO)} \qquad (2)$$

As mentioned above, the analyzers agreed with less than half of the nine in situ H_2O measurements. The WGS calculation, on the other hand, agreed with five of the eight in situ measurements made at steady-state operations (the final in situ measurement occurred after the last steady-state period). One of the in situ measurements that did not have good agreement with the WGS moisture content occurred at hour 257, during a loss of coal feed. The other in situ measurement at hour 142 experienced tar formation, which may have hindered the sampling. In general, the AI475H was usually about 2 to 6 percent higher than the WGS H_2O, but occasionally the WGS has higher, as for TC10A-1 and TC10A-5.

The synthesis gas H_2O concentration should be a function of the amount of steam added to the Transport Gasifier and the amount of nitrogen dilution. Figure 3.3-17 plots the synthesis gas H_2O content against the amount of steam added to the gasifier (based on the hydrogen balance). The main effect is the amount of nitrogen dilution caused by the different modes of operation air- or oxygen-blown. Figure 3.3-17 shows a strong relationship between syngas moisture and steam rate. Note that the two air-blown operating periods had the lowest H_2O content.

The best estimates of the wet gas compositions for the TC10 operating periods are given on Table 3.3-4 and shown on Figure 3.3-18. Also shown on Table 3.3-4 are the synthesis gas molecular weights for each operating period.

The CO concentration started at just over 6 percent. After transitioning to oxygen-blown mode, CO dropped slightly due to a high steam flow rate of over 2,600 pph. Once the steam flow rate decreased, carbon monoxide levels increased to 12 percent, and, besides the air-blown test period at hour 121, the CO level fluctuated between 8 and 12 percent for the remainder of the test run.

The H_2 concentration was around 5 percent from the start of TC10, and increased to over 9 percent upon the transition to oxygen-blown mode and to around 12 percent, upon increasing the coal-feed rate. Except for a decrease in hydrogen to 5 percent during the air-blown test period at hour 121, the hydrogen content remained between 9 and 12 percent until the end of the test run. The H_2 was lower than the CO during the air-blown operation and greater than or equal to the CO during oxygen-blown operation due to the higher steam-flow rate during oxygen-blown operation, which created additional H_2 via the water-gas shift reaction (See Section 3.3.6).

The CO_2 concentration was around 9 percent for the first air-blown period and increased to 14 percent during oxygen-blown operations. During the oxygen-blown testing the CO_2 was mostly between 12 and 15 percent. When the system briefly returned to air-blown operation at hour 121, the CO_2 returned to about 9.5 percent.

The CH_4 concentration started the run at 1.5 percent, decreased slightly due to the high steam flow rate during the first oxygen-blown test period, and then slowly increased to just over 2 percent at the onset of oxygen-blown testing. During oxygen-blown testing, the CH_4 remained steady at slightly above 2 percent. CH_4 concentrations experienced a drop in concentration during the air-blown test period at hour 121.

The CO/CO_2 ratios were calculated from the gas data for each operating period, and are listed on Table 3.3-4. The TC10 CO/CO_2 ratio varied from 0.4 to 0.9, with the lowest ratio occurring during the period of high steam-flow rate. Once the steam-flow rate decreased, the CO/CO_2 ratio increased.

The LHV for each gas composition was calculated and is given on Table 3.3-4 and plotted on Figure 3.3-19.

The LHV value was calculated using the formula:

$$\mathrm{LHV(Btu/SCF)} = \begin{Bmatrix} 275\times(\mathrm{H_2\%})+322\times(\mathrm{CO\%})+ \\ 913\times(\mathrm{CH_4\%})+1641\times(\mathrm{C_2^+\%}) \end{Bmatrix}/100 \qquad (3)$$

The raw LHV was around 50 Btu/scf for the two periods of air-blown operation and ranged from 57 to 100 Btu/scf for oxygen-blown operation. The raw LHV began the test run at about 52 Btu/scf and climbed to 57 Btu/scf when the transition to oxygen-blown operations took place. A high steam-flow rate kept the value low. After the steam-flow rate decreased, the LHV increased to values as high as 100 Btu/scf, before gasifier operations forced a return to air-blown mode where the LHV dropped back to 46 Btu/scf. Upon resuming oxygen-blown mode, the LHV typically remained between 80 and 90 Btu/scf, with a few test periods seeing values around 70 Btu/scf and others having a LHV of over 90 Btu/scf.

Past test runs have indicated that the LHV is most affected by two major operating parameters: the coal-feed rate and the steam-feed rate. The LHV increases as coal rate increases (see Figure 4.5-5 of TC06 Final Report). The coal rate effect is due to the way that the Transport Gasifier operates in that the aeration and instrument nitrogen remains constant as the coal rate increases.

As the coal-feed rate increases, the syngas-flow rate increases, but the nitrogen-flow rate remains constant. The pure nitrogen part of the syngas concentration is thus lessened (less nitrogen dilution), and the syngas LHV increases. When oxygen replaces air in enhanced air- and oxygen-blown operation, the nitrogen content of the syngas also decreases, increasing the LHV.

Unlike the coal-feed rate, an increase in steam flow produces a lower LHV by diluting the syngas with moisture. A way to combine the effects of changes in steam, mode of operation, and coal rates is to determine the overall percent of oxygen of all the gases that are fed to the Transport Gasifier. The overall oxygen percentage compensates for the different amount of nitrogen and steam that are added to the gasifier. The overall percent O_2 is calculated by the following formula:

$$\text{Overall }\%O_2 = \frac{.21 * \text{air} + \text{oxygen}}{\text{air} + \text{oxygen} + (\text{pure nitrogen}) + \text{steam}} \tag{4}$$

The air, oxygen, nitrogen, and steam flows are in moles per hour. At the PSDF, a large amount of pure nitrogen is fed to the gasifier for instrument purges, coal and sorbent transport, and equipment purges. In air-blown operation at the PSDF, about 50 percent of the synthesis gas nitrogen comes from air and 50 percent comes from the pure nitrogen system. In oxygen-blown operation at the PSDF, the removal of nitrogen from air removes about the same amount of nitrogen as if the pure nitrogen was replaced by recycling synthesis gas. The TC10 raw LHV data are plotted against the overall percent O_2 on Figure 3.3-20. Also plotted on Figure 3.3-20 are two straight lines: one a correlation of LHV data from PRB test runs TC06, TC07, and TC08, the other a correlation of LHV data from the Hiawatha bituminous run, TC09. The TC10 data range from 46 Btu/scf at 11.5-percent oxygen to 100-Btu/scf at 18.2-percent oxygen and follows a clear trend of increasing Btu/scf with oxygen percentage. The TC10 results agree with the trend line showing the combination of the TC06, TC07, and TC08 PRB data. The Hiawatha data indicate slightly higher LHV at a given oxygen percentage, partially due to the high heating value (HHV) of the Hiawatha coal with respect to PRB coal.

3.3.5 Nitrogen- and Adiabatic-Corrected Synthesis Gas Lower Heating Values

The PSDF Transport Gasifier produces syngas of a lower quality than a commercially sized gasifier due to the use of recycle gas (in a commercial gasifier) rather than nitrogen, (at the PSDF) for aeration and instrument purges as well as the lower heat loss per pound coal gasified in a commercially sized gasifier when compared to the PSDF Transport Gasifier. To estimate the commercial synthesis LHV data, the following corrections are made to the measured, raw synthesis gas composition:

1. All nonair nitrogen is subtracted from the syngas. This nitrogen is used for Transport Gasifier aeration and instrument purges. In a commercial plant the instrument purges will be lower due to less commercial plant instrumentation and due to commercial instruments requiring the same purge rate independent of the plant size. This correction assumes that recycled syngas or steam will be used in a commercial plant for aeration and instrument purges to replace the nonair nitrogen. The nonair nitrogen was determined by subtracting the air nitrogen from the synthesis gas nitrogen. This

correction increases all the nonnitrogen syngas compositions and decreases the nitrogen syngas composition. The syngas rate will decrease as a result of this correction. For oxygen-blown mode, this correction removes all nitrogen from the syngas and the oxygen-blown syngas will have 0 percent nitrogen. The water-gas shift equilibrium constant and the CO/CO_2 ratios will not change. This correction should be valid in that other gases should be able to replace the nonair nitrogen in the Transport Gasifier. One potential problem to this correction is the use of recycle gas in Transport Gasifier locations where the recycle gas will combust in preference to the coal or recycle standpipe carbon, since this might result in gasifier hot spots or decreased performance. A commercial plant might use some nitrogen for selected aeration and instrument locations.

2. Accounting for the energy required to heat up the nonair nitrogen that has been eliminated by using steam or recycle gas for aeration or instrument purges. Once the nonair nitrogen is removed, the coal and air rates will decrease by the amount of energy no longer required to heat the nonair nitrogen to the maximum gasifier temperature. This results in decreased coal, air, and oxygen rates to the Transport Gasifier. It is assumed that this eliminated coal is combusted to CO_2 and H_2O to heat up the nonair nitrogen. Eliminating this additional coal reduces the syngas CO_2 and H_2O concentrations. The lower corrected air rates for air-blown mode also decreases the nitrogen in the corrected syngas. This correction decreases the synthesis gas-flow rate. For this correction the water-gas shift constant and the CO/CO_2 ratio both change due to the reduction in CO_2 and H_2O. This correction neglects the heat required to heat up the recycle gas replacing the nonair nitrogen used for aeration and instrument purges. The recycle gas will be available at a higher temperature than the nitrogen and less recycle gas will be required to replace the nonair nitrogen. This correction is more aggressive than it should be, but it is difficult to estimate the amount of recycle gas required in a commercial plant.
3. Correcting for the PSDF having a higher heat loss per pound of coal gasified than a commercially sized plant. Smaller scale pilot and demonstration units have higher surface area-to-volume ratios than their scaled up commercial counterparts, and hence the PSDF Transport Gasifier has a higher heat loss per pound of coal gasified than a commercial plant. Since the heat loss of a commercial plant is difficult to estimate, the corrected heat loss is assumed to be zero (adiabatic). The correction uses the same method to correct for the no longer required energy to heat up the nonair nitrogen. The coal, air, and oxygen rates are reduced; the syngas CO_2, H_2O, and N_2 concentrations are reduced; the water-gas shift equilibrium constant and the CO/CO_2 ratio change. This correction is probably good since the commercial plant heat loss per pound of coal gasified is much smaller than the PSDF Transport Gasifier heat loss per pound of coal gasified.
4. Reducing the steam rates for oxygen-blown operation, since in oxygen-blown operation steam is added to control the gasifier temperature. In a commercial plant, as the oxygen rate is decreased, the steam rate will also be decreased. It was assumed that the steam-to-oxygen ratio will be the same for the PSDF and the commercial Transport Gasifier, and hence the corrected steam rate will be lower than the original steam rate. The effect of lowering the steam rate was assumed to decrease the amount of H_2O in the syngas by the amount the steam rate was reduced. This correction reduces the steam rate and the H_2O content of the syngas and hence the LHV and water-gas shift equilibrium constant

also changes. The steam-to-oxygen ratio is a function of the detailed design of the Transport Gasifier and it is difficult to estimate what the commercial steam-to-oxygen ratio will be.

The sum of all these four corrections is the adiabatic nitrogen corrected LHV. These calculations are an oversimplification of the gasification process. A more sophisticated model is required to correctly predict the effects of decreasing pure nitrogen and gasifier heat loss. It should be noted that the corrected syngas compositions are based on a corrected coal rate, corrected air rate, corrected oxygen rate, corrected steam rate, and a corrected syngas rate. Since the corrections change the syngas water-gas shift equilibrium constant, still another correction should be made to the corrected gas compositions since the water-gas shift constant should be a function of the gasifier mixing zone temperature, not whether recycle gas is used. The corrected syngas LHV is probably correct since the WGS reaction does not change the LHV much since H_2 is being replaced by CO (or vice versa). Due to correction 4, the corrected H_2O is probably too high. In a commercial plant the WGS equilibrium will decrease H_2 to create more H_2O, which increases CO and decreases CO_2.

The corrections also change the equilibrium H_2S concentration, since as the H_2O and CO_2 concentrations increases, the equilibrium H_2S concentration increases. The corrected process conditions will result in higher equilibrium H_2S and will increase sulfur emissions if the sulfur emissions are equilibrium controlled.

The adiabatic N_2-corrected LHV for each operating period are given in Table 3.3-5 and plotted on Figure 3.3-21. The N_2-corrected LHV were 94 and 106 Btu/scf for the two air-blown operating periods and between 171 and 227 for the oxygen-blown operating periods. The trends during the run of the corrected LHV followed the raw percent O_2 and LHV. Note that the oxygen-blown operation corrected N_2 syngas concentration is 0 percent by the definition of the adiabatic N_2-corrected LHV. The correction is higher for oxygen blown because there is less syngas in the raw oxygen-blown mode of operation, so taking about the same amount of pure nitrogen out the syngas has a larger effect.

For comparing the raw LHV with the adiabatic N_2-corrected LHV, an equivalent to the overall percent O_2 is defined as:

$$\text{Corrected Overall }\%O_2 = \frac{.21*(\text{corrected air}) + (\text{corrected oxygen})}{(\text{corrected air}) + (\text{corected oxygen}) + (\text{corrected steam})} \qquad (5)$$

All flow rates are expressed as moles per hour. The corrected air rate, corrected oxygen rate, and corrected steam rate are used in the determination of the corrected LHV. The corrected overall percent O_2 for oxygen rate blown mode is a direct function of the steam-to-oxygen ratio, since the corrected air rate is zero.

The adiabatic N_2-corrected LHV data are plotted against the adiabatic overall percent O_2 in Figure 3.3-21. The air- and oxygen-blown LHV data form a smooth plot with overall percent O_2 in the feed gas. Also plotted in Figure 3.3-21 are a correlation of the corrected TC06, TC07, and TC08 corrected PRB results, a correlation of the corrected TC09 Hiawatha results, and the raw TC10 results. The correlation between the TC06, TC07, and TC08 data and the TC10 is good at lower oxygen percentages, but is slightly lower at higher oxygen percentages. The TC09 data indicate higher LHV at a given oxygen percentage than the TC10 data indicate, possibly due to the Hiawatha bituminous type of coal used. Note that the corrected air-blown TC10 data is consistent with the raw oxygen-blown data at the same percent O_2.

3.3.6 Synthesis Gas Water Gas-Shift Equilibrium

The water-gas shift equilibrium constants were calculated for the nine in situ moisture measurements and are given on Table 3.3-6. The measured equilibrium constant varied from 0.67 to 0.83, with one outlier at 0.97, which was taken during a period when the steam rate was decreasing. Two of the other moisture samples were contaminated with tar, suggesting less than desirable gasifier operating conditions. Another sampling took place during a coal feeder trip. The WGS for the remaining samples was relatively constant despite the wide range of H_2O (11.5 to 29.4 percent), CO (6.9 to 16.1 percent), H_2 (6.5 to 14.4 percent), and CO_2 (10.8 to 18.8 percent) during TC10, indicating that the water-gas shift reaction is controlling the relative H_2, H_2O, CO, and CO_2 concentrations in the Transport Gasifier.

The thermodynamic equilibrium temperature for each equilibrium constant was calculated from thermodynamic data and is shown on Table 3.3-6. The thermodynamic equilibrium temperature varied from 1,500 to 1,727°F. These temperatures are approximately the mixing zone temperatures (with the exception of the December 11th sample taken during the period of varying steam-flow rate). The equilibrium temperatures are listed in Table 3.3-6. The WGS constants calculated from the mixing zone temperatures are compared with the measured WGS constants in Figure 3.3-22 using the same approach temperature used in Figure 3.3-16 (-100°F). The WGS constants determined from the mixing zone temperature have much less variation than the measured WGS constants. Since the approach temperature of -100°F was used to curve fit the data, all points other than the outliers are centered around the 45-degree line on Figure 3.3-22.

3.3.7 Synthesis Gas Combustor Oxygen, Carbon, and Hydrogen Balance Calculations

The synthesis gas compositions and synthesis gas flow rate can be checked by oxygen balances, hydrogen balances, and carbon balances around the synthesis gas combustor since the synthesis gas combustor flue gas composition is measured by the following syngas combustor flue gas analyzers (see Figure 3.3-1 for the analyzer location):

- AIT8775 – O_2
- AI476H – H_2O
- AI476D – CO_2

The synthesis gas combustor gas composition was calculated for each operating period by using synthesis gas composition, synthesis gas flow rate, FI463, and the following syngas combustor flows:

- Primary air flow, FI8773.
- Secondary air flow, FIC8772.
- Quench air flow, FI8771.
- Propane flow, FI8753.

The measured and mass-balance-calculated O_2 values are shown in Figure 3.3-23 and Table 3.3-7. The calculated synthesis gas combustor O_2 concentrations measured slightly higher than the measured values for all but two of the operating periods. The maximum error between the two was under 10 percent of the two values. The measured O_2 being lower than the calculated O_2 could indicate that the assumed synthesis gas composition had fewer combustibles (and a lower LHV) than the actual synthesis gas.

Throughout the test run, the measured CO_2 concentrations were always 1 to 3 percent lower than the calculated CO_2 concentrations (a percent error of over 10 percent) due to an analyzer error. The low measured values imply that the carbon conversion and LHV may be higher than indicated by the synthesis gas analyzers. The oxygen data above also seem to support the fact that the syngas LHV was higher than assumed. Later calibrations of AI476D indicated that it was reading about 2 percent low during TC10. Thus, a correction of +2 percent was added to the AI476D analyzer CO_2 data for data analysis. The corrected measured and mass-balance synthesis-gas combustor flue gas calculated CO_2 values are shown in Figure 3.3-24 and Table 3.3-7. The corrected data resulted in relative error of well within 10 percent for most operating periods.

The AI476H measured and mass-balance-calculated H_2O values are shown in Figure 3.3-25 and Table 3.3-7. Most of the measured and calculated H_2O values straddled the 45-degree line, indicating that the syngas gas analyzers were consistent with the syngas combustor H_2O analyzer. The calculated H_2O values agreed closely (less than 10 percent error) with the analyzer values for all but two periods.

The results of the SGC flue gas analyzers all seem to indicate that the syngas may actually have a higher LHV than measured.

The synthesis gas LHV can be estimated by performing an energy balance around the synthesis gas combustor. The synthesis gas combustor energy balance is done by estimating the synthesis gas combustor heat loss by matching the synthesis gas LHV calculated by the synthesis gas combustor energy balance with LHV calculated from the synthesis gas analyzer data. In some of the commissioning tests (GTC test series), the gas analyzers were not operational during the entire run, and the SGC energy balance determined LHV was used to estimate synthesis gas LHV during periods when there was no gas analyzer data. A comparison between the measured TC10 LHV and the synthesis gas combustor energy balance LHV using a synthesis gas combustor heat loss of 1.5×10^6 Btu/hr is given on Figure 3.3-26. This heat loss was consistent with previous test campaigns. The SGC combustor energy balance LHV and analyzer LHV were very consistent with each other during all operating periods. The agreement was very good with the values obtained through gas analysis being within 10 percent of the values obtained from the energy balance.

3.3.8 Sulfur Emissions

The wet H_2S concentration based on chemical equilibrium is plotted on Figure 3.3-27 and compared with the synthesis gas combustor SO_2 analyzer AI476N and the synthesis gas total reduced sulfur (TRS). The synthesis gas combustor SO_2 analyzer, AI476N, measures the total sulfur emissions from the Transport Gasifier. The total sulfur emissions consist of H_2S, COS, and CS_2. The main sulfur species in coal gasification are considered to be H_2S and carbon oxysulfide (COS). There should also be a minor amount of carbonyl sulfide (CS_2). The sulfur emissions for the operating periods of TC10 are listed on Table 3.3-7. Since the synthesis gas combustor exit gas-flow rate is about twice that of the synthesis gas rate during air-blown operations, the synthesis gas total reduced sulfur concentration is about twice that of the measured synthesis gas combustor SO_2 concentration during air-blown operations (at hours 22 and 121). During oxygen-blown operations, the synthesis gas combustor flue-gas rate is about three times the synthesis-gas rate, so the syngas TRS is normally about three times the synthesis gas combustor SO_2 concentration. In the TC10 oxygen-blown operating periods, however, the syngas TRS was usually around two times the measured value, perhaps because the high steam-flow rate adjusted the flow ratio of inlet and outlet of the syngas combustor. The H_2S analyzer, AI419J, was out of service for most of the test run. Therefore, H_2S analyzer AI419J data will not be used for the remainder of this report.

TC10 was operated without sorbent addition for the entire run to determine the amount of sulfur removal that could be obtained by the PRB ash alkalinity. This will be discussed further in Section 3.5.

The TRS emissions began the run at about 300 ppm and increased to around 500 ppm. For the remainder of the test run, the value fluctuated between 400 and 500 ppm, except for decreasing to 300 during the low-steam-flow, air-blown test period at hour 121.

Table 3.3-1

TC10 Operating Periods

Operating Period	Start Time	End Time	Duration Hours	Operating Period Average Time	Operating Period Relative Hours	Notes
TC10A-1	11/19/2002 7:15	11/19/2002 15:15	8:00	11/19/2002 11:15	22	(1)
TC10A-2	11/19/2002 20:00	11/20/2002 7:00	11:00	11/20/2002 1:30	37	
TC10A-3	11/21/2002 0:15	11/21/2002 6:30	6:15	11/21/2002 3:22	62	
TC10A-4a	11/21/2002 7:45	11/21/2002 14:00	6:15	11/21/2002 10:52	70	
TC10A-5	11/21/2002 18:30	11/22/2002 2:00	7:30	11/21/2002 22:15	81	
TC10A-6a	11/22/2002 14:00	11/22/2002 22:00	8:00	11/22/2002 18:00	92	
TC10A-6b	11/22/2002 22:00	11/23/2002 6:00	8:00	11/23/2002 2:00	100	
TC10A-6c	11/23/2002 6:00	11/23/2002 13:45	7:45	11/23/2002 9:52	108	
TC10A-7	11/24/2002 2:15	11/24/2002 6:15	4:00	11/24/2002 4:15	121	(1,2)
TC10A-8	11/25/2002 3:15	11/25/2002 7:15	4:00	11/25/2002 5:15	136	
TC10A-9	11/25/2002 16:30	11/25/2002 22:00	5:30	11/25/2002 19:15	150	
TC10B-1	12/7/2002 22:15	12/8/2002 5:00	6:45	12/8/2002 1:37	182	
TC10B-2a	12/8/2002 7:00	12/8/2002 15:00	8:00	12/8/2002 11:00	191	
TC10B-3b	12/9/2002 10:00	12/9/2002 14:45	4:45	12/9/2002 12:22	216	
TC10B-4a	12/10/2002 5:30	12/10/2002 14:30	9:00	12/10/2002 10:00	231	
TC10B-4b	12/10/2002 14:30	12/10/2002 23:00	8:30	12/10/2002 18:45	240	
TC10B-4c	12/10/2002 23:00	12/11/2002 8:00	9:00	12/11/2002 3:30	248	
TC10B-5	12/11/2002 23:15	12/12/2002 6:00	6:45	12/12/2002 2:37	272	
TC10B-7	12/13/2002 16:15	12/13/2002 23:45	7:30	12/13/2002 20:00	313	
TC10B-8	12/14/2002 2:00	12/14/2002 6:30	4:30	12/14/2002 4:15	321	
TC10B-9	12/14/2002 9:15	12/14/2002 13:15	4:00	12/14/2002 11:15	328	
TC10B-10	12/14/2002 15:45	12/14/2002 20:15	4:30	12/14/2002 18:00	335	

Notes:
1. TC10A-1 and TC10A-7 were air-blown. All others were oxygen-blown.
2. Small amount of coke breeze fed as fuel with coal.

Table 3.3-2

Operating Conditions

Operating Periods	Average Relative Hours	Mixing Zone Temperature TI350 °F	Pressure PI287 psig	PCD Inlet Temperature TI458 °F	Air Rate lb/hr	Oxygen Rate lb/hr	Synthesis Gas Rate lb/hr	Steam Rate[3] lb/hr	Nitrogen Rate[1] lb/hr
TC10A-1	22	1,691	180	772	12,489	0	23,920	1,000	7,610
TC10A-2	37	1,688	146	751	0	2,190	16,595	2,638	7,533
TC10A-3	62	1,720	146	753	0	2,070	14,928	2,043	6,578
TC10A-4a	70	1,756	146	756	0	2,302	14,835	1,698	6,389
TC10A-6a	92	1,751	152	705	0	2,305	15,052	1,739	6,834
TC10A-6b	100	1,754	152	706	0	2,283	14,451	1,764	7,022
TC10A-6c	108	1,751	152	704	0	2,341	14,648	1,921	7,043
TC10A-7	121	1,706	152	769	11,129	0	21,790	875	6,437
TC10A-8	136	1,736	152	758	0	2,457	16,389	2,781	6,386
TC10A-9	150	1,782	152	746	0	2,302	13,801	1,722	6,304
TC10B-1	182	1,735	150	728	0	2,207	13,643	1,738	6,660
TC10B-2a	191	1,716	150	721	0	2,318	14,371	1,610	6,957
TC10B-3b	216	1,728	150	727	0	2,419	14,340	1,556	6,563
TC10B-4a	231	1,723	160	730	0	2,236	14,258	1,435	7,053
TC10B-4b	240	1,737	160	719	0	2,205	14,081	1,627	6,849
TC10B-4c	248	1,747	160	712	0	2,156	13,846	1,666	6,858
TC10B-5	272	1,736	160	712	0	2,243	14,107	1,404	7,119
TC10B-7	313	1,749	158	721	0	2,325	14,993	1,706	6,998
TC10B-8	321	1,743	158	727	0	2,253	14,437	1,807	7,184
TC10B-9	328	1,730	158	732	0	2,166	14,808	1,723	7,158
TC10B-10	335	1,766	158	736	0	2,365	15,162	1,691	6,834

Notes:
1. Nitrogen feed rate reduced by 200 pounds per hour to account for losses in feed systems and seals.
2. TC10A-1 and TC10A-7 were air blown; all other operating periods were oxygen blown.
3. Steam rate by hydrogen balance.

Table 3.3-3

TC10 Gas Analyzer Choices

Operating Periods	Average Relative Hours	Gas Compound					
		CO	H_2	CO_2	CH_4	C_2^+	N_2
TC10A-1	22	AI425	AI464G	AI464D	None[2]	0.25[3]	AI464B
TC10A-2	37	AI425	AI464G	AI464D	AI464E	0.25	AI464B
TC10A-3	62	AI425	AI464G	AI464D	AI464E	0.25	AI464B
TC10A-4a	70	AI425	AI464G	AI464D	AI464E	0.25	AI464B
TC10A-6a	92	AI425	AI464G	AI464D	AI464E	0.25	AI464B
TC10A-6b	100	AI425	AI464G	AI464D	AI464E	0.25	AI464B
TC10A-6c	108	AI425	AI464G	AI464D	AI464E	0.25	AI464B
TC10A-7	121	AI425	AI464G	AI464D	AI464E	0.25	AI464B
TC10A-8	136	AI425	AI464G	AI464D	AI464E	0.25	AI464B
TC10A-9	150	AI425	AI464G	AI464D	AI464E	0.25	AI464B
TC10B-1	182	AI425	AI464G	AI464D	AI464E	0.25	AI464B
TC10B-2a	191	AI425	AI464G	AI464D	AI464E	0.25	AI464B
TC10B-3b	216	AI453	AI464G	AI464D	AI464E	0.25	AI464B
TC10B-4a	231	AI453	AI464G	AI464D	AI464E	0.25	AI464B
TC10B-4b	240	AI453	AI464G	AI464D	AI464E	0.25	AI464B
TC10B-4c	248	AI453	AI464G	AI464D	AI464E	0.25	AI464B
TC10B-5	272	AI453	AI464G	AI464D	AI464E	0.25	AI464B
TC10B-7	313	AI453	AI464G	AI464D	AI464E	0.25	AI464B
TC10B-8	321	AI425	AI464G	AI464D	AI464E	0.25	AI464B
TC10B-9	328	AI425	AI464G	AI464D	AI464E	0.25	AI464B
TC10B-10	335	AI425	AI464G	AI464D	AI464E	0.25	AI464B

Notes:

1. H_2O calculated from water gas shift equilibrium using TI368, and H_2, CO, and CO_2 data.
2. Neither CH_4 anlayzer operating during this oporating period.
3. C_2^+ assumed to be 0.25 when AI464E not reading properly.

Table 3.3-4

Gas Compositions, Molecular Weight, and Heating Value

Operating Period	Average Relative Hour	H_2O Mole %	CO Mole %	H_2 Mole %	CO_2 Mole %	CH_4 Mole %	C_2H_6 Mole %	N_2 Mole %	Total Mole %	Syngas LHV Btu/SCF	Syngas TRS[1] ppm	Syngas MW lb./Mole	O_2 in Feed %	Syngas CO/CO_2 Ratio
TC10A-1	22	8.9	6.4	5.3	8.9	1.4	0.23	68.8	100.0	52	317	27.0	11.9	0.7
TC10A-2	37	24.3	5.9	8.9	13.3	1.2	0.19	46.3	100.0	57	346	25.2	14.1	0.4
TC10A-3	62	21.4	8.4	10.4	13.7	1.8	0.20	44.1	100.0	76	401	25.1	15.7	0.6
TC10A-4a	70	18.2	12.3	12.0	14.0	2.6	0.21	40.6	100.0	100	521	25.0	18.2	0.9
TC10A-6a	92	18.7	11.1	11.2	14.0	2.3	0.21	42.6	100.0	91	489	25.2	17.4	0.8
TC10A-6b	100	19.0	11.0	11.3	14.0	2.5	0.21	42.0	100.0	92	466	25.1	17.0	0.8
TC10A-6c	108	19.9	10.7	11.3	14.1	2.5	0.20	41.3	100.0	92	480	25.0	17.0	0.8
TC10A-7	121	10.2	6.0	5.1	9.6	1.0	0.23	67.9	100.0	46	311	27.1	11.6	0.6
TC10A-8	136	24.1	8.9	11.3	14.6	2.6	0.19	38.3	100.0	87	512	24.7	15.7	0.6
TC10A-9	150	19.6	11.7	11.7	14.1	2.7	0.21	40.1	100.0	98	539	24.9	17.8	0.8
TC10B-1	182	20.8	9.9	11.0	14.5	2.1	0.20	41.5	100.0	84	459	25.1	17.1	0.7
TC10B-2a	191	18.8	10.0	10.6	14.1	2.2	0.21	44.2	100.0	85	460	25.4	17.2	0.7
TC10B-3b	216	18.2	10.8	10.9	14.0	2.5	0.21	43.5	100.0	91	540	25.3	18.7	0.8
TC10B-4a	231	17.2	8.8	9.4	12.6	2.0	0.21	49.8	100.0	76	478	25.6	17.0	0.7
TC10B-4b	240	19.1	9.1	9.9	13.5	2.3	0.21	45.9	100.0	81	505	25.4	16.7	0.7
TC10B-4c	248	19.0	9.6	10.3	13.3	2.6	0.21	45.0	100.0	86	495	25.2	16.6	0.7
TC10B-5	272	17.2	11.1	10.6	13.8	2.8	0.28	44.3	100.0	95	487	25.4	17.4	0.8
TC10B-7	313	18.4	10.0	10.4	13.4	2.5	0.21	45.1	100.0	87	427	25.3	16.7	0.7
TC10B-8	321	19.8	9.4	10.2	14.0	2.5	0.24	43.9	100.0	85	446	25.3	16.5	0.7
TC10B-9	328	19.2	7.8	8.9	13.1	1.9	0.22	48.8	100.0	71	388	25.6	15.1	0.6
TC10B-10	335	18.5	10.1	10.1	13.7	2.5	0.23	44.9	100.0	86	478	25.4	16.8	0.7

Notes:

1. Synthesis gas total reduced sulfur (TRS) estimated from Synthesis gas combustor SO_2 analyzer data.
2. TC10A-1 and TC10A-7 were air blown; all other operating periods were oxygen blown.

Table 3.3-5 Corrected[1] Gas Compositions, Molecular Weight, and Heating Value

Operating Period	Average Relative Hour	H_2O Mole %	CO Mole %	H_2 Mole %	CO_2 Mole %	CH_4 Mole %	C_2H_6 Mole %	N_2 Mole %	Total Mole %	Syngas LHV Btu/SCF	Syngas MW lb./Mole	O_2 in Feed %	Syngas CO/CO_2 Ratio
TC10A-1	22	14.4	13.2	11.0	12.3	2.9	0.5	45.8	100.0	106	25.3	17.2	1.1
TC10A-2	37	24.7	17.5	26.7	27.0	3.6	0.5	0.0	99.9	171	22.5	31.8	0.6
TC10A-3	62	20.7	22.0	27.1	25.0	4.8	0.5	0.0	99.9	198	22.3	36.3	0.9
TC10A-4a	70	17.8	27.2	26.5	22.2	5.8	0.5	0.0	100.0	221	22.2	43.3	1.2
TC10A-6a	92	18.6	26.1	26.2	23.2	5.4	0.5	0.0	100.0	214	22.4	42.7	1.1
TC10A-6b	100	18.9	25.7	26.2	23.0	5.7	0.5	0.0	100.0	215	22.3	42.2	1.1
TC10A-6c	108	19.9	24.6	26.0	23.3	5.7	0.5	0.0	100.0	211	22.3	40.7	1.1
TC10A-7	121	17.0	12.2	10.5	13.7	2.0	0.5	44.1	100.0	94	25.5	17.2	0.9
TC10A-8	136	24.7	19.7	25.0	24.4	5.8	0.5	0.0	100.0	192	22.2	33.2	0.8
TC10A-9	150	20.2	25.6	25.6	22.2	5.9	0.5	0.0	100.0	214	22.2	42.9	1.2
TC10B-1	182	22.4	22.9	25.4	24.1	4.8	0.5	0.0	100.0	195	22.5	41.7	0.9
TC10B-2a	191	20.4	24.1	25.6	24.0	5.4	0.5	0.0	100.0	206	22.5	44.8	1.0
TC10B-3b	216	19.9	25.1	25.5	23.1	5.9	0.5	0.0	100.0	212	22.4	46.7	1.1
TC10B-4a	231	18.6	25.1	27.0	23.0	5.7	0.5	0.0	99.9	217	22.1	46.7	1.1
TC10B-4b	240	20.5	23.5	25.6	23.8	6.1	0.5	0.0	99.9	210	22.4	43.3	1.0
TC10B-4c	248	19.3	24.3	26.2	23.1	6.7	0.5	0.0	99.9	220	22.2	42.2	1.1
TC10B-5	272	17.9	26.5	25.4	22.8	6.7	0.5	0.0	99.8	227	22.5	47.4	1.2
TC10B-7	313	19.0	25.2	26.0	23.2	6.1	0.5	0.0	99.9	217	22.3	43.4	1.1
TC10B-8	321	20.8	23.1	25.0	24.3	6.2	0.5	0.0	99.9	209	22.6	41.2	0.9
TC10B-9	328	20.3	22.6	25.8	25.2	5.5	0.5	0.0	99.8	204	22.6	41.4	0.9
TC10B-10	335	19.7	25.1	25.0	23.6	6.1	0.5	0.0	99.9	214	22.6	44.0	1.1

Notes:

1. Correction is to assume that only air nitrogen is in the synthesis gas and that the reactor is adiabatic
2. TC10A-1 and TC10A-7 were air blown; all other operating periods were oxygen blown.

Table 3.3-6

Water Gas-Shift Equilibrium Constant

In situ Start	In situ End	Average Run Time Hours	Operating Periods	Dry CO %	Dry H2 %	Dry CO2 %	In-situ H_2O %	Kp	WGS Eqm. Temp. F	Mixing Zone Temp. F	Mixing Zone Kp^2
11/19/2002 09:30	11/19/2002 13:18	22	TC11A-1	6.87	6.49	10.75	11.5	0.78	1,627	1,693	0.79
11/20/2002 09:30	11/20/2002 11:52	46	(1)	13.00	14.98	18.80	25.0	0.65	1,748	1,712	0.77
11/21/2002 09:30	11/21/2002 13:30	71	TC11A-4a	14.77	14.36	16.79	18.3	0.73	1,672	1,756	0.72
11/25/2002 11:00	11/25/2002 11:30	142	(1)	7.59	12.71	16.70	29.4	0.67	1,727	1,735	0.74
12/9/2002 09:45	12/9/2002 13:45	216	TC11B-3b	11.90	13.04	16.87	18.1	0.84	1,586	1,727	0.75
12/10/2002 10:35	12/10/2002 14:35	234	TC11B-4a	9.87	11.67	15.41	20.3	0.72	1,684	1,714	0.77
12/11/2002 12:10	12/11/2002 15:10	259	(1)	10.94	12.11	14.87	14.5	0.97	1,500	1,748	0.73
12/12/2002 12:00	12/12/2002 15:00	283	(1)	12.33	12.99	15.52	17.8	0.76	1,649	1,735	0.74
12/18/2002 10:35	12/18/2002 12:26	416	(1)	16.07	13.40	15.83	13.7	0.83	1,589	1,812	0.66

Notes:

1. Data not taken during operating period.
2. Equilibrium constant calculated at mixing zone temperature (TI350), with an -100ºF approach.

Table 3.3-7 Synthesis Gas Combustor Calculations

Operating Period	Average Relative Hour	AIT8775 SGC Exit O_2 M %	Calculated SGC Exit O_2 M %	AI476D SGC Exit CO_2[4] M %	Calculated SGC Exit CO_2 M %	AI476H SGC Exit H_2O M %	Calculated SGC Exit H2O M %	Gas Analyzer LHV Btu/SCF	Energy Balance LHV[1] Btu/SCF	Combustor SO_2 AI476N ppm	Syngas Total Reduced Sulfur[2] ppm	Thermo. Equlibrium H_2S ppm
TC10A-1	22	4.9	5.2	9.9	9.1	12.7	10.7	52	50	154	317	191
TC10A-2	37	4.1	4.6	10.2	11.0	22.9	20.1	57	55	174	346	560
TC10A-3	62	6.0	6.8	9.8	10.0	17.6	16.0	76	74	148	401	499
TC10A-4a	70	7.6	8.2	9.7	9.7	14.3	13.5	100	95	158	521	428
TC10A-6a	92	5.6	6.0	10.8	11.5	16.3	15.9	91	84	198	489	444
TC10A-6b	100	6.0	6.4	10.4	11.1	15.7	15.7	92	87	180	466	453
TC10A-6c	108	6.0	6.4	10.5	11.1	16.0	16.0	92	87	186	480	473
TC10A-7	121	6.1	6.7	9.0	8.3	11.2	10.7	46	40	113	311	212
TC10A-8	136	6.0	6.4	10.4	10.7	17.8	17.9	87	83	199	512	580
TC10A-9	150	5.5	5.8	11.0	11.8	16.3	16.5	98	92	215	539	482
TC10B-1	182	5.6	5.3	10.8	12.1	16.5	17.6	84	78	201	459	528
TC10B-2a	191	5.6	5.2	10.8	11.9	15.6	16.7	85	79	201	460	516
TC10B-3b	216	6.2	6.3	10.7	11.2	14.8	15.4	91	89	213	540	447
TC10B-4a	231	5.3	5.5	10.9	10.9	16.1	15.6	76	75	213	478	391
TC10B-4b	240	5.6	5.8	10.6	11.0	16.0	16.2	81	81	214	505	445
TC10B-4c	248	6.1	6.6	10.5	10.4	15.8	15.4	86	89	194	495	449
TC10B-5	272	6.2	6.2	10.5	11.2	14.8	15.0	95	89	190	487	413
TC10B-7	313	5.9	5.9	10.6	11.2	15.6	15.8	87	83	177	427	438
TC10B-8	321	5.8	5.8	10.6	11.3	16.0	16.6	85	82	187	446	480
TC10B-9	328	4.7	4.6	10.7	11.6	16.7	17.3	71	69	188	388	453
TC10B-10	335	5.8	5.8	10.5	11.4	15.3	15.8	86	83	199	478	444

Notes:

1. Energy LHV calcualted assuming the sythesis gas combustor heat loss was 1.5×10^6 Btu/hr.
2. Synthesis gas total reduced sulfur (TRS) estimated from synthesis gas combustor SO_2 analyzer data
3. TC10A-1 and TC10A-7 were air blown; all other operating periods were oxygen blown.
4. CO_2 Analyzer data adjusted by +2% to account for analyzer miscalibration.

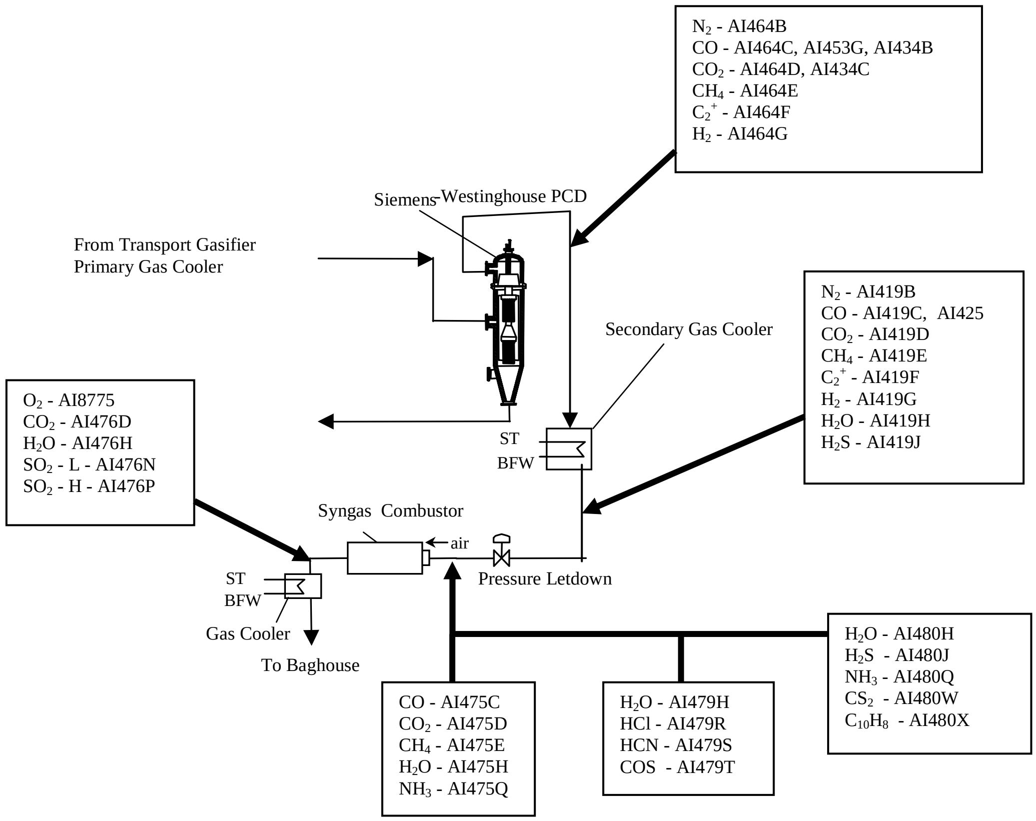

Figure 3.3-1 Gas Sampling Locations

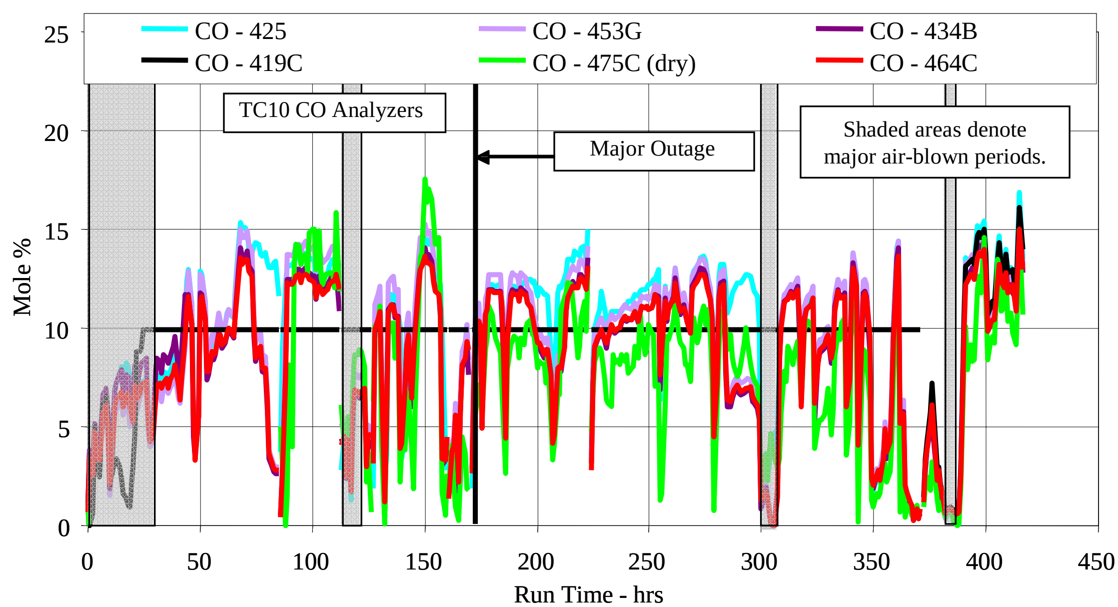

Figure 3.3-2 CO Analyzer Data

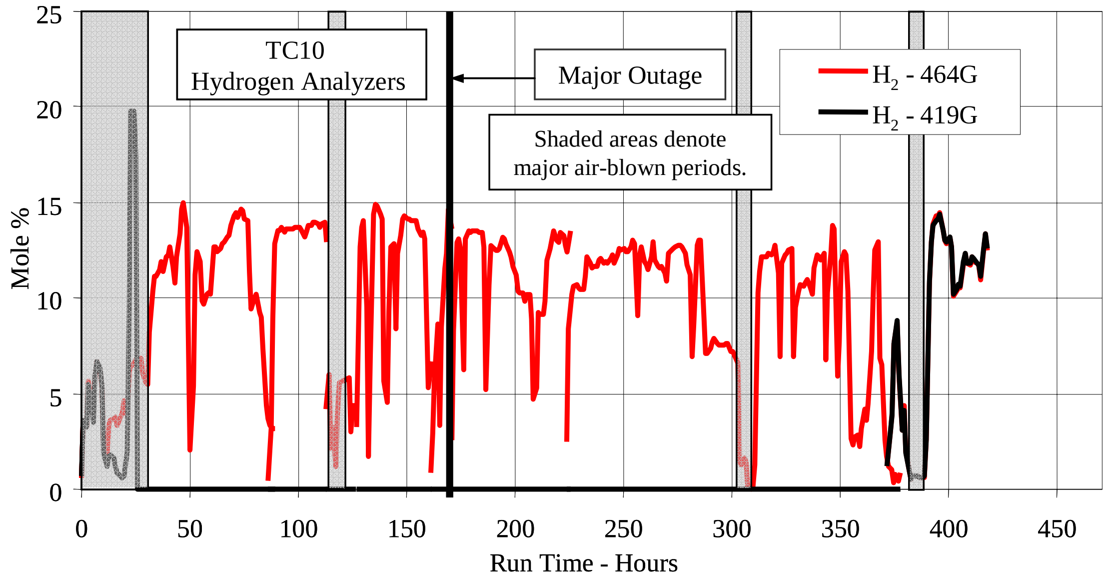

Figure 3.3-3 Hydrogen Analyzer Data

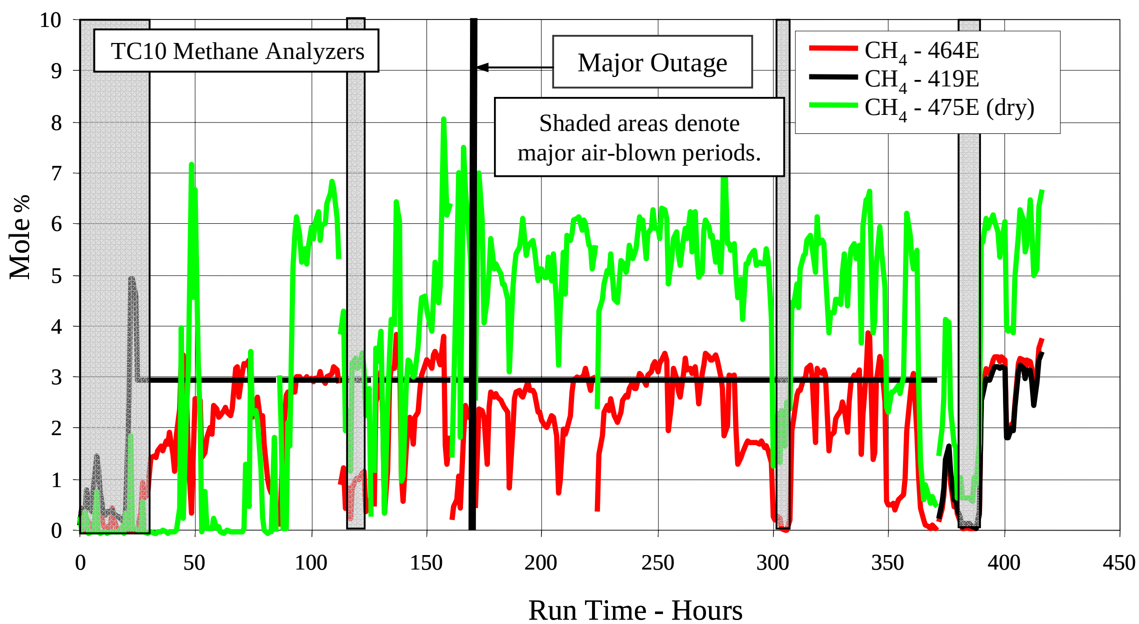

Figure 3.3-4 Methane Analyzer Data

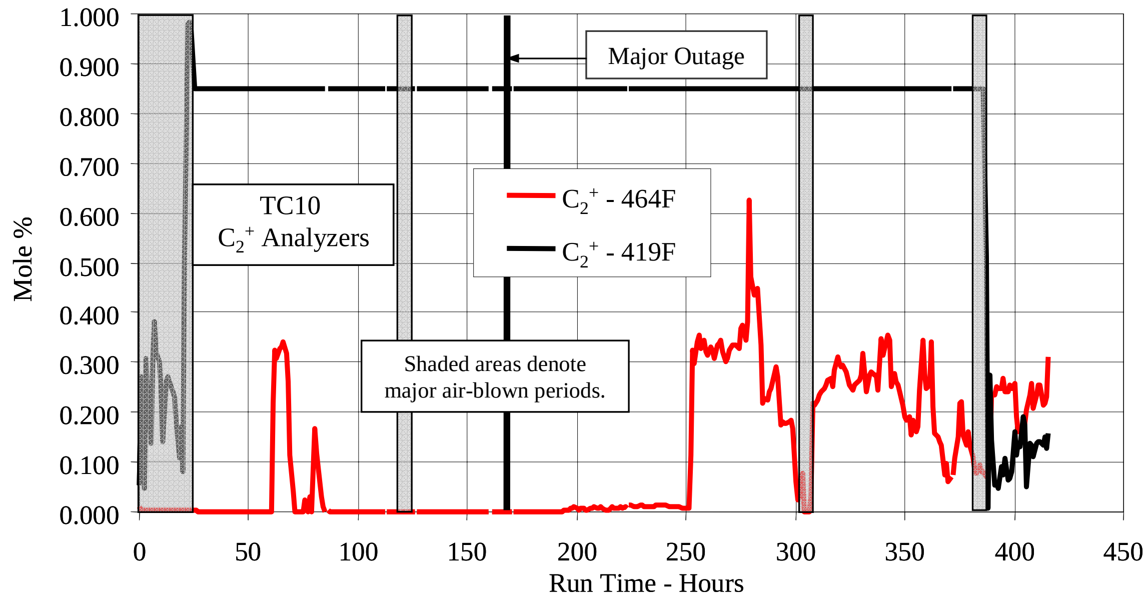

Figure 3.3-5 C_2^+ Analyzer Data

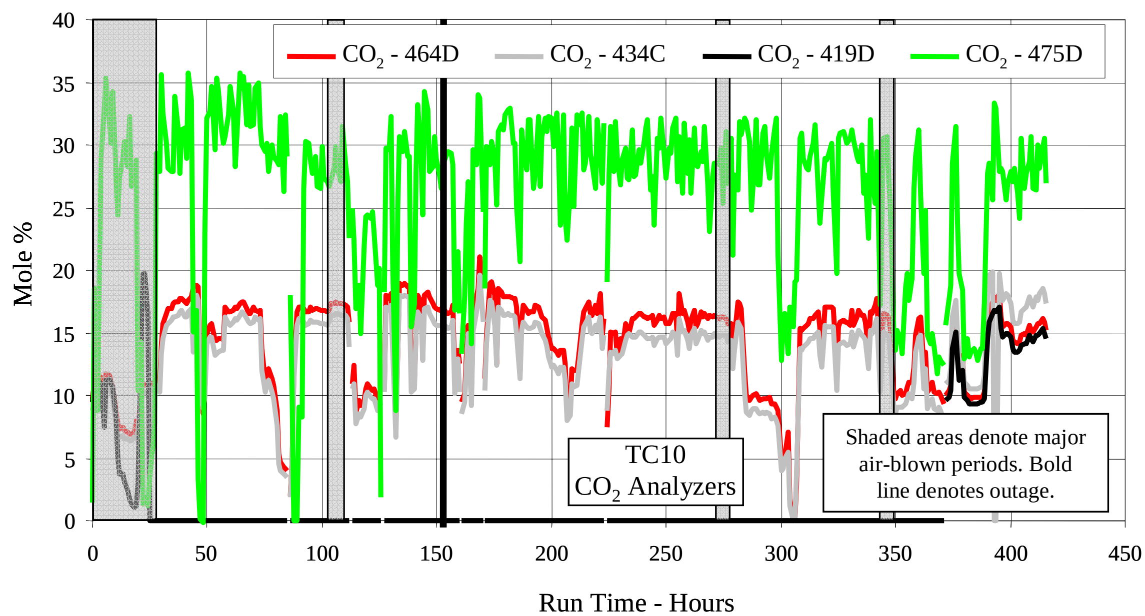

Figure 3.3-6 CO_2 Analyzer Data

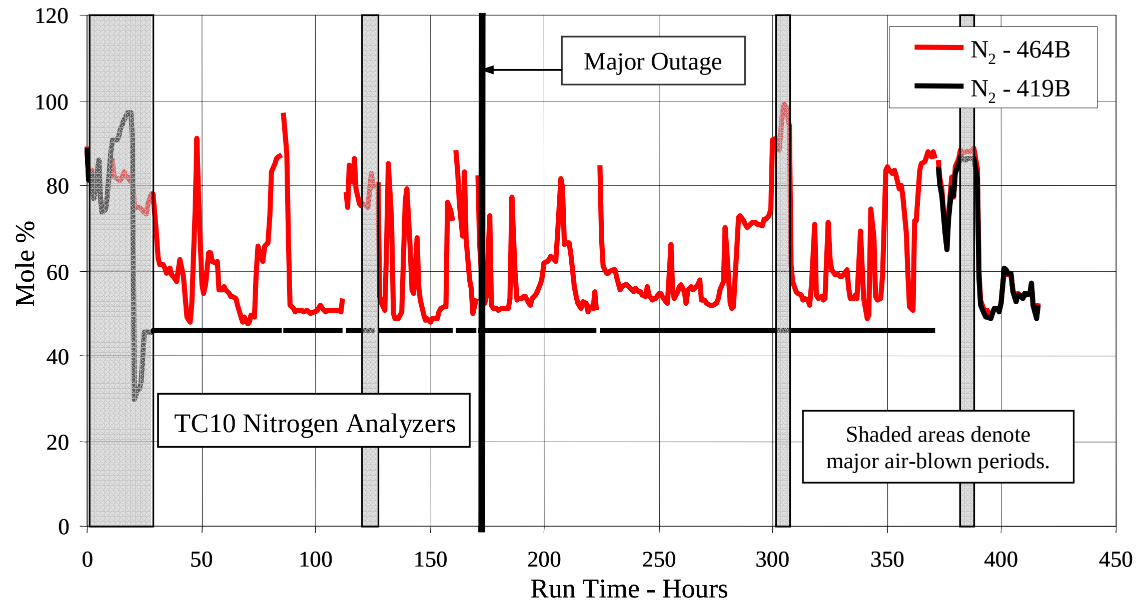

Figure 3.3-7 Nitrogen Analyzer Data

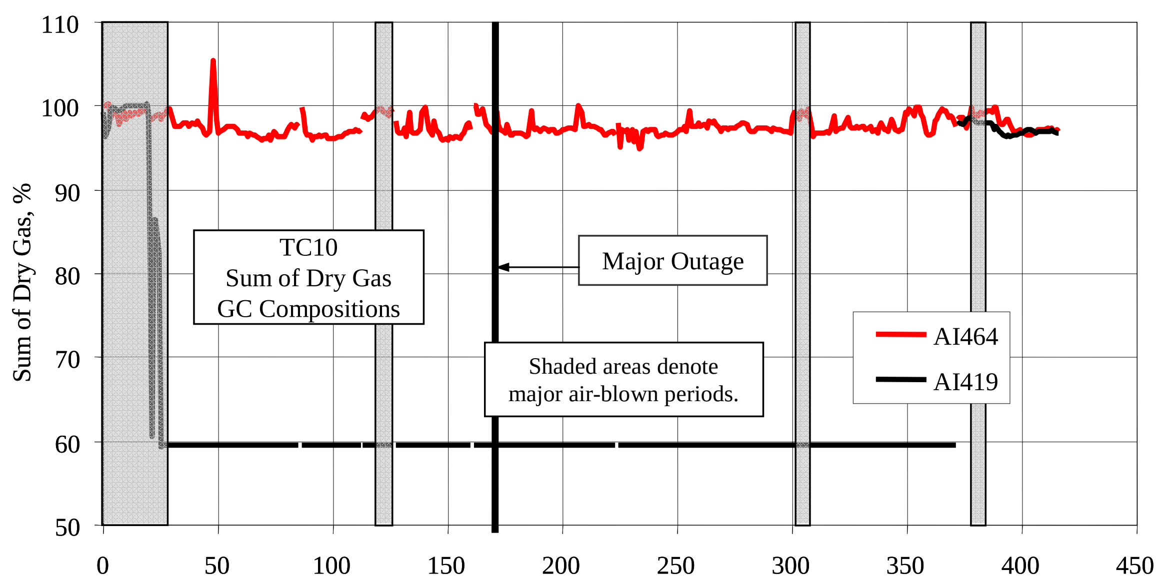

Figure 3.3-8 Sum of GC Gas Compositions (Dry)

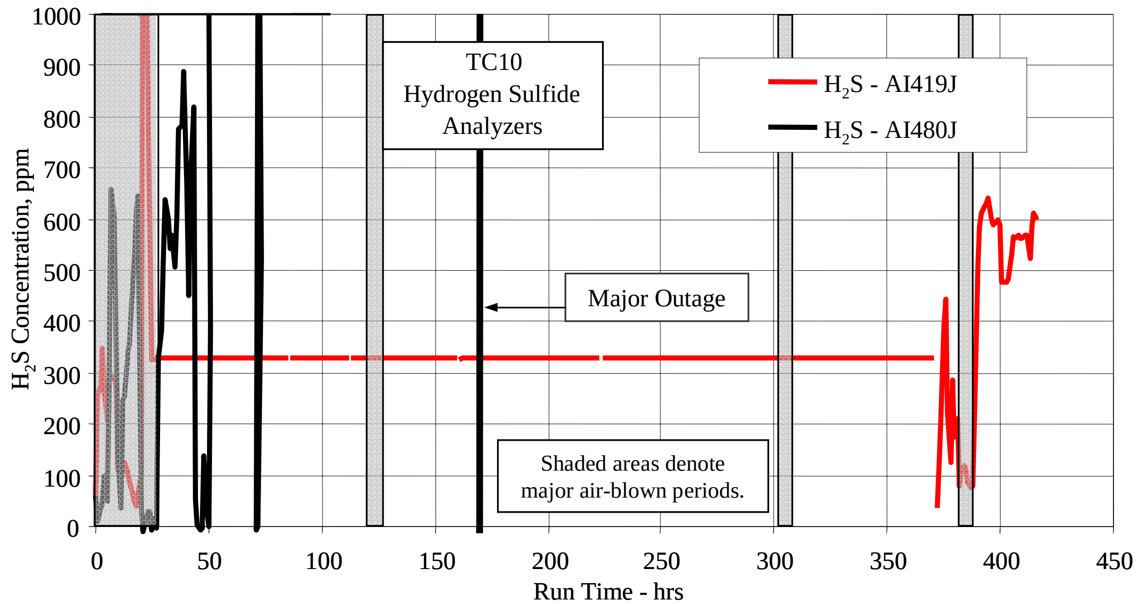

Figure 3.3-9 Hydrogen Sulfide Gas Analysis

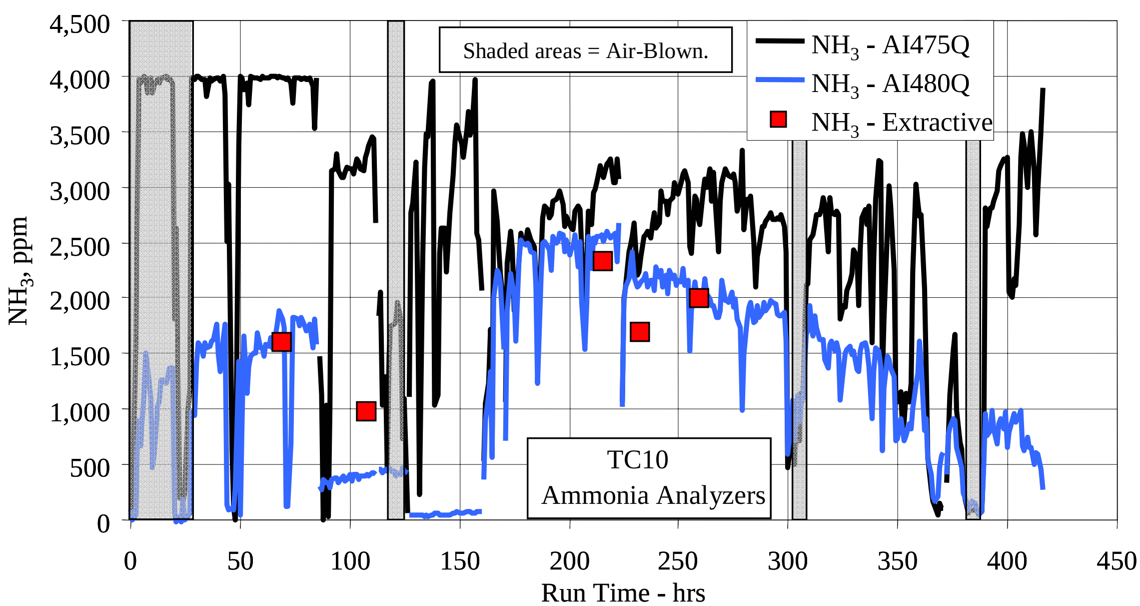

Figure 3.3-10 Ammonia Gas Analysis

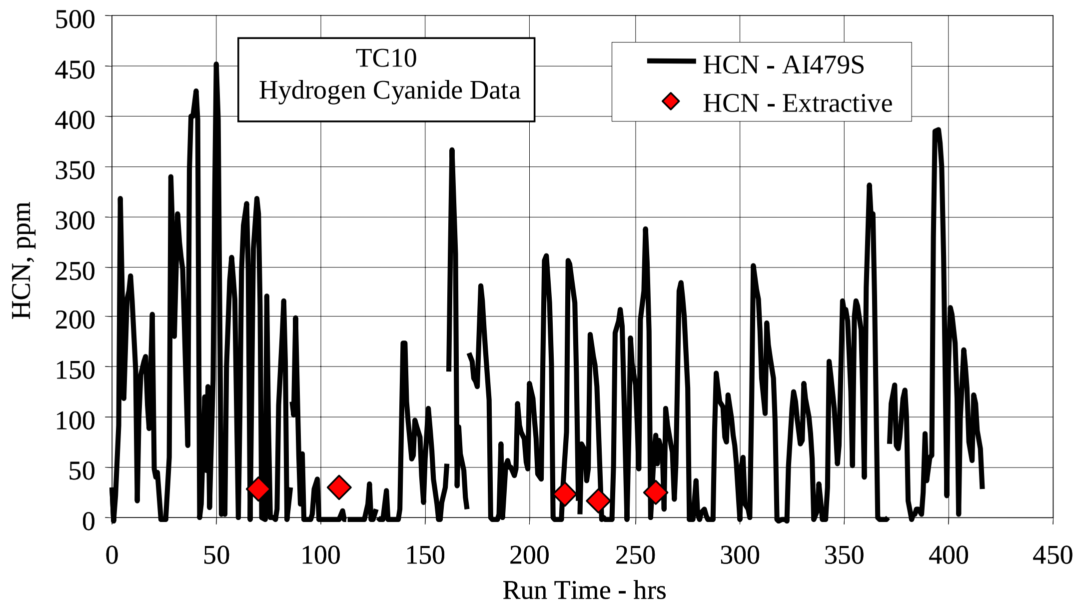

Figure 3.3-11 Hydrogen Cyanide Gas Analysis

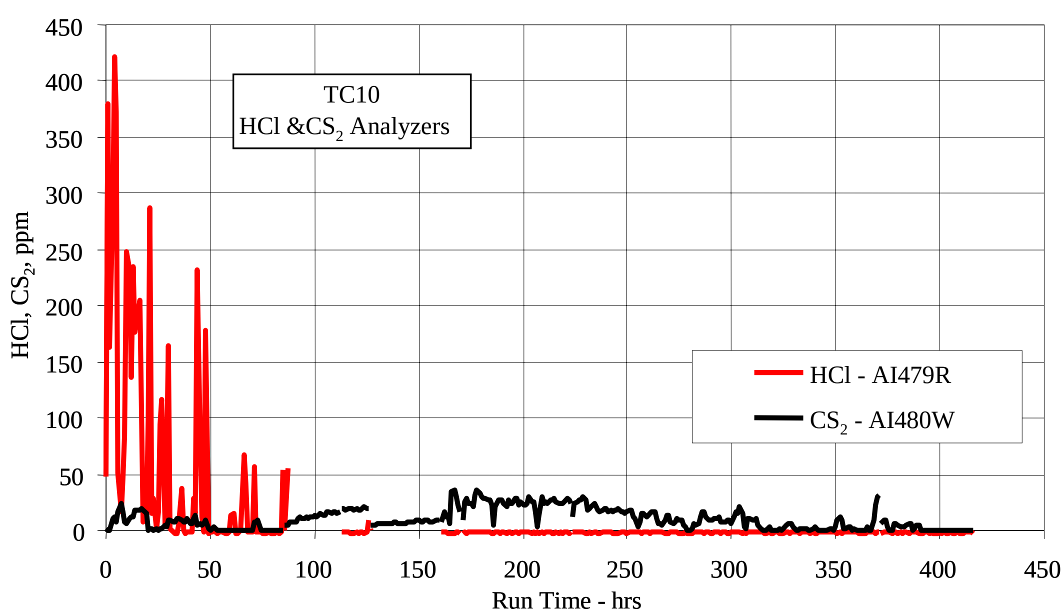

Figure 3.3-12 HCl and CS_2 Gas Analysis

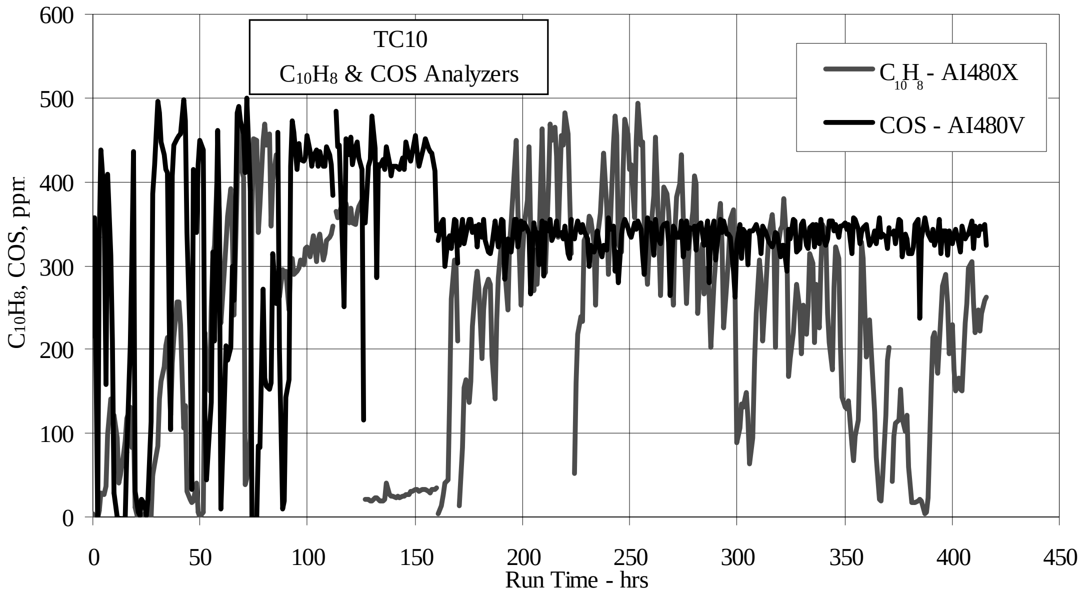

Figure 3.3-13 $C_{10}H_8$ and COS Gas Analysis

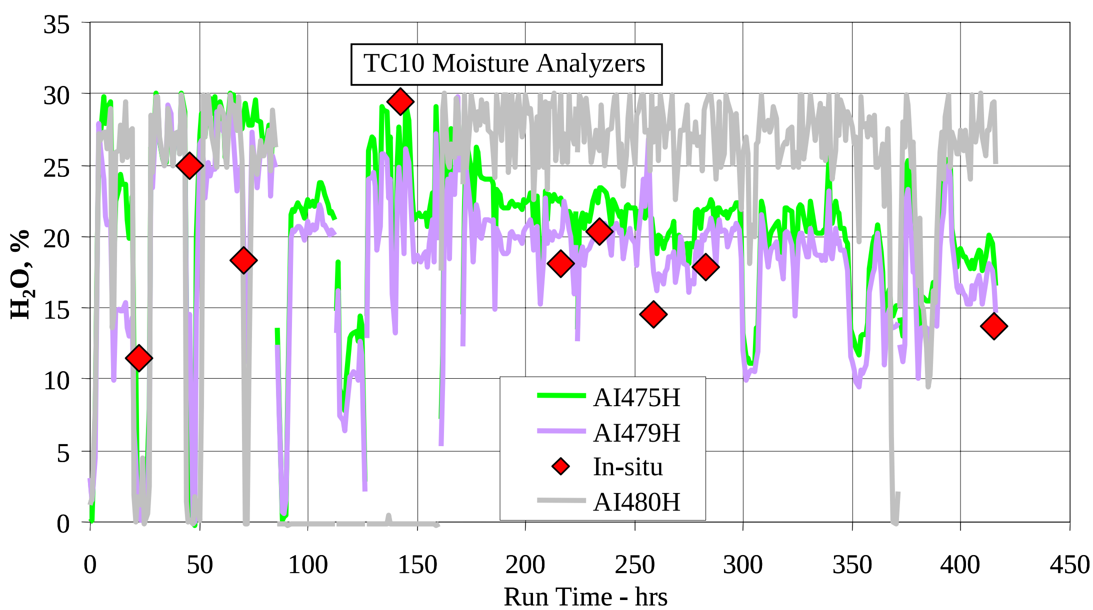

Figure 3.3-14 Moisture Gas Analysis

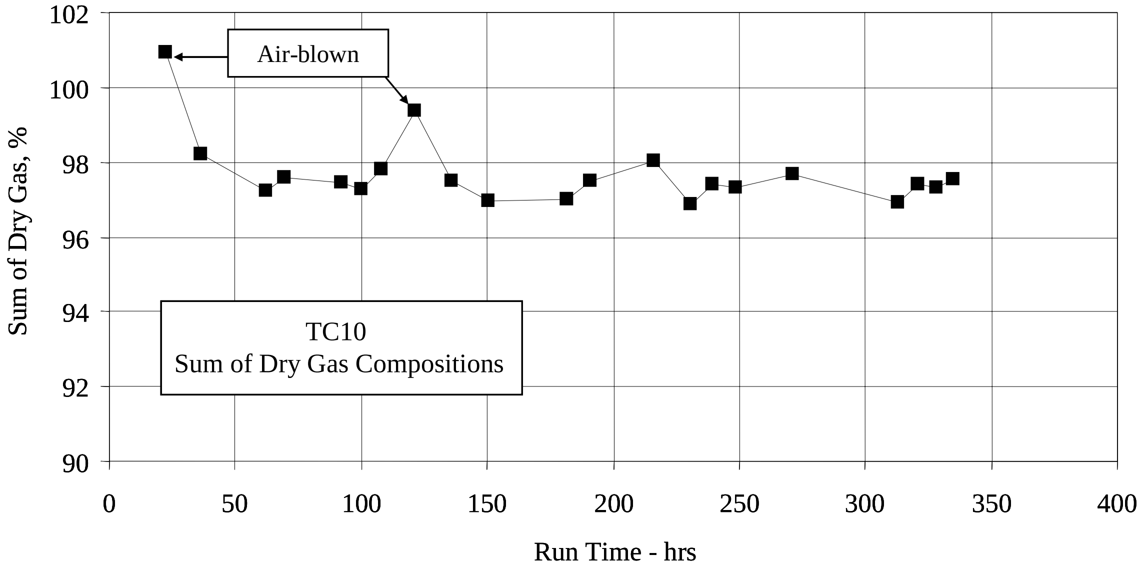

Figure 3.3-15 Sum of Dry Gas Compositions

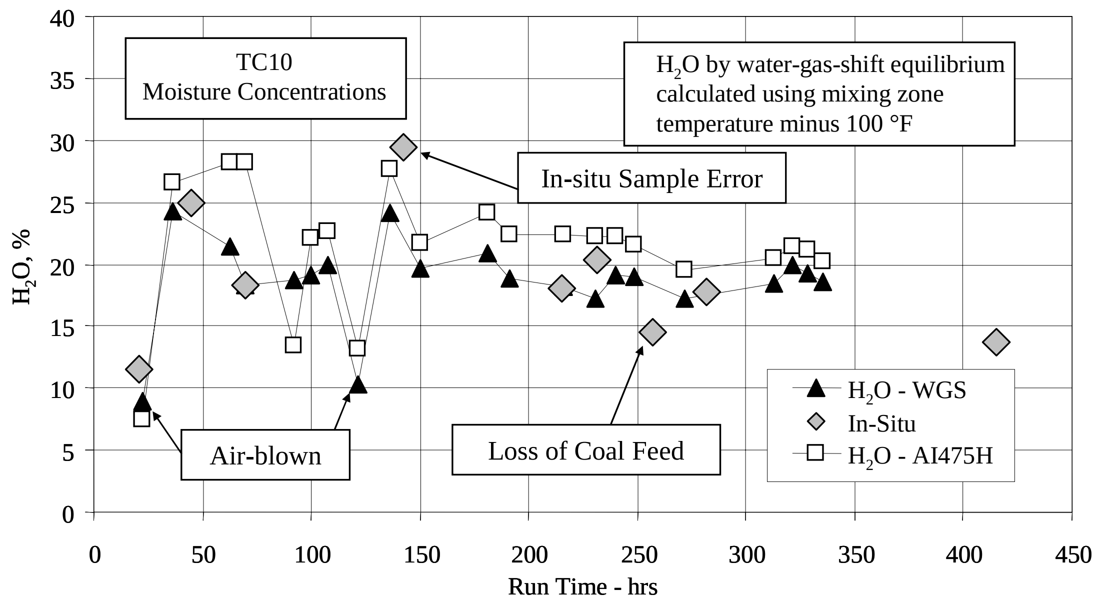

Figure 3.3-16 Comparison of Operating Period Moisture Data

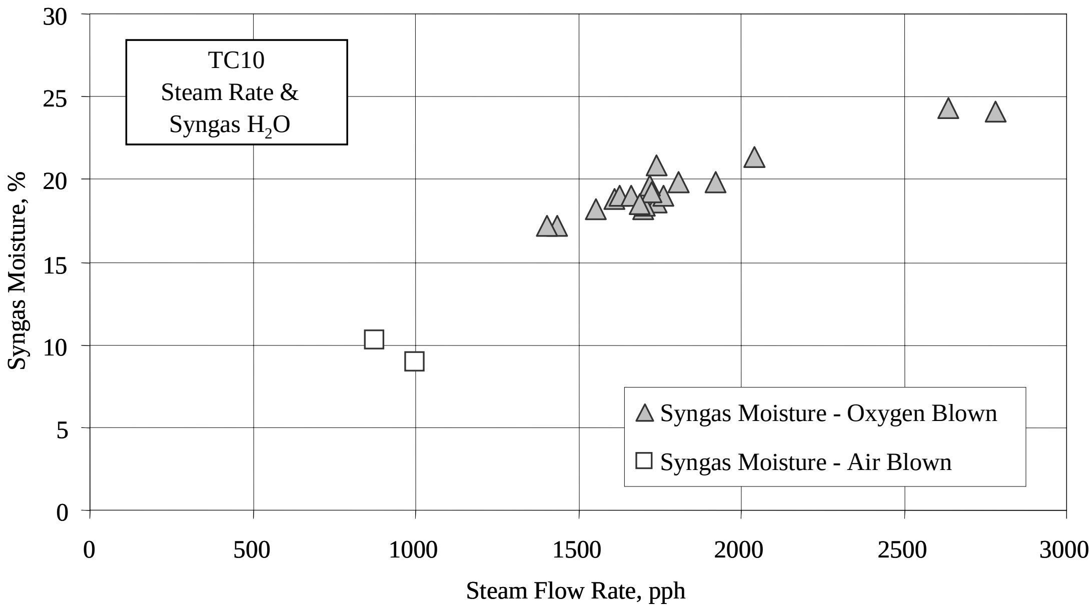

Figure 3.3-17 Comparison of Operating Period Moisture Data

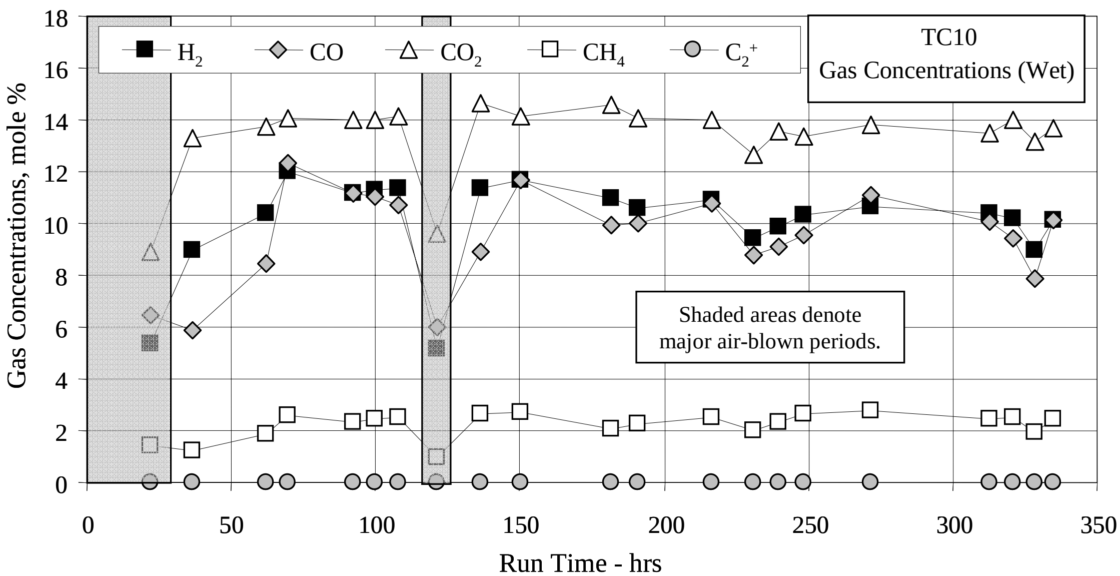

Figure 3.3-18 Wet Syngas Composition

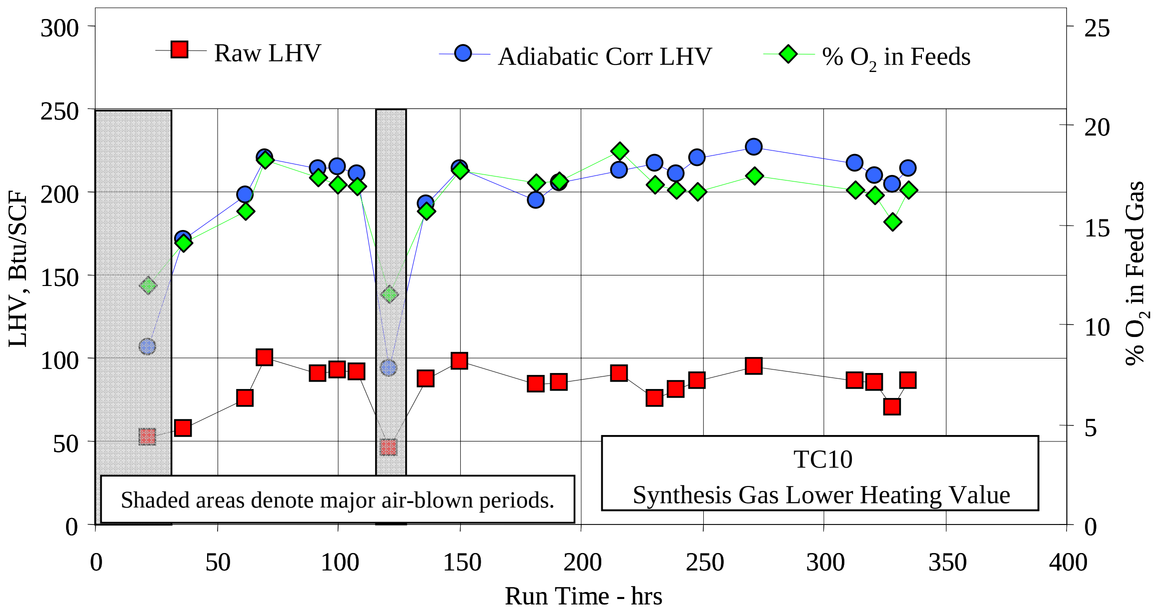

Figure 3.3-19 Synthesis Gas Lower Heating Values

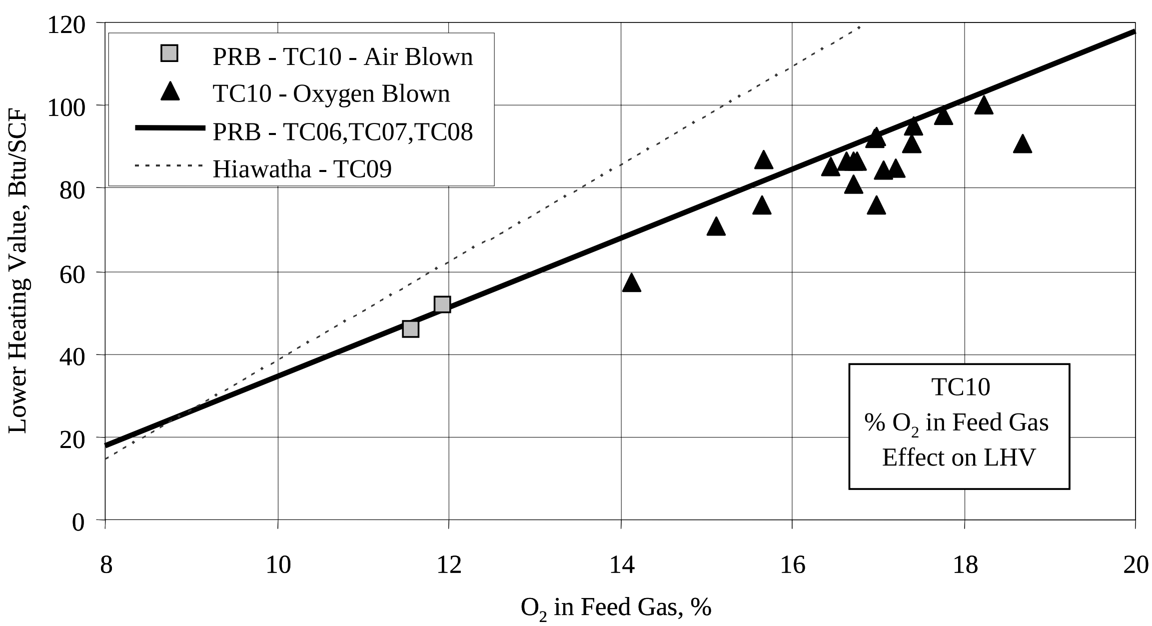

Figure 3.3-20 Raw Lower Heating Value and Overall Percent O_2

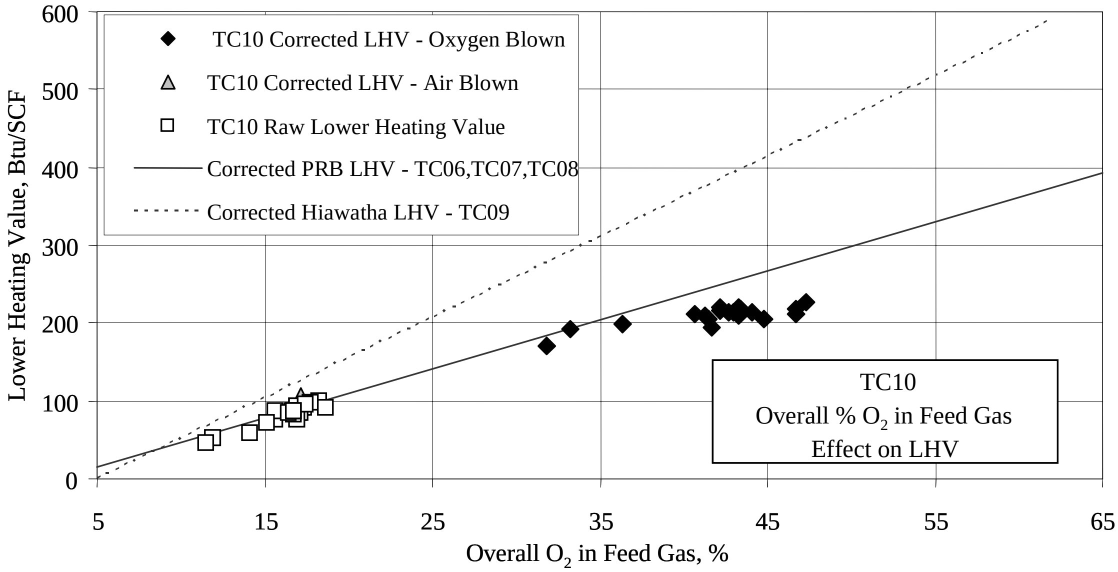

Figure 3.3-21 Corrected Lower Heating Value and Corrected Overall Percent O_2

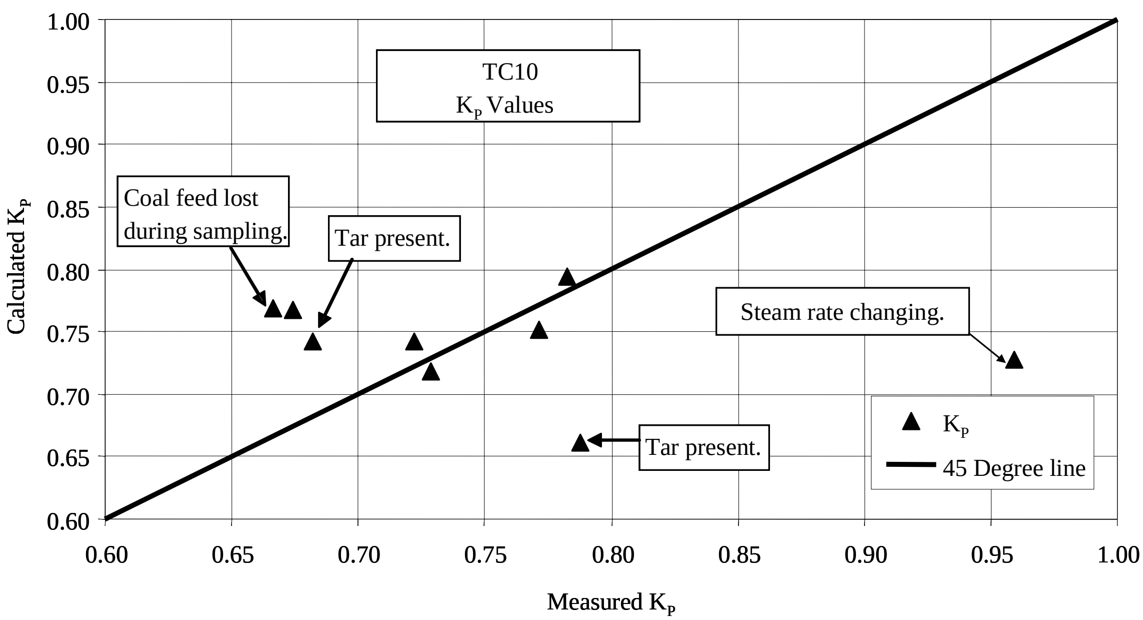

Figure 3.3-22 Water-Gas-Shift Constant

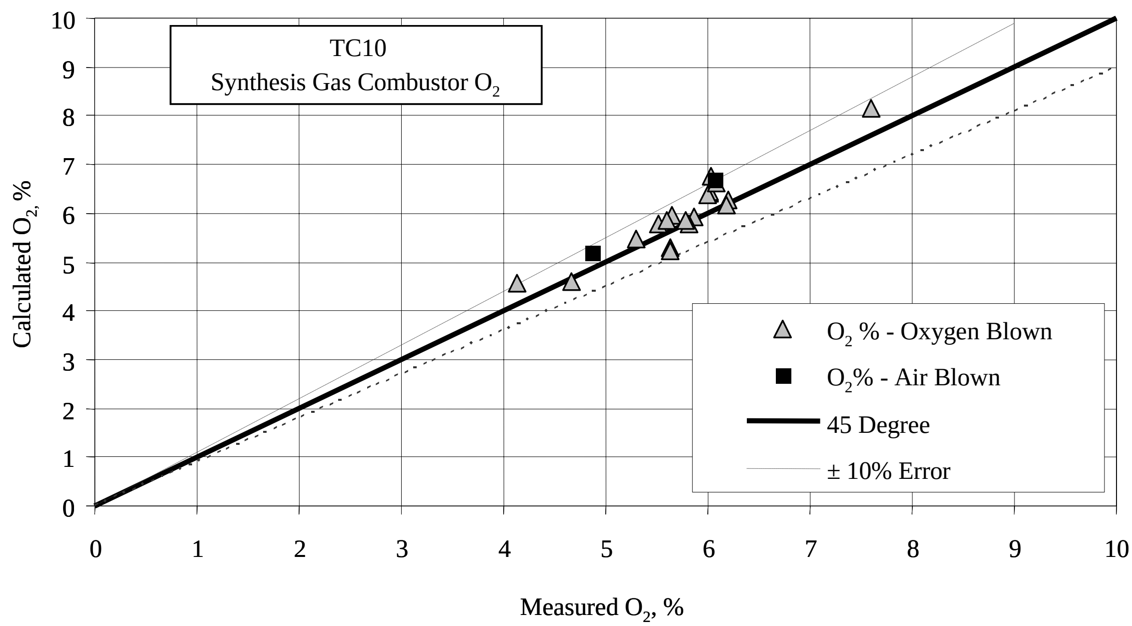

Figure 3.3-23 Synthesis Gas Combustor Outlet Oxygen

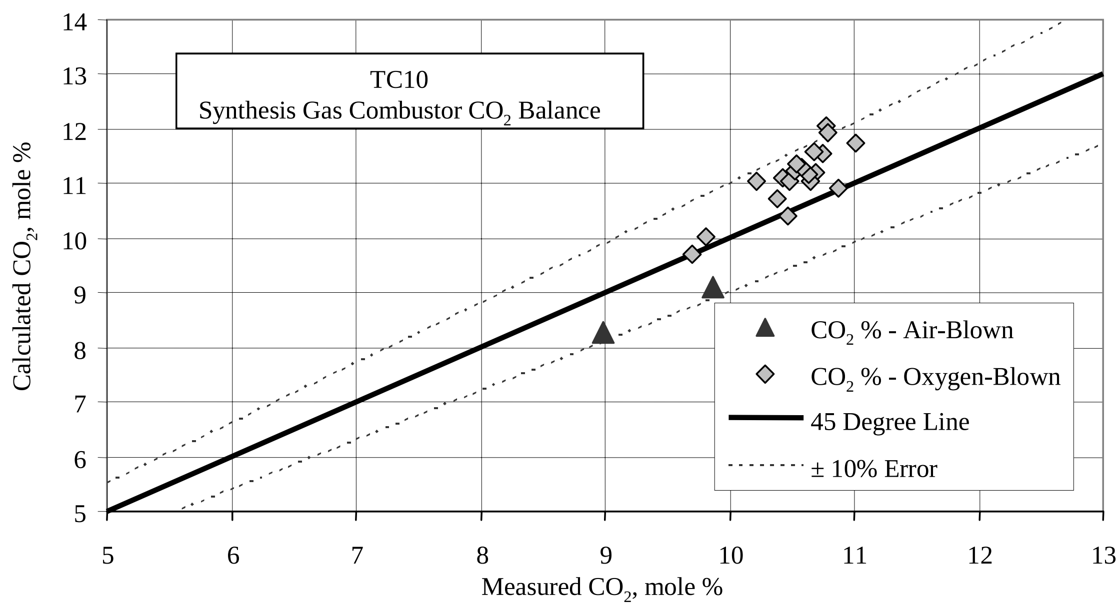

Figure 3.3-24 Synthesis Gas Combustor Outlet Carbon Dioxide

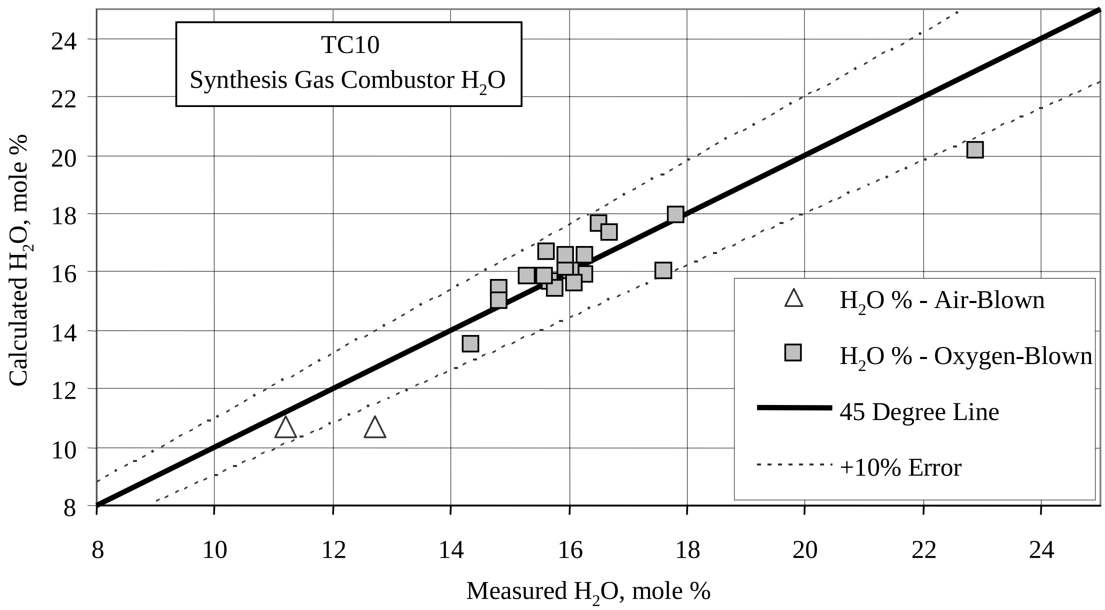

Figure 3.3-25   Synthesis Gas Combustor Outlet Moisture

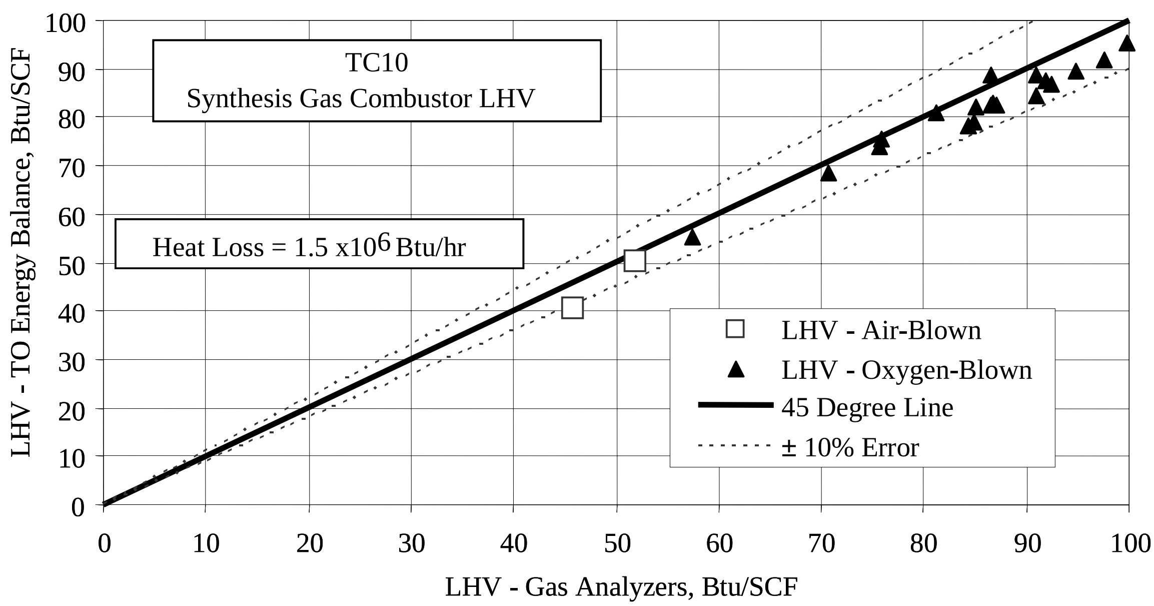

Figure 3.3-26   Synthesis Gas Combustor LHV

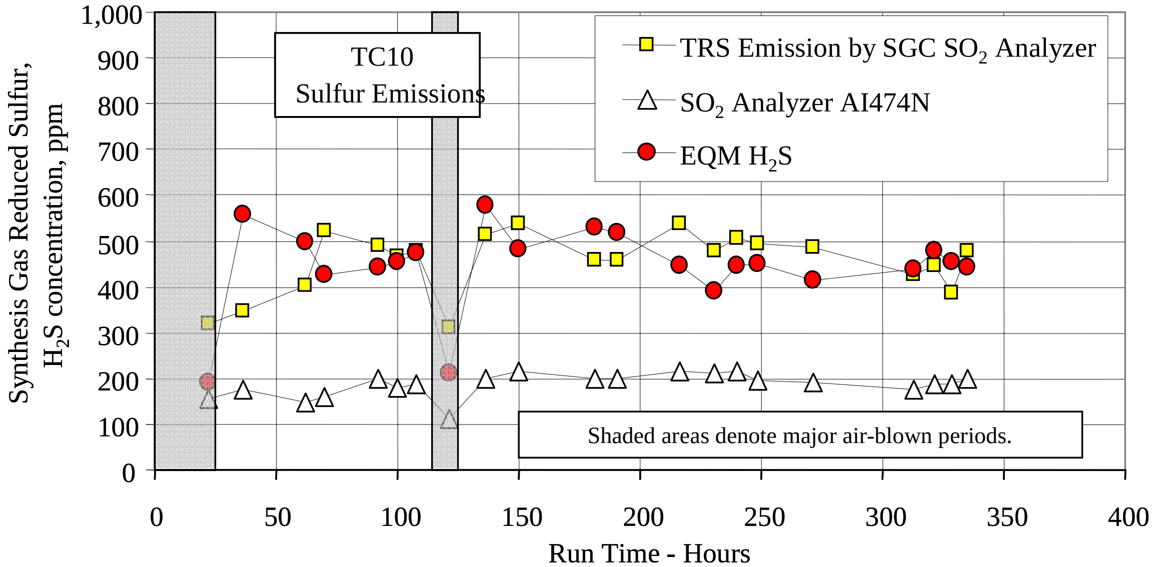

Figure 3.3-27 Sulfur Emissions

3.4 SOLIDS ANALYSES

3.4.1 Summary and Conclusions

- PRB coal composition was not constant during TC10 testing due to an increase in coal moisture that coincided with a decrease in heating value.
- For steady operating periods without coke breeze addition, the standpipe carbon content was between 0.1 and 0.4 weight percent.
- The standpipe solids did not completely reach a steady composition with respect to SiO_2, CaO, Al_2O_3, and MgO in TC10.
- The standpipe solids contained a negligible amount of CaS.
- The PCD fines sulfur, the cyclone dipleg sulfur, and the standpipe solids sulfur content indicate very little overall Transport Gasifier sulfur capture.
- The cyclone dipleg solids contained a higher amount of SiO_2 than the PCD solids, but a lower amount than the standpipe solids.
- The cyclone dipleg carbon content varied widely from 0 to 40 weight percent, but always possessed a value between that of the standpipe solids and that of the PCD solids.
- In situ PCD inlet solids samples generally had higher carbon and lower SiO_2 than the solids sampled from FD0520.
- The use of coke breeze seemed to increase the carbon content of the PCD fines.
- The PCD fines calcium was typically 80 to 90 percent calcined.
- A lack of sorbent feed produced lower calcium concentrations in the standpipe solids and the PCD fines than in previous PRB testing.
- The coal feed particle size was constant at the beginning of the test run, at about 300 μ (mass mean diameter, D_{50}). At the end of the test run, the removal of the screen in the coal mill increased the particle size to over 500 μ (D_{50}).
- The coal fed had large amounts of fines towards the end of the test run.
- The standpipe solids particle size increased during testing.
- As the test run progressed, the standpipe solids bulk density decreased from around 90 to 80 lb/ft^3, increasing again as sand was added.
- During TC10, the standpipe solids particle size was higher than the standpipe solids particle sizes measured in previous test runs that included sorbent addition.
- The cyclone dipleg solids bulk density fluctuated between 30 and 90 lb/ft^3 during TC10.

- During TC10, the particle size of the cyclone dipleg solids was between 20 and 150 μ SMD.
- The PCD solids particle size was between 6 to 18 μ SMD during most of the test run.
- The PCD solids bulk density fluctuated between 16 and 40 lb/ft^3.

3.4.2 Introduction

During TC10, solid samples were collected from the fuel feed system (FD0210), the sorbent feed system (FD0220), the Transport Gasifier standpipe, the Transport Gasifier cyclone dipleg, and the PCD fine solids transport system (FD0520). In situ solids samples were also collected from the PCD inlet. The sample locations are shown in Figure 3.4-1. These solids were analyzed for chemical composition and particle size. During TC10, coke breeze and sand were added through FD0220. Sorbent was not added through FD0220 during TC10.

3.4.3 Feeds Analysis

Table 3.4-1 gives the average coal composition for the samples analyzed during TC10. The coal carbon and moisture contents as sampled from FD0210 are shown in Figure 3.4-2. The average PRB coal carbon was 53.7-weight percent and the average PRB moisture was 22.6-weight percent. All averages excluded the first sample which possessed very different characteristics than the others. Note the increase in coal moisture between the start of TC10 and hour 140.

Figure 3.4-3 shows the fuel sulfur and ash as sampled from the fuel feed system during TC10. The average values are given on Table 3.4-1; the PRB coal average sulfur was 0.28 percent and the average ash was 5.92 percent. The first three coal samples had high (above 0.30 percent) sulfur content.

The coal HHV and LHV are given on Figure 3.4-4 with the TC10 average values given on Table 3.4-1. The LHV was determined from the HHV by reducing the heating value to account for the coal moisture and hydrogen. The low moisture in the coal during the first samples after startup caused the LHV and HHV to be higher than the averages. The average HHV was 9,088 Btu/lb and the average LHV was 8,528 Btu/lb. The HHV and LHV of the first sample were excluded from the average HHV and LHV.

Average values for TC10 coal moisture, carbon, hydrogen, nitrogen, sulfur, ash, oxygen, volatiles, fixed carbon, higher heating value, lower heating value, CaO, SiO_2, Al_2O_3, Fe_2O_3, and MgO are given in Table 3.4-1. Also given on Table 3.4-1 are the molar ratios for coal calcium to sulfur (Ca/S) and coal iron to sulfur (Fe/S). PRB has sufficient alkalinity in the ash to remove all of the coal sulfur.

3.4.4 Gasifier Solids Analysis

The chemical compositions of the solid compounds produced by the Transport Gasifier were determined using the solids chemical analysis and the following assumptions:

1. All carbon dioxide measured came from $CaCO_3$, hence moles CO_2 measured = moles $CaCO_3$.
2. All sulfide sulfur measured came from CaS.
3. All calcium not taken by CaS and $CaCO_3$ came from CaO.
4. All magnesium came from MgO.
5. Total carbon is measured, which is the sum of organic and inorganic (CO_2) carbon. The organic carbon is the total carbon minus the inorganic carbon (CO_2).
6. All iron reported as Fe_2O_3 is assumed to be present in the gasifier and PCD solids as FeO.
7. Inerts are the sum of the P_2O_5, K_2O, Na_2O, and TiO_2 concentrations.

It will be assumed that all iron in the standpipe, the cyclone dipleg, and the PCD solids is in the form of FeO and not in the form of Fe_3O_4 or Fe_2O_3. Thermodynamically, the mild reducing conditions in the Transport Gasifier should reduce all Fe_2O_3 to FeO. The assumption of iron as FeO seemed to give solids compositions totals that add up to around 100 percent.

It will also be assumed that no FeS is formed in the Transport Gasifier and that all the sulfur in the standpipe, cyclone dipleg, and PCD fines solids is present as CaS. It is thermodynamically possible that some FeS is formed. Most of the captured sulfur should be in the form of CaS due to the larger amount of calcium than iron in the system.

Table 3.4-2 gives the results from the standpipe analyses. Notes indicate standpipe solids that were sampled before the start of steady period coal feed or between periods of coal feed. The standpipe solids are solids that recirculate through the mixing zone, riser, and standpipe and change slowly with time, since a small amount of solids are taken out of the standpipe via FD0510. FD0510 was operated intermittently during TC10 to control the standpipe level. The flow rates for FD0510 and FD0520 solids during the stable operating periods will be given in Section 3.5.

On startup, the standpipe solids were mainly composed of sand containing 96.7-percent SiO_2. The standpipe did not contain pure sand at zero hours since there were several periods of coal and coke breeze operation prior to the starting of the clock for the test, which diluted the standpipe sand.

As the run progressed, the start-up sand was slowly replaced by CaO, Al_2O_3, Fe_2O_3, and other inerts. This is shown in Figure 3.4-5, which plots SiO_2, CaO, and Al_2O_3 and run time. The SiO_2 content slowly decreased and both the Al_2O_3 and the CaO increased to replace the SiO_2. There were several sand additions to the gasifier during TC10. The TC10 sand additions increased the standpipe SiO_2 as shown in the samples taken at hours 94, 184, and 369. The gasifier tripped several times during TC10 and some of the standpipe solids were lost and had to be replaced by sand. The standpipe solids SiO_2, Al_2O_3, and CaO compositions never seemed to reach steady conditions, although the values were leveled out for the standpipe samples taken just prior to the sand addition prior to the sample taken at hour 369.

The standpipe solids data in Table 3.4-2 shows that none of the volatile elements (sulfur and carbon) were present in high concentrations after the unit was in operation for a few days. The organic carbon, also shown in Figure 3.4-6, was generally 0.2 percent or less, with the exception of two samples that contained an organic carbon content of around 2 percent. The high carbon content of sample AB12056 occurred while feeding coke breeze only, and sample AB12054 occurred during a period of unstable standpipe operation. One period of coal feed with a small amount of coke breeze feed only produced a slightly higher standpipe carbon content, since hour 121 had coal and coke breeze feed, and the standpipe carbon only rose to 0.4 percent. The organic carbon content in TC10 was similar to the contents seen in other PRB test runs and lower than the organic carbon contents seen in the TC09 Hiawatha coal test run.

The standpipe $CaCO_3$ was at very low levels, less than 0.1 percent, indicating that there was very little inorganic carbon in the gasifier. Since there were much higher levels of CaO than $CaCO_3$, all calcium that circulated in the standpipe was nearly completely calcined. Since there was no sorbent calcium, all the standpipe solids calcium came from the fuel calcium.

The sulfur level in the solids was very low, less than the detectable limit for all of the samples taken during coal feed, indicating that all of the sulfur removed from the synthesis gas leaves the system via the PCD solids and does not accumulate in the gasifier or leave with the gasifier solids. The MgO, Fe_2O_3, and other inert compounds contents are not plotted on Figure 3.4-5, but they follow the same trends as the CaO and Al_2O_3, that is, they accumulate in the gasifier as the feed solids replace the start-up sand.

Table 3.4-3 gives the cyclone dipleg solids chemical analysis data. The cyclone dipleg solids consist of the particles that escape the disengager, but not the primary cyclone. Thus, their chemical and physical characteristics are usually between those of the standpipe solids and the PCD fines.

The cyclone dipleg CaO, SiO_2, and Al_2O_3 compositions are shown in Figure 3.4-7. The CaO and Al_2O_3 compositions were relatively constant at around 3- to 5-weight percent each, with a major exception at hour 265. The SiO_2 content ranged from 65- to 90-weight percent, and it tended to decline as the test run progressed. At hour 265, the SiO_2 content dropped to 42-weight percent. A corresponding increase in carbon content, as shown in Figure 3.4-8, accompanied the drop in SiO_2 content. The increase in carbon content occurred at a time of standpipe instability when material was emptied from the gasifier to the PCD, perhaps affecting the properties of the material in the standpipe. Other than the sample at hour 265, when the carbon content soared to 38-weight percent, Figure 3.4-8 illustrates that the carbon content varied over a moderate range from less than 1 to greater than 20-weight percent throughout the test run.

3.4.5 Gasifier Products Solids Analysis

Figure 3.4-9 plots the organic carbon (total carbon minus CO_2 carbon) for the PCD solids sampled from FD0520. The organic carbon content for every PCD fines sample analyzed is given on Table 3.4-4. Since FD0520 ran continuously during TC10, solid samples were taken often, with a goal of one sample every 4 hours. Only a fraction (coinciding with the steady operating periods) of the TC10 PCD solids that were sampled were analyzed. Since no steady operating periods occurred after hour 350, PCD samples were not analyzed after hour 350. Solids recovered in situ during the PCD inlet particulate sampling were also analyzed. The in situ carbon contents are compared with the FD0520 solids on Figure 3.4-9. The in situ solids organic carbon analyses compared reasonably well with the FD0520 solids for 7 of the 10 in situ solid samples. Two of the in situ samples did not have a corresponding sample from FD0520, and the remaining sample read abnormally high due to a coal feeder trip during the sampling period. The in situ analyses generally indicated a lower carbon conversion (higher carbon content) than the FD0520 analyses. Some of the data early in the test run seem to indicate that additional carbon conversion takes place between the PCD inlet and the solids sampled at FD0520. This phenomenon seems very unlikely, however, due to the temperature and the residence time available for carbon conversion between the in situ sampling point and the FD0520 sampling point.

The two FD0520 samples taken at hours 121 and 139 were taken at unstable operating conditions due to intermittent coal feed accompanied by coke breeze feed. The sample taken at hour 110 seems to be an anomaly. Higher organic carbon is also present in samples taken during the coke breeze feed from hours 222 and 306 (oxygen-blown testing).

The organic carbon started the run at 22 percent, and then decreased down to 17 percent at hour 39. The organic carbon then increased to 38 percent before coal feeder difficulties made steady operation infrequent, resulting in fluctuating carbon content until the outage at hour 160. After the outage, the organic carbon content remained between 29 and 40 percent for most of the remainder of the TC10.

Figure 3.4-10 and Table 3.4-4 give the amounts of SiO_2 and CaO in the PCD solids as sampled from FD0520. Also plotted on Figure 3.4-10 are the in situ solids concentrations for SiO_2 and CaO. The 10 in situ CaO concentrations showed very good agreement with the FD0520 solids CaO concentrations. The CaO concentrations were constant at around 10 percent during TC10. The CaO concentrations in TC10 FD0520 solids were similar to those seen in TC08 and about one-half of the concentrations in test runs TC06 and TC07 that featured sorbent feed to the gasifier. The TC09 CaO composition was slightly lower due to the lack of sorbent addition and less calcium in the entering coal.

At the beginning of the test run, the SiO_2 in situ analyses indicated a value 10 to 20 percent lower than the FD0520 solids analyses. As the run progressed, the two values began to compare well, except for the in situ sample taken at hour 257 when the coal feeder tripped. Previous test runs have indicated periods of good agreement and periods of poor agreement between in situ and FD0520 SiO_2 analyses.

The SiO_2 concentrations decreased from 50 to 30 percent during the early part of TC10 (up to hour 83). Then, the SiO_2 composition fluctuated over the next few samples, since gasifier conditions were unstable due to wet coal frequently plugging the coal feeder. After the deposit-induced outage at hour 160, the oxygen-blown SiO_2 slowly climbed from 33 to 44 percent over a period of roughly 120 hours. Due to the lack of unsteady gasifier operating conditions, no more FD0520 samples were analyzed. The in situ samples taken at hours 393 and 417, however, seemed to indicate that the SiO_2 content steadied out at the end of TC10.

Figure 3.4-11 and Table 3.4-4 give the amounts of $CaCO_3$ and CaS in the PCD solids as sampled from FD0520. Also plotted on Figure 3.4-11 are the in situ solids concentrations for $CaCO_3$ and CaS. The in situ sample $CaCO_3$ concentrations agreed fairly well with the FD0520 solids $CaCO_3$ concentrations, averaging about 1 percent higher. In TC06, the in situ $CaCO_3$ concentrations were consistently higher than the FD0520 $CaCO_3$ concentrations, while in TC07 and TC08, the in situ $CaCO_3$ concentrations were either equal to or slightly higher than the FD0520 $CaCO_3$ concentrations. A possible explanation is the decarbonization of the solids between the in situ sampling and the FD0520 sampling. In TC09, however, the in situ values were actually less than the FD0520 values.

The first $CaCO_3$ FD0520 solids concentrations were around 2 to 3 percent. The concentration dipped to 0.6 percent at 110 hours into the run and returned to 3 percent just before the outage at hour 160. During the second portion of the test run, the $CaCO_3$ concentration remained around 3 percent. Due to the lack of sorbent feed, the TC10 $CaCO_3$ FD0502 solids concentrations were similar to those in TC08 and TC09 and lower than those in TC06 and TC07 (which were from 5- to 10-percent $CaCO_3$).

As in previous test runs, the FD0520 solids CaS concentration agreed well with the in situ CaS concentration throughout TC10. The CaS remained fairly constant at values between 0.3 and 0.5 percent. These data indicate consistently low sulfur capture by the PCD solids.

The PCD fines calcination is defined as:

$$\%\,Calcination = \frac{M\%\,CaO}{M\%\,CaO + M\%\,CaCO_3 + M\%\,CaS} \tag{1}$$

The PCD fines calcination is plotted on Figure 3.4-12. The calcination at the beginning of TC10 was 90 percent and then dropped to 80 percent; before climbing back to 96 percent at 110 hours, where it began to fluctuate, possibly due to unstable gasifier conditions. Later the readings stabilized, and the PCD fines calcination percentage remained virtually constant at around 80 percent with one outlier at 87 percent. These results are consistent with the PCD fines calcination values exhibited in previous PRB test runs (values which averaged about 85 percent).

The data suggest that the presence or absence of sorbent makes no difference in the amount of PCD fines calcination.

The calcium sulfation is defined as:

$$\%\ Sulfation = \frac{M\%CaS}{M\%CaO + M\%CaCO_3 + M\%CaS} \qquad (2)$$

The PCD fines sulfation is plotted on Figure 3.4-12 with the limestone calcination. The PCD fines sulfation held steady at about 1 to 2 percent for the first part of the test run. At hour 121 the sulfation spiked to 11 percent due to the low calcium content of the PCD fines. This was caused by high carbon content of the PCD fines due to coke breeze feed rather than high sulfur content—before settling between 3 and 4 percent, where it remained for the balance of the test run.

Table 3.4-4 gives the PCD fines composition for the samples collected in FD0520. The consistency is excellent in that the totals usually add up to between 98.0 and 101.2 percent. The average of the totals was 99.8 percent, indicating a virtually no bias. Additional components on Table 3.4-4, other than those plotted on Figures 3.4-9, -10, and -11 are MgO, FeO, and Al_2O_3. The MgO concentration was between 1.5 and 2.8 percent. The Al_2O_3 concentration was between 8.4 and 13.2 percent. Also given on Table 3.4-4 are the HHV, LHV, and organic carbon values for the PCD fines. As expected, the trend of heating values follows the carbon content of the PCD fines.

No FD0510 solid samples were analyzed during TC10 because the standpipe samples should give a more accurate view of the circulating solids composition.

3.4.6 Gasifier Solids Analysis Comparison

A comparison of the total organic carbon contents for the standpipe, cyclone dipleg, and spent fines samples yield the data shown in Figure 3.4-13. Ranging from 15 to 45 percent, the PCD solids always contained the highest amounts of organic carbon, followed by the cyclone dipleg solids, whose values ran mostly between 0 and 38 percent. The standpipe solids always possessed the lowest carbon content (less than 2.5 percent by weight).

Figure 3.4-14 compares the SiO_2 content between the standpipe, cyclone dipleg, and PCD solids samples. As suggested by the carbon contents discussed above, the standpipe solids have the highest SiO_2 content, and the PCD solids contain the lowest SiO_2 content. The cyclone dipleg solids, while ranging widely, always contain a silica content between that of the PCD solids and that of the standpipe solids at any given sampling time.

A comparison of the calcium content in the gasifier solids in shown in Figure 3.4-15. The PCD fines had the highest calcium content throughout the test run. The standpipe and cyclone dipleg solids calcium contents were similar during the test run, but the standpipe calcium content occasionally fluctuated above and below the calcium level of the cyclone dipleg solids.

3.4.7 Feeds Particle Size

The TC10 SMD and D_{50} particle sizes of the coal sampled from FD0210 are plotted on Figure 3.4-16. The PRB coal SMD particle size was fairly constant at the beginning of TC10 with values between 220 and 265 μ and two outliers at 158 and 286 μ, respectively. The PRB D_{50} was not constant during TC10. It started consistently between 280 and 320 μ, but as the run progressed, the particle size became increasingly larger, attaining values of 500 μ and above. The D_{50} values may be the more accurate in that the coal mill screen did not operate in the later part of the run since it constantly plugged with wet coal while in service. The D_{50} was always greater than the SMD, usually by 100 μ or more.

In past testing, high fines content resulted in an increased number of coal feeder outages due to coal feeder plugging caused by the packing of coal fines. A measure of the amount of fines in the coal is the percent of the smallest size fraction. To show the level of fines in the coal feed, the percent of ground coal less than 45 μ is plotted in Figure 3.4-17. The percentage of fines less than 45 μ in size was 3 to 7 percent during the majority of TC10. At the end of the test run, the percentage of fines increased dramatically, causing difficulty in feeding the coal. Keeping the percent fines under 15 percent for TC10 helped the coal feeder performance, but high coal moisture offset the positive effects of low fines percentage by making the conveying line more prone to plug throughout the test run. Thus, although coal fines were present toward the end of the test run, coal moisture, rather than coal particle size, presented the largest problems for the feeder in TC10.

3.4.8 Gasifier Solids Particle Size

The TC10 standpipe solids particle sizes are given in Figure 3.4-18. The particle size of the solids increased as the start-up sand was replaced by sorbent and coal ash. When the gasifier lost large amounts of solids during gasifier upsets, the bed material was replaced by 122 μ D_{50} sand, which had a smaller particle size. Sand additions occurred between hours 79 and 86, between hours 147 and 166, and intermittently from hour 337 until the end of the test run. The added sand decreased the standpipe solids particle size. The SMD values of the gasifier solids began at 170 μ and increased to 210 μ during the first 80 hours of TC10 operation. The SMD diameter decreased to 160 μ after the sand addition before hour 86, then slowly climbed back to 230 μ. During the last portion of the test run, the SMD of the standpipe solids reached a high value of 420 μ, possibly because of the large coal particles entering the gasifier from the coal mill operating without its 1,200 μ screen in service. Due to the several sand additions, the gasifier never reached a “steady-state” particle size. The last PRB test runs which had a steady-state particle size in the standpipe, were TC06 and TC07. The steady-state TC06 SMD was about 160 μ (see TC06 report Figure 4.4-14) and the steady-state TC07 SMD was about 170 μ (see TC07 report Figure 4.4-14). Thus, the TC10 standpipe solids were larger than the TC06 and TC07 solids, perhaps because of the lack of 10 μ sorbent during TC10 and the aforementioned lack of the coal mill screen, both of which would decrease the standpipe particle size.

The TC10 standpipe Mass Mean Diameter (D_{50}) sizes were about 20 μ less than the TC10 SMD, excepting the highest particle sizes. At the highest particle sizes, the D_{50} values were actually higher than the SMD values.

The cyclone dipleg particle sizes (SMD), shown in Figure 3.4-19, varied widely at the beginning of the test run from less than 20 to over 150 μ, the latter appearing to be more indicative of the average particle size. During the last 150 hours of the test run, the particle size dropped to between 10 and 30 μ, where it remained until the end of the test run.

As seen in the standpipe, the TC10 cyclone dipleg D_{50} sizes, also shown in Figure 3.4-19, averaged about 15 μ higher than the TC10 SMD, excepting some of the higher particle sizes.

Figure 3.4-20 plots the SMD and D_{50} for the PCD solids sampled from FD0520 and for the in situ solids collected upstream of the PCD. All but two of the in situ particle sizes agreed well with the FD0520 solids, while the remaining points were in the general range of the FD0520 particle size. The PCD fines SMD was fairly constant at about 9 μ for the first portion of TC10. Just before and after the outage at 160 hours, the size increased to 12 μ, with occasional spikes to 15 μ, before decreasing to around 10 μ again toward the end of the test run. These values are consistent with previous PRB data. For example, TC06 PCD fines had 9 to 14 μ SMD (TC06 Report, Figure 4.4-15), TC07 PCD fines had 9 to 13 μ SMD (TC07 Report, Figure 4.4-15), TC08 PCD fines had a slightly higher size of between 8 and 20 μ (TC08 Report, Figure 4.4-13), and TC09 PCD fines were similar at a 10 to 20 μ SMD (TC09 Report, Figure 4.4-14).

The D_{50} was about 5 μ larger than the SMD and follows the same trends as the SMD particle sizes.

3.4.9 TC10 Particle Size Comparison

Figure 3.4-21 plots all the solids SMD particle sizes. The Transport Gasifier was fed approximately 250 μ SMD coal and produced 7 to 18 μ SMD PCD fines, 20 to 150 μ cyclone dipleg solids, and 150 to 250 μ SMD gasifier solids—with some values exceeding 400 μ.

The D_{50} diameters were larger than the SMD for the FD210 (coal), and FD0520 (PCD fines), while the TC10 SMD particle sizes are larger than the D_{50} particle sizes for the standpipe and cyclone dipleg solids. This trend was also seen in PRB test runs TC06, TC07, and TC08 and Hiawatha bituminous test run TC09. The standpipe and cyclone dipleg solids have a non-

Gaussian distribution (bimodal), which probably caused the standpipe SMD to be larger than the standpipe D_{50}.

3.4.10 TC10 Standpipe and PCD Fines Bulk Densities

The TC10 standpipe, cyclone dipleg, and PCD fines bulk densities are given in Figure 3.4-22. The standpipe bulk density of the solids decreased slightly as the start-up sand was replaced by ash after both the original startup and the sand additions before hours 86, 166, and 369. The standpipe solids bulk density decreased from 85 to 78 lb/ft^3 during the first 79 hours of TC10 operation. The standpipe bulk density then fluctuated around 80 lb/ft^3 as sand was added, and the gasifier experienced a few unsteady periods leading up to the brief outage at hour 160. After the outage and subsequent sand addition, the gasifier bulk density decreased from 90 to 76 lb/ft^3 until the sand addition that brought the density up to 98 lb/ft^3 around hour 369. During the final periods of air-blown operation the gasifier bulk density again decreased 93 lb/ft^3. The standpipe solids bulk density from previous test runs behaved as did the TC10 standpipe bulk density, starting around 90 lb/ft^3 just after sand addition and then decreasing to around 80 lb/ft^3.

The cyclone dipleg bulk density ranged widely, from around 20 μ to values in excess of 80 μ. Despite the varied data, the majority of the test run saw dipleg densities between those of the standpipe and the PCD solids.

The bulk densities for the FD0520 PCD are also plotted on Figure 3.4-22. The bulk densities of the PCD fines decreased from 26 to 16 lb/ft^3 for the first 80 hours of TC10. The bulk densities then increased and fluctuated around 30 lb/ft^3 at hour 90 until the 10-day outage at hour 160. Upon restart, the density remained around 20 lb/ft^3 until around hour 360 when the constant feeding of sand caused the value to increase before decreasing again at the end of the test run.

Table 3.4-1

Coal Analyses

	Powder River Basin	
	Value	Standard Deviation
Moisture, wt%	22.64	1.04
Carbon, wt%	53.73	0.54
Hydrogen[1], wt%	3.53	0.06
Nitrogen, wt%	0.71	0.02
Oxygen, wt%	13.19	0.23
Sulfur, wt%	0.28	0.03
Ash, wt%	5.92	0.39
Volatiles, wt%	32.27	0.34
Fixed Carbon, wt%	39.17	0.55
Higher Heating Value, Btu/lb	9,088	99
Lower Heating Value, Btu/lb	8,528	104
CaO, wt %	0.87	0.11
SiO_2, wt %	2.24	0.28
Al_2O_3, wt %	1.04	0.14
MgO, wt %	0.25	0.04
Fe_2O_3, wt %	0.34	0.03
Ca/S, mole/mole	2.65	0.51
Fe/S, mole/mole	0.41	0.06

Notes:
1. All analyses are as sampled at FD0210.
2. Hydrogen in coal is reported separately from hydrogen in moisture.
3. Samples AB11721 excluded.

Table 3.4-2

Standpipe Analysis

Sample Number	Sample Date & Time	Sample Run Time Hours	SiO_2 Wt. %	Al_2O_3 Wt. %	FeO Wt. %	Other Inerts[1] Wt. %	$CaCO_3$ Wt. %	CaS Wt. %	CaO Wt. %	MgO Wt. %	Organic Carbon Wt. %	Total Wt. %
AB11723	11/19/2002 12:00	(2)	91.5	3.0	0.8	1.6	0.0	0.0	2.1	0.4	0.2	99.7
AB11726	11/20/2002 0:00	35	91.2	3.2	0.9	1.7	0.0	0.0	2.1	0.4	0.0	99.6
AB11779	11/21/2002 12:00	(3)	80.2	6.3	2.5	2.4	0.0	0.0	6.4	1.3	0.2	99.3
AB11816	11/22/2002 20:00	94	88.1	4.2	1.3	2.4	0.0	0.0	3.1	0.6	0.1	99.8
AB11817	11/23/2002 4:00	102	83.6	4.9	2.1	2.2	0.0	0.0	5.2	1.1	0.1	99.1
AB11851	11/24/2002 4:00	121	82.0	5.2	2.5	2.0	0.0	0.0	6.1	1.2	0.4	99.3
AB11854	11/25/2002 4:00	135	78.5	6.1	3.1	2.1	0.0	0.0	7.2	1.4	0.2	98.5
AB11872	11/25/2002 20:00	151	75.2	7.1	3.6	2.6	0.0	0.0	8.7	1.8	0.2	99.1
AB11937	12/8/2002 4:00	184	90.6	3.2	1.3	1.5	0.0	0.0	2.6	0.5	0.0	99.7
AB11977	12/9/2002 12:00	216	82.8	4.9	2.3	2.0	0.0	0.0	6.3	1.2	0.1	99.7
AB12052	12/14/2002 11:00	328	74.5	7.4	3.0	2.8	0.0	0.0	9.8	1.9	0.1	99.5
AB12054	12/15/2002 4:00	345	74.7	6.1	3.4	2.8	0.0	0.0	9.5	1.9	2.3	100.7
AB12056	12/16/2002 4:00	369	77.5	5.2	3.1	2.3	0.0	0.1	7.2	1.5	2.1	98.9
AB12105	12/17/2002 12:00	392	78.8	5.8	3.7	2.1	0.0	0.0	7.2	1.5	0.1	99.4

Notes:

1. Other inerts consist of P_2O_5, Na_2O, K_2O, & TiO_2
2. Sample AB11723 was taken prior to start of coal feed.
3. Sample AB11779 was taken prior to the re-start of coal feed.
4. Samples AB12054 and AB12056 were taken after periods of coke breeze feed.

Table 3.4-3

Cyclone Dipleg Analysis

Sample Number	Sample Date & Time	Sample Run Time Hours	SiO_2 Wt. %	Al_2O_3 Wt. %	FeO Wt. %	Other Inerts[1] Wt. %	$CaCO_3$ Wt. %	CaS Wt. %	CaO Wt. %	MgO Wt. %	Organic Carbon Wt. %	Total Wt. %
AB11724	11/19/2002 13:00	24	90.4	3.3	0.9	1.8	0.4	0.0	2.3	0.4	0.1	99.7
AB11780	11/21/2002 12:00	71	73.4	5.5	1.9	2.2	1.3	0.1	5.0	1.1	12.9	103.4
AB11826	11/23/2002 8:00	106	76.3	5.5	2.4	2.0	2.2	0.0	4.5	1.2	5.4	99.4
AB11972	12/9/2002 12:00	216	67.6	7.7	2.2	2.2	1.3	0.0	6.5	1.5	22.3	111.3
AB12021	12/11/2002 20:00	265	41.7	7.0	1.9	1.9	1.7	0.6	5.6	1.4	38.1	99.7
AB12099	12/16/2002 20:00	376	64.7	6.5	2.9	2.2	1.6	0.0	5.3	1.3	15.5	100.0
AB12106	12/17/2002 12:00	392	74.7	6.7	3.2	2.4	1.0	0.0	5.4	1.3	5.1	99.8

Notes:
1. Other inerts consist of P_2O_5, Na_2O, K_2O, & TiO_2
2. Sample AB12099 was taken during a period of coke breeze feed.

Table 3.4-4

PCD Fines From FD0520

Sample Number	Sample Date & Time	Sample Run Time Hours	SiO_2 Wt. %	Al_2O_3 Wt. %	FeO Wt. %	Other Inerts[1] Wt. %	$CaCO_3$ Wt. %	CaS Wt. %	CaO Wt. %	MgO Wt. %	Organic C ($C-CO_2$) Wt. %	Total Wt. %	HHV Btu/lb.	LHV Btu/lb.
AB11719	11/19/2002 12:00	23	48.4	11.2	2.8	3.0	2.0	0.2	9.7	2.3	21.6	101.2	2,796	2,762
AB11730	11/20/2002 4:00	39	47.8	12.3	3.4	3.1	1.7	0.1	12.8	2.8	16.8	100.7	2,239	2,208
AB11761	11/21/2002 4:00	63	36.1	11.5	2.9	2.7	2.7	0.3	9.6	2.3	31.4	99.6	4,528	4,476
AB11788	11/22/2002 0:00	83	30.8	10.0	2.5	2.4	3.3	0.3	8.2	2.1	38.2	98.0	5,810	5,751
AB11820	11/23/2002 0:00	98	41.7	11.1	2.7	3.0	2.5	0.4	8.8	2.2	29.0	101.4	3,863	3,816
AB11829	11/23/2002 12:00	110	59.4	10.3	3.8	2.7	0.5	0.2	7.7	1.7	13.0	99.3	1,232	1,215
AB11844	11/24/2002 4:00	121	33.0	9.3	2.6	2.3	1.6	1.0	5.3	1.5	44.4	101.0	6,013	5,969
AB11863	11/25/2002 8:00	139	46.7	13.2	3.8	3.1	2.0	0.2	11.4	2.6	15.4	98.5	2,135	2,110
AB11878	11/26/2002 0:00	155	30.9	9.5	2.2	2.0	2.8	0.4	6.1	1.7	42.4	98.1	6,393	6,326
AB11950	12/8/2002 16:00	196	33.8	10.4	2.6	2.7	3.3	0.4	8.1	2.1	36.2	99.6	5,253	5,194
AB12030	12/12/2002 8:00	277	35.2	8.4	2.1	2.4	2.9	0.4	6.4	1.7	39.7	99.2	5,822	5,761
AB12060	12/13/2002 20:00	313	38.6	9.6	2.4	2.4	3.0	0.5	7.4	1.9	34.8	100.5	4,868	4,815
AB12061	12/14/2002 8:00	325	44.1	10.4	2.6	2.7	2.4	0.2	8.5	2.1	28.0	100.9	3,971	3,928

Notes:

1. Other inerts consist of P_2O_5, Na_2O, K_2O, & TiO_2
2. Samples AB11844 and AB11863 were taken during a period of coke breeze feed.

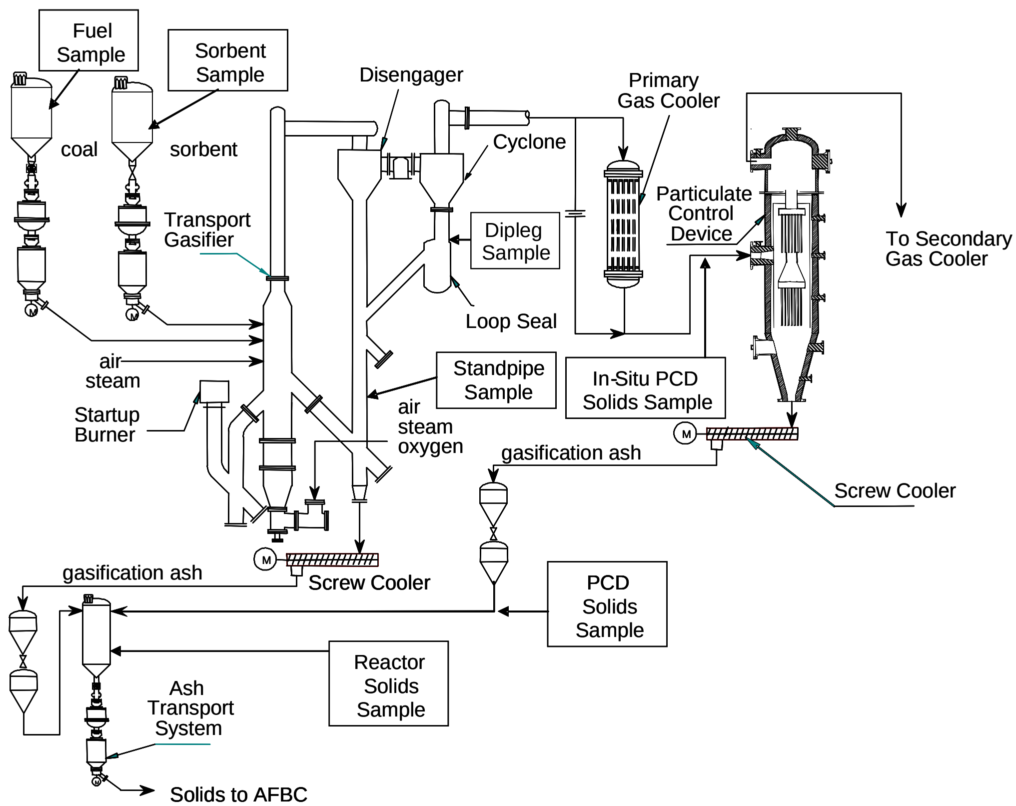

Figure 3.4-1 Solids Sample Locations

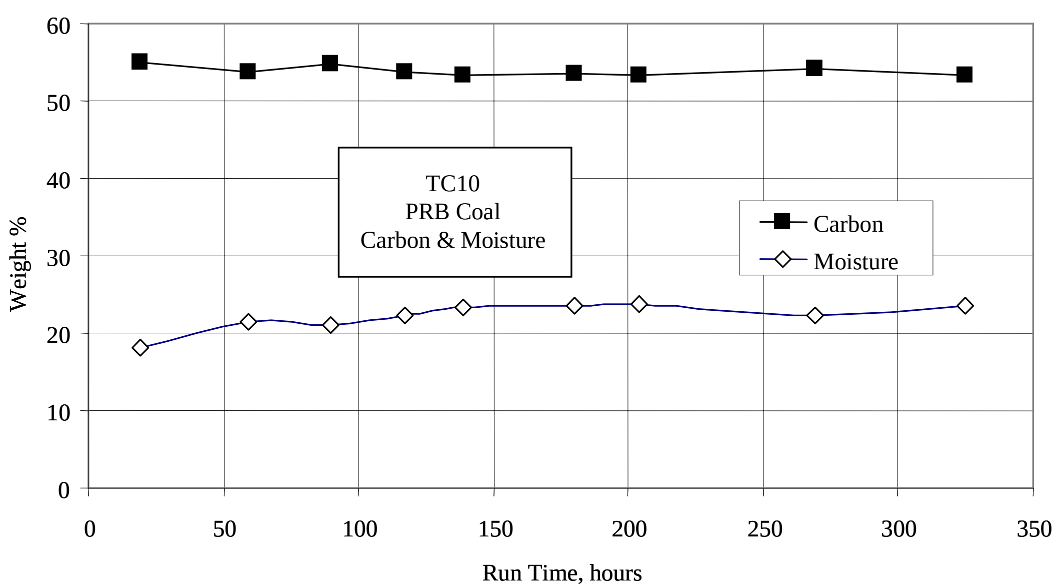

Figure 3.4-2 Coal Carbon and Moisture

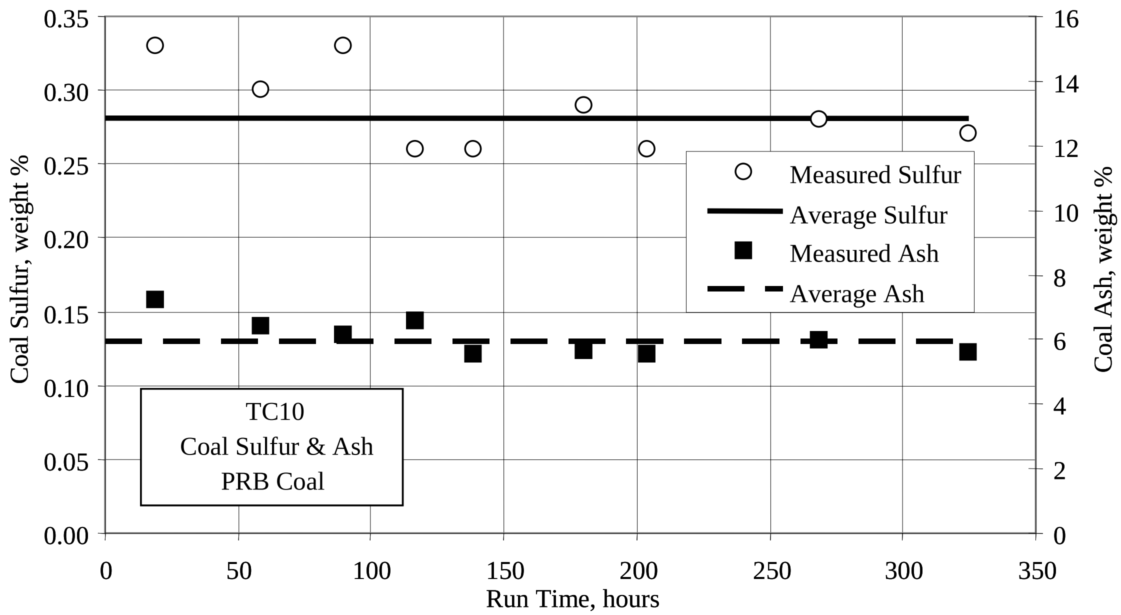

Figure 3.4-3 Coal Sulfur and Ash

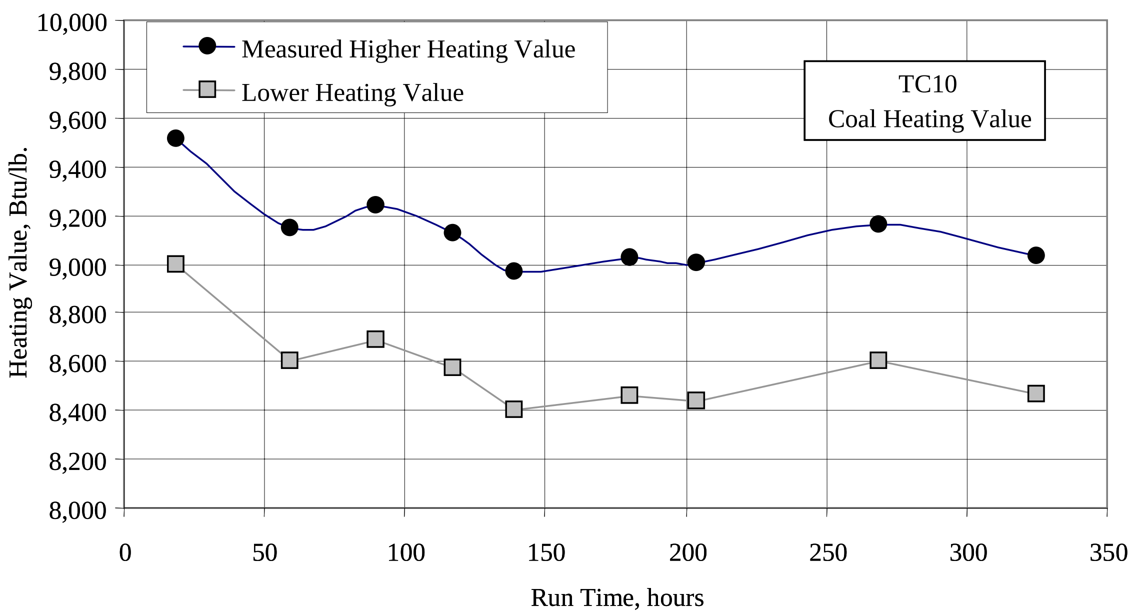

Figure 3.4-4 Coal Heating Value

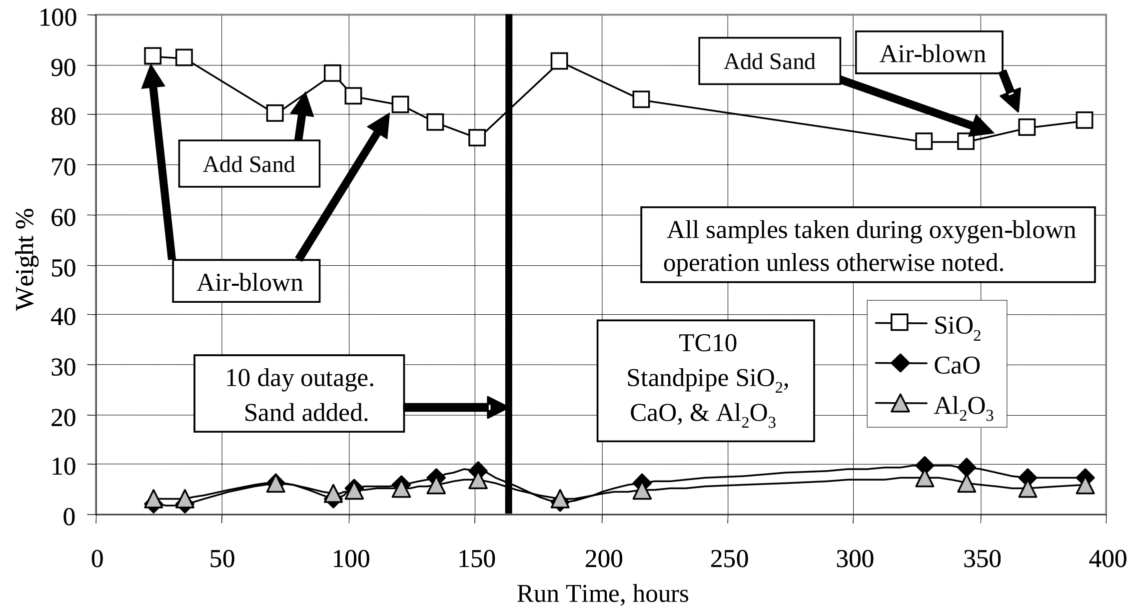

Figure 3.4-5 Standpipe SiO_2, CaO, and Al_2O_3

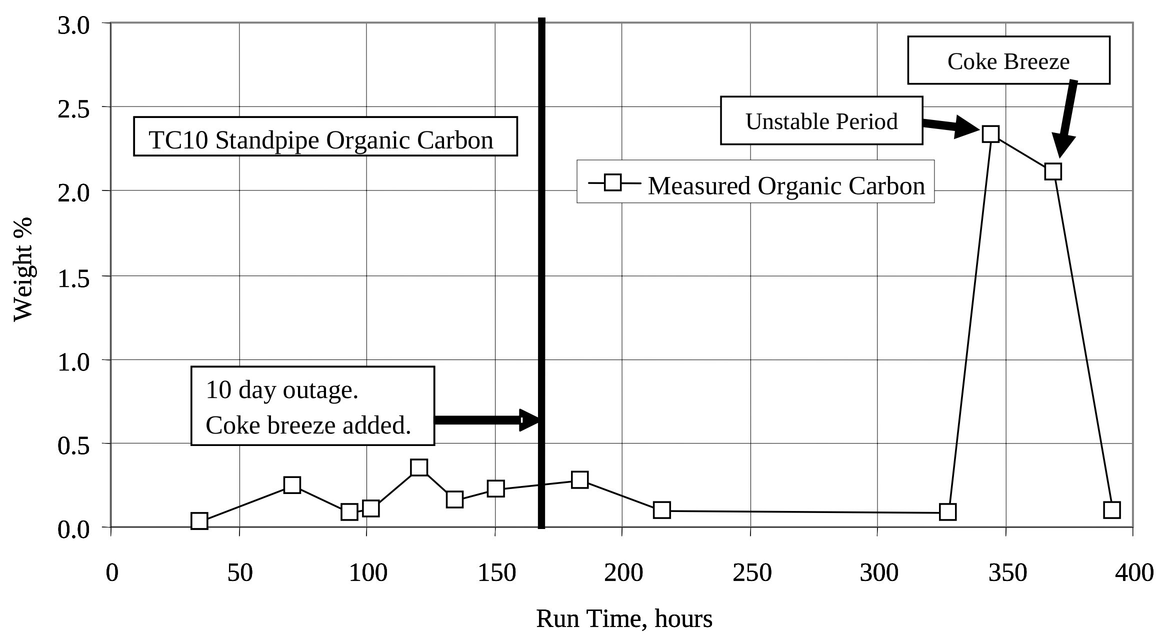

Figure 3.4-6 Standpipe Organic Carbon

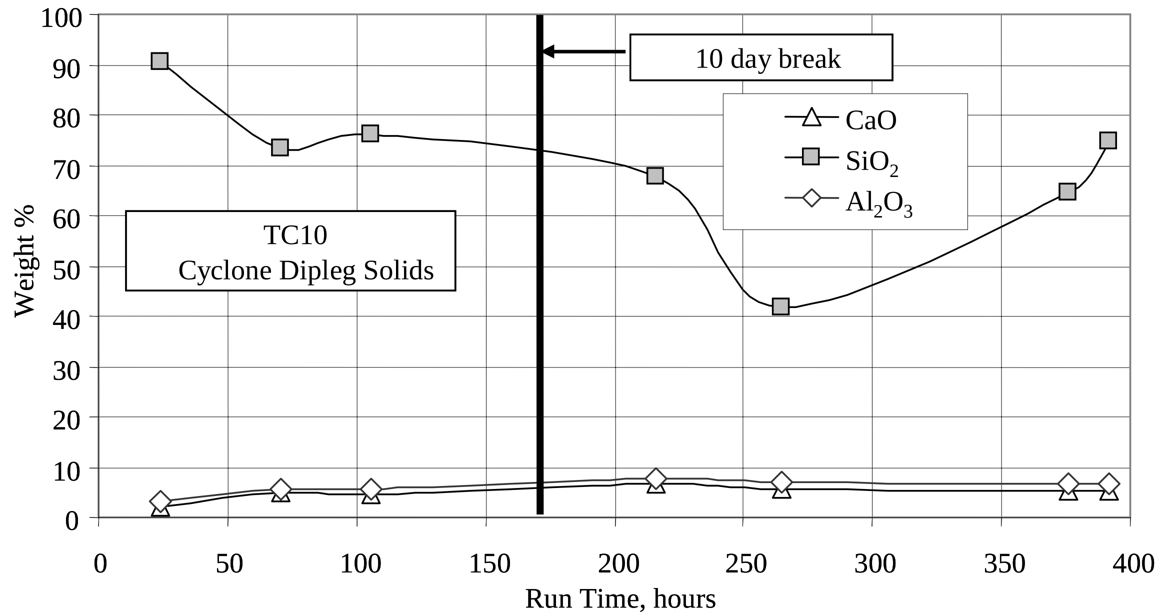

Figure 3.4-7 Cyclone Dipleg Solids SiO_2, CaO, and Al_2O_3

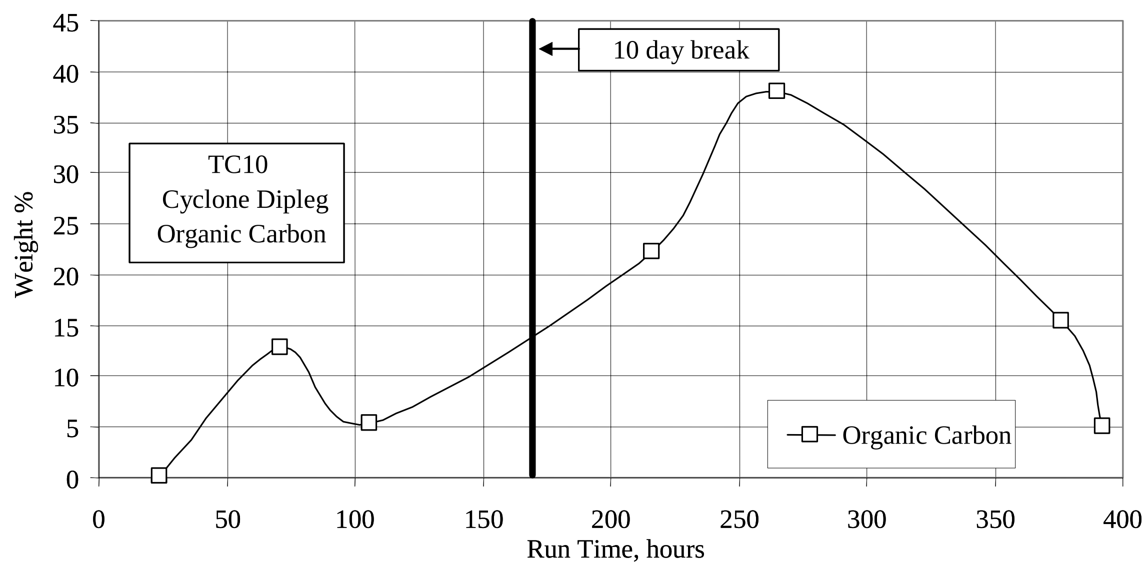

Figure 3.4-8 Cyclone Dipleg Organic Carbon

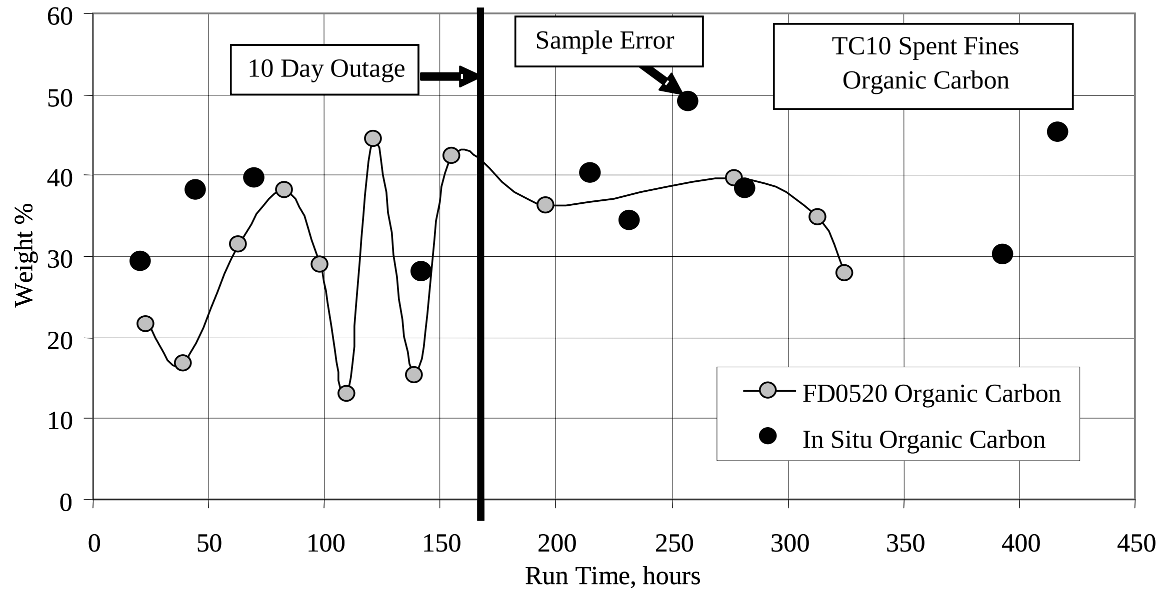

Figure 3.4-9 PCD Fines Organic Carbon

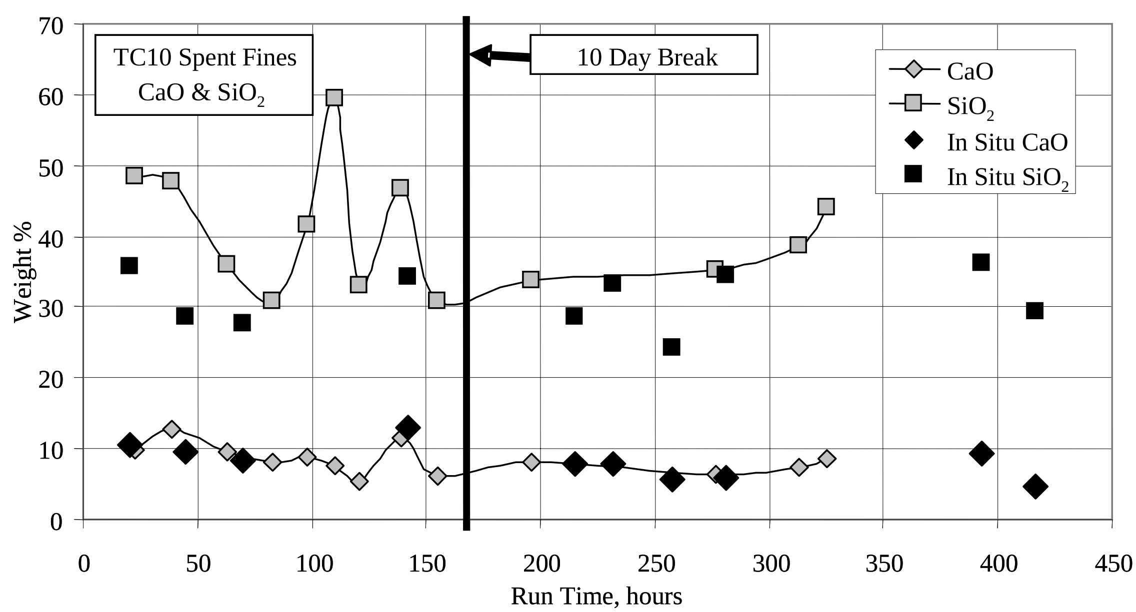

Figure 3.4-10 PCD Fines CaO and SiO_2

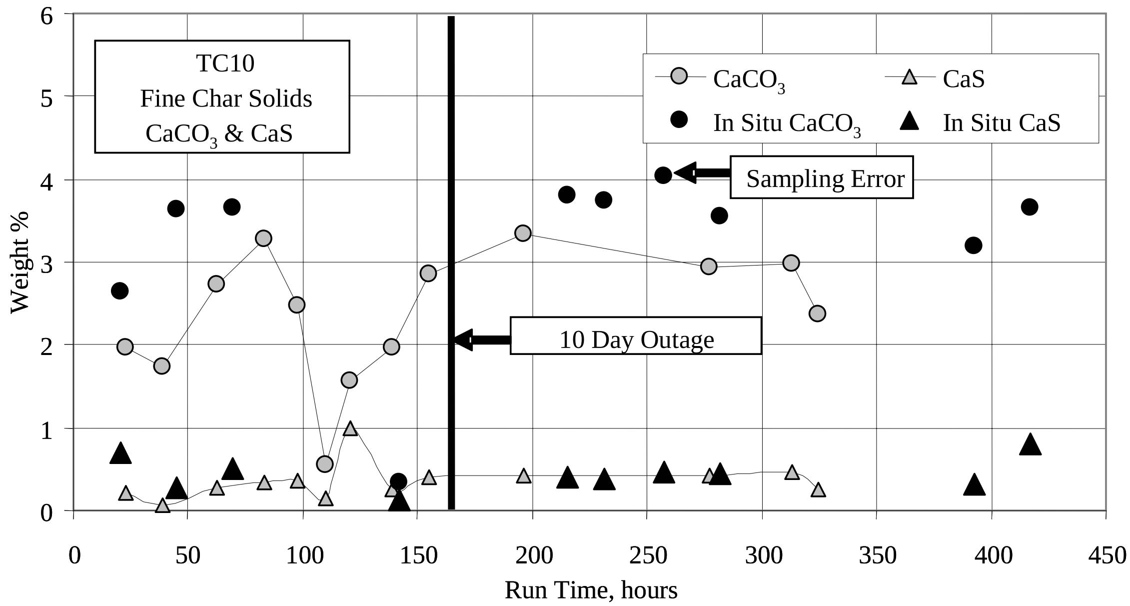

Figure 3.4-11 PCD Fines $CaCO_3$ and CaS

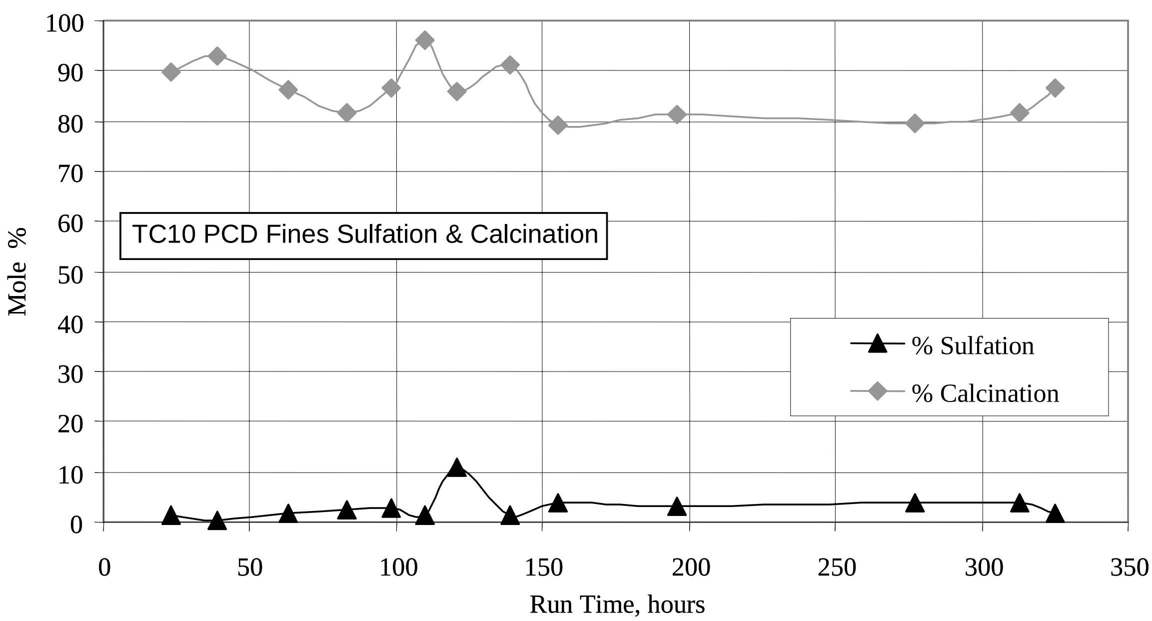

Figure 3.4-12 PCD Fines Sulfation and Calcination

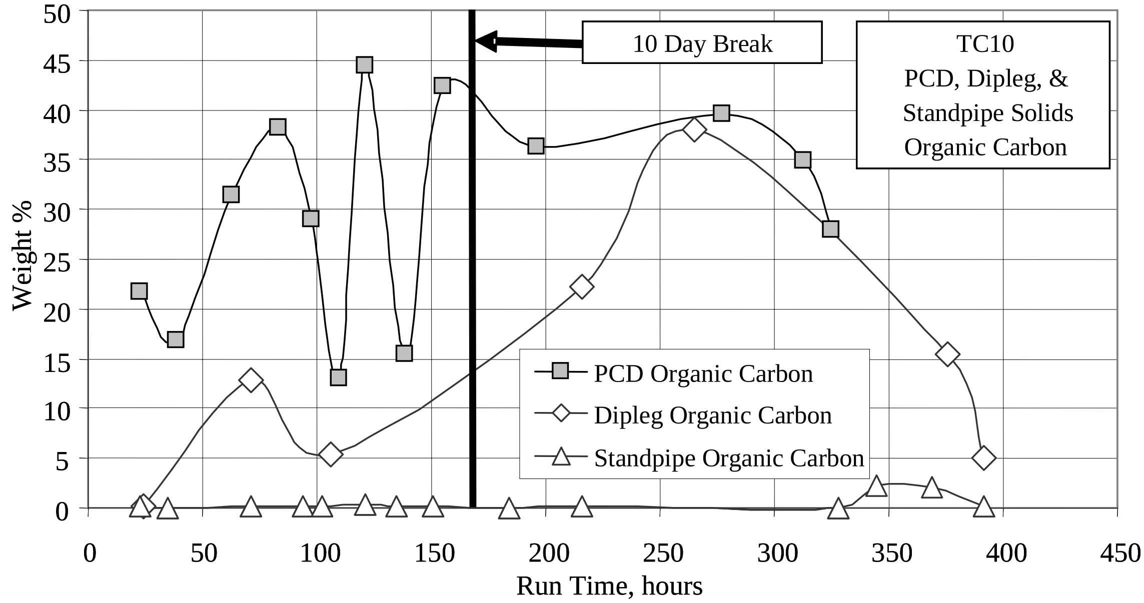

Figure 3.4-13 Gasifier Solids Organic Content

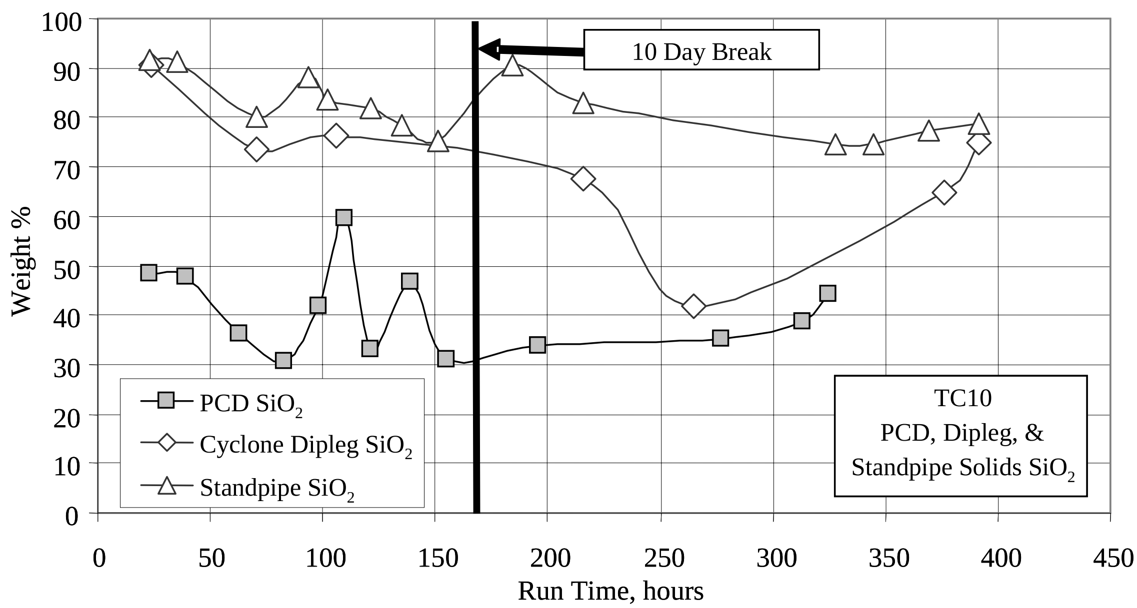

Figure 3.4-14 Gasifier Solids SiO_2 Content

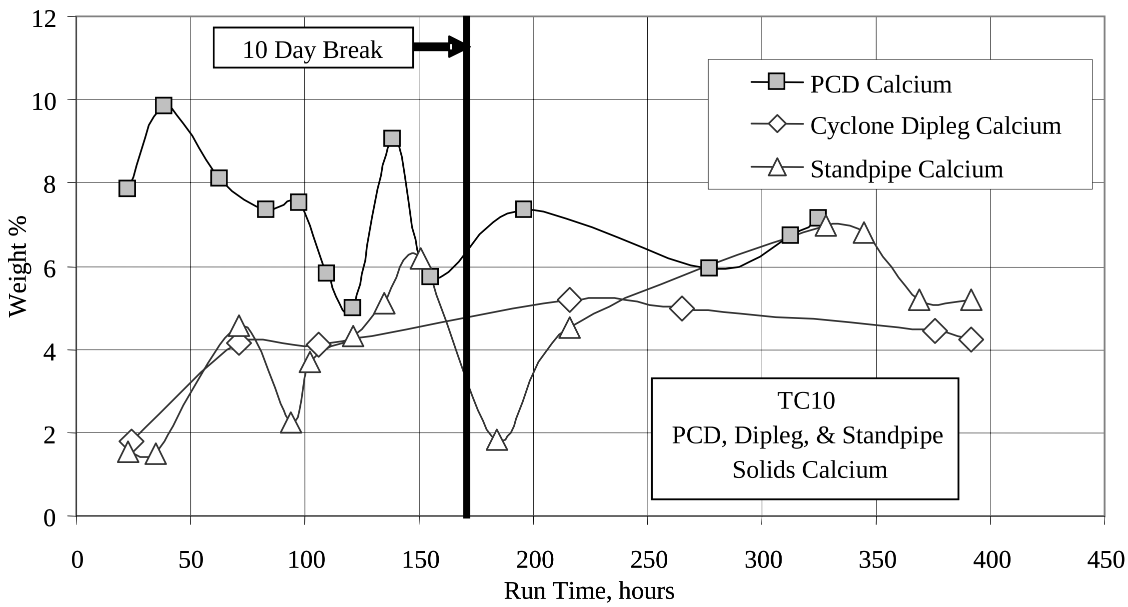

Figure 3.4-15 Gasifier Solids Calcium Content

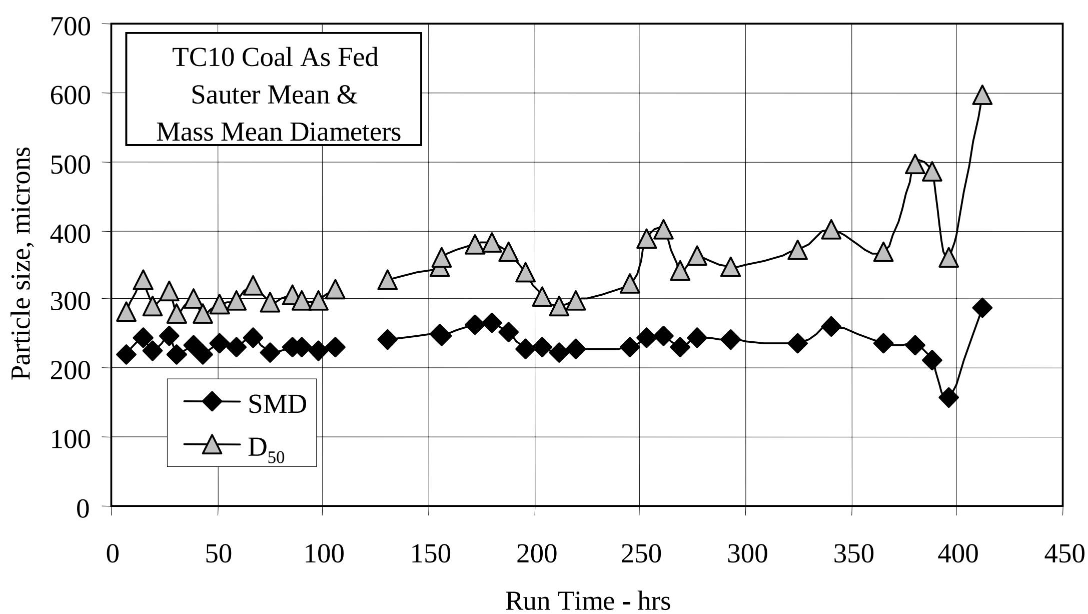

Figure 3.4-16 Coal Particle Size

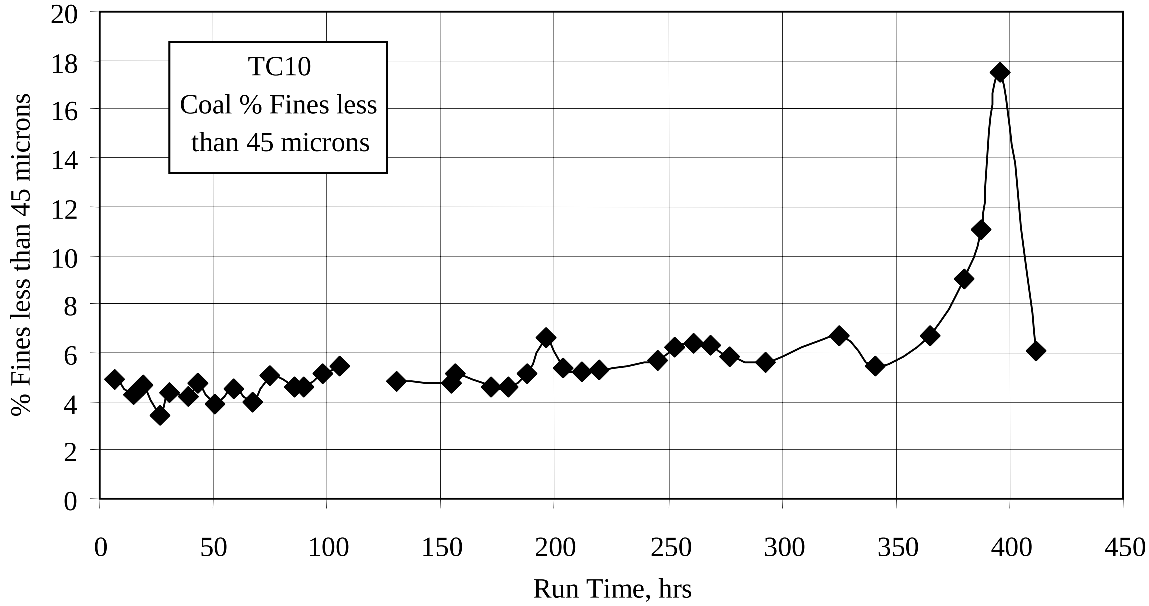

Figure 3.4-17 Percent Coal Fines

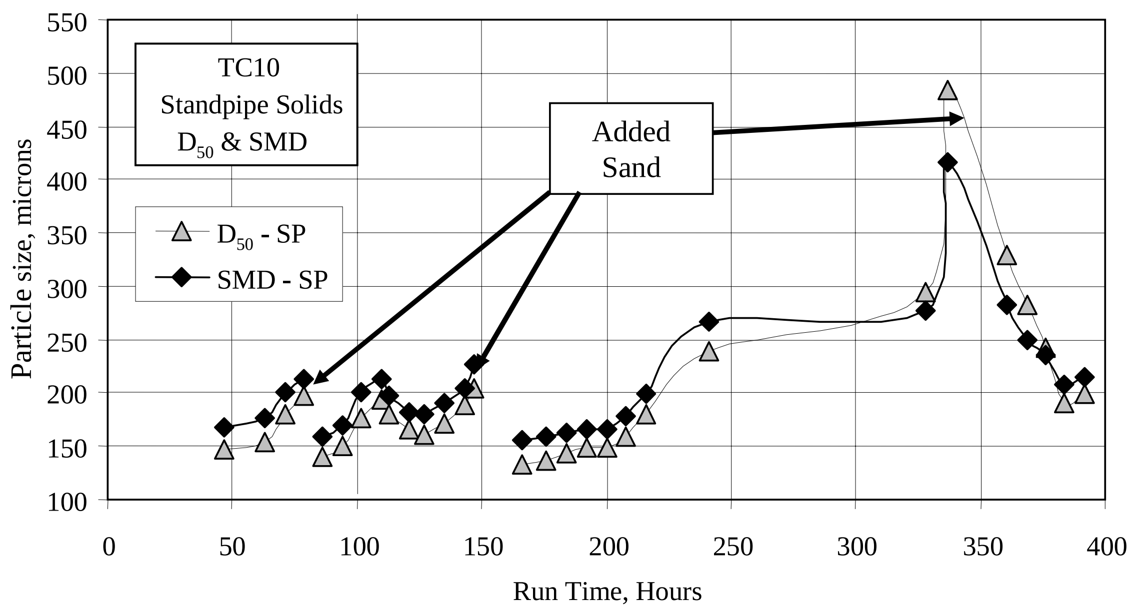

Figure 3.4-18 Standpipe Solids Particle Size

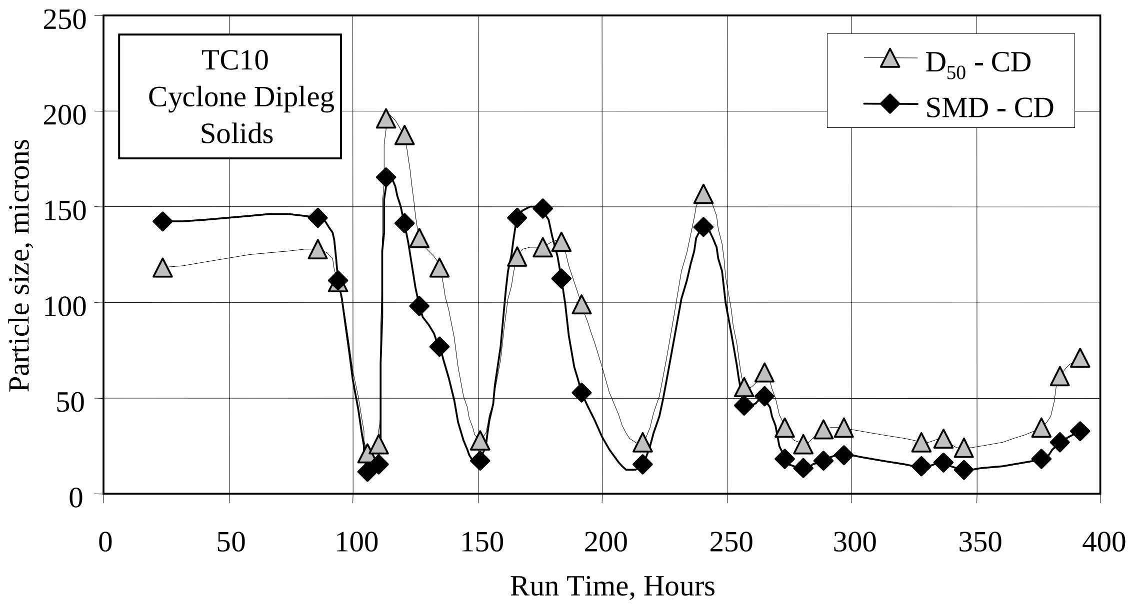

Figure 3.4-19 Cyclone Dipleg Solids Particle Size

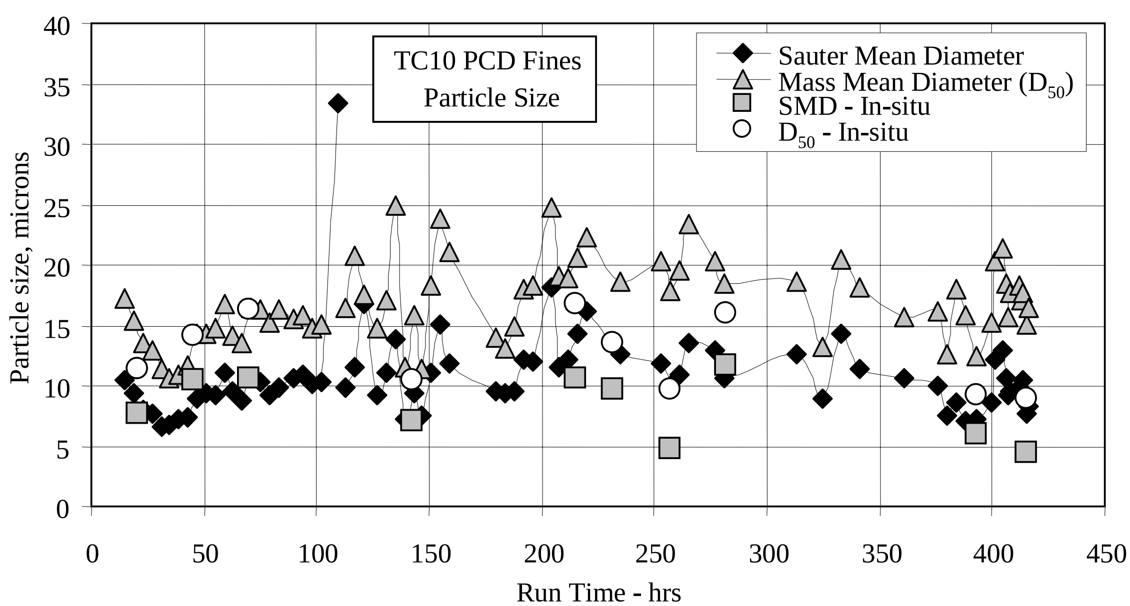

Figure 3.4-20 PCD Fines Particle Size

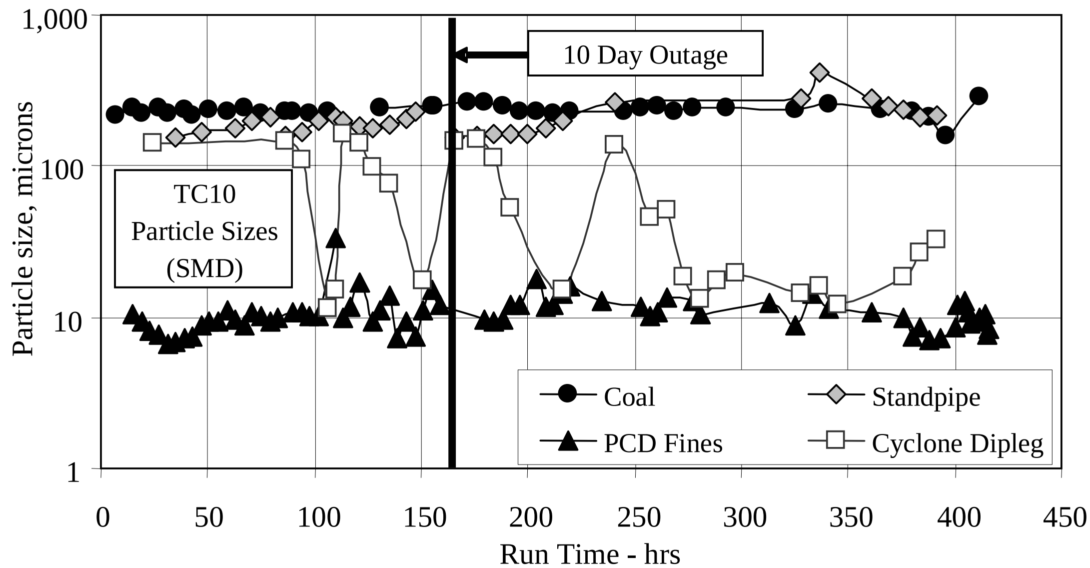

Figure 3.4-21 Particle Size Distribution

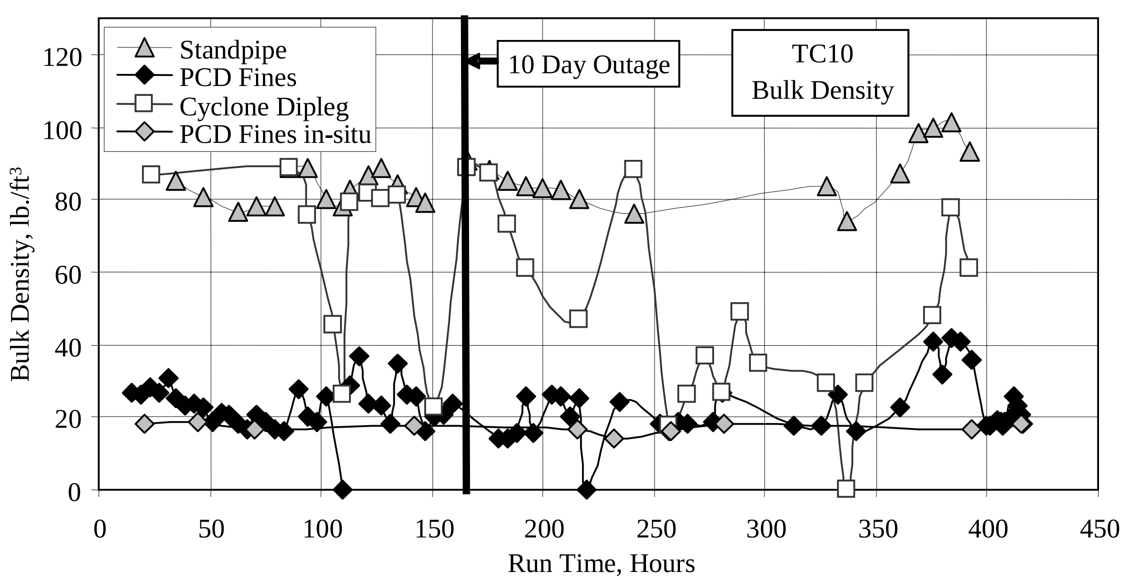

Figure 3.4-22 Standpipe, Cyclone Dipleg, and PCD Fines Solids Bulk Density

3.5 MASS AND ENERGY BALANCES

3.5.1 Summary and Conclusions

- Carbon conversions were 93 and 96 percent in air-blown mode and between 92 and 98 percent in oxygen-blown mode.
- To achieve a good mass and energy balances, the coal-feed rate based on the Transport Gasifier carbon balance was selected rather than the coal-feed rate based on the coal feeder weigh cells.
- Coal rates were from 3,100 to 4,100 lb/hr.
- The oxygen-to-coal ratios (pound-per-pound) were 0.79 and 0.84 in air-blown mode and between 0.56 and 0.70 in oxygen-blown mode.
- Overall mass balance was good, with most periods at ±6 percent.
- Nitrogen balances were good, with most at ±7 percent, assuming 200 lb/hr FI609 nitrogen did not enter the gasifier.
- Sulfur balance was marginal for air-blown mode at ±18 percent, and poor for oxygen-blown mode at about -7 to +25 percent.
- Sulfur removal was from 2 to 12 percent. All removal came from the PRB coal alkalinity, since no sorbent was added.
- Sulfur emissions were from 0.47 to 0.57 pounds SO_2/MBtu coal.
- Sulfur capture was sometimes limited by the H_2S equilibrium when the syngas H_2O concentrations was high.
- Equilibrium H_2S calculations indicated that sulfur capture would not have been increased by the use of sorbent at high syngas moisture conditions, but perhaps could at lower syngas moisture conditions.
- Use of the measured steam rate did not produce acceptable hydrogen and oxygen balances, so the hydrogen balance was used to calculate the steam rate. Hydrogen balance steam rates were 10 to 40 percent higher than the measured steam rates.
- Oxygen balances were excellent for air-blown mode at ±4 percent and good for oxygen-blown mode at ±9 percent with a negative bias.
- Calcium balances were poor with most of the calcium balances outside of ±20 percent, with a negative bias.
- Energy balances were acceptable at 2 to 17 percent, with a positive bias in both modes. The air-blown balances were significantly closer than the oxygen-blown balances.
- The raw cold-gasification efficiency was 52 and 57 percent for the two air-blown operating periods and 58 to 69 percent for the oxygen-blown periods (feed energy basis, not feed coal basis).

- The raw hot gasification efficiency was 88 and 92 percent for the air-blown operating periods and between 85 to 93 percent for the oxygen-blown operating periods.
- The corrected cold gas efficiency was 68 and 73 percent for air-blown mode and 79 to 83 percent for oxygen-blown mode.

3.5.2 Introduction

The process flows into the KBR Transport Gasifier process are:

- Coal flow through FD0210.
- Coke breeze flow through FD0220.
- Air flow measured by FI205.
- Oxygen flow measured by FI726.
- Pure nitrogen flow measured by FI609.
- Steam flow measured by the sum of FI204, FI727b, FI734, and FI733.

Sand was added through FD0220 to increase the Transport Gasifier bed height both during outages and coal feed. Limestone was not fed to the Transport Gasifier during TC10.

The process flows from the KBR Transport Gasifier are:

- Synthesis gas-flow rate from the PCD measured by FI465.
- PCD solids flow through FD0520.
- Gasifier solids flow through FD0510.

The coal flow through FD0210 can be determined by three different methods:

- The coal feeder surge bin weigh cell.
- Transport Gasifier carbon balance.
- Syngas Combustor carbon balance.

The FD0210 surge bin weigh cell uses the time between filling cycles and the weigh differential between dumps to determine the coal rate. This method was used to determine the coal rate in GCT4 and resulted in both the carbon and energy balance being 10- to 20-percent high. The coal rates determined from the FD0210 weigh cell data were consistently higher than the actual coal rate. For TC10, the energy balance based on the FD0210 weigh cells coal rate was between 15 and 20 percent too high with 15 to 20 percent more energy entering the Transport Gasifier than accounted for in the product streams.

The Transport Gasifier carbon balance method uses the syngas carbon rate from the syngas flow rate and composition plus the PCD carbon rate from the PCD fines carbon concentration and PCD solids flow rate. This method was used in TC06, TC07, and TC08. The energy balanced averaged about 11-percent high using the Transport Gasifier carbon balance for determining the coal-feed rate.

The syngas combustor carbon balance method uses the syngas combustor flue gas CO_2 analyzer and the syngas combustor flue gas rate to determine the carbon in the synthesis gas. The carbon in the synthesis gas plus the carbon in the PCD fines determines the coal-feed rate. The TC09 mass and energy balances used this method. In TC10, the syngas combustor carbon balance coal rates energy balance averaged 11-percent high—virtually the same as the Transport Gasifier carbon balance. Since the two carbon balances performed similarly, most of the previous PRB test runs featured the Transport Gasifier carbon balance, and the syngas combustor CO_2 analyzer did not read reliably in TC10, the Transport Gasifier carbon balance coal rate was used for TC10.

3.5.3 Feed Rates

The operating period steam, oxygen, and nitrogen flow rates are shown in Figure 3.5-1 and on Table 3.5-1. It is estimated that during air-blown mode about 200 lb/hr of the nitrogen from FI609 does not enter the process but is used to seal valves, to pressurize and depressurize feed and ash lock hopper systems, and to serve to seal the screw coolers. Values in Table 3.5-1 and Figure 3.5-1 assume that 200 lb/hr of nitrogen from FI609 does not enter the Transport Gasifier. In TC07, it was assumed that 500 lb/hr was lost, and in TC08 it was assumed that 1,000 lb/hr of nitrogen were lost, while in TC09 1,250 pph were lost in air-blown mode and no loss occurred in oxygen-blown mode. A small amount of nitrogen (~200 lb/hr) is added via FI6080 to the Transport Gasifier through the coke breeze feed line to keep the line clear between periods of coke breeze feed. This value is included in the feed nitrogen.

Nitrogen rates were at 6,400 and 7,600 lb/hr during the two air-blown periods and were between 6,300 and 7,500 pph during oxygen-blown mode. Increasing the nitrogen rate decreases the syngas LHV.

The oxygen rate was zero for the two air-blown periods. For oxygen-blown mode, the oxygen rate was about 2,200 lb/hr.

No coke breeze was fed to the gasifier during any of the operating periods. Therefore, it does not come into any of the calculations.

The steam rate to the gasifier should be determined from the sum of FI204 (total steam flow to the UMZ), FI727 or FI727B (steam mixed with the air fed to the LMZ), FI734 (steam fed into the LMZ), and FI733 (steam fed to a shroud into the LMZ). FI727 and FI727B are two flow meters on the same line and both should read the same. Using the TC10 steam rates from the steam-flow meters resulted in poor Transport Gasifier hydrogen and oxygen balances, so the steam rate by hydrogen balance was used rather than the measured steam rate. Section 3.5.9 below compares the hydrogen balance and measured steam-flow rates in more detail.

TC10 began at 1,000 lb/hr steam during the first operating period, and then increased to 2,600 lb/hr steam fed to the gasifier in preparation for oxygen-blown operations. The rate was reduced to below 2,000 pph, then reduced to 850 for the second air-blown period. Upon resuming oxygen-blown operations, the rate achieved a high value of around 2,800 pph before it was again reduced to between 1,500 and 1,700 pph, where it remained until the end of the test run. Lower steam rates tend to increase the synthesis gas LHV. Air-blown mode tests in previous test runs show the trend more clearly due to the large variation in steam rates.

The operating period air-feed rates are shown on Figure 3.5-1 and listed on Table 3.5-1. The air rates were 12,500 and 11,100 lb/hr for the two air-blown test periods. During oxygen-blown mode, the air-flow rate was zero.

3.5.4 Product Rates

The operating period synthesis-gas rates are shown on Figure 3.5-2 and listed on Table 3.5-1. The synthesis-gas rates were taken from FI463.

The synthesis gas rate was checked for all the operating periods using an oxygen, carbon, and hydrogen balance around the synthesis gas combustor and found to be in good agreement with the synthesis gas combustor data for most of the operating periods (see Figures 3.3-23, -24, and -25). The synthesis gas rates were 23,900 and 21,700 lb/hr respectively for the two air-blown periods. During oxygen-blown mode, the synthesis-gas rate was from 13,500 to 16,600 lb/hr. The synthesis-gas rate is a strong function of the air and oxygen rates and a weak function of the steam and nitrogen rates.

The solids flow from the PCD can be determined from two different methods by using:

- In situ particulate sampling data upstream of the PCD.
- FD0530 weigh-cell data.

The best measurements of the PCD solids flow are the in situ PCD inlet particulate determinations. Using the synthesis gas-flow rate and the in situ PCD inlet particulate measurement, the solids flow to the PCD can be determined since the PCD captures all of the solids.

The FD0530 weigh-cell data can be used to determine the PCD solids flow only if both the FD0530 feeder and the FD0510 feeder (standpipe solids) are off because FD0520 and FD0510 both feed into FD0530, and FD0530 feeds the sulfator. This method assumes that the PCD solids level in the PCD and FD0502 screw cooler are constant, that is, the PCD solids level is neither increasing nor decreasing. A good check on the PCD fines rates is the calcium balance, since calcium is only present in the feed coal and the PCD fines. The two PCD fines rates methods are compared on Figure 3.5-3 where the nine in situ rates are plotted against rates determined by the FD0530 weigh cells at about the same time. The in situ rates were higher than the FD0530 weigh-cell rates for all nine in situ samples. Only one sample agreed well.

The results for all of the FD0530 weigh-cell data are compared with the in situ data in Figure 3.5-4. The FD0530 weigh-cell measurements had a large scatter and were usually lower than the in situ samples PCD fines rates. Also plotted on Figure 3.5-4 are the interpolated PCD solids rates used for the operating periods.

The operating period PCD fines rates ranged from 220 to 480 lb/hr and did not change during the transitions to and from oxygen-blown mode. The operating period rates were used in mass balances shown on Table 3.5-1. As indicated in the table, FD0510 did not operate during any of the operating periods.

3.5.5 Coal Rates and Carbon Conversion

In GCT3 and GCT4, both the carbon balance and energy balance were off by 10 to 20 percent, and it was speculated that this was due to FD0210 weigh-cell data reading about 15 percent too high. Using coal rates determined by TC06, FD0210 weigh-cell data would have produced a TC06 carbon balance that had 10 to 20 percent more carbon entering than exiting the Transport Gasifier. The other large carbon flows (synthesis gas carbon flow and PCD solids carbon flow) are independently checked, so it is likely that the weigh-cell coal rate was in error. In TC10, the coal rate was determined by a Transport Gasifier carbon balance, the PCD carbon, the standpipe carbon, and the PCD solids rate. Table 3.5-2 gives the TC10 Transport Gasifier carbon flows for each operating period.

The Transport Gasifier carbon balance coal rates, synthesis gas combustor carbon balance coal rates, and FD0210 weigh-cells coal rates for the operating periods are compared on Figure 3.5-5. The FD0210 weigh-cell coal rates were determined from a spreadsheet which calculated the coal rate for every filling of the FD0210 surge vessel. The values for the FD0210 weigh cell were averaged for each operating period. FEED210 is a DCS-calculated value that simulates the weigh-cell feed rate on a real-time basis.

The weigh-cell coal-feed rate was slightly higher than both the Transport Gasifier carbon balance coal rate for most of the TC10 oxygen-blown test periods. The weigh-cell feed rate was lower than the gasifier carbon balance values for the two air-blown periods. In all except the first two periods, the weigh-cell feed rate was higher than the values obtained from the syngas combustor carbon balance. During TC10, the coal-feed rate by the Transport Gasifier carbon balance was usually higher than the coal rate by the syngas analyzers. The syngas combustor values were close to those of the gasifier carbon balance, once the CO_2 data were corrected, since the syngas combustor CO_2 (see Figure 3.3-24) analyzer was consistently lower than the CO_2 calculated from the gasifier gas composition.

The Transport Gasifier carbon balance coal rate will be used for all further data analysis in this section because it provides a satisfactory energy balance, and it is consistent with data from previous test runs. The syngas combustor method energy balance is as accurate as the gasifier carbon balance method, but it relies on a single CO_2 analyzer whose data is slightly inconsistent with the rest of the gas analyzer data. The use of the higher weigh cell coal-feed rates (during oxygen-blown operation) decreases the carbon conversion when compared to using the coal rates by the Transport Gasifier or syngas combustor carbon balance.

The carbon balance coal-flow rates for the operating periods are given in Table 3.5-1. The coal rate started at about 3,500 lb/hr for the first operating period and decreased to 3,100 lb/hr for the second (the first oxygen-blown period). The next five oxygen-blown tests occurred at a feed rate of between 3,400 and 4,100 pph, followed by another air-blown test at 3,300 pph. The remaining test periods (all oxygen-blown) featured coal-feed rates that varied from 3,100 pph to 4,100 pph.

Carbon conversion is defined as the percentage of the fuel carbon that is gasified to CO, CO_2, CH_4, C_2H_6, and higher hydrocarbons. The carbon conversion is inversely proportional to the percentage of carbon that is rejected by the gasifier with the PCD and gasifier solids. Coke breeze carbon is considered potential carbon for gasification; however, none of the operating periods in TC10 took place during coke breeze feed. The rejected carbon to the gasifier or PCD fines solids is typically burned in a less efficient combustor and/or disposed of—a less efficient use of fuel.

The carbon conversions for each operating period are given on Table 3.5-2 and in Figure 3.5-6. The carbon conversion started at 96 percent during the first air-blown operating period and ranged from 94 to 98 percent during the subsequent oxygen-blown testing. The carbon conversion for the second air-blown period dipped to below 94 percent, and ranged from 91 to 98 percent for the oxygen-blown periods that occurred during the remainder of the test run. The average carbon conversion for the entire test run was 95 percent, a value that is consistent with previous PRB testing.

The carbon conversion should be a function of gasifier temperature, with the carbon conversion increasing as the temperature increases. The TC10 products method carbon conversions are plotted against riser exit temperature in Figure 3.5-7. The products method carbon conversion is defined as the carbon in the syngas divided by the total amount of carbon leaving the gasifier (in the syngas as well as in the solids). The data indicate only a slight increase of carbon conversion occurs as the riser temperature increases. This observation is consistent with TC06, TC07, TC08, and TC09 data.

3.5.6 Overall Material Balance

Material balances are useful in checking the accuracy and consistency of data as well as determining periods of operation where the data is suitable for model development or commercial plant design. Total material balances for each operating period are given on Figure 3.5-8, which compare the total mass in and the total mass out. The overall material balance was good, with all but two of the relative differences at ±6 percent. The two outliers had a relative difference of under ±10 percent. The relative difference (relative error) is defined as the Transport Gasifier feeds in minus products out divided by the feeds ({In-Out}/In). Note that the air-blown operating periods had higher overall mass flow rates than the oxygen-blown operating periods.

The details of the overall mass balance are given in Table 3.5-1 with the relative differences and the absolute differences. The absolute difference (absolute error) is defined as the difference between the feeds and the products (In-Out).

The gas composition data in Section 3.3 and the solids composition data in Section 3.4 affect the mass balance through the coal rate determined by carbon balance. The main contributors to the material balance are the synthesis gas rate (13,600 to 23,900 lb/hr), air rate (0 to 12,500 lb/hr), oxygen rate (0 to 2,500 lb/hr), steam rate (900 to 2,800 lb/hr), nitrogen rate (6,300 to 7,600 lb/hr), and coal rate (3,100 to 4,100 lb/hr).

The oxygen-to-coal ratios are listed on Table 3.5-1. The oxygen-to-coal ratio was 0.79 and 0.84 for air-blown operation and 0.56 to 0.70 for oxygen-blown operation. The differences in oxygen-to-coal ratios between air- and oxygen-blown is because less oxygen per pound of coal is required for oxygen-blown operation since air-blown operation requires more coal and air to heat up the nitrogen in the air.

3.5.7 Nitrogen Balance

The TC10 operating period nitrogen balances are plotted in Figure 3.5-9 by comparing the nitrogen in and the nitrogen out and as listed in Table 3.5-3. Nitrogen flows for air-blown test TC10A-1 are shown in Table 3.5-4 and nitrogen flows for oxygen-blown test TC10A-6c are shown on Table 3.5-5. Both the air- and oxygen-blown nitrogen balances were good with errors less than 7 percent for all but two operating periods. TC10A-2 and TC10A-3 had errors of 13 and 11 percent, respectively. The nitrogen balances were made by assuming that 200 lb/hr of nitrogen was lost though seals and lock hopper purges for both air- and oxygen-blown testing. The 200 lb/hr assumption is different than in previous test runs where higher nitrogen losses appeared to be present in air-blown operations. In TC10, however, the air-blown operating pressure was significantly lower (and closer to that of oxygen-blown operation) than it was in previous test runs. Less nitrogen would be lost at lower pressures than at higher pressures.

The nitrogen flows as shown in Tables 3.5-4 and 3-5-5 are dominated by the air, nitrogen, and synthesis-gas flows. None of the solid streams contribute significantly to the nitrogen balance. The TC06 nitrogen balances had a ±5-percent error assuming 1,000 lb/hr of nitrogen lost while TC07 had nitrogen balance errors of ±2 percent assuming 500 lb/hr of nitrogen lost. TC08 nitrogen balances were at 1 to 7 percent for air-blown mode, 2 to 4 percent for enhanced air mode, and -16 to 5 percent for oxygen-blown mode, assuming 1,000 lb/hr nitrogen did not enter the gasifier. TC09 nitrogen balances were within ±5 percent for both air- and oxygen-blown testing, with 1,250 pph of nitrogen assumed lost in air-blown mode and no loss in oxygen-blown mode. The TC10 nitrogen balances are consistent with TC06, TC07, TC08, and TC09 air-blown nitrogen balances. Although the TC10 oxygen-blown nitrogen balances were, for the most part, better than the TC08 oxygen-blown nitrogen balances, they were not quite as good as the oxygen-blown nitrogen balances in TC09.

3.5.8 Sulfur Balance and Sulfur Removal

Sulfur balances for all the TC10 operating periods are given in Figure 3.5-10 and Table 3.5-6. The synthesis gas sulfur compounds used in the mass balance were not directly measured, but estimated from syngas combustor SO_2 analyzer data and synthesis gas combustor flue gas flow. The coal sulfur values were interpolated between the solids sampling times. The sulfur balances for the two air-blown periods had relative errors of +18 and -7 percent. Five of the oxygen-blown sulfur balances were poor with relative errors between +18 and +25 percent. The remaining 14 balances were fair, with relative errors ranging from -7 to 15 percent.

Overall, the TC10 sulfur balances were better than the sulfur balances for TC06, TC07, TC08, and TC09. The TC10 balances appeared to be biased low. Most of the operating period sulfur balances were biased high in TC06 and TC07, and the first TC08 air-blown sulfur balance was neutral with the second air-blown sulfur balance biased high. The TC08 enhanced air sulfur balances were biased high and the TC08 oxygen-blown sulfur balances were biased slightly negative. The TC09 sulfur balances were biased high in oxygen-blown mode and unbiased in air-blown mode.

With the errors in the sulfur balances, it is difficult to determine the correct sulfur removal rate. Similarly to the coal conversions calculations, three different methods exist to determine the Transport Gasifier sulfur removal:

1. From synthesis gas sulfur emissions (using the synthesis gas combustor flue-gas rate and synthesis gas combustor flue-gas SO_2 measurement) and the feed-sulfur rate (using the feed-coal rate and coal sulfur content). (Gas analyses method)
2. From PCD solids analysis (using PCD solids-flow rate and PCD solids sulfur content) and the feed-sulfur rate. (Solids analyses method)
3. From the gas analysis data and the PCD solids data. (Product analyses method)

The three sulfur removals are plotted on Figure 3.5-11 and given on Table 3.5-6. The sulfur in the fuel is an inaccurate measurement due to the multiplication of a very small number (coal sulfur) by a large number (coal-feed rate). The coal rate is determined by carbon balance rather than an actual measurement. The low coal sulfur content (around 0.3-weight percent sulfur) increases the error. The gaseous sulfur flow should be accurate, although it is also the product of a small number (the syngas combustor SO_2 content) and a large number (the syngas combustor flue-gas rate). The PCD fines sulfur rates have inaccuracies due to the low sulfur in the PCD solids. No accumulation of sulfur-containing solids in the gasifier took place during TC10, because the standpipe samples contained negligible amounts of sulfur.

The TC10 results indicate that the gas method is less accurate than the product and the solids methods. The solids and products methods usually agreed with each other and seemed to change slowly and consistently during the run. The gas method varied a lot during the run, and one period actually had a negative sulfur removal (according to the gas method). The negative sulfur removal occurred because the sulfur flow out was larger than the sulfur flow in. The sulfur removal by the products is probably the most reliable sulfur removal calculation method.

The sulfur removal by the products method was 3 and 12 percent during the two air-blown periods, respectively. During the oxygen-blown periods, the products sulfur removal ranged between 2 to 9 percent, with more periods around 6 percent. The solids method sulfur removal tracked the products method sulfur removal. The three methods agreed when the sulfur balance had less than about 2-percent error.

The synthesis gas combustor SO_2 data was used for the sulfur emissions shown in Table 3.5-6. The sulfur emissions were from 0.47 to 0.57 lb SO_2/MBtu coal fed.

Figure 3.5-12 plots the measured sulfur emissions against the coal maximum reduced sulfur emissions. The coal maximum sulfur emissions are the maximum sulfur emissions possible based on the coal-feed rate, coal sulfur level, and syngas-flow rate assuming 0-percent sulfur capture. On Figure 3.5-12, the 45-degree line is the 0-percent sulfur removal line (sulfur emissions equal maximum coal sulfur emissions) and the X-axis is the 100-percent sulfur removal line (0 sulfur emissions). The area of the plot above the 45-degree line indicates less than 0-percent removal—data in this region is the result of errors in the sulfur balance that indicate more sulfur leaving the Transport Gasifier than entering in the feed stocks. This plot is a replotting of the gas method sulfur removal calculation since it is based on the coal-feed sulfur and the syngas sulfur. The data indicate that only a small amount of sulfur removal takes place. No points are above the 0-percent capture line, indicating that some sulfur removal did occur in both operating modes.

The calculation of the minimum equilibrium synthesis H_2S concentration has been described in previous PSDF reports. In summary, the minimum equilibrium H_2S concentration is a function of the partial pressures of H_2O and CO_2 as long as there is calcium sulfide present in the solids. (The equilibrium H_2S concentration is a function of system temperature, while the minimum equilibrium H_2S concentration is not a function of temperature.) As the partial pressures of H_2O and CO_2 increase, the H_2S concentration should increase. Using Aspen simulations, the minimum equilibrium H_2S concentrations were determined for all of the operating periods and listed in Table 3.5-6.

Figure 3.5-13 plots the TRS and equilibrium H_2S directly against each other for TC10. The data should have all fallen above the 45-degree line since the minimum equilibrium H_2S concentration should be the lowest H_2S concentration in a system with calcium sulfide present. Both of the air-blown operating points and about half of the oxygen-blown operating points are above the line, indicating that not enough calcium sulfide was present to capture sulfur to the point of equilibrium. The addition of sorbent would have increased the sulfur capture for these periods, since the sulfur capture was not limited by H_2S equilibrium, but by insufficient sorbent.

The rest of the oxygen-blown data indicate sulfur emissions less than equilibrium. These data points occurred at periods at which the equilibrium H_2S concentration was high. The high H_2S equilibrium concentrations are a result of the higher steam rates and resulting H_2O concentrations used in TC10. If the H_2S equilibrium concentrations are above the measured sulfur emissions, no sulfur capture is possible. Put another way, the comparison of the equilibrium H_2S and measured sulfur emissions indicates that insufficient sulfur exists in the system to form CaS at high syngas moisture levels and low coal sulfur levels, and no amount of sorbent would be able to remove the sorbent at these conditions.

3.5.9 Hydrogen Balance

In previous testing, the steam rate was blamed for most of the errors in the hydrogen and oxygen balances. The TC10 hydrogen and oxygen balances were both poor if the measured steam rate was used in the material balances. For TC10, it was assumed that the steam rate determined by the hydrogen balance was more accurate than the measured steam rate. The steam rate for each operating period was calculated using a hydrogen balance, which is essentially the difference in hydrogen between the coal-feed and synthesis gas rate. The hydrogen balance steam rate is compared with the measured steam rate on Figure 3.5-14. The measured steam rate is from a PI tag that sums the steam rate to the gasifier from FI204 (total steam flow to the UMZ), FI727B (steam mixed with the air fed to the LMZ), FI734 (steam fed into the LMZ), and FI733 (steam fed to a shroud into the LMZ). The tag rejects any steam flows that are negative. The hydrogen balance steam rates were usually 10 to 40 percent higher than the measured steam rates, with one outlier. Using the measured steam rates would cause the hydrogen and oxygen balances to be severely in error.

Typical hydrogen flows for air-blown test TC10A-1 are shown in Table 3.5-4 and typical hydrogen flows for oxygen-blown test TC10A-6c are shown on Table 3.5-5. Note the lower steam rate in the air-blown mode example. The coal, steam, and synthesis gas streams dominate the hydrogen balance. The hydrogen balance was -20 to 0 percent for TC06, -30 to 0 percent for TC07, and 0 to 12 percent in TC08. Like TC10, TC09 used the calculated steam-flow rate, and thus, the balance was perfect.

In TC07, the hydrogen balance indicated that there was about 500 pounds more steam per hour than measured being fed to the Transport Gasifier. During TC08, with either the enhanced air- or oxygen-blown modes, the steam rate by hydrogen balance was less than the measured steam rate by about 200 to 500 lb/hr of steam. The second air-blown mode indicates that about 500 pounds more steam per hour is being fed to the Gasifier than reported by the measured steam rate. The TC09 hydrogen balance was very similar to that observed in TC10, with the calculated steam rates running between 10 and 50 percent higher than the measured steam-flow rates.

3.5.10 Oxygen Balance

Operating period oxygen balances are given in Figure 3.5-15 and Table 3.5-3. Typical oxygen flows for air-blown test TC10A-1 are shown in Table 3.5-4 and typical oxygen flows for oxygen blown test TC10A-6c are shown on Table 3.5-5. The oxygen balance is determining if the steam and oxygen or air rates are consistent with the synthesis gas rate and composition.

The TC10 operating period oxygen balances for air-blown mode were good with less than ±4 percent relative error. The TC10 oxygen-blown mode oxygen balances were good with all operating periods less than ±9 percent relative error with a low bias. Using the measured steam rates would have put the oxygen balances off by about 15 to 20 percent. The good oxygen balances indicate that the measured steam rates were not consistent with the rest of the TC10 data, while the hydrogen balance steam rates were consistent.

The TC06 oxygen balances were off by -20 to -4 percent and the TC07 oxygen balances were off by -20 to -5 percent. The TC08 oxygen balances were from 0 to 12 percent (0 to 859 lb/O_2/hr). The TC09 (off by about ±7) oxygen balances were better than the TC06 through TC08 oxygen balances, which used the measured steam rates. Although the TC10 balances were not quite as close as TC09, they were still much better than those in TC06, TC07, and TC08.

3.5.11 Calcium Balance

Operating period calcium balances are given in Figure 3.5-16 and Table 3.5-3. Typical calcium flows for air-blown test TC10A-1 are shown in Table 3.5-4 and typical calcium flows for oxygen-blown test TC10A-6c are shown on Table 3.5-5. The calcium balances are essentially a comparison between the coal calcium and the PCD fines calcium, since no sorbent feed to the gasifier occurred during TC10. There was minimal flow through FD0510, and the gasifier accumulation term was assumed to be small. The gasifier accumulation term was assumed to be negligible because typically the gasifier solids level does not vary much during operating periods.

Except for one operating period with 5-percent relative error, the calcium balances were unacceptable during the TC10 operating periods. The relative errors ranged from 5 to 111 percent. All of the calcium balances had a negative bias. Obtaining a good calcium balance is difficult because the comparison is between two difficult-to-measure solid streams. The calcium balances were the best during the middle of TC10, around hour 136, and the worst around hours 37 and 272. Note that the TC10 calcium rates are lower than TC06 and TC07 due to no sorbent feed in TC10. TC10 calcium rates were consistent with TC08 and TC09 that also had no sorbent feed. In TC06 the calcium balances were off by -50 to +40 percent, in TC07 the calcium balances were off by -100 to +40 percent, and the TC08 calcium balances were off by ±40 percent. The TC09 calcium balances were off by -20 to +80 percent with a negative bias.

Figure 3.5-17 plots TC10 sulfur removal by-products method as a function of calcium to sulfur molar ratio (Ca/S, molecular weight) measured in the PCD solids samples from FD0520. The sulfur removals were 2 to 7 percent with one outlier at 9 percent and another at 12 percent. The removals were consistent with TC08 PRB sulfur removals with no sorbent addition. The trends in the PCD solids Ca/S with sulfur emissions on Figure 3.5-17 seem to suggest that the sulfur removal decreased with increasing Ca/S ratio, but increased sorbent should lead to increased sulfur removal, and the sulfur removal should increase with Ca/S. Since the sulfur capture is in fact limited by gas phase equilibrium, the amount of excess calcium does not always effect sulfur capture. The results seen on Figure 3.5-17 demonstrate that when the PCD solids contain very little sulfur (high Ca/S) the sulfur removals are low, which is reasonable by sulfur balance. The calcium sulfation percent is the reciprocal (times 100) of the Ca/S ratio based on the PCD fines solids. The PCD fines Ca/S and the percent sulfation are both based on the sulfur captured by the PCD fines. TC06 had 10- to 55-percent sulfur removal, TC07 had 5- to 50-percent sulfur removal, and TC08 had 0- to 17-percent sulfur removal. TC09 experienced 0- to 18-percent sulfur removal. The lower sulfur removal for test runs TC08 through TC10 were due to the absence of limestone feed, the high steam rates, and the resulting high syngas H_2O concentrations. Due to the low sulfur level in the coals gasified to date and the low sulfur removals without sorbent, it is difficult to determine the effect of equilibrium H_2S on the sulfur removals. However, it can be concluded that sorbent addition increases sulfur capture.

Figure 3.5-18 plots TC10 sulfur emissions (expressed as lb of SO_2 emitted per MBtu coal fed) as a function of moles calcium/moles sulfur (Ca/S) measured in the PCD solids sampled from FD0520. The sulfur emissions varied from 0.47 to 0.57 pounds SO_2 emitted per MBtu coal fed with no trend with Ca/S ratio. The sulfur emissions were similar for both oxygen- and air-blown mode. TC06 sulfur emissions were from 0.13 to 0.37 pounds SO_2 per MBtu, TC07 sulfur emissions were from 0.15 to 0.47 pounds SO_2 per MBtu, and TC08 were from 0.4 to 0.7 as pounds SO_2 emitted per MBtu coal. TC09 sulfur emissions were from 0.6 to 1.0 lb/MBtu. TC08 and TC09 had similar sulfur emissions due to the higher steam rates than in TC06 and TC07. The steam flow rates in TC10 were slightly lower than those in TC08 and TC09, allowing for lower sulfur emissions.

3.5.12 Energy Balance

The TC10 Transport Gasifier energy balance is given in Figure 3.5-19 with standard conditions chosen to be 1.0 atmosphere pressure and 80°F temperature. Table 3.5-7 breaks down the individual components of the energy balance for each operating period. The "energy in" consists of the coal, air, and steam fed to the Transport Gasifier. The nitrogen, oxygen, and sorbent fed to the gasifier were considered to be at the standard conditions (80°F) and hence have zero enthalpy. The energy out consisted of the synthesis gas and PCD solids. The lower heating value of the coal and PCD solids were used in order to be consistent with the lower heating value of the synthesis gas. The energy of the synthesis gas was determined at the Transport Gasifier cyclone exit. About 1,200 pounds of N_2 per hour fed to the PCD inlet and outlet particulate sampling trains has been subtracted from the synthesis gas rate to determine the actual syngas rate from the cyclone. The sensible enthalpy of the synthesis gas was determined by overall gas heat capacity from the synthesis gas compositions and the individual gas heat capacities. The synthesis gas and PCD solids energy consists of both latent and sensible heat. The heat loss from the Transport Gasifier was estimated to be 1.5 x 10^6 Btu/hr based on a previous combustion test. It is possible that the actual Transport Gasifier heat losses are higher than the 1.5 x 10^6 Btu/hr measured. The energy balance errors would all be between $\pm$ 0 percent if the gasifier heat loss is increased to 3.5 MBtu/hr.

The TC10 energy balances had from +2- to +17-percent errors, with a consistent positive bias. The two air-blown energy balances (errors of 2 and 7 percent) were much closer than the oxygen-blown energy balances (errors between 9 and 17 percent). The negative carbon balance errors and the positive energy balance errors were both minimized by choosing the Transport Gasifier carbon balance coal rate.

3.5.13 Gasification Efficiencies

Gasification efficiency is defined as the percent of energy in (coal energy and steam energy) that is converted to potentially useful synthesis gas energy. Two types of gasification efficiencies have been defined, which are the cold-gas efficiency and the hot-gas efficiency. The cold-gas efficiency is the amount of energy feed that is available to a gas turbine as synthesis gas latent heat.

Similar to sulfur removal, the cold-gas efficiency can be calculated at least three different ways. Since the energy balance is off by up to 17 percent, each result could be different. If there were a perfect energy balance, all three calculations would produce the same result. Three calculation methods were performed for cold-gasification efficiency consistent with the three methods of sulfur removal:

1. Based on the feed heat (coal latent heat plus steam heat) and the latent heat of the synthesis gas. This assumes that the feed heat and the synthesis gas latent heat are correct. (Gas analyses)
2. Based on the feed heat (coal latent heat plus steam heat) and the latent heat of the synthesis gas determined by a Transport Gasifier energy balance, not the gas analyses. This assumes that the synthesis gas latent heat is incorrect. (Solids analyses)
3. Based on the feed heat determined by Transport Gasifier energy balance and the synthesis gas sensible heat. This assumes that the coal feed or the steam rate is in error. (Products analyses)

The cold-gas gasification efficiencies for the three calculation methods are plotted in Figure 3.5-20. For all of the operating periods, the products method is between the solids and gas methods. The gas method is lower than the solids method and the products method for all TC10 operating periods, since all of the energy balances are biased high. The three methods agree more closely with each other whenever the energy balance is close to being perfect (hours 22 and 121). Only the products method is listed on Table 3.5-7 because the products method is the most accurate method, since it does not use the coal-feed rate.

The products analysis cold-gas gasification efficiencies started TC10 at nearly 57 percent due to the high coal rate and low steam rate. The cold-gas efficiency increased to over 60 percent, once the system was placed in oxygen-blown mode. The oxygen-blown tests had higher cold-gas efficiency than the air-blown modes at the same steam to coal ratio by about 10 percent because the air blown modes had the inefficiency of heating up the air nitrogen. Later the efficiency increased to as high as 69 percent before falling to 52 percent, when the system returned to air-blown operations. Once placed back in oxygen-blown mode, the system again experienced efficiencies between 62 and 68 percent for the remainder of TC10.

The hot-gasification efficiency is the amount of feed energy that is available to a gas turbine plus a heat recovery steam generator. The hot-gas efficiency counts both the latent and sensible heat of the synthesis gas. Similar to the cold-gasification efficiency and the sulfur removal, the hot-gas efficiency can be calculated at least three different ways. The three calculation methods for hot gasification are identical with the three methods of cold-gasification efficiency calculation except for the inclusion of the synthesis gas sensible heat into the hot-gasification efficiency.

The hot-gasification efficiency assumes that the sensible heat of the synthesis gas can be recovered in a heat recovery steam generator, so the hot-gasification efficiency is always higher than the cold-gasification efficiency. The three hot gasification calculation methods are plotted in Figure 3.5-21 and the product method shown on Table 3.5-7.

For all of the operating periods the products method is essentially equal to the solids method, because the amount of inlet coal heat is about the same as the total synthesis gas heat, and whether the synthesis gas heat or the coal heat is corrected makes little difference. The gas method is lower than the solids and products when the energy balance has a high bias.

As with the cold-gasification efficiencies, the hot-gasification efficiencies started TC10 high, at 92 percent due to low steam rates and high coal rates. During the oxygen-blown mode testing, the hot-gasification efficiencies were between 85 and 92 percent. Oxygen-blown hot-gasification efficiencies tend to be lower than air-blown hot-gasification efficiencies, since the air blown syngas sensible heat is higher than the oxygen-blown syngas sensible heat due to the higher air-blown syngas rate. In TC10, however, the oxygen- and air-blown values were close.

Two main sources of losses in efficiency are the gasifier heat loss and the latent heat of the PCD solids. The gasifier heat loss of 1.5 million Btu/hr was about 5 percent of feed energy, while the total energy of the PCD solids was about 4 percent of the feed energy. The heat loss percentage will decrease as the gasifier size is increased. While the Transport Gasifier does not recover the latent heat of the PCD solids, this latent heat could be recovered in a combustor. The total enthalpy of the PCD solids can be decreased by decreasing both the PCD solids carbon content (heating value) and the PCD solids rate.

Gasification efficiencies can be calculated from the adiabatic nitrogen-corrected gas heating values and corrected flow rates that were determined in Section 3.3. The products adiabatic nitrogen-corrected cold-gasification efficiencies are plotted on Figure 3.5-22 and are listed on Table 3.5-7 for all of the operating periods. Only the cold gasification efficiencies based on the products are given in Figure 3.5-22 and Table 3.5-7, because they are the most representative of the actual gasification efficiencies. Since the nitrogen and adiabatic syngas LHV corrections reduce the coal rate and the steam rate (for oxygen-blown operating periods only), the corrected coal rates and the corrected steam rates were used in Figure 3.5-22. The corrected efficiencies are calculated assuming an adiabatic gasifier, since zero heat loss was one of the assumptions in determining the corrected LHV in Section 3.3. The corrected cold-gas efficiencies were 68 and 73 percent for the two air-blown operating periods and from 79 to 83 percent for oxygen-blown mode. The nitrogen and adiabatic corrections increased the cold-gasification efficiencies by about 15 percent in air-blown mode and by about 20 percent in oxygen-blown mode due to the use of recycle gas rather than nitrogen for aeration and instrument purges.

The adiabatic nitrogen correction does not increase the hot gasification efficiency because the deleted nitrogen lowers the synthesis gas sensible heat and increases the synthesis gas latent heat. Both changes effectively cancel each other out.

Table 3.5-1

Feed Rates, Product Rates, and Mass Balance

Operating Period	Average Relative Hours	Feeds (In) Coal[4] lb/hr	Coke Br.[5] FD0220 lb/hr	Air FI205 lb/hr	Oxygen FI726 lb/hr	Nitrogen FI609[1] lb/hr	Steam lb/hr	Total lb/hr	Products (Out) Syngas FI465 lb/hr	PCD Solids FD0520 lb/hr	SP Solids FD0510[2] lb/hr	Total lb/hr	Mass Balance In - Out lb/hr	(In- Out)/In %	Oxygen/ Coal Ratio
TC10A-1	22	3,463	0	12,489	0	7,610	1,000	24,563	23,920	345	0	24,264	298	1.2	0.84
TC10A-2	37	3,116	0	0	2,190	7,533	2,638	15,477	16,595	365	0	16,960	-1,483	-9.6	0.70
TC10A-3	62	3,427	0	0	2,070	6,578	2,043	14,117	14,928	354	0	15,282	-1,166	-8.3	0.60
TC10A-4a	70	4,079	0	0	2,302	6,389	1,698	14,468	14,835	343	0	15,179	-711	-4.9	0.56
TC10A-6a	92	3,839	0	0	2,305	6,834	1,739	14,718	15,052	314	0	15,366	-648	-4.4	0.60
TC10A-6b	100	3,691	0	0	2,283	7,022	1,764	14,760	14,451	303	0	14,754	5	0.0	0.62
TC10A-6c	108	3,698	0	0	2,341	7,043	1,921	15,003	14,648	293	0	14,940	63	0.4	0.63
TC10A-7	121	3,271	0	11,129	0	6,437	875	21,712	21,790	275	0	22,065	-353	-1.6	0.79
TC10A-8	136	4,062	0	0	2,457	6,386	2,781	15,686	16,389	255	0	16,644	-958	-6.1	0.60
TC10A-9	150	3,766	0	0	2,302	6,304	1,722	14,094	13,801	257	0	14,057	36	0.3	0.61
TC10B-1	182	3,472	0	0	2,207	6,660	1,738	14,077	13,643	292	0	13,935	143	1.0	0.64
TC10B-2a	191	3,603	0	0	2,318	6,957	1,610	14,488	14,371	302	0	14,673	-185	-1.3	0.64
TC10B-3b	216	3,758	0	0	2,419	6,563	1,556	14,296	14,340	331	0	14,671	-374	-2.6	0.64
TC10B-4a	231	3,211	0	0	2,236	7,053	1,435	13,936	14,258	346	0	14,604	-669	-4.8	0.70
TC10B-4b	240	3,388	0	0	2,205	6,849	1,627	14,069	14,081	348	0	14,429	-360	-2.6	0.65
TC10B-4c	248	3,422	0	0	2,156	6,858	1,666	14,102	13,846	348	0	14,194	-92	-0.6	0.63
TC10B-5	272	3,828	0	0	2,243	7,119	1,404	14,595	14,107	482	0	14,588	7	0.0	0.59
TC10B-7	313	3,680	0	0	2,325	6,998	1,706	14,709	14,993	283	0	15,275	-567	-3.9	0.63
TC10B-8	321	3,521	0	0	2,253	7,184	1,807	14,765	14,437	250	0	14,686	79	0.5	0.64
TC10B-9	328	3,142	0	0	2,166	7,158	1,723	14,189	14,808	223	0	15,031	-842	-5.9	0.69
TC10B-10	335	3,744	0	0	2,365	6,834	1,691	14,634	15,162	312	0	15,474	-840	-5.7	0.63

Notes:

1. Nitrogen feed rate reduced by 200 pounds per hour to account for losses in feed systems and seals.
2. FD0510 was not operated during any test period.
3. TC10A-1 to TC10A-7 were air-blown; all others were oxygen-blown.
4. Coal Rate by Transport Gasifier carbon balance.
5. Coke breeze was not added during the TC10 operating periods.

Table 3.5-2

Carbon Rates

	Average	Carbon In (Feed)			Carbon Out (Products)				Carbon
Operating Period	Relative Hours	Coal[1] lb/hr	Coke B. lb/hr	Total lb/hr	Syngas lb/hr	Standpipe[2] lb/hr	PCD Solids lb/hr	Total lb/hr	Conversion %
TC10A-1	22	1,904	0	1,904	1,829	0.0	75	1,904	96.1
TC10A-2	37	1,699	0	1,699	1,633	0.0	66	1,699	96.1
TC10A-3	62	1,848	0	1,848	1,738	0.0	110	1,848	94.1
TC10A-4a	70	2,209	0	2,209	2,091	0.0	117	2,209	94.7
TC10A-6a	92	2,098	0	2,098	1,994	0.0	104	2,098	95.1
TC10A-6b	100	2,006	0	2,006	1,926	0.0	80	2,006	96.0
TC10A-6c	108	1,998	0	1,998	1,948	0.0	50	1,998	97.5
TC10A-7	121	1,754	0	1,754	1,639	0.0	115	1,754	93.4
TC10A-8	136	2,167	0	2,167	2,114	0.0	52	2,167	97.6
TC10A-9	150	2,006	0	2,006	1,916	0.0	90	2,006	95.5
TC10B-1	182	1,858	0	1,858	1,751	0.0	107	1,858	94.2
TC10B-2a	191	1,924	0	1,924	1,813	0.0	111	1,924	94.2
TC10B-3b	216	2,007	0	2,007	1,883	0.0	124	2,007	93.8
TC10B-4a	231	1,720	0	1,720	1,588	0.0	132	1,720	92.3
TC10B-4b	240	1,819	0	1,819	1,685	0.0	134	1,819	92.6
TC10B-4c	248	1,841	0	1,841	1,705	0.0	135	1,841	92.7
TC10B-5	272	2,070	0	2,070	1,878	0.0	192	2,070	90.7
TC10B-7	313	1,970	0	1,970	1,872	0.0	98	1,970	95.0
TC10B-8	321	1,882	0	1,882	1,806	0.0	76	1,882	95.9
TC10B-9	328	1,678	0	1,678	1,615	0.0	63	1,678	96.2
TC10B-10	335	1,999	0	1,999	1,911	0.0	88	1,999	95.6

Notes:

1. Coal carbon determined by Transport Gasifier carbon balance.
2. Standpipe carbon flow intermittent. Rate shown is average FD0510 rate during operating period.
3. TC10A-1 to TC10A-7 were air-blown; all others were oxygen-blown.

Table 3.5-3

Nitrogen, Oxygen, and Calcium Mass Balances

		Nitrogen[1]		Oxygen		Calcium	
	Average	(In- Out)		(In- Out)		(In- Out)	
Operating	Relative	In	In - Out	In	In - Out	In	In - Out
Period	Hours	%	lb/hr	%	lb/hr	%	lb/hr
TC10A-1	22	0.5	93	4.0	200	-17.2	-5
TC10A-2	37	-12.8	-969	-7.6	-422	-96.2	-24
TC10A-3	62	-10.9	-718	-8.9	-446	-73.3	-20
TC10A-4a	70	-5.2	-332	-8.2	-423	-41.2	-13
TC10A-6a	92	-3.1	-216	-8.1	-416	-37.1	-11
TC10A-6b	100	4.0	282	-5.7	-290	-37.8	-11
TC10A-6c	108	4.4	309	-4.7	-251	-32.6	-10
TC10A-7	121	3.8	607	-3.0	-134	-41.0	-11
TC10A-8	136	2.1	155	-5.5	-344	-5.3	-2
TC10A-9	150	6.9	462	-3.9	-198	-14.2	-4
TC10B-1	182	5.9	397	-6.2	-306	-40.9	-11
TC10B-2a	191	3.7	272	-4.6	-231	-40.5	-12
TC10B-3b	216	-1.2	-85	-2.7	-136	-47.5	-14
TC10B-4a	231	-5.6	-415	-0.1	-5	-80.7	-21
TC10B-4b	240	-0.4	-26	-2.9	-140	-72.2	-20
TC10B-4c	248	-0.4	-31	-2.0	-96	-70.5	-19
TC10B-5	272	3.6	255	-4.9	-236	-111.0	-34
TC10B-7	313	0.3	21	-3.8	-194	-28.7	-8
TC10B-8	321	3.1	221	-4.1	-209	-18.9	-5
TC10B-9	328	1.1	88	-4.1	-195	-19.2	-5
TC10B-10	335	2.3	173	-4.9	-252	-39.8	-12

Notes:

1. Nitrogen feed rate reduced by 200 pounds per hour to account for losses in feed system.
2. TC10A-1 and TC10A-7 were air blown. All others were oxygen-blown.

Table 3.5-4

Typical Air-Blown Component Mass Balances

	Nitrogen[1]	Hydrogen	Oxygen	Calcium
Operating Period	TC10A-1	TC10A-1	TC10A-1	TC10A-1
Date Start	11/19/2002	11/19/2002	11/19/2002	11/19/2002
Time Start	7:15	7:15	7:15	7:15
Time End	15:15	15:15	15:15	15:15
Fuel	PRB	PRB	PRB	PRB
Riser Temperature, ^{O}F	1,751	1,751	1,751	1,751
Pressure, psig	180	180	180	180
In, pounds/hr				
Fuel	25	205	1,163	28
Coke Breeze				
Air	9,526		2,894	
Nitrogen	7,613			
Steam		111	889	
Total	17,164	316	4,946	28
Out, pounds/hr				
Synthesis Gas	17,071	314	4,706	
PCD Solids	1	2	41	32
Reactor				
Total	17,071	316	4,747	32
(In-Out)/In, %	0.5%	0.0%	4.0%	-17.2%
(In-Out), pounds per hour	93	0	200	-5

Note: 1. Feed nitrogen decreased by 200 pounds per hour.

Table 3.5-5

Typical Oxygen-Blown Component Mass Balances

	Nitrogen[1]	Hydrogen	Oxygen	Calcium
Operating Period	TC10A-6c	TC10A-6c	TC10A-6c	TC10A-6c
Date Start	11/23/02	11/23/02	11/23/02	11/23/02
Time Start	6:00	6:00	6:00	6:00
Time End	13:45	13:45	13:45	13:45
Fuel	PRB	PRB	PRB	PRB
Riser Temperature, ^{O}F	1,723	1,723	1,723	1,723
Pressure, psig	152	152	152	152
In, pounds/hr				
Fuel	27	219	1,242	30
Coke Breeze				
Oxygen			2,341	
Nitrogen	7,043			
Steam		213	1,708	
Total	7,070	432	5,291	30
Out, pounds/hr				
Synthesis Gas	6,762	431	5,507	
PCD Solids	1	1	35	39
Reactor				
Total	6,763	432	5,542	39
(In-Out)/In, %	4.3%	0.0%	-4.7%	-32.6%
(In-Out), pounds per hour	307	0	-251	-10

Note: 1. Feed nitrogen decreased by 200 pounds per hour.

Table 3.5-6

Sulfur Balances

Operating Period	Average Relative Hours	Feeds (In) Coal lb/hr	Products (Out) Syngas lb/hr	PCD Solids lb/hr	SP Solids lb/hr	Total lb/hr	In - Out lb/hr	(In- Out)/In %	Sulfur Removal Gas[4] %	Products %	Solids %	Sulfur Emissions lb SO_2/MMBtu	Equilibrium H_2S ppm	Measured TRS ppm
TC10A-1	22	11.3	9.0	0.3	0.0	9.3	2.1	18.1	21	3	3	0.55	191	317
TC10A-2	37	9.9	7.3	0.2	0.0	7.4	2.4	24.6	26	2	2	0.50	560	346
TC10A-3	62	10.4	7.6	0.4	0.0	8.0	2.3	22.5	27	5	4	0.47	499	401
TC10A-4a	70	12.7	9.9	0.4	0.0	10.3	2.3	18.4	22	4	4	0.52	428	521
TC10A-6a	92	12.4	9.4	0.5	0.0	9.8	2.6	20.8	25	5	4	0.52	444	489
TC10A-6b	100	11.2	8.6	0.4	0.0	9.0	2.2	19.7	24	5	4	0.50	453	466
TC10A-6c	108	10.5	9.0	0.3	0.0	9.3	1.2	11.5	14	3	3	0.52	473	480
TC10A-7	121	8.5	8.0	1.1	0.0	9.1	-0.6	-7.4	6	12	13	0.52	212	311
TC10A-8	136	10.6	10.9	0.4	0.0	11.3	-0.7	-7.1	0	4	4	0.57	580	512
TC10A-9	150	9.8	9.5	0.4	0.0	9.9	-0.2	-1.6	3	4	4	0.54	482	539
TC10B-1	182	10.0	8.0	0.6	0.0	8.5	1.4	14.5	20	6	6	0.49	528	459
TC10B-2a	191	10.0	8.3	0.6	0.0	8.9	1.0	10.5	16	6	6	0.49	516	460
TC10B-3b	216	9.9	9.8	0.6	0.0	10.4	-0.5	-5.5	1	6	6	0.55	447	540
TC10B-4a	231	8.5	8.5	0.7	0.0	9.2	-0.6	-7.4	0	7	8	0.56	391	478
TC10B-4b	240	9.1	9.0	0.7	0.0	9.6	-0.5	-6.0	1	7	7	0.56	445	505
TC10B-4c	248	9.2	8.7	0.7	0.0	9.3	-0.1	-1.3	6	7	7	0.54	449	495
TC10B-5	272	10.7	8.7	0.9	0.0	9.6	1.1	10.5	19	9	8	0.48	413	487
TC10B-7	313	10.0	8.1	0.6	0.0	8.7	1.4	13.6	19	7	6	0.47	438	427
TC10B-8	321	9.5	8.1	0.4	0.0	8.5	1.0	10.9	15	4	4	0.49	480	446
TC10B-9	328	8.5	7.2	0.2	0.0	7.4	1.1	12.5	15	3	3	0.49	453	388
TC10B-10	335	10.1	9.1	0.3	0.0	9.5	0.6	6.4	10	4	3	0.52	444	478

Notes:

1. Synthesis gas sulfur emissions determined from synthesis gas combustor SO_2 analyzer.
2. There was no sorbent feed to the Transport Gasifier during TC10
3. Negative sulfur removals were assumed to actually be 0% sulfur removal.

Table 3.5-7

Energy Balance[3]

Operating Period[4]	Average Relative Hours	Feeds (In)[1]				Products (Out)					In - Out	(In- Out)/In	Efficiency		
													Raw		Corrected[2]
		Coal	Air	Steam	Total	Syngas	PCD Solids	Gasifier Solids	Heat Loss	Total			Cold	Hot	Cold
		10^6 Btu/hr	10^6 Btu/hr	10^6 Btu/hr	10^6 Btu/hr	10^6 Btu/hr	10^6 Btu/hr	10^6 Btu/hr	10^6 Btu/hr	10^6 Btu/hr	10^6 Btu/hr	%	%	%	%
TC10A-1	22	29.5	0.8	1.1	31.4	28.0	1.1	0.00	1.5	30.6	0.7	2.3	56.9	91.5	72.5
TC10A-2	37	26.6	0.0	3.6	30.1	22.4	1.0	0.00	1.5	24.9	5.3	17.4	57.6	89.8	78.8
TC10A-3	62	29.2	0.0	2.7	31.9	24.2	1.7	0.00	1.5	27.4	4.5	14.0	62.2	88.3	79.2
TC10A-4a	70	34.8	0.0	2.0	36.8	29.8	1.8	0.00	1.5	33.1	3.6	9.8	67.9	89.9	81.1
TC10A-6a	92	32.7	0.0	2.2	34.9	27.8	1.6	0.00	1.5	30.9	4.0	11.5	66.8	90.0	81.1
TC10A-6b	100	31.5	0.0	2.1	33.6	27.1	1.2	0.00	1.5	29.8	3.8	11.5	67.8	91.1	82.2
TC10A-6c	108	31.5	0.0	2.2	33.8	27.4	0.7	0.00	1.5	29.6	4.2	12.3	68.9	92.6	83.3
TC10A-7	121	27.9	0.7	0.1	28.6	23.5	1.7	0.00	1.5	26.6	2.0	6.9	52.5	88.1	68.0
TC10A-8	136	34.6	0.0	3.2	37.8	30.1	0.8	0.00	1.5	32.5	5.3	14.1	67.6	92.9	81.7
TC10A-9	150	32.1	0.0	1.6	33.7	27.1	1.4	0.00	1.5	30.0	3.7	10.9	68.2	90.2	81.4
TC10B-1	182	29.6	0.0	2.2	31.8	23.7	1.6	0.00	1.5	26.8	5.0	15.6	64.7	88.3	79.2
TC10B-2a	191	30.7	0.0	1.8	32.6	24.8	1.7	0.00	1.5	28.0	4.5	13.9	65.2	88.6	79.9
TC10B-3b	216	32.0	0.0	1.7	33.8	26.1	1.9	0.00	1.5	29.5	4.3	12.6	66.3	88.4	80.0
TC10B-4a	231	27.4	0.0	1.7	29.1	22.2	2.0	0.00	1.5	25.8	3.3	11.4	62.2	86.3	79.1
TC10B-4b	240	28.9	0.0	1.7	30.6	23.3	2.1	0.00	1.5	26.8	3.7	12.2	63.6	86.7	79.0
TC10B-4c	248	29.2	0.0	1.6	30.8	24.1	2.1	0.00	1.5	27.6	3.2	10.3	65.1	87.0	79.9
TC10B-5	272	32.6	0.0	1.2	33.8	26.2	3.0	0.00	1.5	30.7	3.1	9.2	65.2	85.5	78.4
TC10B-7	313	31.4	0.0	1.6	33.0	26.0	1.5	0.00	1.5	28.9	4.1	12.3	67.3	89.7	82.0
TC10B-8	321	30.0	0.0	1.5	31.5	24.6	1.2	0.00	1.5	27.3	4.2	13.5	67.5	90.2	82.4
TC10B-9	328	26.8	0.0	1.7	28.5	21.8	1.0	0.00	1.5	24.3	4.2	14.8	63.8	89.8	82.1
TC10B-10	335	31.9	0.0	1.6	33.6	26.2	1.4	0.00	1.5	29.1	4.5	13.4	67.3	90.2	82.0

Notes:

1. Nitrogen and sorbent assumed to enter the system at ambient temperature and therefore have zero enthalpy.
2. Correction is to assume that only air nitrogen is in the synthesis gas and that the gasifier is adiabatic
3. Reference conditions are 80°F and 14.7 psia.
4. TC10A-1 and TC10A-7 were air-blown. All others were oxygen-blown.

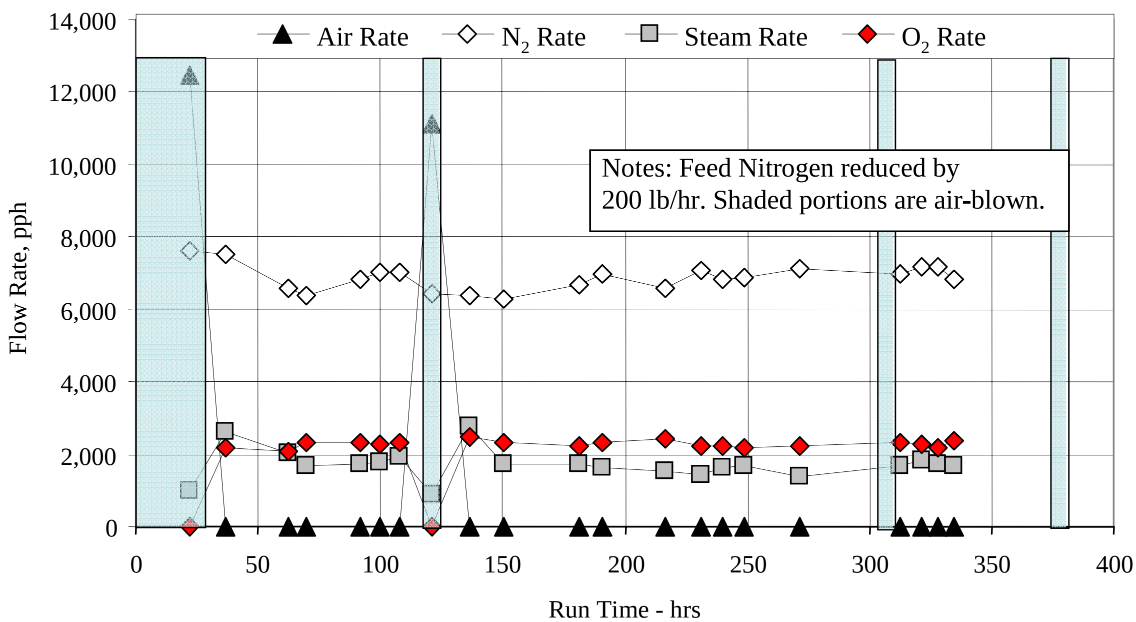

Figure 3.5-1 Air, Nitrogen, Oxygen, and Steam Rates

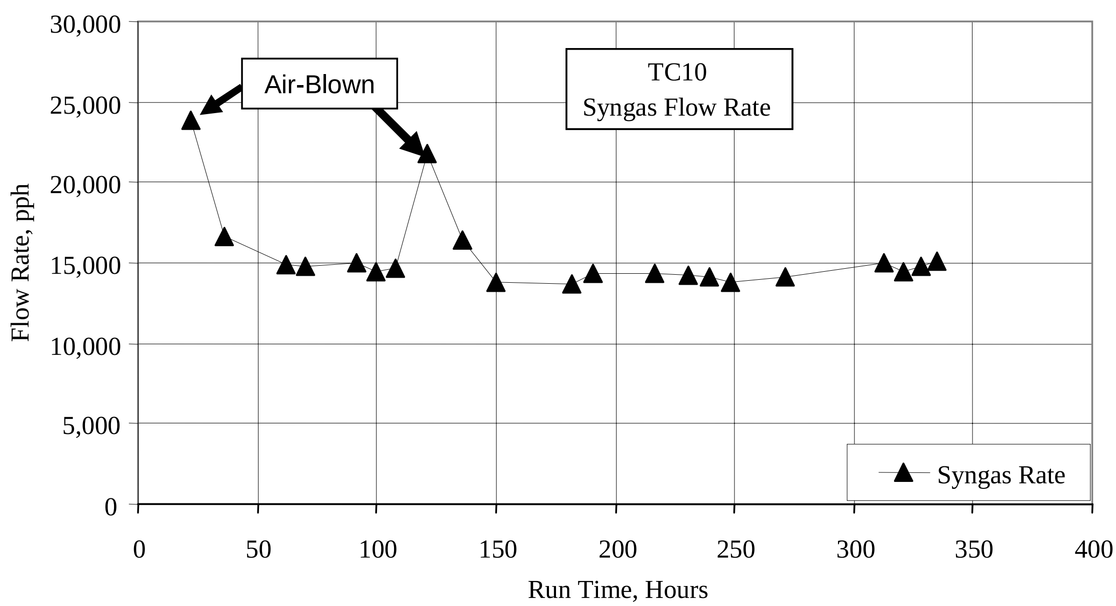

Figure 3.5-2 Syngas Flow Rates

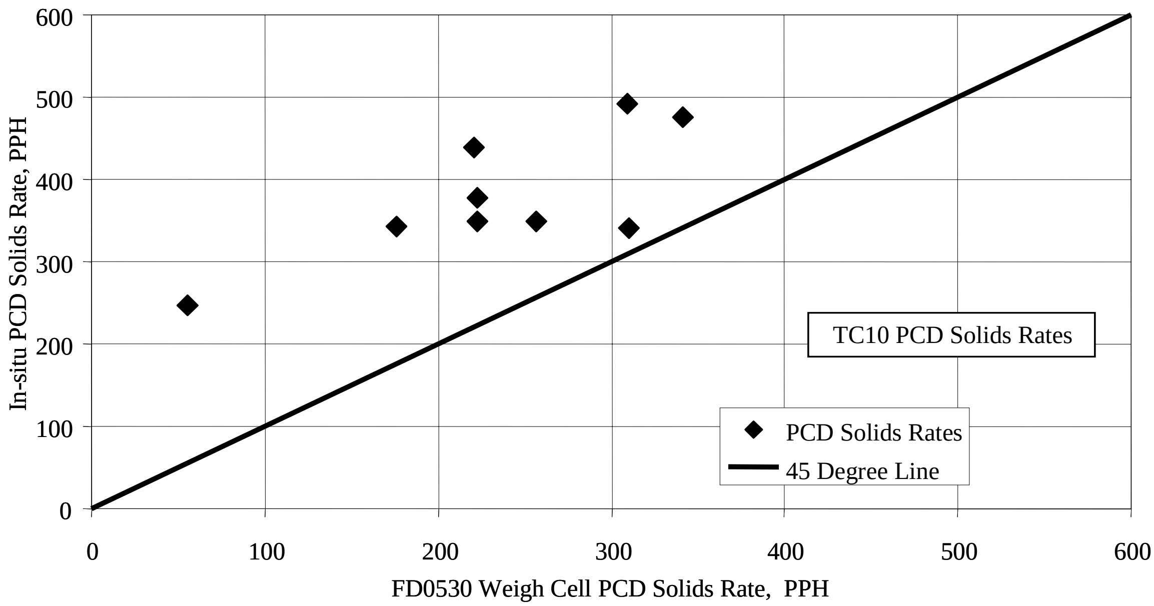

Figure 3.5-3 PCD Fines Rates

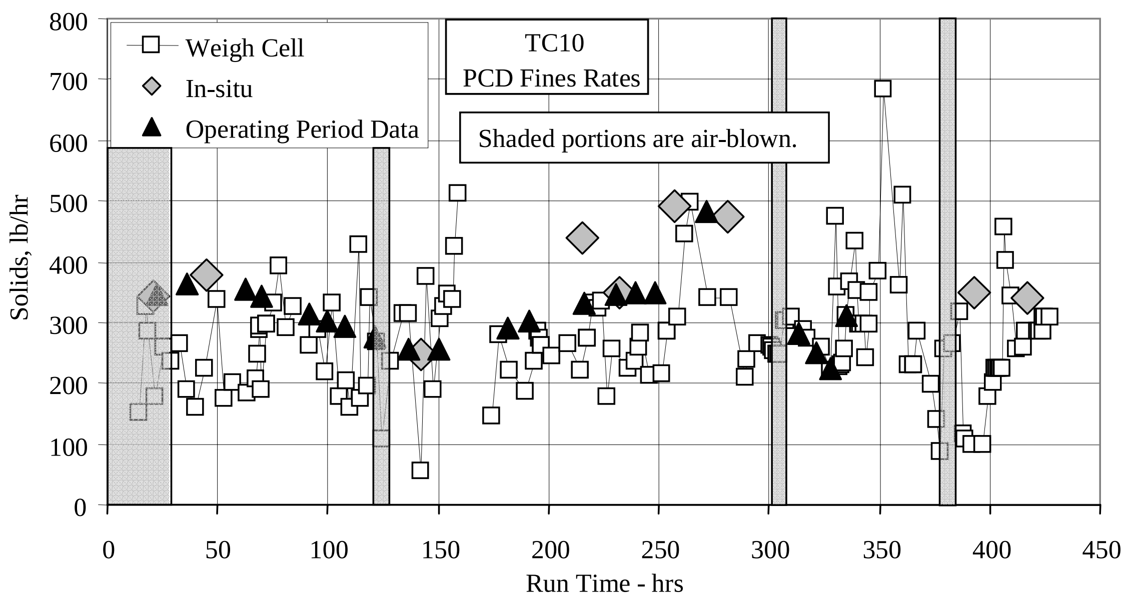

Figure 3.5-4 PCD Fines Rates

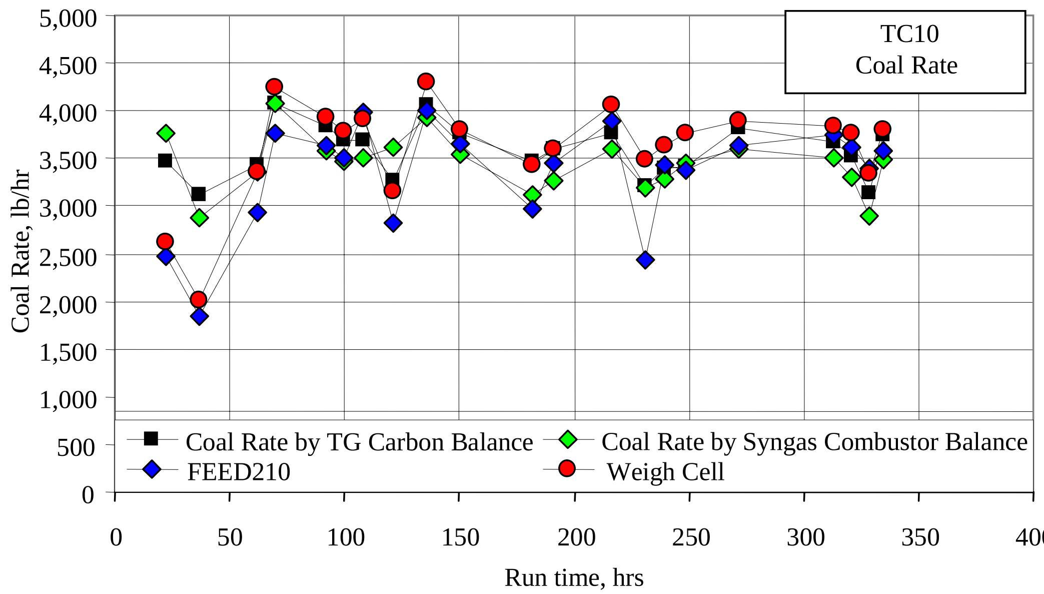

Figure 3.5-5 Coal-Feed Rates

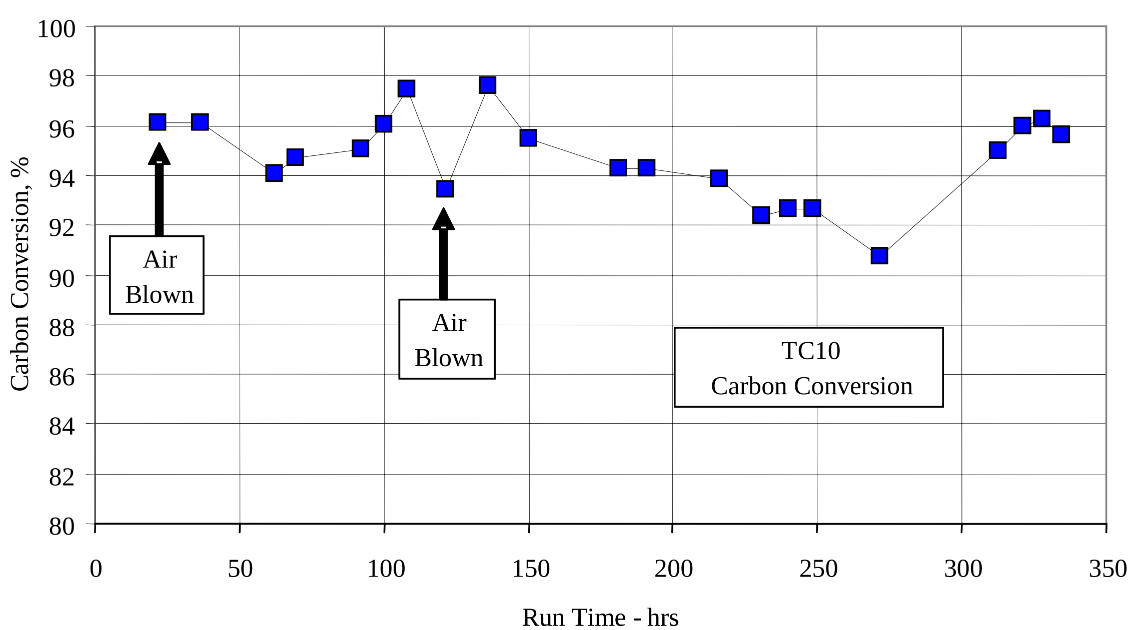

Figure 3.5-6 Carbon Conversion

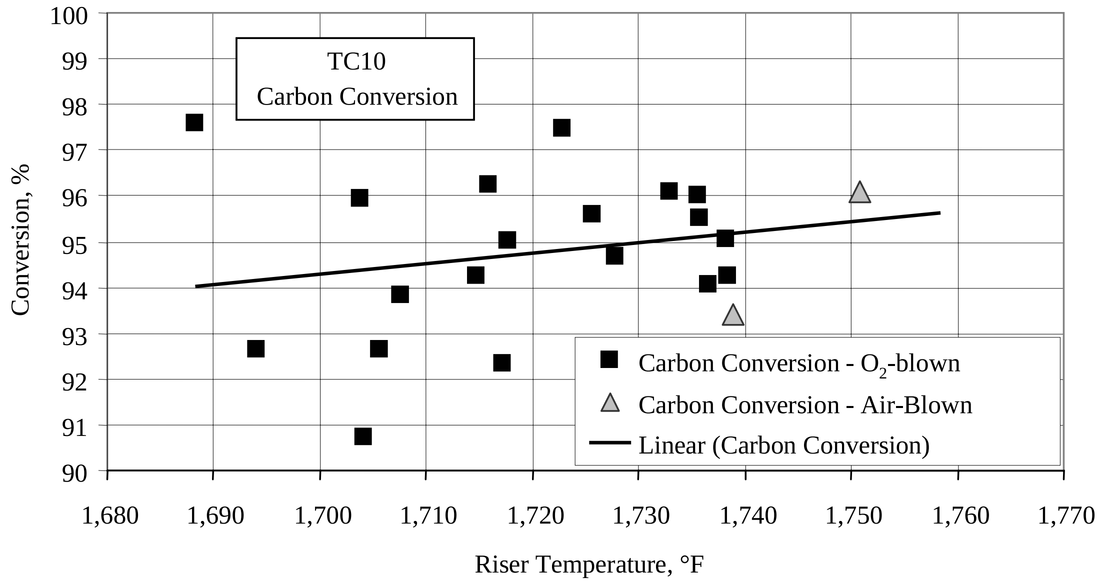

Figure 3.5-7 Carbon Conversion and Riser Temperature

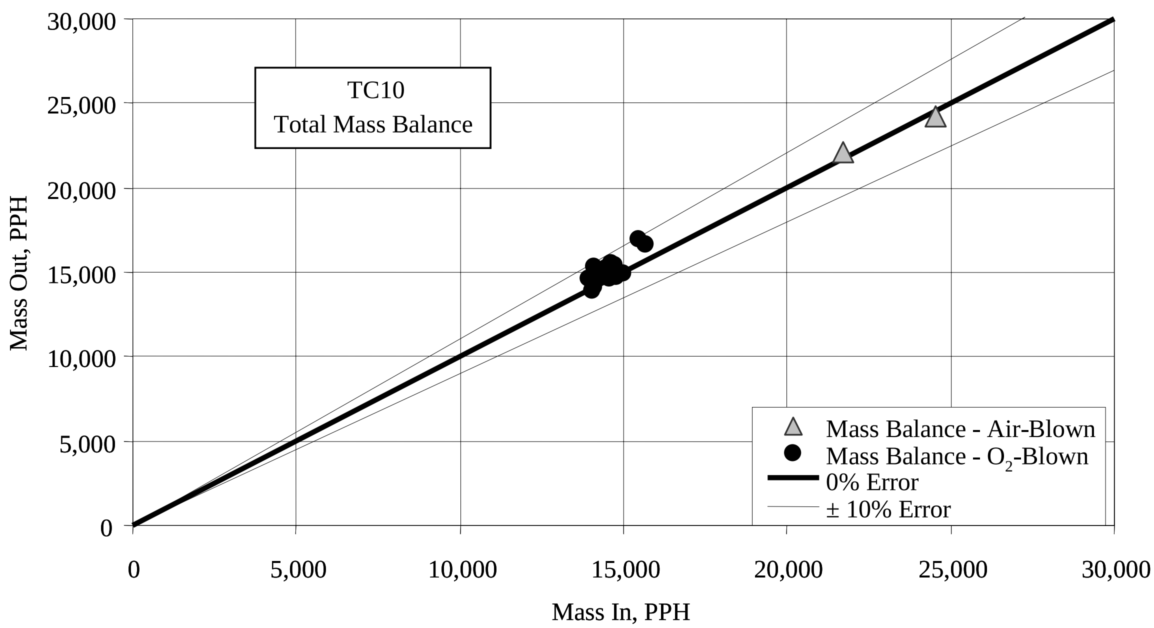

Figure 3.5-8 Overall Material Balance

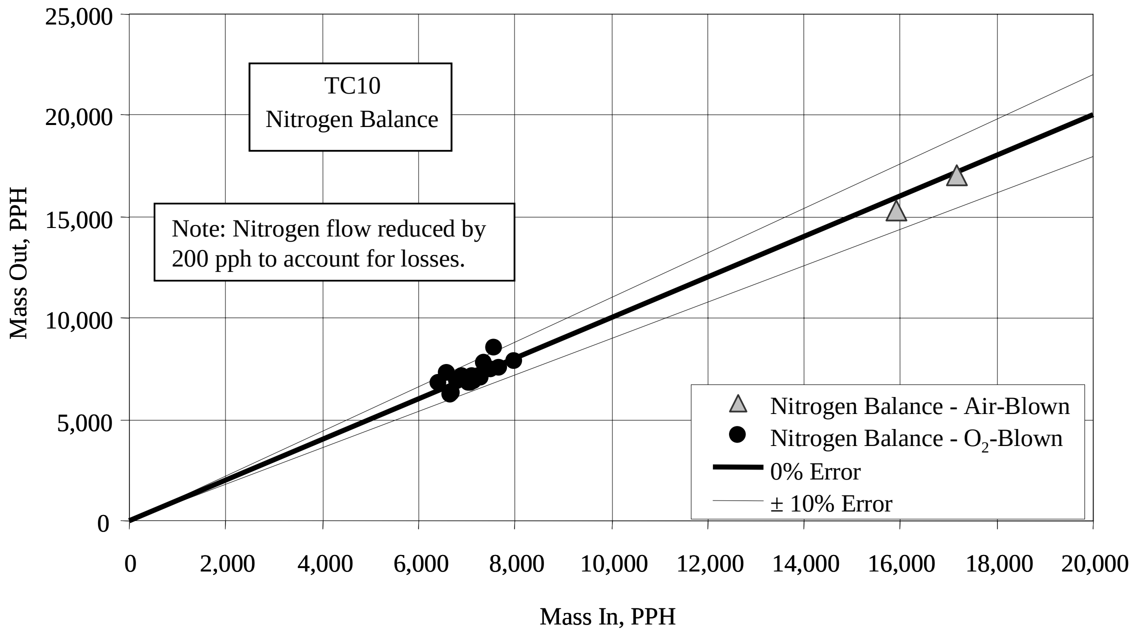

Figure 3.5-9 Nitrogen Balance

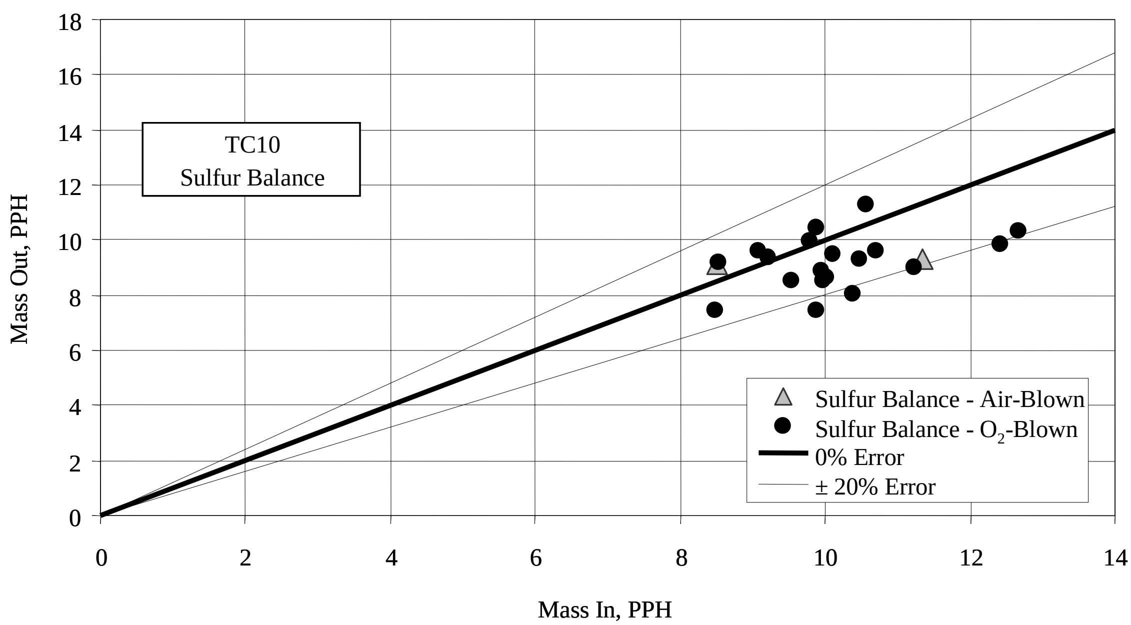

Figure 3.5-10 Sulfur Balance

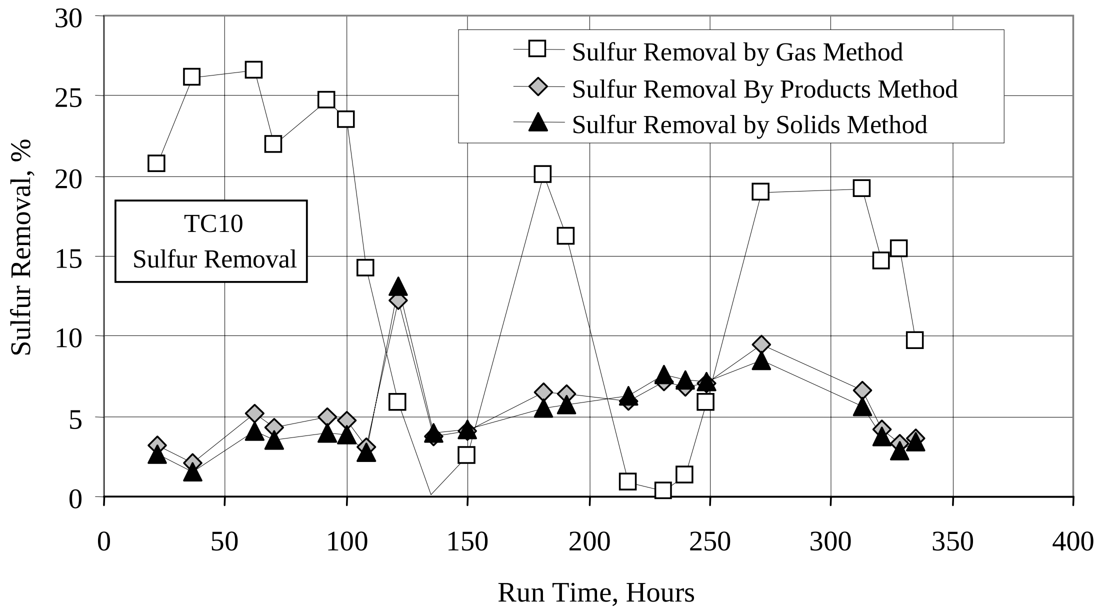

Figure 3.5-11 Sulfur Removal

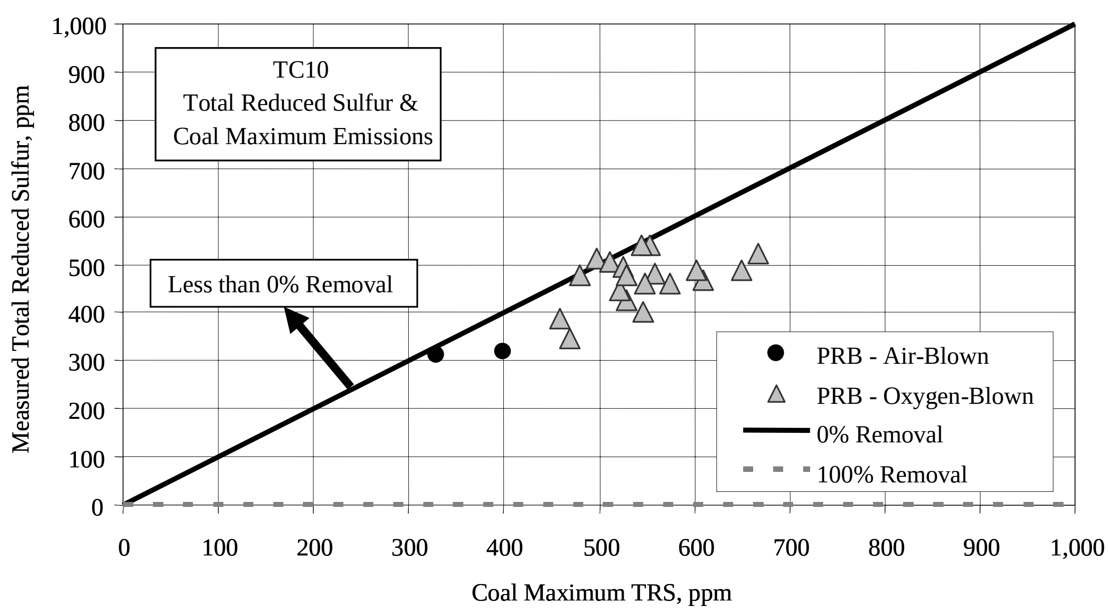

Figure 3.5-12 Measured and Maximum Sulfur Emissions

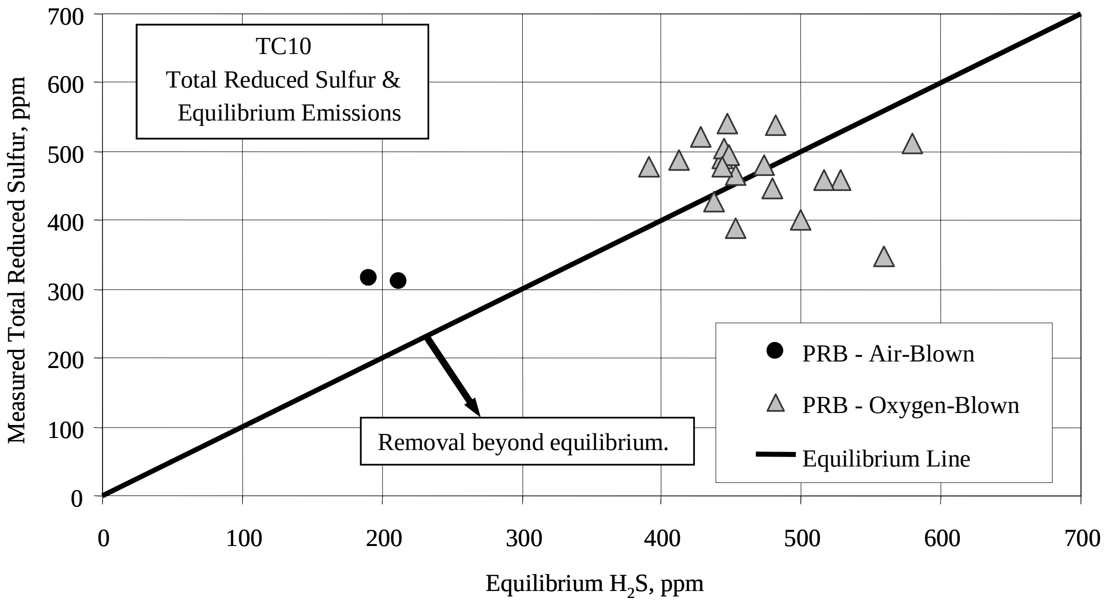

Figure 3.5-13 Measured and Equilibrium Sulfur Emissions

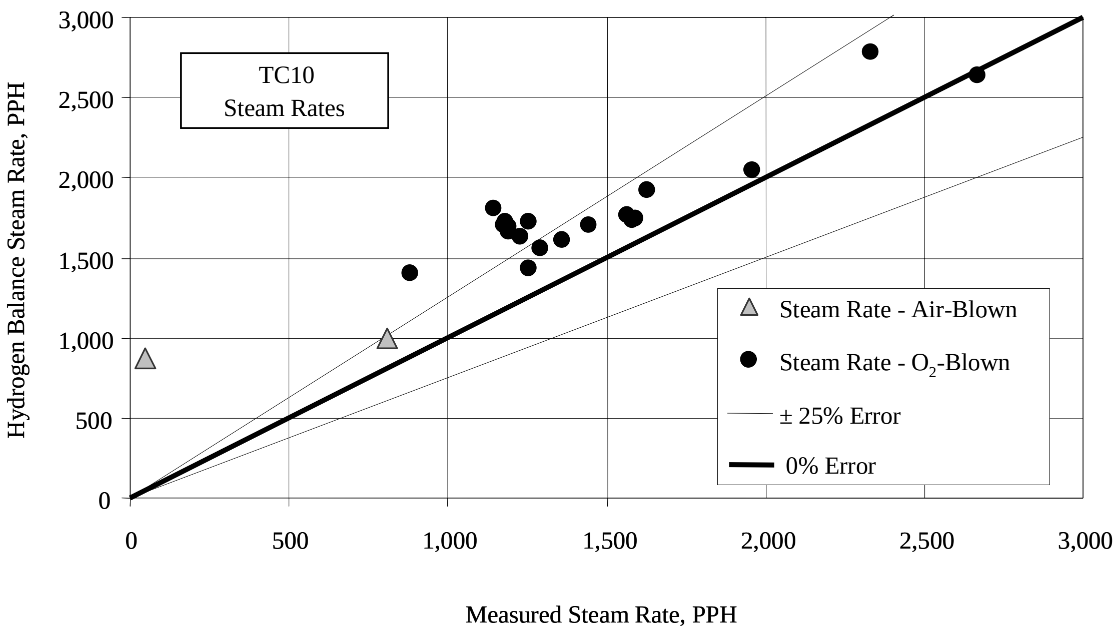

Figure 3.5-14 Measured and Calculated Steam-Flow Rates

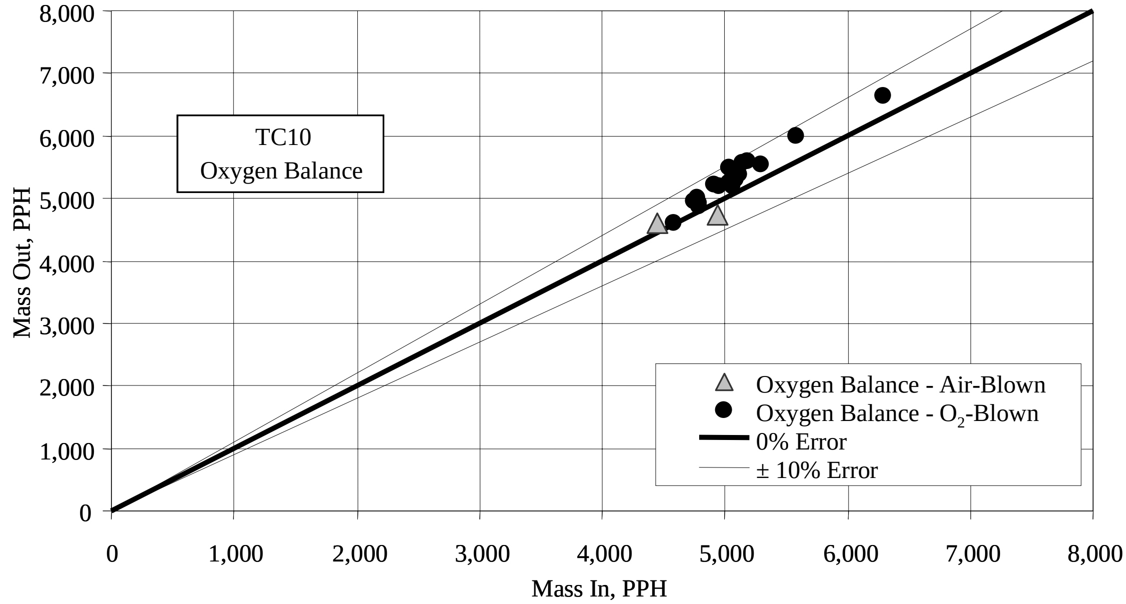

Figure 3.5-15 Oxygen Balance

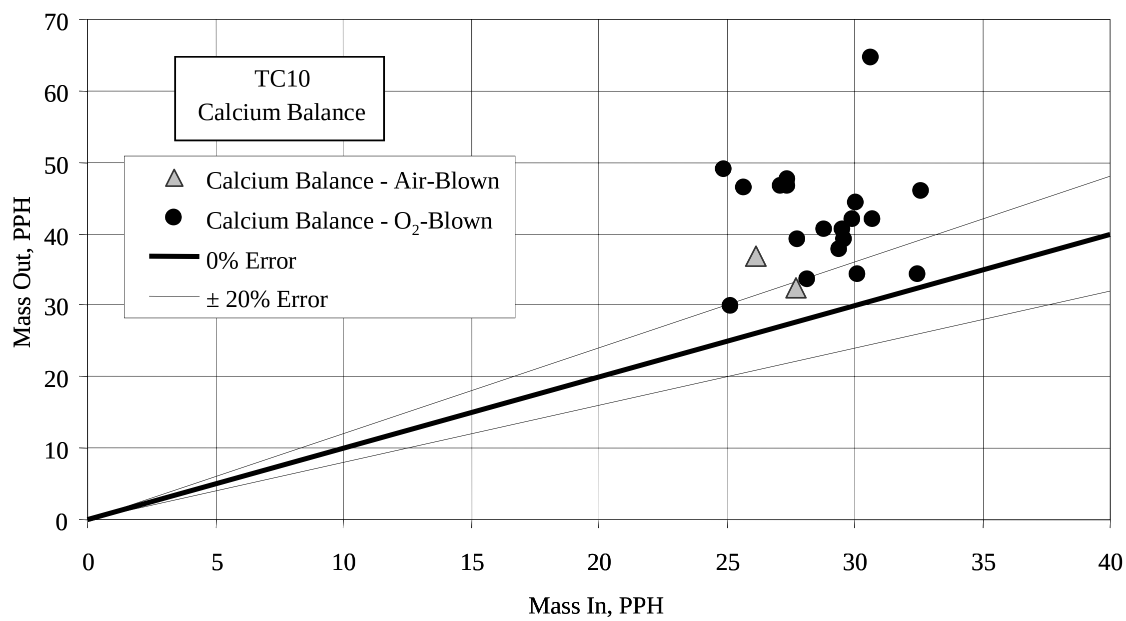

Figure 3.5-16 Calcium Balance

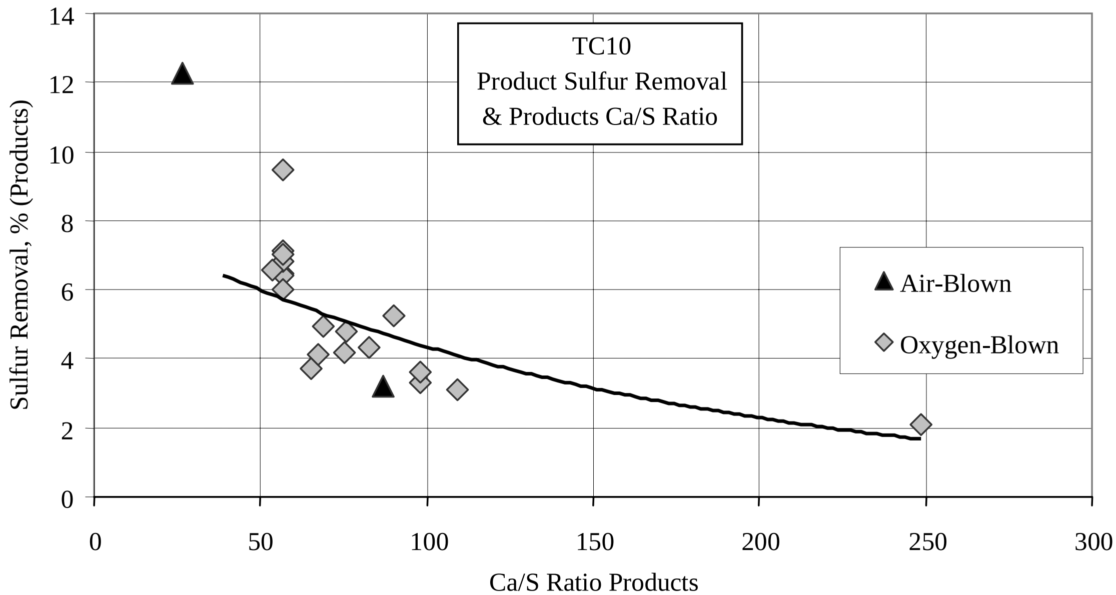

Figure 3.5-17 Sulfur Removal and PCD Solids Ca/S Ratio

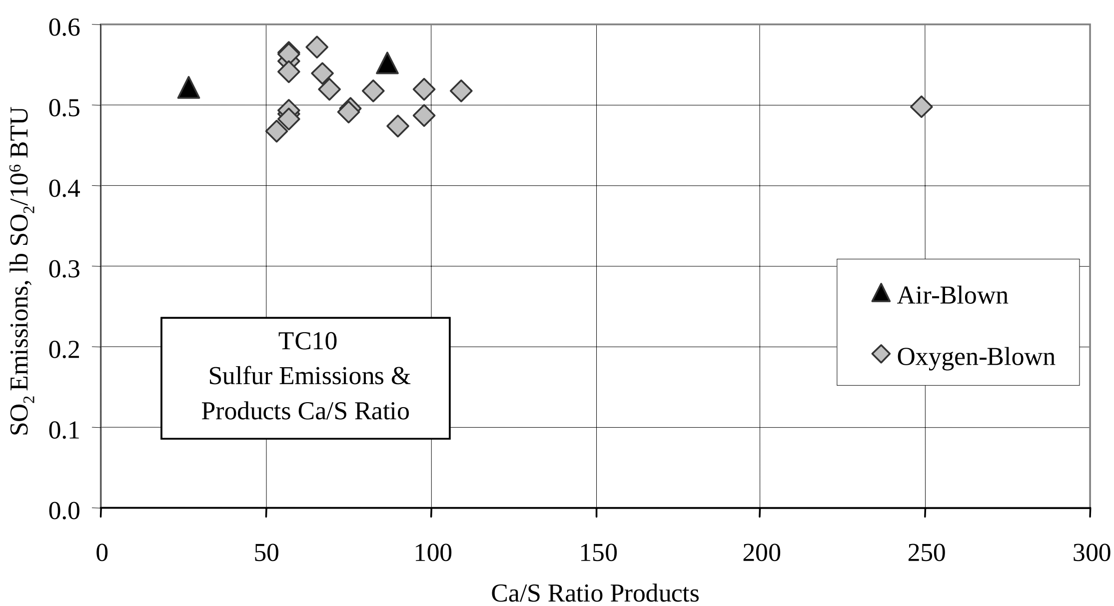

Figure 3.5-18 Sulfur Emissions and PCD Solids Ca/S Ratio

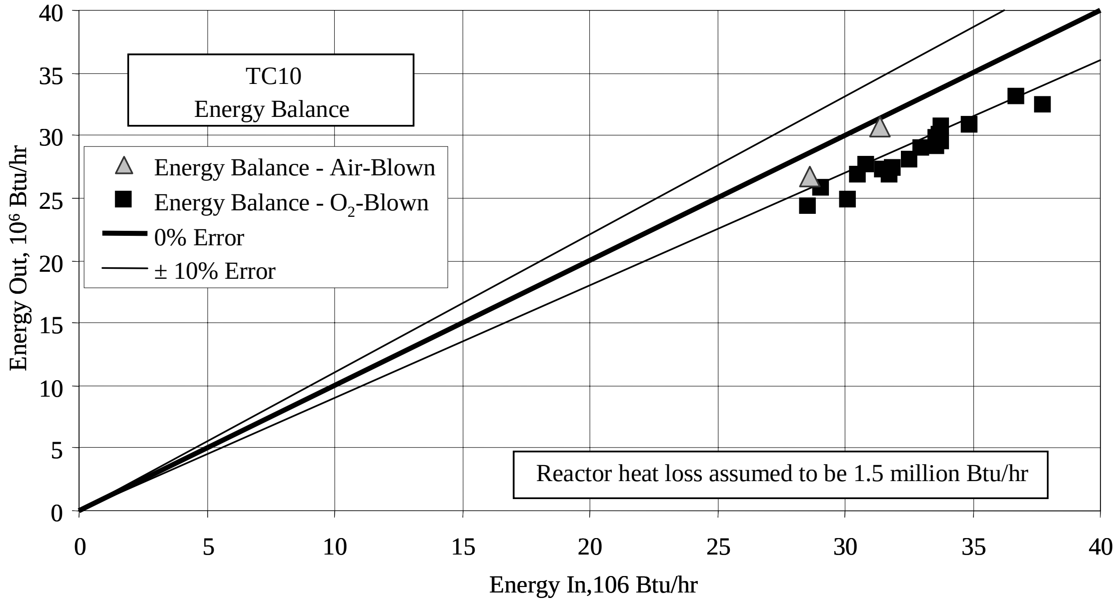

Figure 3.5-19 Energy Balance

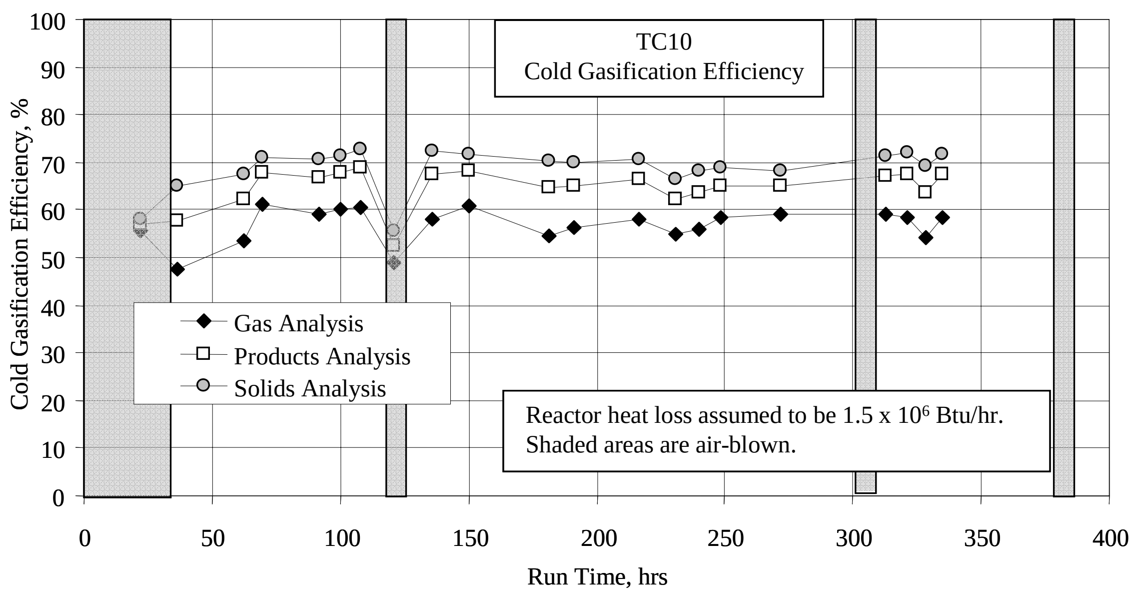

Figure 3.5-20 Cold Gasification Efficiencies

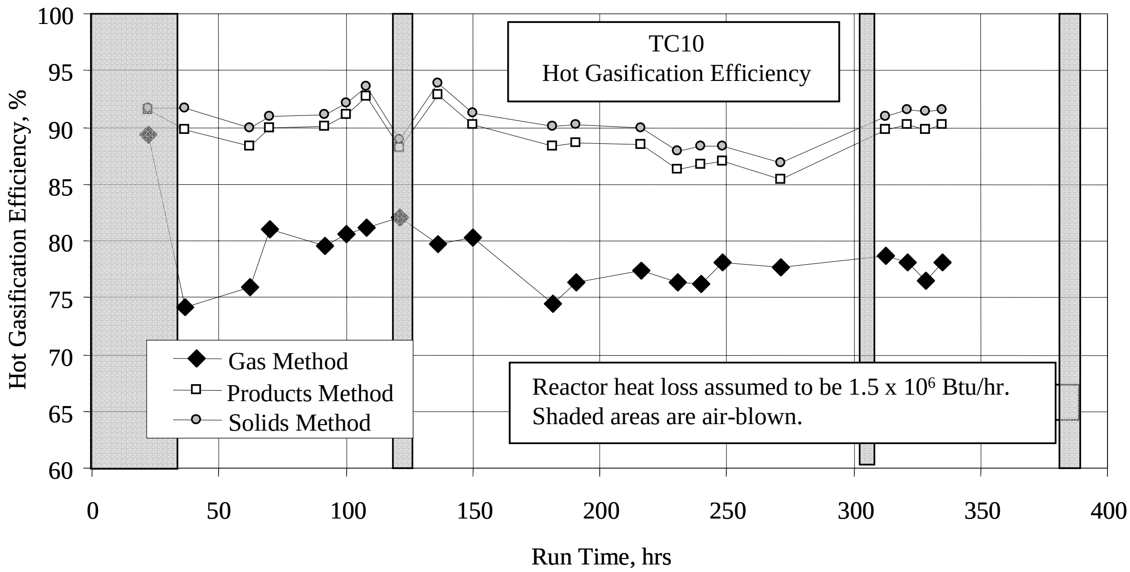

Figure 3.5-21 Hot Gasification Efficiencies

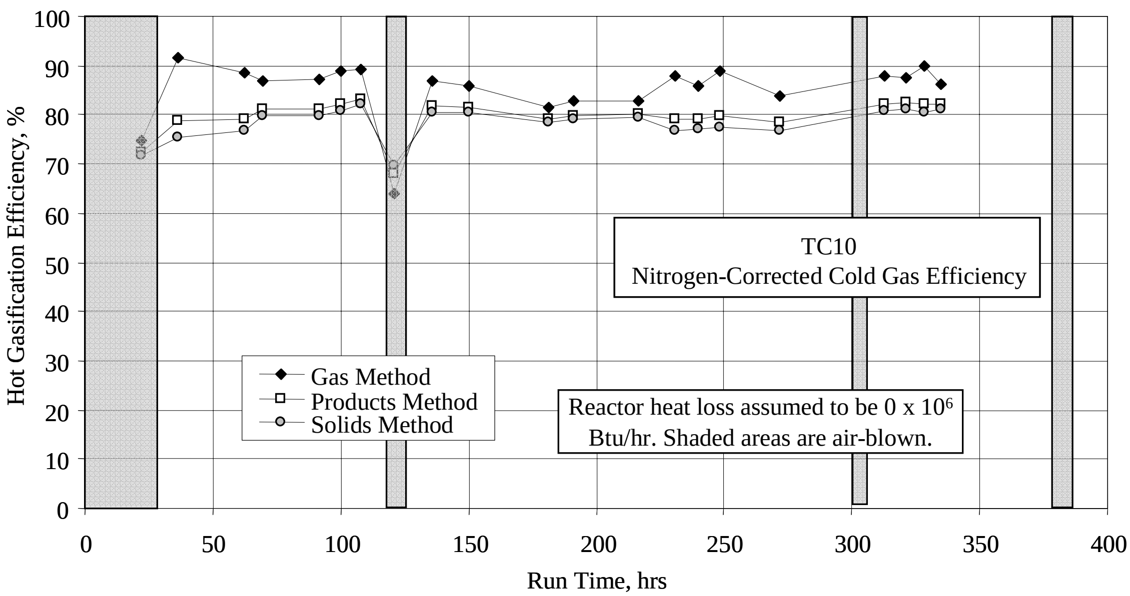

Figure 3.5-22 Adiabatic Nitrogen-Corrected Cold Gasification Efficiencies

3.6 ATMOSPHERIC FLUIDIZED-BED COMBUSTOR (AFBC) OPERATIONS

The AFBC system operated for 622 hours during TC10. Included were 70 hours of g-ash feed to the AFBC and 390 hours of diesel firing. The average bed temperature during TC10 was 1,410°F, slightly less than the design temperature of 1,600 to 1,650°F. The AFBC operated for about 15 hours at the design temperature.

During startup, the air distribution grid was found to be partially plugged with solids. It was most likely plugged during the outage by an accidental pressurization of the system when the outlet flue gas valve was closed while purges remained flowing to the combustor. The main air compressor was used to successfully blow the material out of the distribution grid.

The AFBC bed temperature profile from TC10 is shown in Figure 3.6-1. The graph shows that the bed was well mixed and that the normal bed temperature was below design. The lower temperature was not a problem. A closer inspection of the temperature profile reveals that on more than one occasion, the AFBC was operated such that the freeboard region was well over 1,850°F, and exceeded 1,900°F early on December 7th. After this, the AFBC began to operate at higher than design pressures causing problems for the AFBC compressor. At the end of TC10, the AFBC was opened for inspection and it was found that the high temperatures had caused deposits to form in the AFBC exit to cyclone crossover. These were then removed.

The loss of bed material to the baghouse was less in TC10 than in previous test runs with it only becoming necessary to add sand a few times during the course of the run. Towards the end of TC10, the gasification ash feed system (FD0530) gearbox was damaged beyond repair. The result was a complete lack of feed-rate control for the gasification ash. As a result, FD0530 was piped directly to the ash silo bypassing the AFBC.

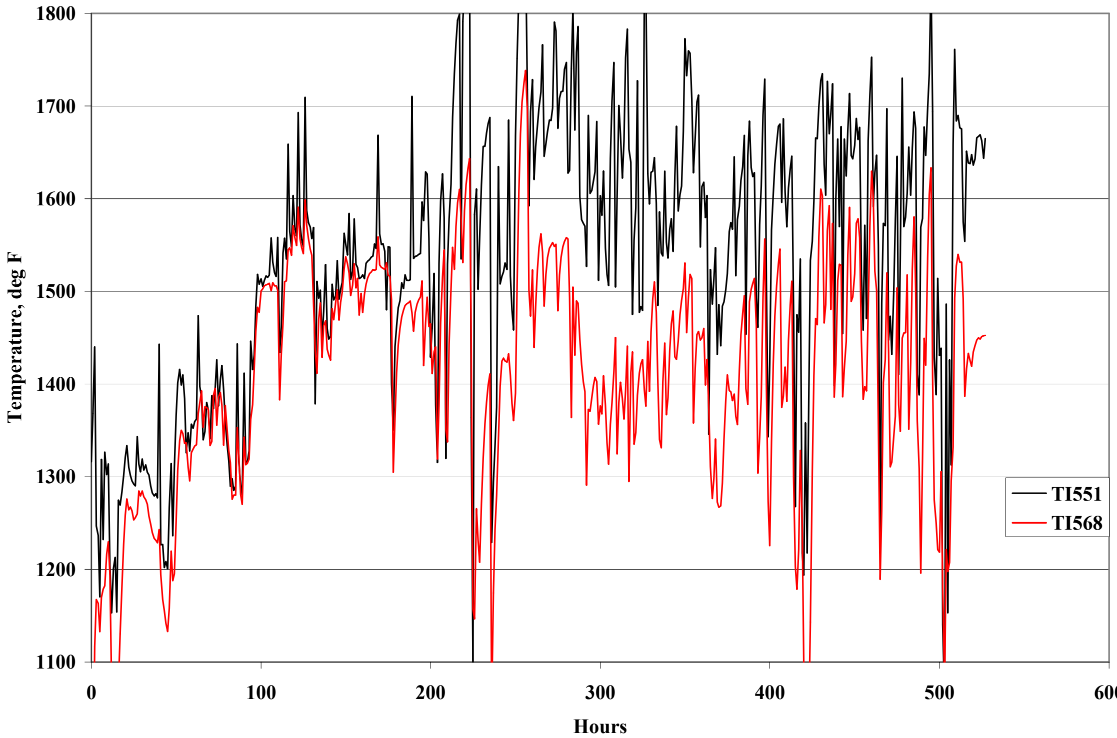

Figure 3.6-1 Temperature Profile of Bed

3.7 PROCESS GAS COOLERS

Heat transfer calculations were performed for the primary gas cooler (HX0202) and the secondary gas cooler (HX0402) to determine if their performance had deteriorated during TC10 due to tar or other compounds depositing on the tubes.

The primary gas cooler is between the Transport Gasifier cyclone (CY0201) and the Westinghouse Siemens PCD (FL0301). During TC10, HX0202 was not bypassed, and took the full gas flow from the Transport Gasifier. The primary gas cooler is a single-flow heat exchanger with hot gas from the gasifier flowing through the tubes and the shell side operating with the plant steam system. The pertinent equations are:

$$Q = UA\Delta T_{LM} \tag{1}$$

$$Q = c_p M(T_1 - T_2) \tag{2}$$

$$\Delta T_{LM} = \frac{(T_1 - t_2) - (T_2 - t_1)}{\ln \frac{(T_1 - t_2)}{(T_2 - t_1)}} \tag{3}$$

Q = Heat transferred, Btu/hour
U = Heat transfer coefficient, Btu/hr/ft^2/°F
A = Heat exchanger area, ft^2
ΔT_{LM} = Log mean temperature difference, °F
c_p = Gas heat capacity, Btu/lb/°F
M = Mass flow of gas through heat exchanger, lb/hr
T_1 = Gas inlet temperature, °F
T_2 = Gas outlet temperature, °F
t_1 = t_2 = Steam temperature, °F

Using Equations (1) through (3) and the process data, the product of the heat transfer coefficient and the heat exchanger area (UA) can be calculated. The TC10 HX0202 UA is shown on Figure 3.7-1 as 4-hour averages, along with the design UA of 5,200 Btu/hr/°F and the pressure drop across HX0202. If HX0202 is plugging, the UA should decrease and the pressure drop should increase. The UA deterioration is a better indication of heat exchanger plugging because the pressure drop is affected by changes in flow, pressure, and temperature.

The UA was fairly unsteady and below the design UA of 5,200 Btu/hr/°F, for most of TC10. During this time the UA ranged from 4,000 to 5,300 Btu/hr/°F. During the last 80 hours the UA further declined and finished TC10 averaging about 3,600 Btu/hr/°F. The UA was below design for essentially all of TC10.

For the first 50 hours of TC10, the pressure drop across HX0202 was about 1.5 psi. After that, the pressure drop declined to 0.7 to 0.8 psi over the next 75 hours. The pressure drop held steady for the next 200 hours before rising slightly to 1.2 psi over the last 80 hours.

While the UA during TC10 was below design, it was very close to the 3,900 to 5,200 Btu/hr/°F observed during TC09. The pressure drop was also in the same range as previous oxygen-blown testing. The slight increase in the pressure drop and decrease in UA over the last few days of the test run could indicate the inlet to a few of the tubes becoming plugged. The UA and pressure drop in TC10 for HX0202 are charted in Figure 3.7-1.

The secondary gas cooler is a single-flow heat exchanger with hot gas from the PCD flowing through the tubes and the shell side operating with the plant steam system. Heat transfer and pressure drop calculations were done around HX0402 to determine if there was any plugging or heat exchanger performance deterioration during TC10. HX0402 is not part of the combustion gas turbine commercial flow sheet. In the commercial gas turbine flow sheet, the hot synthesis gas from the PCD would be directly sent to a combustion gas turbine. HX0402 would be used commercially if the synthesis gas was used in a fuel cell or as a chemical plant feedstock.

Using Equations (1) through (3) and the process data, the product of the heat transfer coefficient and the heat exchanger area (UA) can be calculated. The UA for TC10 testing is shown on Figure 3.7-2 as 2-hour averages, along with the design UA of 13,100 Btu/hr/°F and the pressure drop across HX0402. If HX0402 is plugging, the UA should decrease and the pressure drop should increase.

For the first day of operation in TC10, the UA of HX0402 was above design and averaged 13,500 and 14,500 Btu/hr/°F. After the first day, the UA declined to about 10,500 Btu/hr/°F and held very steady for the next 300 hours. The UA came back up to the 11,000 to 12,000 Btu/hr/°F range during the last 3 days. Except for the first day, the UA was below the design UA of 13,100 Btu/hr/°F for the whole of TC10.

During the first 3 days of TC10, the pressure drop across HX0402 dropped from 2.4 to 0.8 psi. The pressure drop held at 0.8 psi for the next 300 hours. During the last few days of TC10, the pressure drop varied from 0.7 to 1.8 psi.

While below design, the UA of HX0402 was 11,000 to 12,000 Btu/hr/°F for most of TC10 which compares closely to the UA of 10,200 to 10,800 Btu/hr/°F in TC09 and of UA of 11,000 to 11,800 Btu/hr/°F in TC08 oxygen blown operations. The pressure drop for TC10 was in general lower than the 1.2 to 3.1 psi from TC09.

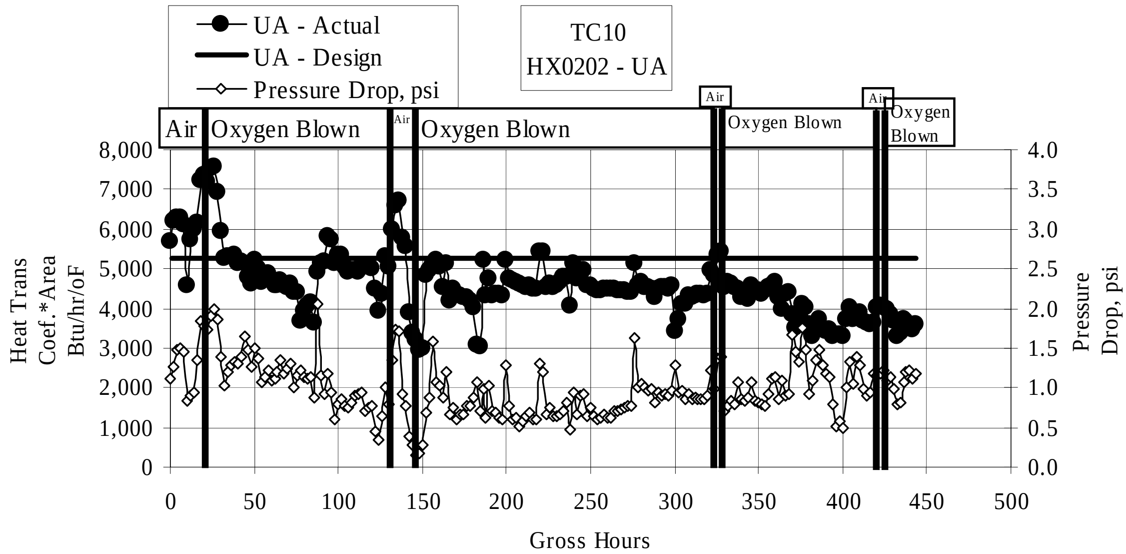

Figure 3.7-1 HX0202 Heat Transfer Coefficient and Pressure Drop

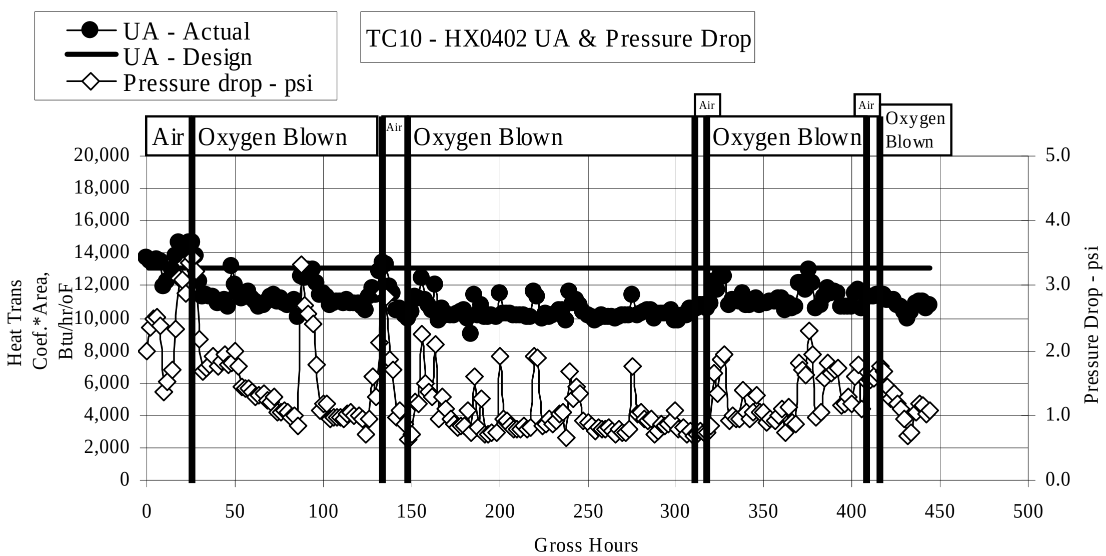

Figure 3.7-2 HX0402 Heat Transfer Coefficient and Pressure Drop

4.0 PARTICLE FILTER SYSTEM

4.1 TC10 RUN OVERVIEW

TC10 was a test run using PRB coal and oxygen-blown gasifier operation in order to further characterize system operation under these conditions. As in other recent test runs, this run was a demonstration of reliable particulate control device (PCD) performance. Since January 2002, when hardware modifications to the gasifier were completed, particulate properties such as drag changed. The result was a lower pressure drop in the particulate control device and more stable PCD performance. Although gasification ash (g-ash) bridging had been a recurring problem in the 2001 runs, bridging had not occurred since the modifications were completed, except in the unusual circumstance of g-ash buildup due to overfilling the PCD. In TC10, the trend of a lower pressure drop and absence of bridging continued. The PCD was leak tight during the run and no filter element failures occurred. Despite some unstable system conditions, the PCD proved to be robust and reliable.

TC10 consisted of two major periods of operation including 167 hours on coal in November 2002, and 249 on-coal hours in December 2002. Both of these portions of the run ended due to poor solids circulation in the gasifier. Because of numerous coal feeder trips, system operation was often unstable. Several thermal excursions occurred in the PCD due to oxygen breakthrough following coal feeder trips, but no major problems with PCD operation occurred.

Good sealing of the filter vessel allowed high collection efficiency. Nonetheless, many of the outlet samples were contaminated with condensed material. Unlike the measurements taken during most test runs, which showed outlet loading to be below the sampling system lower limit of detection, 0.1 ppmw, some measurements taken in TC10 showed detectable concentrations, up to 2.6 ppmw. (However, these particulate levels should still satisfy expected turbine specifications.) This contamination was largely responsible for the elevated outlet loadings, and it precluded failsafe testing since outlet loading sampling is a primary method of failsafe performance evaluation.

This report contains the following sections:

- PCD Operation Report, Section 4.2—This section describes the main events and operating parameters affecting PCD operation. Operation of the fines removal system is also included in this section.

- Inspection Report, Section 4.3—The complete inspection performed following TC10 is discussed in this section including details of the post-run conditions of various PCD components and of the fines removal system.

- Gasification Ash Characteristics and PCD Performance, Section 4.4—This section includes a detailed discussion of g-ash physical and chemical properties, as well as the effects of these characteristics on PCD performance. The results of PCD inlet and outlet solids concentration sampling are presented in this section.

- Filter Material Testing, Section 4.5— This section presents results of on-going testing of various types of filter media in an effort to characterize material properties such as degradation and useful filter life in gasification operation.

4.2 TC10 PCD OPERATION REPORT

4.2.1 Introduction

Despite unstable system conditions during TC10, PCD operation was successful. There were no filter element failures and or bridging. In addition, outlet loading samples showed that the PCD was leak tight. Several thermal excursions occurred during the run, which resulted from coal feeder trips and subsequent periods of oxygen breakthrough. However, PCD operation was not critically affected by these transients.

Ranging from approximately 40 to 60 inH_2O, the baseline pressure drop was comparable to that of test runs conducted since the addition of the lower mixing zone (LMZ) on the gasifier. Overall, the baseline pressure drop showed a slight upward trend throughout the run, although there was much variation in the baseline due to the unstable coal-feed rate. Typically, the inlet temperature was 710 to 775°F, and the face velocity was 3 to 4 ft/min. The back-pulse frequency was consistently kept at 5 minutes, while the back-pulse pressures were kept at 400 psid (that is, 400 psi above system pressure) on the top plenum and 600 psid on the bottom plenum.

The fines removal system operated reliably during the majority of the run. However, on three occasions, one of the FD0520 lock hopper system spheri valve seals required replacement. The FD0520 lock hopper system required frequent cycle-time adjustment, and the FD0502 screw cooler required daily maintenance attention to control leaking seals.

Run statistics for TC10 are shown in Table 4.2-1. Layout 26, the filter element layout implemented for the run, is shown in Figure 4.2-1.

4.2.2 Test Objectives

For TC10, the primary objectives for the filter system were the following:

- G-ash Bridging – Several measures were taken in previous runs to prevent g-ash bridging and were continued in TC10. These measures included using six blanks in place of a partial row of filters on the bottom plenum, reducing the number of support bars, and keeping the back-pulse intensity consistently at 400 psid (top) and 600 psid (bottom) with the pulse timer at 5 minutes during coal feed. Additionally, filter element instrumentation including thermocouples and resistance probes were installed and monitored during the run for the presence of g-ash bridging.

  In TC09, solids rate to the PCD often exceeded the capacity of the PCD solids removal system, causing solids accumulation in the PCD cone. This affected both gasifier and PCD operation. The existing PCD cone thermocouples could not provide detailed information about how the solids accumulated in the cone and how the accumulation affected the PCD operation. To better monitor the solids level in the PCD cone, seven thermocouples and six resistance probes were installed on four rods mounted on the bottom of filter elements and extended into the cone cavity. This arrangement together with the existing thermocouples in the cone provided more thorough information for profiling the solids accumulation.

Two inverted filter element assemblies, which were designed by Siemens Westinghouse to prevent bridging, were tested in TC08 and TC09. Because they performed well without problems, seven of the assemblies were installed on the top plenum in TC10 to further evaluate their performance.

- Filter Element Testing – Exposure of metallic filter elements continued in TC10. Many of the filter elements from TC09 were reinstalled and included Pall iron aluminide, Pall Hastelloy X and Pall/Fluid Dynamics HR-160 filter elements. A greater number of HR-160 filters were installed to more extensively characterize the material. In TC09, thick residual cake and signs of patchy cleaning were observed on the Pall Hastelloy X filter elements. However, after further off-line cleaning, all of them resumed normal flow resistance. To continue the evaluation, 10 Pall Hastelloy-X filter elements exposed in TC09 were reinstalled in TC10.

- FailSafe Device Testing – Three types of failsafe devices were exposed during TC10: Pall fuses, PSDF-designed failsafes, and Siemens Westinghouse metal-fiber-filled failsafes. To accommodate filter elements not equipped with Pall fuses, 50 PSDF-designed failsafes were installed in TC10. The g-ash injection testing of this type of failsafe in TC08 demonstrated its excellent performance with outlet particulate loading of less than 0.1 ppmw. More PSDF-designed failsafes will be continuously evaluated for their long-term performance. Six metal-fiber-filled Siemens Westinghouse failsafes remained on top of six blanks to continue the syngas exposure for material evaluation. Failsafe testing with g-ash injection had been planned for both the PSDF design and the Pall fuse, but contamination in the outlet duct precluded those tests.

- Venturi Pressure Drop Measurements – In TC10, two pressure differential transmitters (PDTs) were installed in the venturi devices on the top and bottom plenum exit pipes. Pressure drop measurements during normal filtration process were conducted to characterize the flow through each plenum in different periods of the back-pulse cycle. The data were used in evaluating flow distribution and characterizing overall PCD operation. As a secondary objective, a fast PDT was also installed in parallel with the two regular PDTs to explore if the dynamic response of the jet flow during a back-pulse could be obtained using a fast data acquisition device.

- Inlet Particulate Sampling and Characterization – In situ particulate samples were collected at the PCD inlet to determine the effects of various gasifier operating conditions on the characteristics of the g-ash. These tests examined how the various gasifier operating conditions affected the g-ash physical properties, chemistry, and flow resistance; and how the changes in g-ash characteristics impacted PCD performance. To the extent that the various operating conditions could be maintained during available sampling periods, in situ samples were collected at each of the coal-feed rates, gasifier control temperatures, and process pressures (residence times) specified in the test plan.

The measured inlet particulate loadings were used in combination with the PCD pressure drop data obtained over the sampling time intervals to determine the drag of the transient dustcake under various conditions. The transient dustcake drag values were compared to the drag values measured in the laboratory to determine whether the pressure drop was influenced by any outside factors other than the buildup of the dustcake. The drag of the TC10 g-ash generated from PRB coal was compared to the drag of PRB g-ashes from previous runs to better understand how the drag was affected by changes in the process (e.g., the new LMZ) or by changes in operating conditions.

- Outlet Particulate Sampling and Monitoring – As in previous tests, the ability of the PCD to maintain acceptable levels of particulate control was documented by regular particulate sampling. In addition to the regular sampling, the output from the PCME DustAlert-90 was monitored continuously to provide rapid detection of any particle leakage through the PCD. The measured outlet loadings were plotted against the corresponding outputs from the PCME DustAlert-90 and compared to similar data from previous runs to supplement the ongoing evaluation of the PCME monitor.

4.2.3 Observations/Events – November 15, 2002, Through December 18, 2002

Refer to Figures 4.2-2 through 4.2-11 for operating trends corresponding to the following list of events.

A. System Startup. Back-pulsing for the PCD began at 11:50 on November 15, 2002. The TC10 run began on November 16, 2002, with startup of the main air compressor and lighting of the gasifier start-up burner, however, startup was delayed when a spheri valve seal on the FD0502 lock hopper system ruptured. The main air compressor and the start-up burner were restarted at 20:00 on November, 17, 2002. On November 18, 2002, at 11:20, the back-pulse pressure was increased to 400 psid (i.e., 400 psi above gasifier pressure) on the top plenum and 600 psid on the bottom plenum.

B. Coal Feed Started. At 12:55 on November 18, 2002, coal feed was started. The coal-feed rate and the PCD pressure drop were erratic while commissioning the FD0200 coal feeder.

C. Coal Feeder Trip. At 11:50 on November 20, 2002, coal feed was lost and was reestablished at 12:15.

D. Coal Feeder Trip. At 02:20 on November 22, 2002, coal feed was lost. System pressure was reduced so that the start-up burner could be lit. At 05:20 on November 22, 2002, a sudden carryover of gasifier solids caused a trip of the solids removal system.

E. Restarted Coal Feed. At 11:20 on November 22, 2002, coal feed was reestablished.

F. Coal Feeder Trips. Beginning on November 23, 2002, at 14:10, several coal feeder trips occurred. On November 24, 2002, at 11:00, coal feed was stopped so that the coal feed conveying line could be cleared.

G. Coal Feed Restarted. At 19:35 on November 24, 2002, coal feed resumed.

H. Coal Feeder Trip. At 00:25 on November 25, 2002, a coal feeder trip occurred. Coal feed continued to be unsteady over the following day.

I. System Shutdown. Beginning at 02:35 on November 26, 2002, several coal feeder trips occurred. Because of lack of sufficient circulation in the gasifier, the system was shutdown. This concluded TC10A.

J. System Restart. Back-pulsing was resumed at 21:15 on December 5, 2002, and the start-up burner and main air compressor were started at 21:50. On December 6, 2002, at 11:00, the back-pulse pressure was set to 400 psid on the top plenum and 600 psid on the bottom plenum, and coke breeze feed was started at 11:35.

K. Coal Feed Started. At 14:43 on December 6, 2002, coal feed was started. A coal feeder trip occurred at 18:32, and coal feed was quickly reestablished.

L. Loss of Coal Feed. Due to a loss of nitrogen, coal feed was stopped at 00:40 on December 7, 2002. The start-up burner was lit at 03:30, and by 11:50, coke breeze feed was established.

M. Coal Feed Started. Coal feed was started again at 14:20 on December 7, 2002.

N. Coal Feeder Trips. At 19:15 on December 7, 2002, a coal feeder trip occurred which caused oxygen breakthrough to the PCD. Coal feed was quickly reestablished. Another feeder trip occurred on December 8, 2002, at 05:12, and this also caused oxygen breakthrough.

O. Coal Feeder Trip. At 19:30 on December 9, 2002, the coal feeder tripped. At that time, coal feed could not immediately be reestablished. While reheating the gasifier on coke breeze, a gasifier upset occurred at 21:37 which caused a sudden carryover of gasifier solids to the PCD.

P. Coal Feeder Trip. At 09:30 on December 11, 2002, the coal feeder tripped. A high solids carryover occurred while restarting coal feed.

Q. Gasifier Upset. At 09:10 on December 12, 2002, a gasifier upset caused a surge of solids carryover to the PCD.

R. Coal Feeding Difficulty. Beginning at around 06:00 on December 13, 2002, coal feeding became very unstable. Over the next few hours, several coal feeder trips occurred.

S. Loss of Coal Feed. Two coal feeder trips occurred on December 14, 2002, one at 00:05, and one at 06:40. Both of these trips caused oxygen breakthrough and subsequently thermal transients on the filter element surfaces. Coal feed was lost momentarily at 20:42 on December 14, 2002, due to a problem with the coal transport system, and oxygen breakthrough also occurred at this time.

T. Coal Feeder Trips. A coal feeder trip occurred at 01:30 on December 15, 2002. Numerous coal feeder trips occurred throughout the day, and these often caused oxygen breakthrough to the PCD.

U. Coal Feeder Trips. Following several feeder trips, coal feed was discontinued at 06:35 on December 16, 2002, so that the conveying line could be cleared. Coal feed began again at 15:35 on December 16, 2002.

V. Coal Feed Trips. A series of trips occurred beginning at 17:05 on December 16, 2002.

W. System Shutdown. At 12:28 on December 18, 2002, coal feed was discontinued due to deficient gasifier circulation.

4.2.4 Run Summary and Analysis

The system was pressurized and the back-pulsing sequence was first started on November 15, 2002. The TC10 run began on November 16 but startup was delayed to replace a ruptured spheri valve seal on the FD0520 lock hopper system. Coal feed was started on November 18, 2002, and during this period of coal feed, both the FD0210 feeder and the new FD0200 feeder were used to feed coal. Many coal feed disruptions occurred over the next few days, which appeared to be at least in part due to excess moisture in the coal. These periods of unsteady coal-feed rate caused irregular PCD pressure drop and temperature trends. The first portion of TC10 ended on November 26, 2002, with an unscheduled shutdown due to difficulty with coal feeding and lack of adequate circulation in the gasifier.

The second part of TC10 began after the gasifier was cleared of deposits. Coal feed was established on December 6, 2002. This portion of the run was also marked by numerous interruptions in coal feed. Oxygen breakthrough and subsequent thermal transients often resulted from coal feeder trips. However, there apparently was no consequent permanent damage to the filter elements. The filter element temperature increases were often rapid enough to trigger rate-of-change alarms (at least 2°F/second), although the actual temperature increases were usually less than 100°F. These rate-of-change alarms caused emergency back-pulsing, which was effective in controlling the temperature rises. On December 18, 2002, the system was shutdown again due to poor solids circulation through the gasifier.

Throughout the run, the baseline pressure drop showed an upward trend. However, the pressure drop was relatively low, with the baseline usually below 75 inH_2O. Despite the frequent system upsets, usually due to coal feeding difficulty, PCD operation was successful.

Table 4.2.1

TC10 Run Statistics and Steady-State Operating Parameters
November 15, 2002, Through December 18, 2002

Start Time:	11/15/02 11:50 (for back-pulse system)
End Time:	12/18/02 12:28
Coal Type:	Powder River Basin
Hours on Coal:	Approx. 416 hrs
Number of Filter Elements:	85
Filter Element Layout No.:	26 (Figure 4.2-1)
Filtration Area:	241.4 ft^2 (22.4 m^2)
Pulse Valve Open Time:	0.2 sec
Pulse Time Trigger:	5 min
Pulse Pressure, Top Plenum	400 psi Above System Pressure
Pulse Pressure, Bottom Plenum:	600 psi Above System Pressure
Pulse dP Trigger:	275 inH_2O
Inlet Gas Temperature:	Approx. 710 to 775°F (375 to 412°C)
Face Velocity:	Approx. 3 to 4 ft/min (1.5 to 2 cm/sec)
Inlet Loading Concentration:	Approx. 14,600 to 33,300 ppmw
Outlet Loading Concentration:	Below detection limit of 0.1 ppmw to 2.6 ppmw
Baseline Pressure Drop:	Approx. 40 to 60 inH_2O (100 to 150 mbar)

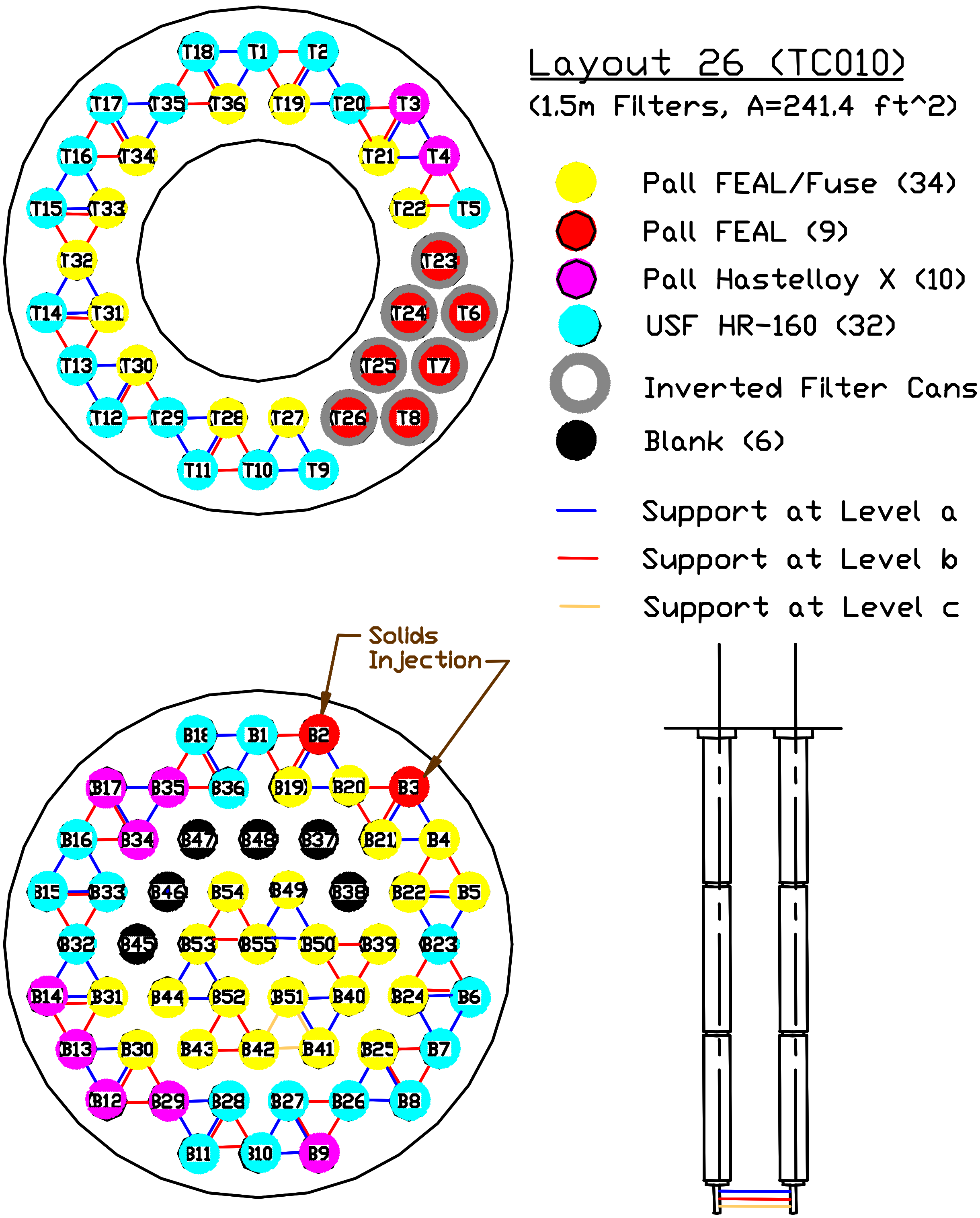

Figure 4.2-1 TC10 Filter Element Layout 26

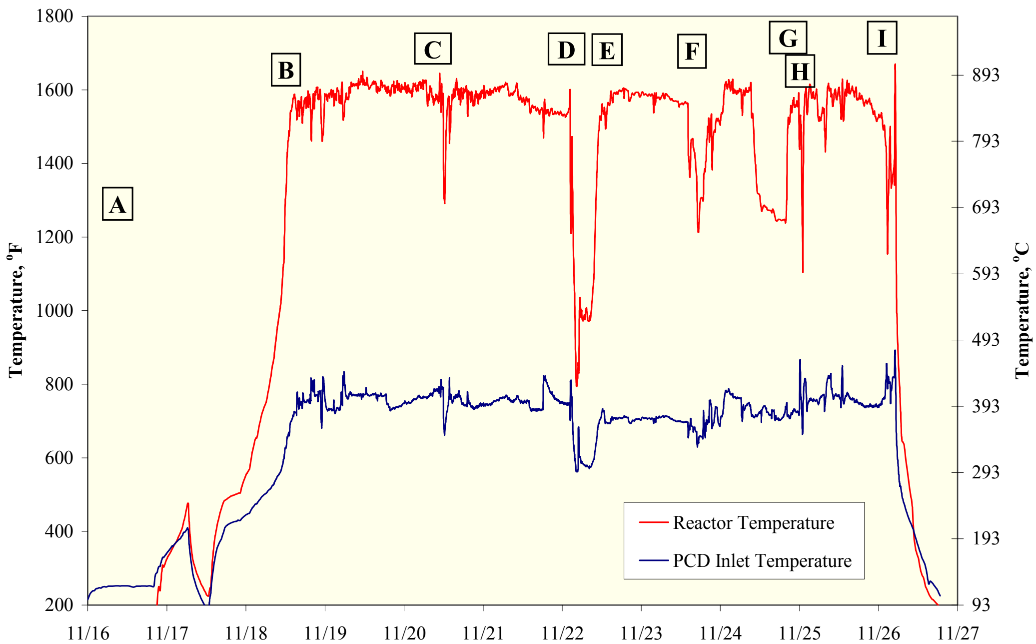

Figure 4.2-2 Reactor and PCD Temperatures, TC10A

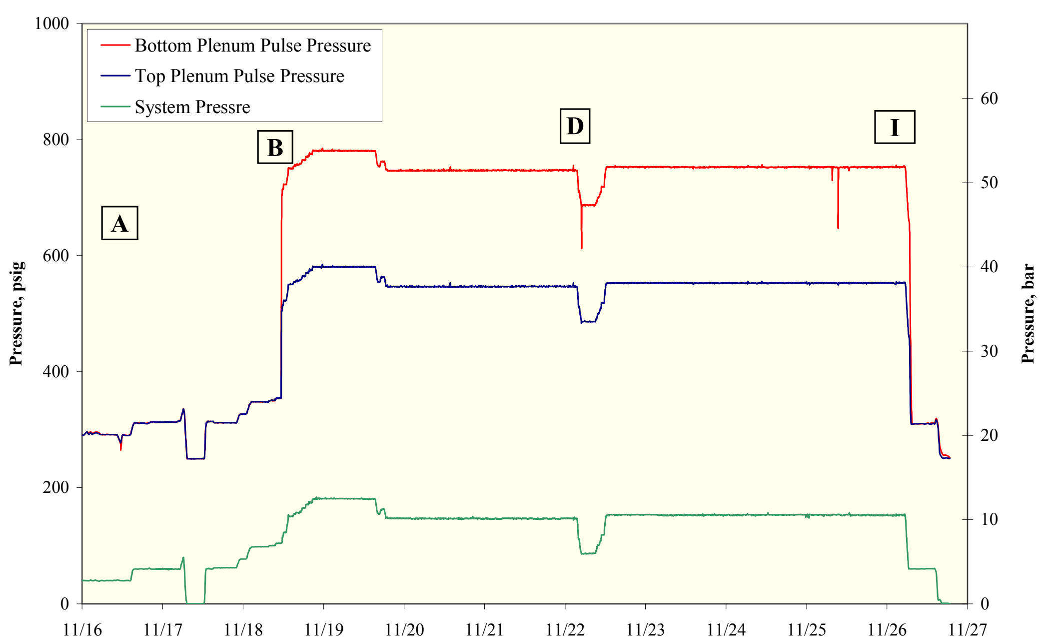

Figure 4.2-3 System and Pulse Pressures, TC10A

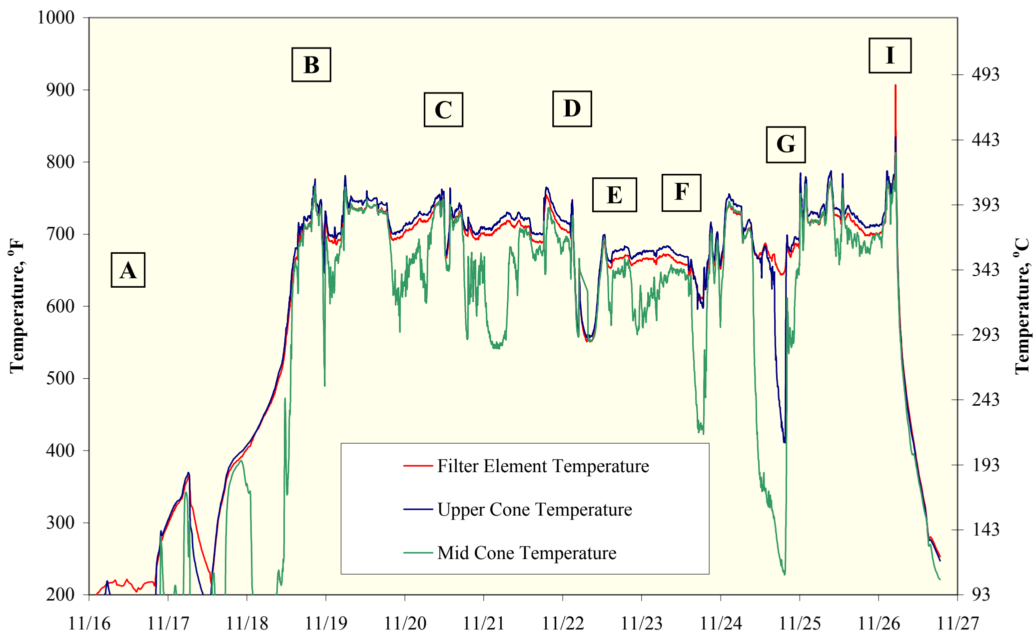

Figure 4.2-4 Filter Element and Cone Temperatures, TC10A

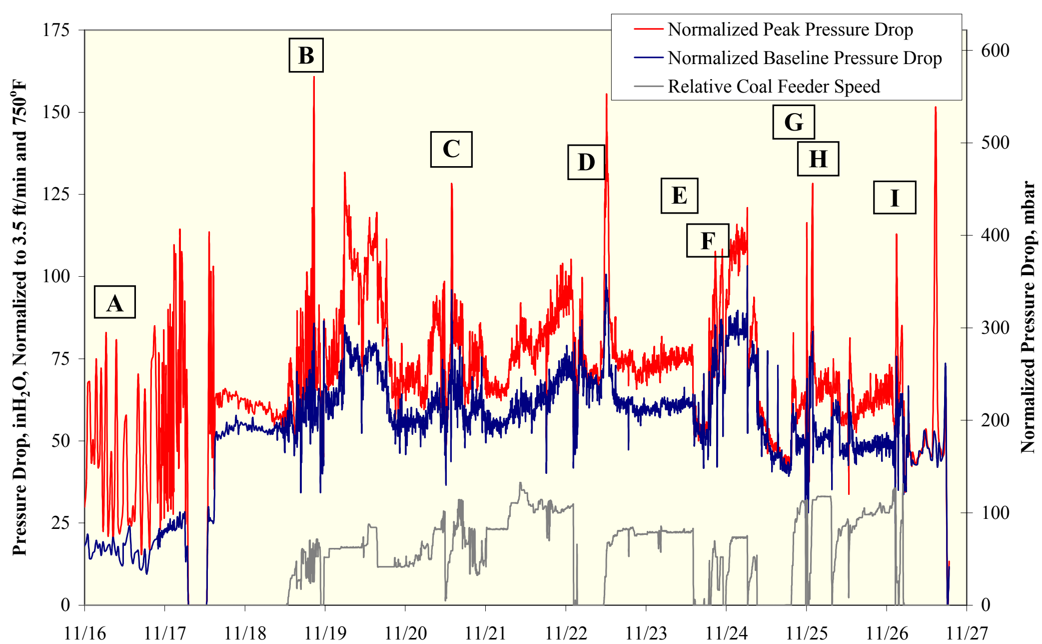

Figure 4.2-5 Normalized PCD Pressure Drop, TC10A

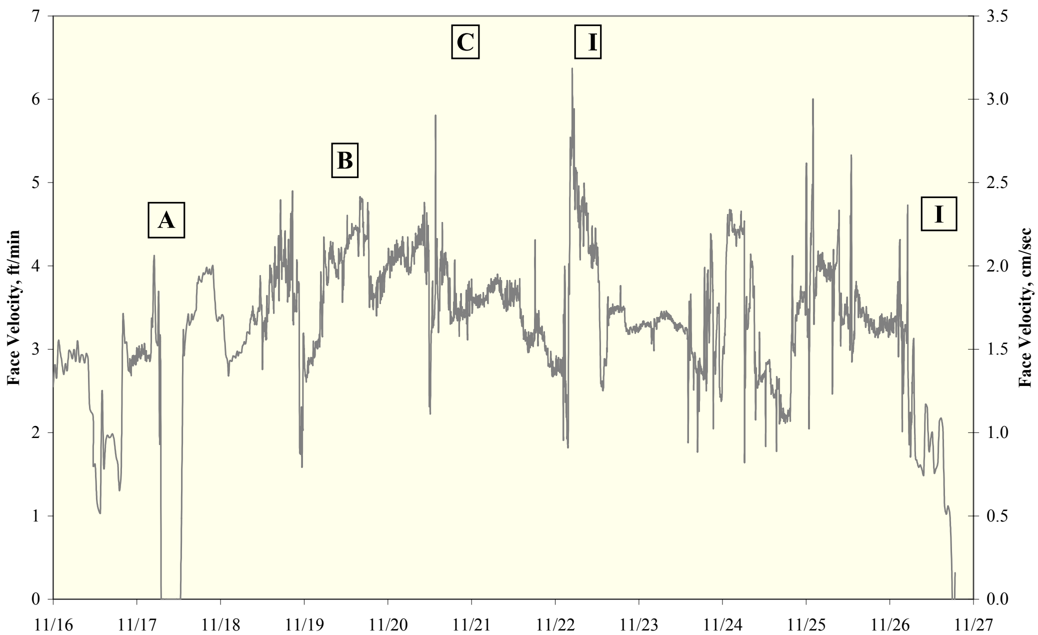

Figure 4.2-6 PCD Face Velocity, TC10A

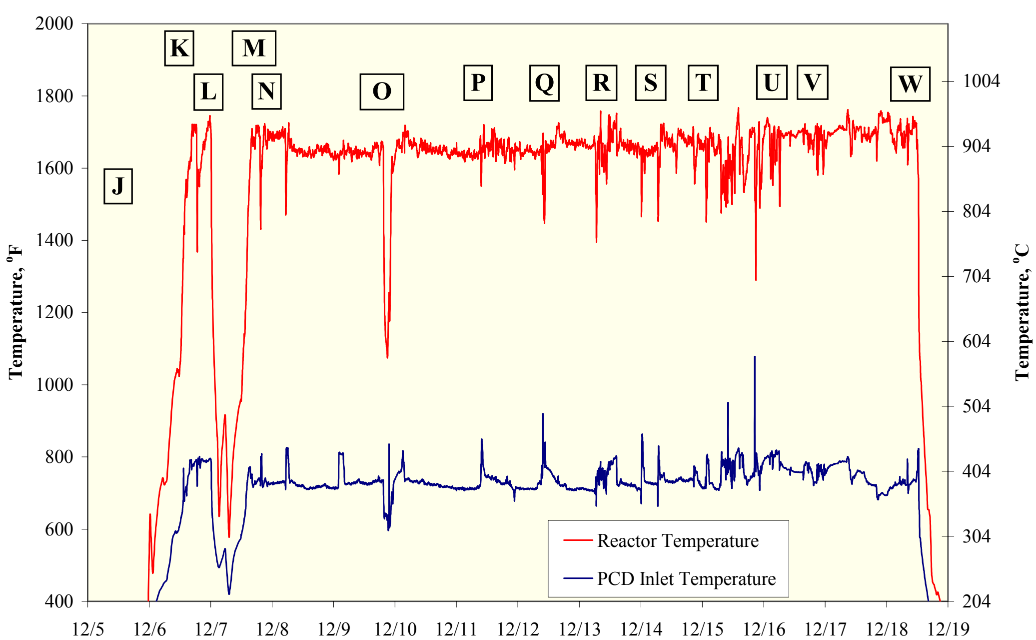

Figure 4.2-7 Reactor and PCD Temperatures, TC10B

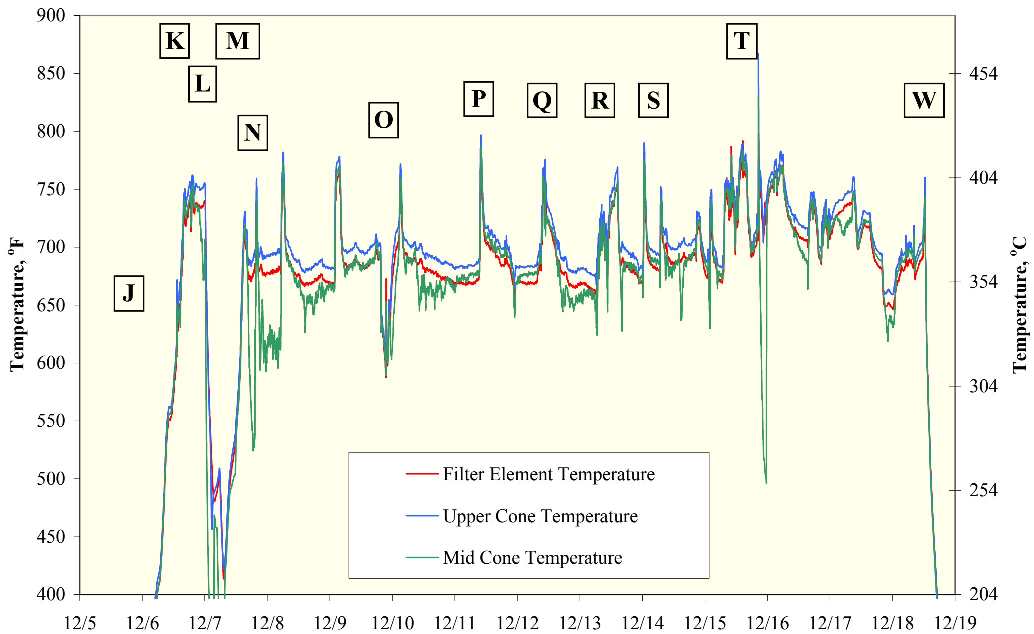

Figure 4.2-8 Filter Element and Cone Temperatures, TC10B

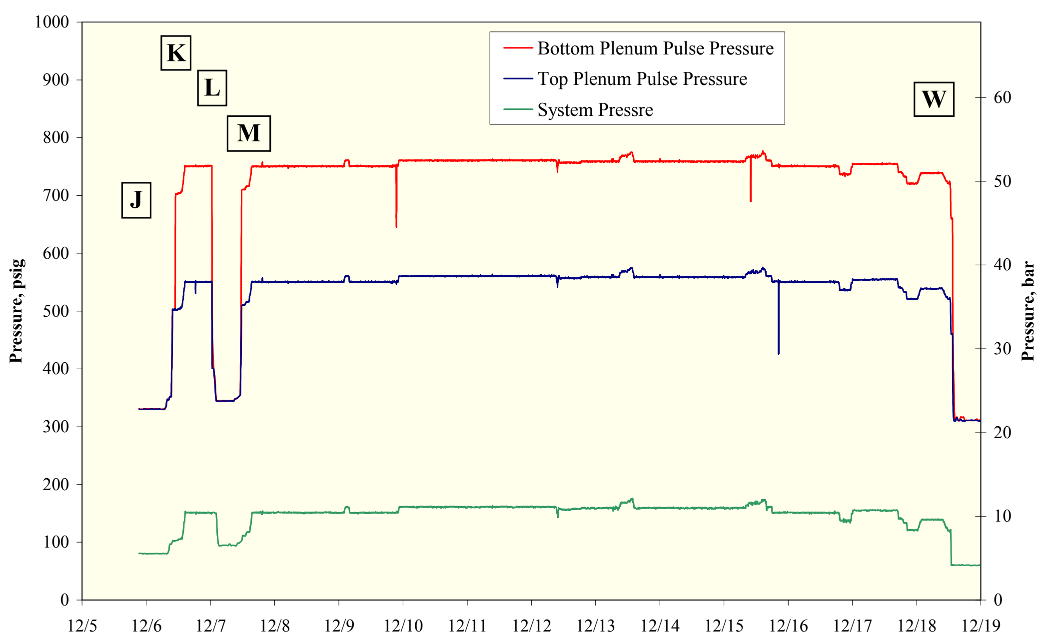

Figure 4.2-9 System and Pulse Pressures, TC10B

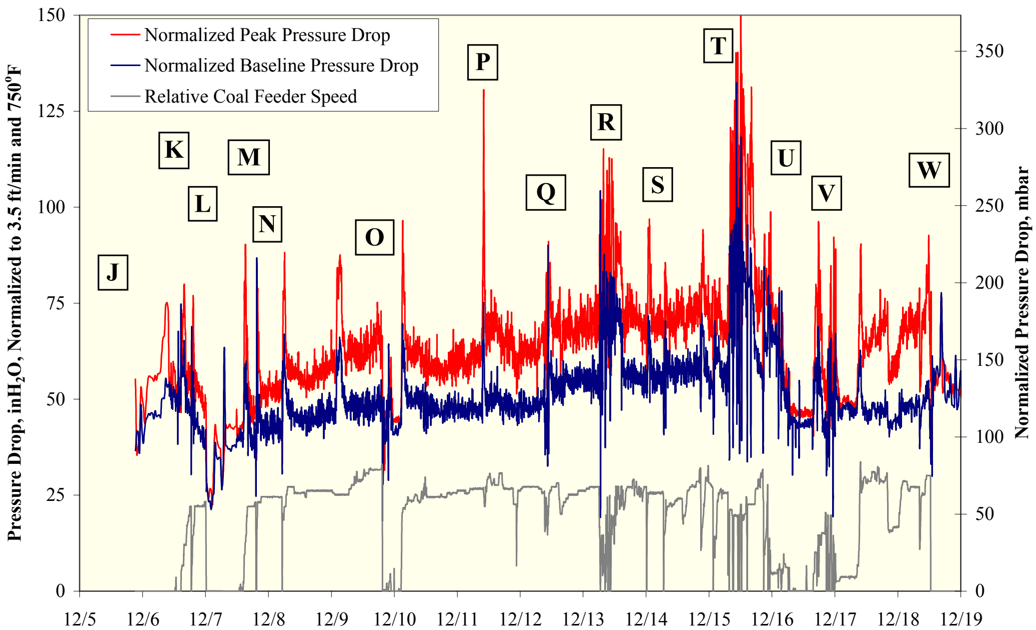

Figure 4.2-10 Normalized PCD Pressure Drop, TC10B

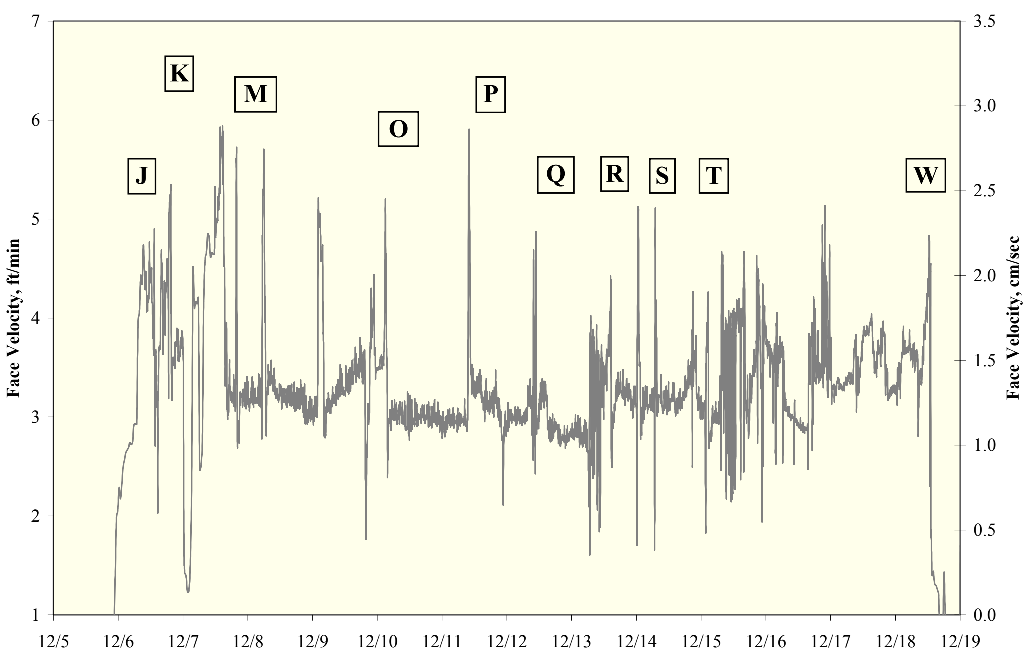

Figure 4.2-11 PCD Face Velocity, TC10B

4.3 TC10 INSPECTION REPORT

4.3.1 Introduction

During the TC10 gasification test run, November 16 through December 18, 2002, the PCD operated for 416 on-coal hours. During TC10, the Transport Gasifier operated 104 on-coal hours under air-blown operation, 293.5 on-coal hours under oxygen-blown operation, and 18.5 on-coal hours under enriched air operation. The test run consisted of two periods of testing. A short inspection outage occurred between the first and second part of TC10. The reason for the outage was to remove solid deposits in the lower mixing zone of the Transport Gasifier.

Overall, the PCD performed well was based on the following:

- No filter failures.
- No g-ash bridging was noted.
- Outlet particle loading from the PCD was maintained below 1 ppmw.
- Screw cooler (FD0520) seal modifications increased reliability.

Therefore, TC10 was considered a successful run for the PCD.

However, TC10 was not without its challenges. There were many process upsets that were a result of coal feeder problems. The coal used during this run was from the Powder River Basin. The as-received coal had a high moisture content that frequently plugged the FD0210 coal feeder. Also, a new coal feeder design was commissioned during TC10. The new feeder was not able to reliably feed the high moisture content coal to the gasifier, leading to several thermal events in the PCD.

During TC10, the solids removal system below the PCD experienced several challenges. There were several incidents of solids carryover from the Transport Gasifier standpipe. This carryover material had a high concentration of sand that plugged the solids removal system conveying line. Also, the top sphere valve seal failed on three occasions, while the lower sphere valve seal failed once, and the exit line sphere valve failed once as well.

The PCD internals were removed from the vessel and inspected after TC10. The outage inspection included examinations of the filter elements, their fixtures to the plenums, solids deposition, filter element gaskets, and auxiliary equipment. The subsequent sections will detail the findings of the inspections.

4.3.2 Filter Elements

For TC10, the following filter elements were installed (See Figure 4.2-1):

- Nine 1.5-meter Pall FEAL filter elements.
- Thirty-four 1.5-meter Pall FEAL filter elements with fuse.
- Ten Pall Hastelloy-X filter elements.

- Thirty-two 1.5-meter Pall Fluid Dynamics Division HR-160 sintered metal fiber filter elements.

During the outage between TC10 and TC11, all the Hastelloy X and HR-160 filter elements were removed from the PCD. During this outage, a cold-flow PCD model was commissioned. The cold-flow PCD model was designed to test filter elements and failsafe devices as a screening tool. HR-160 filter elements were used during the commissioning of the cold-flow model. It was noted that the HR-160 filter elements were leaking during the back-pulse. Also, the Hastelloy-X filter elements were tested, and it was found that they were leaking during the back-pulse as well. Finally, the FEAL filter elements were tested, and no solids penetration was noted. Based on these findings, it was decided to remove all the Hastelloy X and HR-160 filter elements from the PCD. These findings helped determine the source of the solids contamination that SRI has been reporting since TC07D (see past run reports). It is expected that once these filter elements are removed from service and replaced with FEAL filter elements, the solids contamination should disappear. Currently, we are working with Pall Corporation to rectify this problem with these filter elements.

A total of 10 Pall FEAL filter elements were removed. Each filter element was closely inspected and no obvious damage was noted. The welds were examined and no obvious separation from the filter media or cracks were noticed. The Pall FEAL filter elements have accumulated many gasification hours. The following table outlines the exposure hours of the Pall FEAL filter elements that were installed before TC10.

Exposure Hours after TC10	Number of FEAL Filters Exposed
2,897	6
2,427	2
1,484	22
1,334	1
416	12

Several of the FEAL filters that were removed were flow tested. The results of these tests are discussed in section 4.5.

As mentioned above, all the HR-160 filter elements were removed due to the solids penetration through the filter media. Once the HR-160 filter elements were removed, they were visually inspected. No obvious damage was noted upon inspection. Even though these filter elements were removed, there is still interest in testing the HR-160 alloy material. The following table outlines the exposure hours of the HR-160 filter elements that were installed before TC10.

Exposure Hours After TC10	Number of HR-160 Filters Exposed
1,630	1
970	1
824	3
416	27

The table above shows that one HR-160 filter element has accumulated over 1,600 on-coal hours. This filter element has been through many process upsets without failure. Also, there is no indication of corrosion with this alloy in gasification environment. Therefore, we are working with Pall Corporation to resolve the solids penetration issue.

In addition to removing all the HR-160 filter elements, all the Pall Hastelloy-X filter elements were removed during this outage due to solids penetration through the porous media. Once the Hastelloy-X filter elements were removed, they were visually inspected. There was no damage noted upon inspection. Just as with the HR-160, there is still interest in testing Pall Hastelloy-X filter elements based on their strength characteristics. Several of these filter elements have been through many process upsets without failure. The following table outlines the exposure hours of the Hastelloy-X filter elements that were installed before TC10.

Exposure Hours	Number of Hastelloy-X Filters Exposed
2,655	1
1,630	2
824	1
416	6

Once the solids penetration issues are resolved, testing will resume with the Pall Hastelloy-X filter elements.

4.3.3 G-ash Deposition

The plenum was pulled out of the PCD vessel on January 7, 2003. Figure 4.3-1 shows the internals after TC10 as it was being lifted out of the PCD. Figure 4.3-1 shows that there was no g-ash bridging present after TC10. The shutdown was clean, which means that both the top and bottom plenums were back-pulsed after shutdown.

The average residual dustcake thickness was ~0.01 inches. The dustcake was not as sticky or adherent as seen in past gasification test campaigns. The inspection revealed that the g-ash buildup on the filter element holders, upper and lower ash shed, and filter element support brackets was not very significant. The thin residual dustcake on the filter elements and the small buildup on the different PCD internals appear to indicate that tar condensation was not an issue during TC10. Also, it appears that all the changes that have been incorporated over the last several gasification runs have promoted a more stable operation within the PCD.

4.3.4 Filter Element Gasket

The current filter gasket arrangement used in past gasification runs has continued to be very reliable; therefore, it was used during TC10. The gasket types have been outlined in past run reports (see TC06 Inspection Report). During this outage, all the gaskets of the filter elements and failsafe devices that were removed were inspected. The following observations were made:

- There were no apparent leak paths in the area of the failsafe holder flanges that would indicate a leak past the primary gasket.
- Some of the gaskets were cut to inspect the extent of the g-ash penetration. The inside of the primary gaskets was relatively clean.
- The gaskets between the failsafe and plenum were clean, indicating a tight seal.

Based on these findings, the gasket material performed well through the 416-hour test run.

4.3.5 Fail-safes

During TC10, the following failsafe devices were tested: 50 PSDF-designed fail-safe devices and 35 Pall fuses. Also, 6 metal fiber fail-safe devices designed by Siemens Westinghouse were installed above blanks to expose different alloys to the reducing environment. Figure 4.3-2 shows the layout of the different failsafe devices during TC10. It was initially planned to test two fail-safe devices during TC10 by injecting dust. However, the higher-than-usual (>0.1 ppmw) outlet loading contamination from the PCD prevented the failsafe tests.

During the outage, two Pall FEAL fuses were removed, inspected, and flow tested. The fuses appeared to be in good condition with no obvious damage. The welds appeared to be in good condition as well, with no evidence of cracking. Both of the fuses were flow tested using air at ambient temperature and pressure. The flow tests did not reveal that the resistance to flow had increased significantly during the run. Figures 4.3-3 and -4 show the flow curves for the two Pall fuses after 416 hours of operational exposure. Based on these flow curves, there does not appear to be any pore blinding due to corrosion or solids penetration. Future plans are to continue testing the Pall fuses by exposing them to the reducing environment and solids injection tests.

After TC10, 12 PSDF-designed failsafe devices were removed for inspection. Each failsafe appeared to be in good condition with no damage noted. One of the test objectives for the PSDF-designed failsafe is to determine whether or not the porous material blinds over time. Each failsafe that was removed was flow tested during the outage. Figures 4.3-5 through -16 show the results of the flow tests for each PSDF failsafe. The table below outlines the total hours for each failsafe device that was tested and its corresponding ratio of flow coefficients.

Failsafe ID	Total Exposure Hours	Ratio of Flow Coefficients
PSDF #2	2,258	1.06
PSDF #5	1,383	0.94
PSDF #1	2,553	1.06
PSDF #4	1,383	1.03
PSDF #24	1,088	1.11
PSDF #13	724	1.16
PSDF #14	823	1.23
PSDF #15	724	1.13
PSDF #16	724	1.17
PSDF #35	416	0.87
PSDF #36	416	0.89
PSDF #37	416	0.81

The ratio of flow coefficients in the table above is determined by taking the flow coefficient after TC10 and dividing it by the flow coefficient before TC10. The table shows that there was no significant change in the flow coefficients. It is interesting to note that all but one of the failsafe devices with exposure hours greater than 416 regained some of the flow coefficient, while the flow coefficient of the failsafe devices that were installed new before TC10 decreased. It has been noted in past run reports that solids penetration into the porous media decreased the flow coefficient. Therefore, it is possible that the recovery of flow coefficient is due to some of the solids being dislodged during a back-pulse. It appears that the flow coefficient of each failsafe device decreases until all the available pores that are smaller than the particle mean size plug. It is believed that the poor collection efficiency of the HR-160 and Hastelloy-X filter elements caused the loss in flow coefficient. This phenomenon of pore plugging should disappear once these filter elements are removed and replaced with filter elements with higher collection efficiency.

4.3.6 Auxiliary Equipment

During TC10, seven prototype inverted filter element assemblies supplied by SWPC were installed in the PCD and tested. Figure 4.3-2 shows their position on the top plenum. Two inverted filter assemblies using 1.5-meter Pall FEAL filter elements were tested during TC08 and TC09. During the post test inspection after TC08 and TC09, no indication of dust leakage or bridging was noted. Since the initial test results were positive for TC08 and TC09, it was decided to install seven inverted filter element assemblies for TC10. The TC10 inspection did not reveal any indication of leakage or plugging. Therefore, further testing will continue during TC11.

Six g-ash resistance probes were tested during TC10. These probes have been described in past run reports (see TC08 Run Report). The probes were installed to detect g-ash bridging between the filter elements. The inspection did not reveal any damage; therefore, further testing will continue.

For TC10, six new resistance probes were installed in the PCD hopper in addition to the existing six between the filter elements. Four probes were installed on a rod at the centerline of the PCD vessel, with the lowest probe located approximately halfway down the hopper. These probes were utilized as a solids level detection within the hopper of the PCD. The data collected during TC10 was useful in establishing that these probes can be utilized for level detection in the PCD hopper. Inspection of the hopper probes did not reveal any damage. Since operational testing proved that the probes could be used to monitor the solids level and no damage was noticed after the inspection, future testing on these probes will continue during TC11.

The back-pulse pipes were removed and inspected during this outage (See Figure 4.3-17). There was no significant damage on the pulse pipes. Figure 4.3-17 shows tar deposits on the back-pulse pipe. This deposit was spongy in texture. Tar deposits on the back-pulse pipes have been noted and reported in the past. It does not appear that these tar deposits caused significant corrosion. The back-pulse pipes did not reveal any significant changes from before TC10. Finally, the inner liner of each back-pulse pipe was inspected. The liner appeared to be in good condition with no obvious damage (See Figure 4.3-18).

4.3.7 Fine Solid Removal System

The screw cooler (FD0502) performed well during TC10. Other than minor packing adjustments, FD0502 did not require any attention from the maintenance or operation personnel during operation, which was encouraging in light of the modifications made to FD0502. Before TC07D, several modifications were made to the drive-end stuffing box in an attempt to increase reliability. These modifications were documented in the TC07 run report. Since the modifications improved performance during TC07, it was decided to implement the same changes to the nondrive end before TC08. The same set of seals have been tested on the drive-end since TC07D for a total of 1,398 on-coal hours. The same set of seals have been tested on the nondrive end since TC08 for a total of 1,097 on-coal hours. The new modifications continued to perform well during TC10. Therefore, it was decided not to disassemble the stuffing box during this outage.

One of the methods that is used to determine the success of the new stuffing box modifications is tracking the packing follower gap. Figure 4.3-19 shows the packing follower gap that is being measured. The packing follower is used to compress the shaft seal rings to prevent process gas from leaking. Once there is no more room to compress the follower, it is time to replace the seals. The packing follower gap has been monitored since TC08. The following table summarizes the packing follower measurements:

Time Period	Drive-End Gap, in.	Nondrive-End Gap, in.
Before TC08	1.75	1.75
After TC08/Before TC09	1.375	1.625
After TC09/Before TC10	1.125	1.375
After TC10	1.0625	1.25

The table above shows that both the drive-end and nondrive-end packing follower gaps still have room for compression. Therefore, it was decided not to disassemble FD0502 during this outage in order to accumulate operating experience with the new modifications.

The fine solids depressurization system (FD0520) required a large amount of attention by process engineers and operations during TC10. Many of the problems associated with FD0520 were related to periodic increases of solids loading to the PCD or failed seals. It has been noticed in past test runs that FD0520 operates properly as long as the solids consist mainly of g-ash. However, FD0520 has trouble conveying solids carried over from the gasifier after a gasifier upset. One of the problems with the Clyde Pneumatic system is that the bottom of the dense phase vessel has a reducing 90º bend. The 90º bend reduces from 6-inch ID to 2-inch Schedule 160 pipe, which promotes packing within the conveying line. Therefore, changes to the bottom of FD0520 were made during the TC10 outage.

Figure 4.3-20 shows the original 90º bend on FD0520. Figure 4.3-21 shows the new modification. The original design was replaced with a new design that has the potential to fluidize the solids while conveying. Also, the new design allows easier access in the event of a conveying line plug, which will save time. The new outlet design gives the operators the flexibility to try many things to unplug the conveying line before calling maintenance out to disassemble FD0520. Nozzle A on Figure 4.3-21 will allow operations to connect to a higher pressure source to blow the line out, while nozzle B will give operations a rod-out port. The addition of this modification should increase reliability and reduce the amount of downtime in the event of a conveying line plug. However, a reliable solids level detector needs to be identified and installed in FD0520 in order to increase the cycle efficiency and reduce problems associated with high solids loading.

During TC10, there were a lot of problems associated with the sphere valve seals. In past run reports, it has been reported that the Nomex-filled Viton seals cracked during operation because they were too brittle at temperatures below 200°F. Therefore, Clyde Pneumatics suggested that a Nomex-filled Silicon material should be used instead. The Nomex-filled Silicon material was installed before TC10.

During the leak check before TC10, the Nomex-filled Silicone on the top sphere valve failed twice. The cause of these failures was determined to be sticking pilot valves that vent the pressure off the seals. It was found that the seal pressure did not vent until ~4 seconds after the dome was fully open, meaning that the dome was rotating on a fully inflated seal. The pilot valve was replaced, and the problem disappeared on the top vessel. In order to prevent this from happening again in the future, a pressure switch was added to keep the spheri valve from rotating while there is still pressure on the seal.

The lower sphere valve seal failed a couple of days later. The root cause of the failure was solids plugging the pneumatic controls. It appears that the solids were introduced into the control nitrogen through a failed sphere valve in the conveying line. Figure 4.3-22 shows the outlet spheri valve seal after TC10. The purpose of this valve on the outlet is to keep solids from flowing down the exit pipe while the lower vessel is being filled. Therefore, there was no alarm on this valve to indicate that it had failed. This failure gave direct access to the control nitrogen. So each time solids were conveyed out of the lower vessel to FD0530, solids were being forced in the pneumatic control system, which interrupted the normal operations. During this outage, an in-line filter was installed in the control line to the outlet sphere valve seal to prevent this from occurring again.

Finally, the top sphere valve failed again midway through the run. The seal would not hold pressure; therefore, it was thought that the seal had failed. However, once the seal was removed, no damage was found. It appears that the leaking was a result of material problems. It is believed that the more pliable Nomex-filled Silicone material may be too pliable. Therefore, it was decided to replace the Nomex-filled Silicone seal with the Nomex-filled Viton seal. This was a short-term fix to allow the completion of TC10. For TC11, an Everlasting Valve is going to be installed and tested. It is believed that the Everlasting Valve is a more robust design that should increase the reliability of the fine-solids removal system.

Figure 4.3-1 Filter Internals After TC10

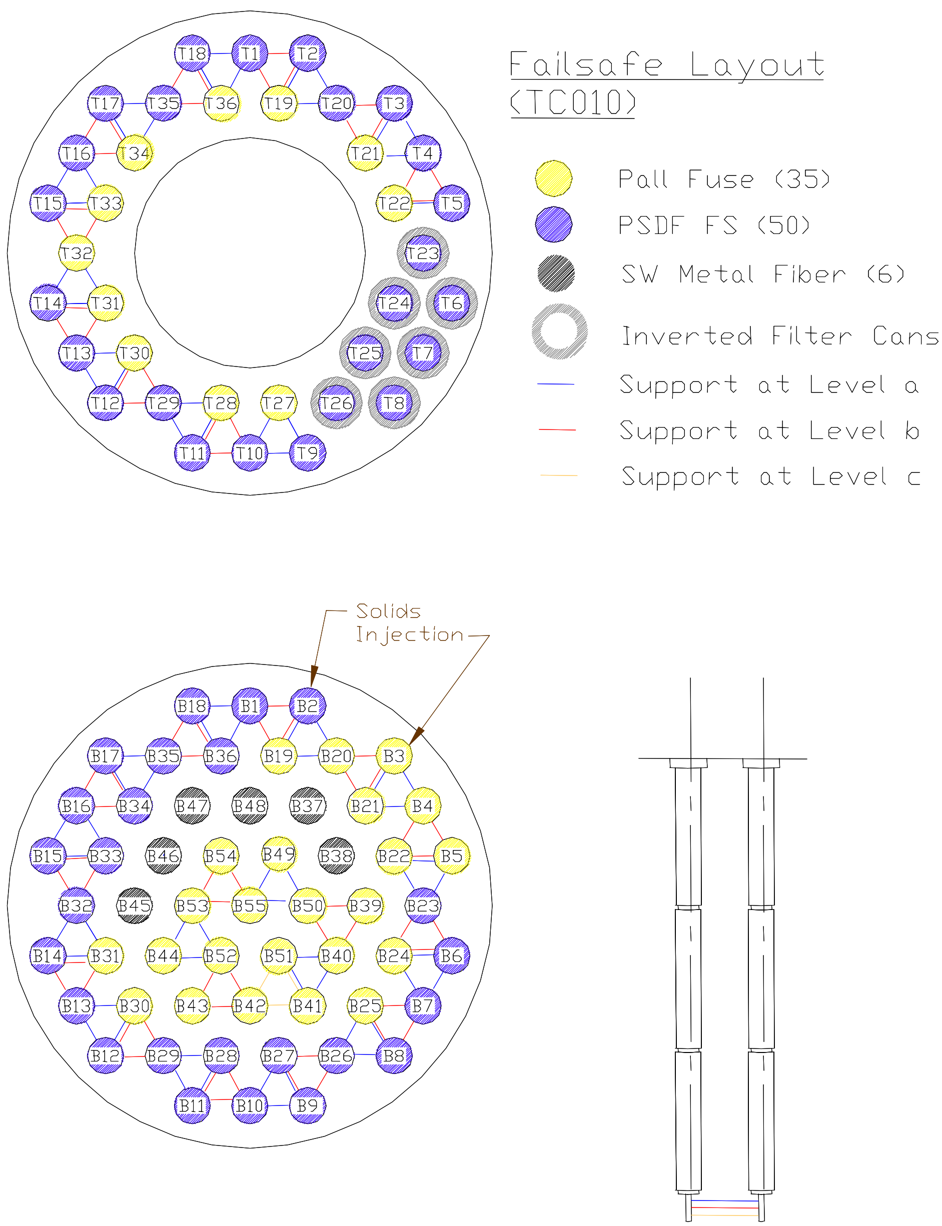

Figure 4.3-2 Failsafe Layout for TC10

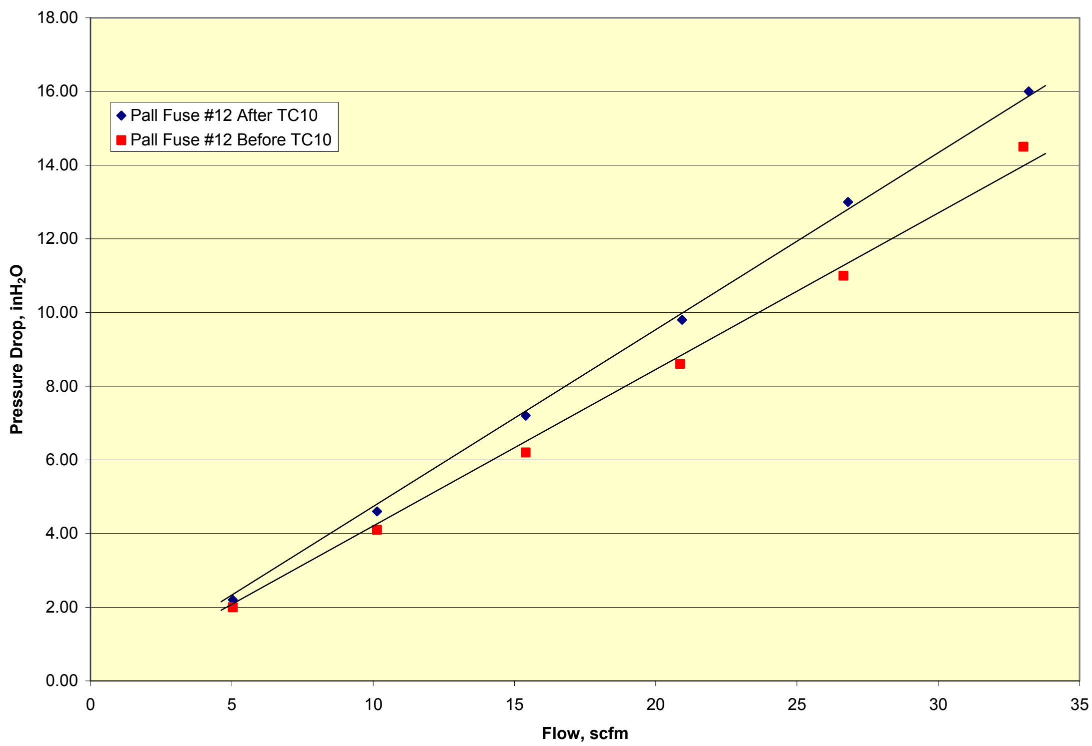

Figure 4.3-3 Flow Curve for Pall Fuse #12

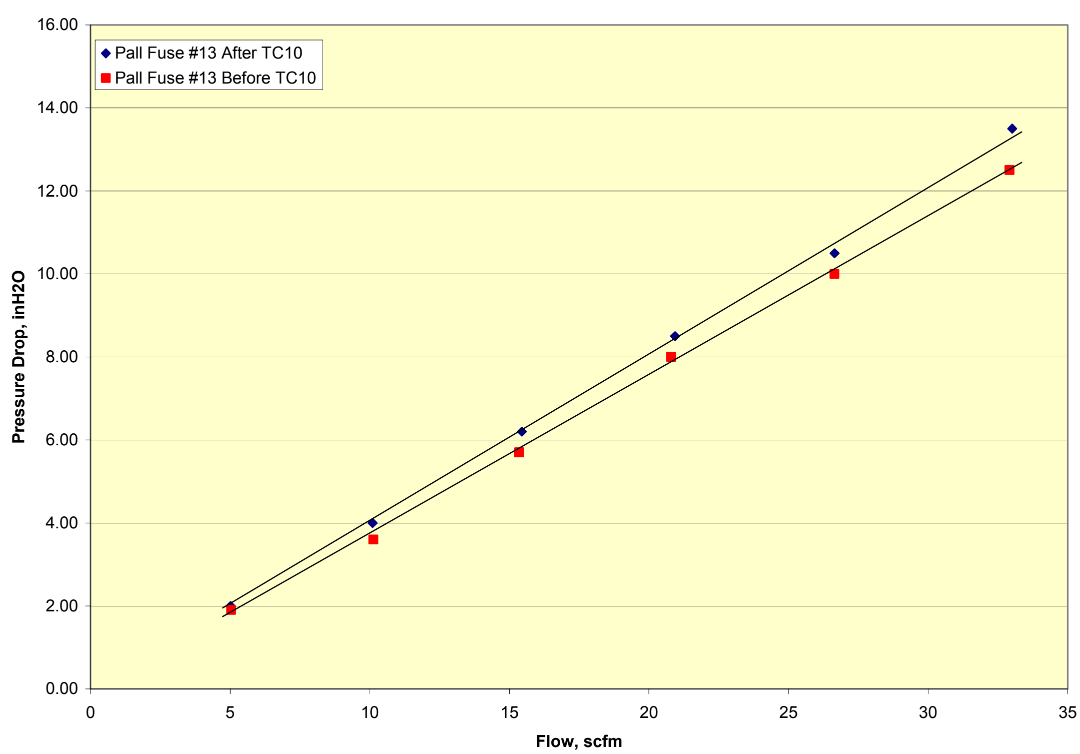

Figure 4.3-4 Flow Curve for Pall Fuse #13

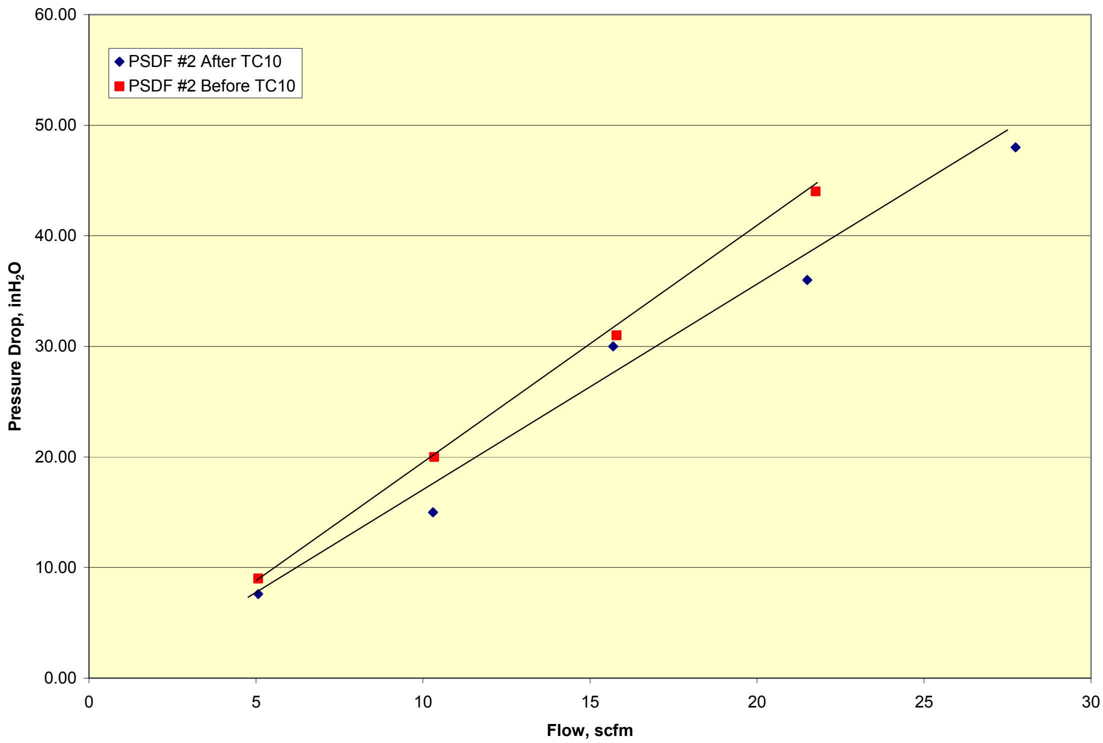

Figure 4.3-5 Flow Curve for PSDF #2 Before and After TC10

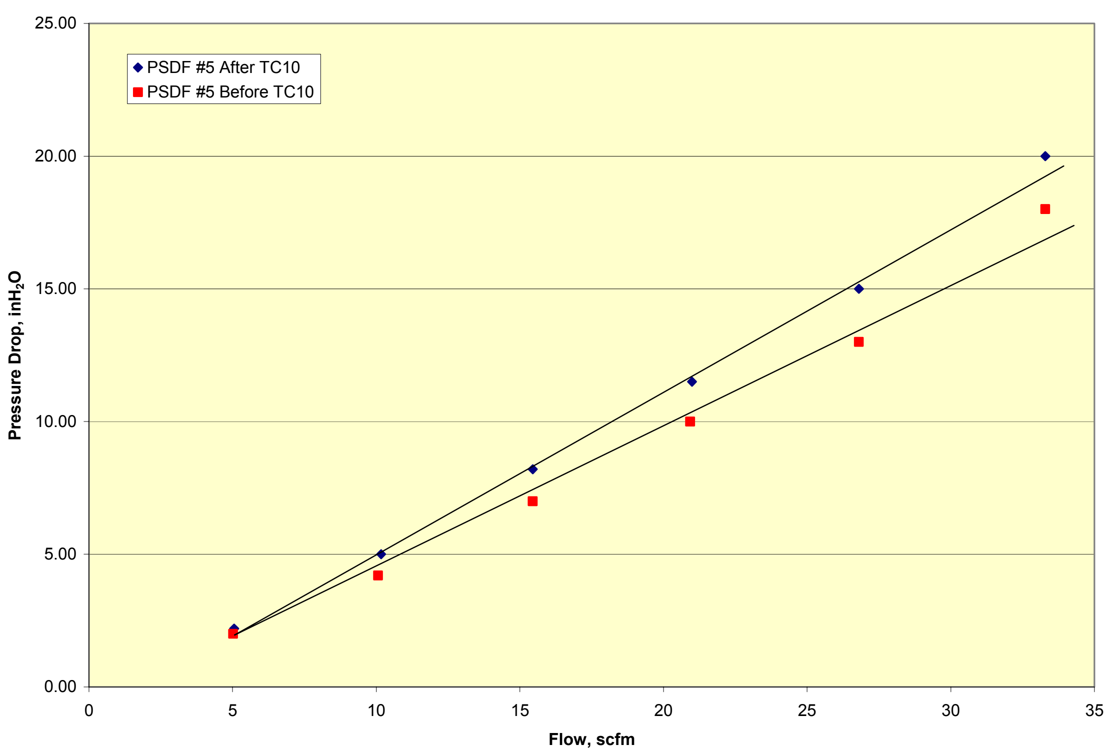

Figure 4.3-6 Flow Curve for PSDF #5 Before and After TC10

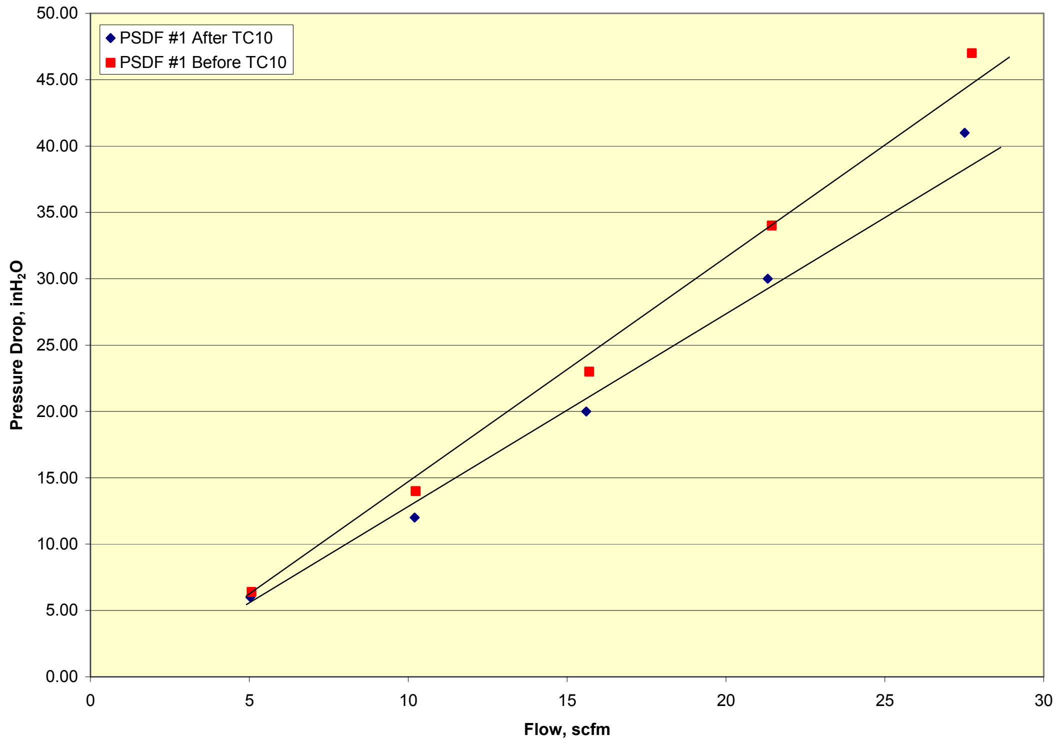

Figure 4.3-7 Flow Curve for PSDF #1 Before and After TC10

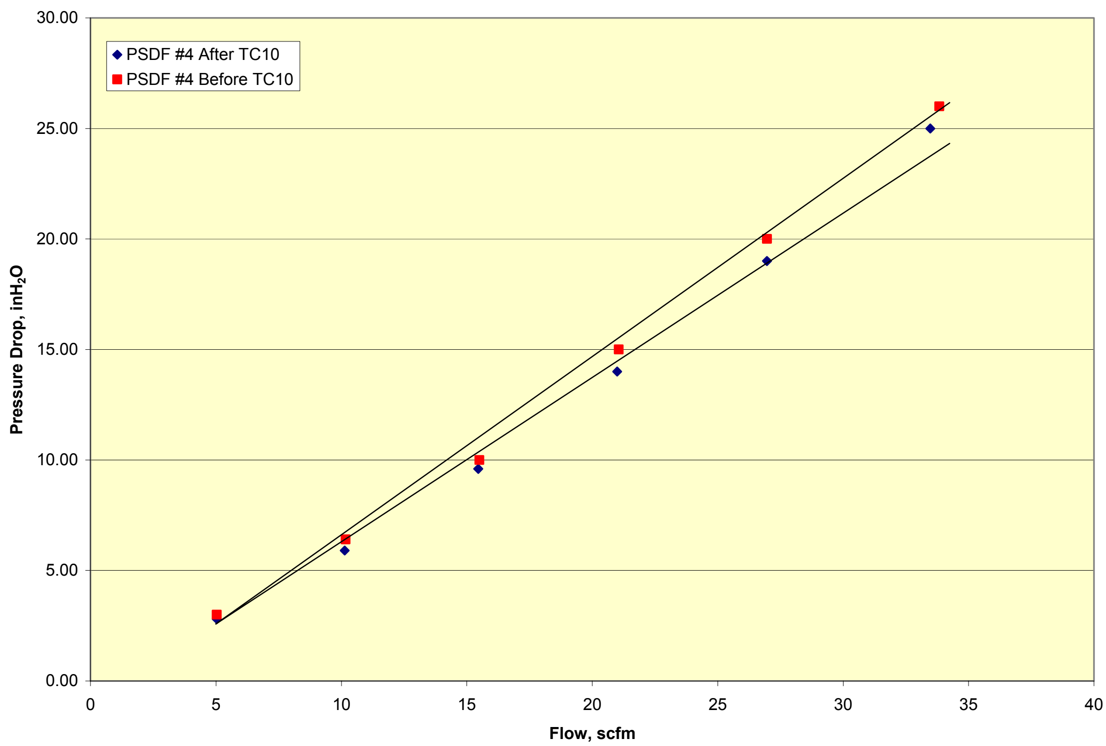

Figure 4.3-8 Flow Curve for PSDF #4 Before and After TC10

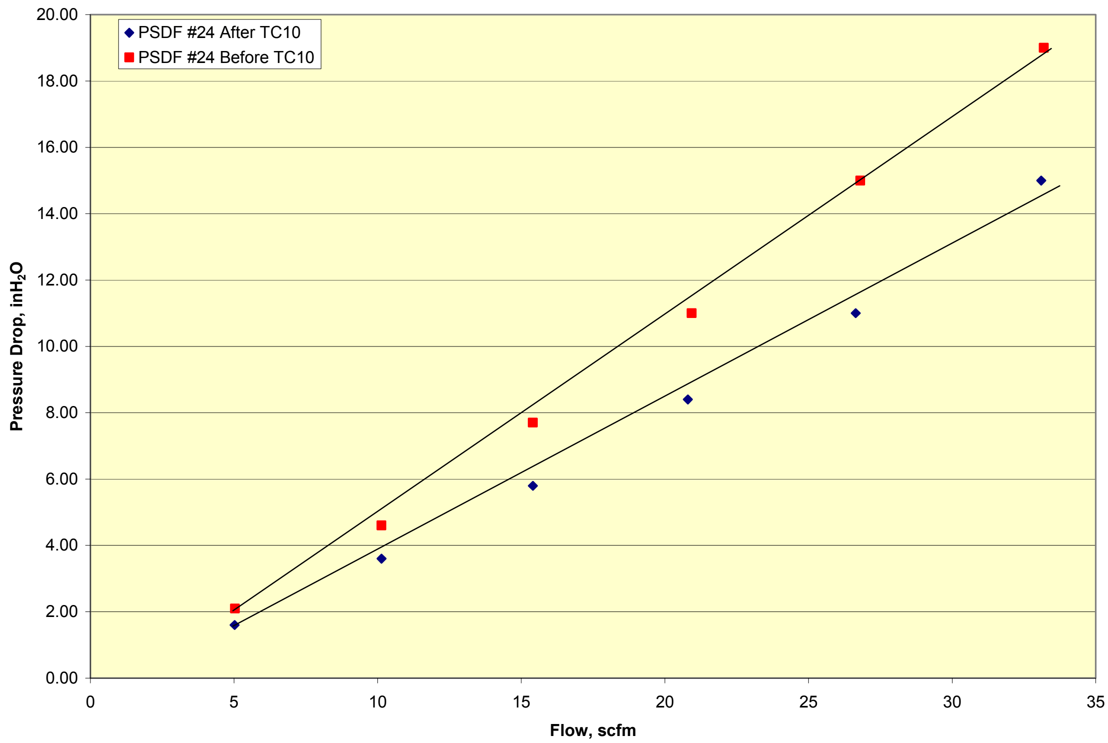

Figure 4.3-9 Flow Curve for PSDF #24 Before and After TC10

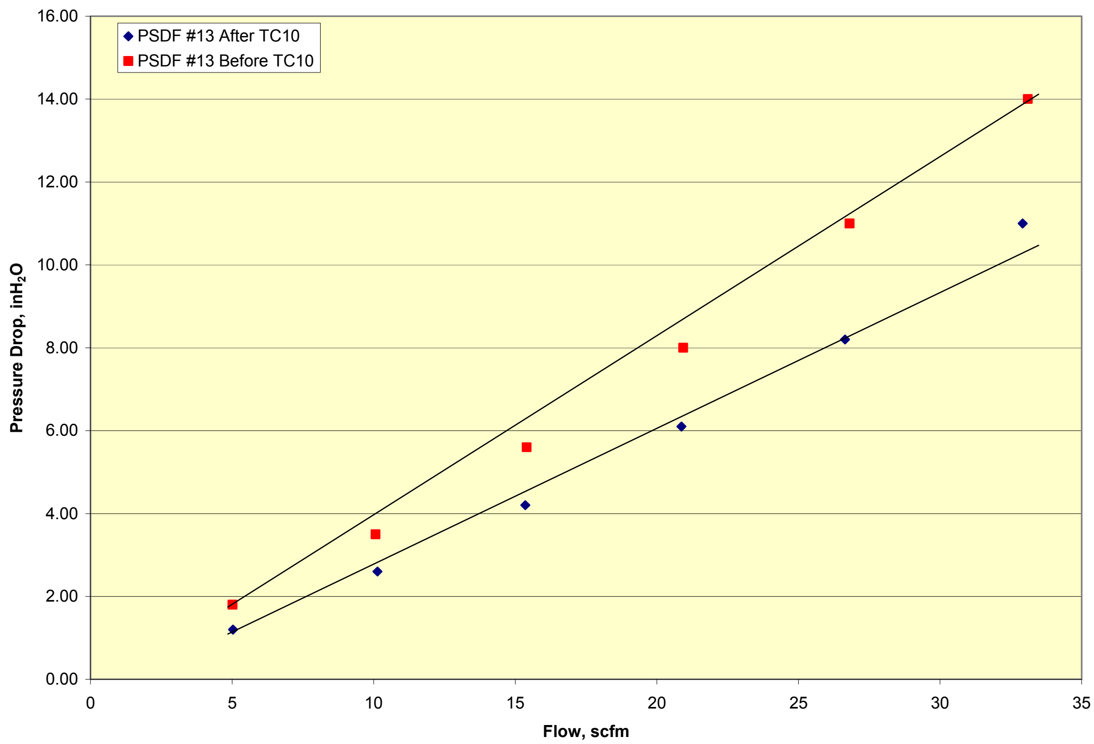

Figure 4.3-10 Flow Curve for PSDF #13 Before and After TC10

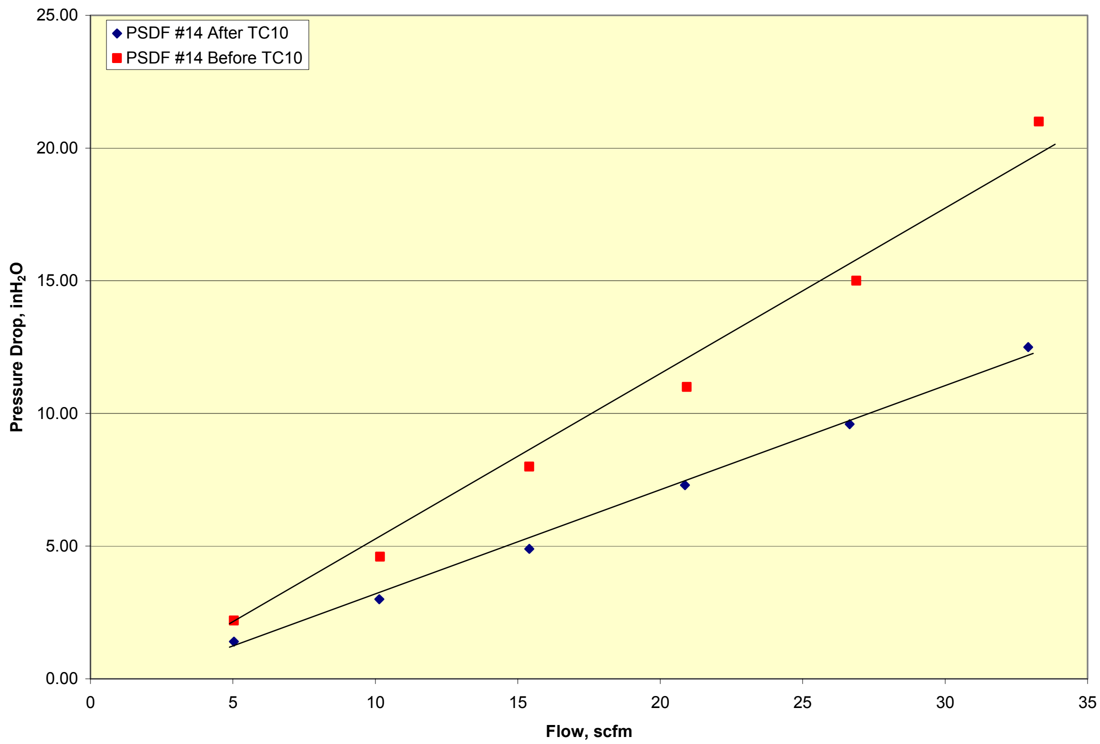

Figure 4.3-11 Flow Curve for PSDF #14 Before and After TC10

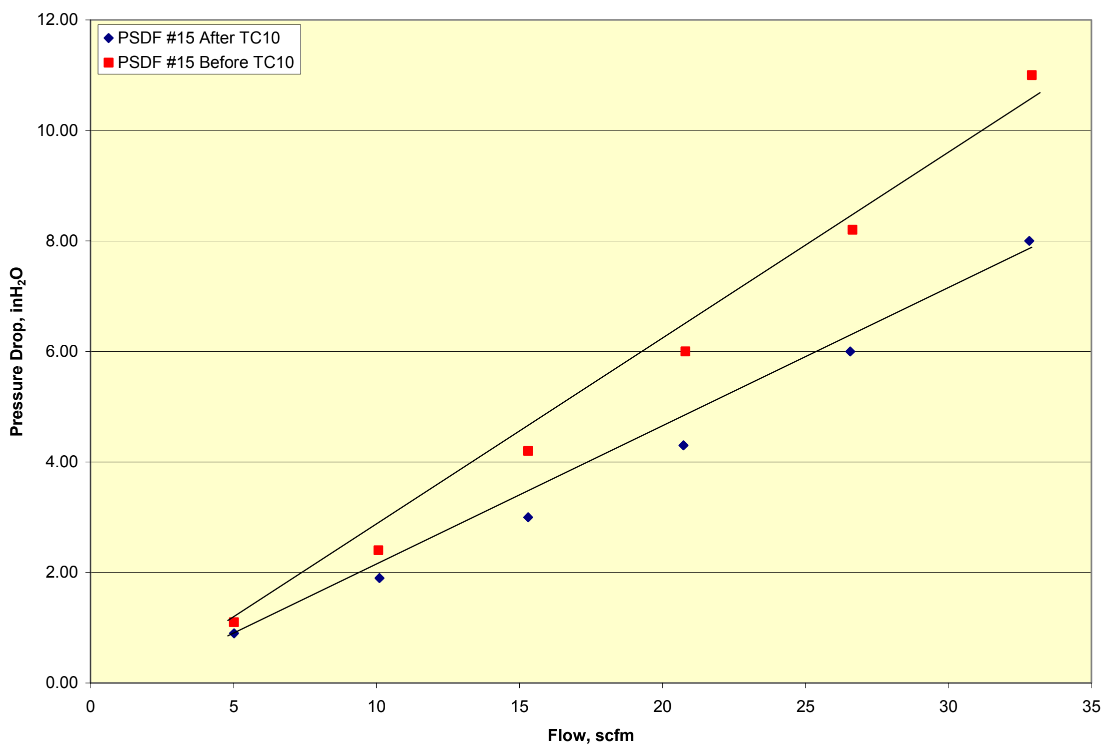

Figure 4.3-12 Flow Curve for PSDF #15 Before and After TC10

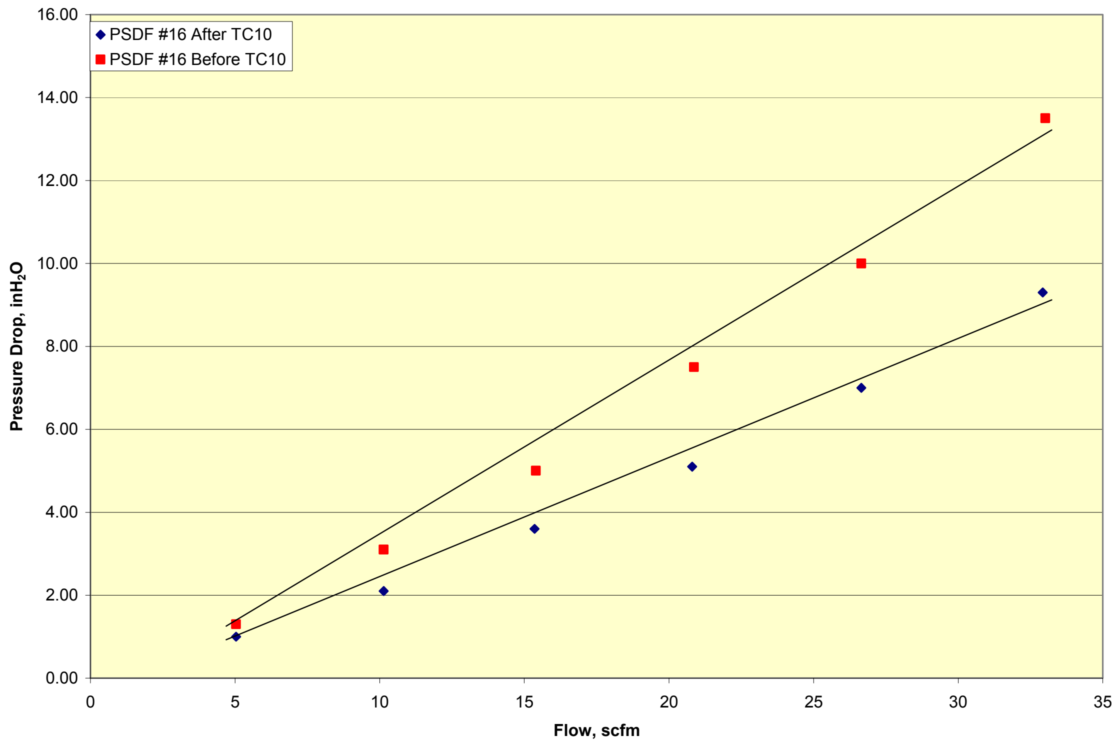

Figure 4.3-13 Flow Curve for PSDF #16 Before and After TC10

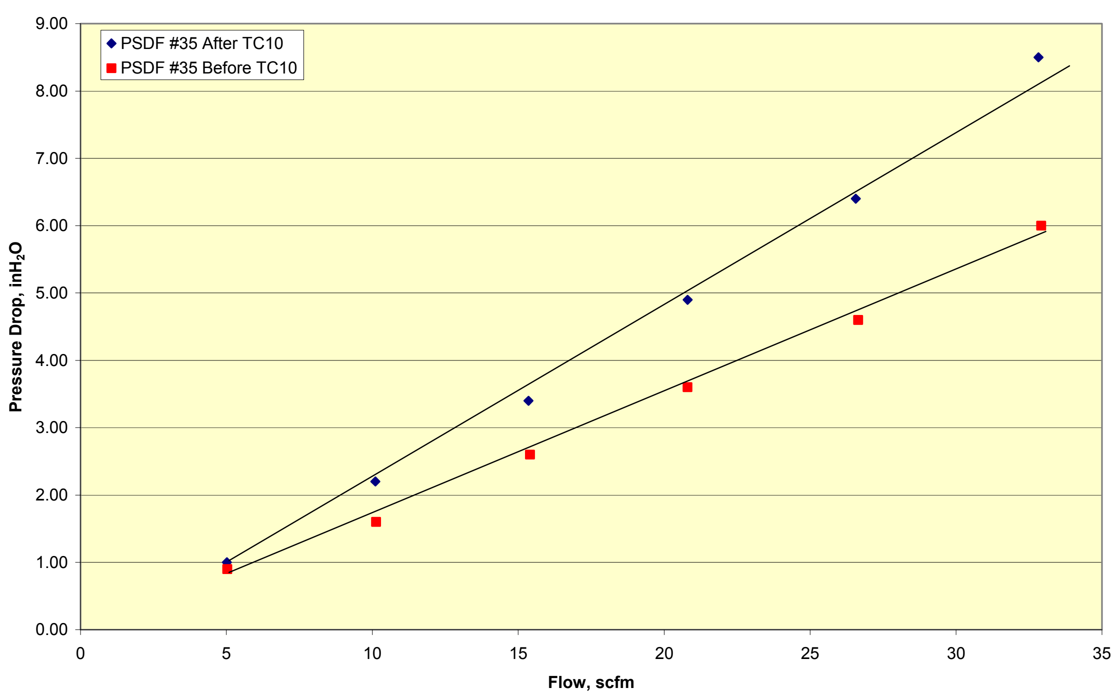

Figure 4.3-14 Flow Curve for PSDF #35 Before and After TC10

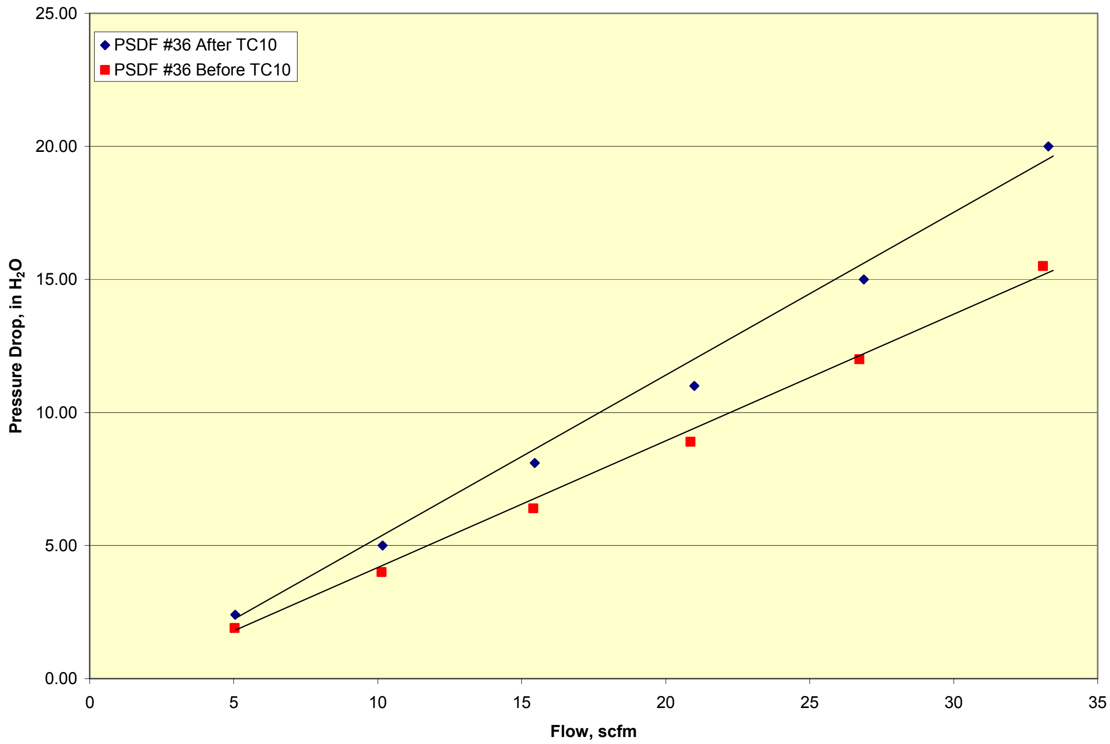

Figure 4.3-15 Flow Curve for PSDF #36 Before and After TC10

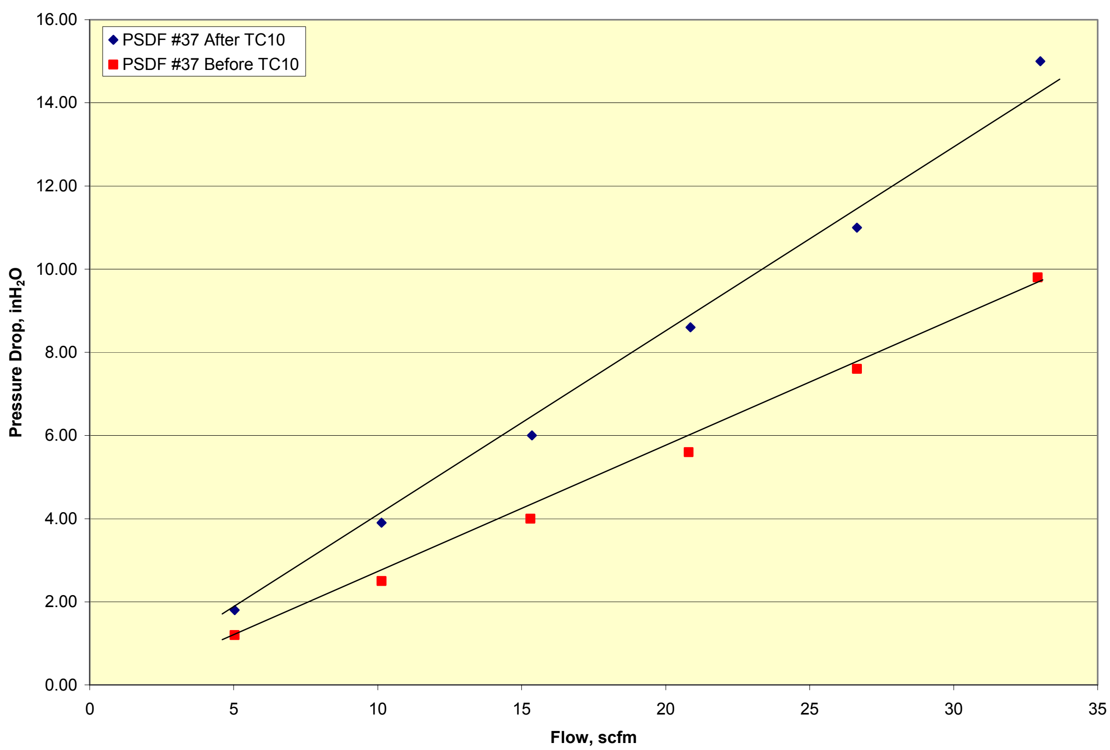

Figure 4.3-16 Flow Curve for PSDF #37 Before and After TC10

Figure 4.3-17 Back-Pulse Pipe After TC10

Figure 4.3-18 Back-Pulse Pipe Inner Liner After TC10

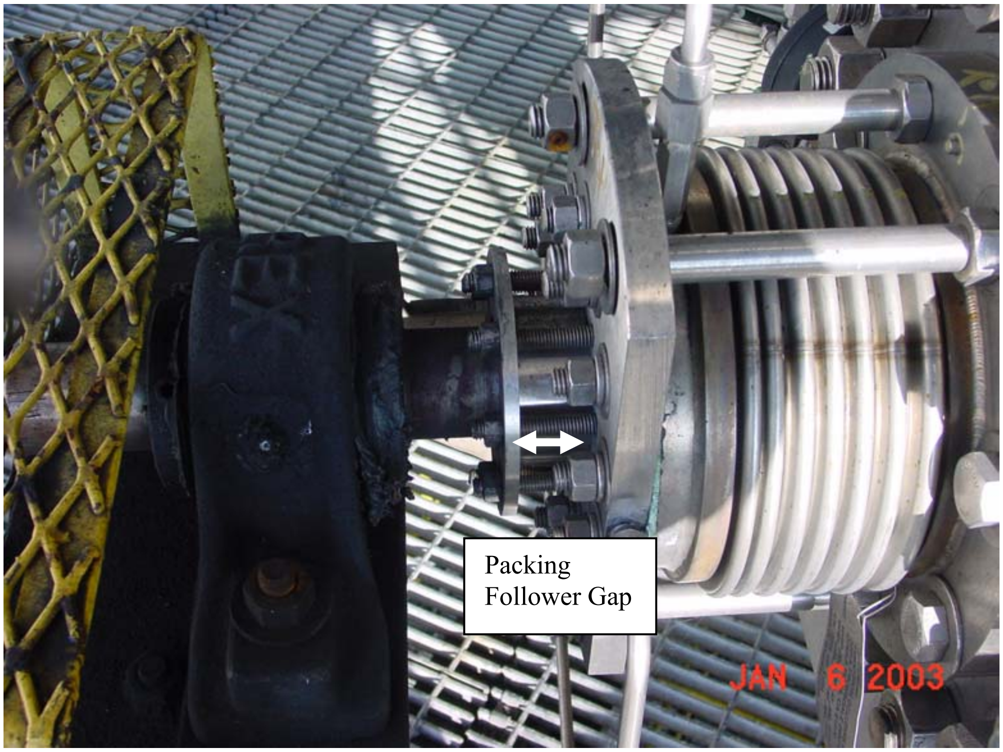

Figure 4.3-19 Packing Follower Gap on Nondrive End of FD0502 After TC10

Figure 4.3-20 Original 90˚ Bend From FD0520

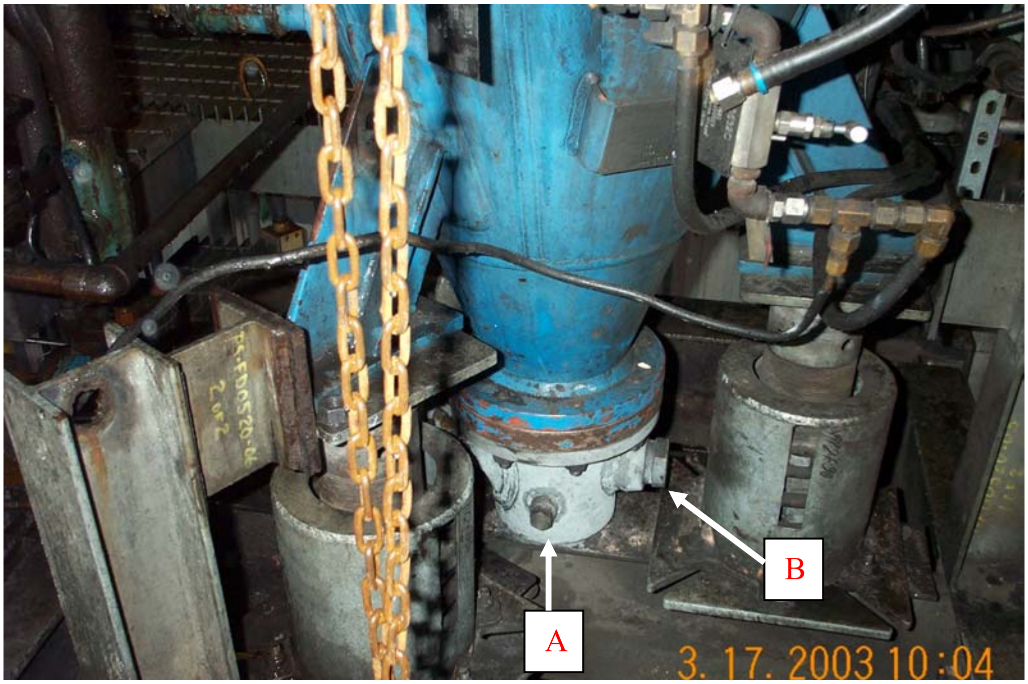

Figure 4.3-21 New FD0520 Modification Before TC11

Figure 4.3-22 Outlet Conveying Line Spheri-Valve Seal After TC10

4.4 TC10 GASIFICATION ASH CHARACTERISTICS AND PCD PERFORMANCE

This section deals with the characteristics of the g-ash produced during TC10 and the relationship between the g-ash characteristics and particulate control device (PCD) performance. As in previous tests, in situ samples and dustcake samples from TC10 were thoroughly characterized in an effort to better understand the effects of the g-ash characteristics on PCD pressure drop (ΔP). Characterization of the in situ samples and dustcake samples included measurements of the true particle density, bulk density, uncompacted bulk porosity, and specific-surface area; chemical analyses; particle-size analyses; and laboratory drag measurements. As in the previous gasification tests, drag measurements were made using the resuspended ash permeability tester (RAPTOR) as modified to allow measurements as a function of particle size. As in previous tests, the RAPTOR drag measurements were compared to transient drag values determined from PCD performance data. The results were used to better understand the contribution of the dustcake to PCD ΔP and to gain insight into the effect of particle size and morphology on drag. Physical, chemical, and drag characteristics of the TC10 samples were compared to discern any differences between air- and oxygen-blown operation, as well as any differences between TC10 and previous tests with PRB coal.

The TC10 test campaign began with a brief period of air-blown gasification followed by oxygen-blown operation during the majority of the testing. Throughout the TC10 test program, there were frequent disruptions in the coal feed, possibly related to the high moisture content of the coal. As a result of the coal feed disruptions, temperatures in the gasifier apparently dropped below the threshold required for tar cracking, resulting in episodes of tar carryover to the PCD. As discussed in the section on the outlet particulate sampling, evidence of the tar carryover could be seen in the form of yellow or black deposits on some of the outlet sampling filters. Four of the nine outlet sampling filters were contaminated with some form of these oils/tars. The oil/tar contamination of the sampling filters made it difficult to determine the true outlet particulate loading during some of the sample runs. The contamination may have also had some effect on the specific-surface area of the g-ash entering the PCD, as discussed in the section on physical properties. Because of these tar-related effects, the properties of the TC10 g-ash may not reflect the true nature of PRB g-ash produced under stable gasification conditions.

4.4.1 In situ Sampling

The system and procedures used for the in situ particulate sampling have been described in previous reports. In situ samples were collected at the PCD inlet and outlet throughout TC10. One inlet sample and one outlet sample were collected during air-blown operation, and nine inlet samples and eight outlet samples were collected during oxygen-blown gasification. Table 4.4-1 gives a summary of the particulate loadings measured at the PCD inlet and outlet.

4.4.1.1 PCD Inlet Particle Mass Concentrations

As shown in Table 4.4-1, the particulate loading entering the PCD varied from 18,100 to 33,300 ppmw in oxygen-blown operation, corresponding to a PCD solids mass rate of 250 lb/hr to 500 lb/hr. As seen in previous tests, the variation in inlet particulate loading was directly related to changes in the coal-feed rate. Because of differences in coal-feed rate, the range of inlet loadings obtained in TC10 was slightly lower than the range of inlet particle concentrations obtained with

PRB coal in TC08 (18,100 to 33,300 ppmw in TC10 versus 25,900 to 38,500 ppmw in TC08). The single measurement obtained under air-blown conditions (14,600 ppmw) was within the range of loadings obtained during the air-blown portion of TC08 (12,500 to 16,700 ppmw). Therefore, the particulate loadings measured at the PCD inlet were apparently not biased significantly by the problems with coal feed disruptions and unstable operation.

4.4.1.2 PCD Outlet Particle Mass Concentrations

Particulate loadings measured at the PCD outlet are included in Table 4.4-1 and plotted along with data from previous runs in Figure 4.4-1. The lower dashed line on the graph indicates the lower limit of detection, which is currently about 0.1 ppmw. The upper dashed line at 1 ppmw is included to guide the eye and does not reflect an acceptable emissions limit. The acceptable emissions limit is a function of the specifications on downstream equipment (gas turbine, fuel cell, gas separation membrane, etc.).

As shown in Table 4.4-1 and Figure 4.4-1, four of the outlet particulate samples were contaminated with either a yellow liquid or a black tar substance. The presence of these contaminants led to biased filter weights as noted in the table and figure. If these biased samples are disregarded, the remaining measurements indicate that the outlet particulate loading was initially 0.22 ppmw and then declined to 0.13 ppmw by the third day of the test and then to less than 0.1 ppmw by the sixth day of the test. Even when the measured concentration was less than 0.1 ppmw, however, particles could still be seen on the sampling filters under the optical microscope.

In addition to the restrictions placed on the total particulate loading, many turbine specifications also place stringent limits on the concentration of large (>10-μm) particles. Microscopic inspections of the noncontaminated TC10 sampling filters revealed that almost all of the particles were smaller than 10 μm, but some particles were larger than 10 μm. Although these large particles are very few in number, their presence could be a violation of the turbine specifications.

The appearance and size distribution of the particles on the noncontaminated sampling filters suggested that they were g-ash particles that had penetrated through the PCD. They did not appear to be any type of tar or other extraneous contaminant. The same conclusion was reached in TC09. As discussed in the TC09 report, subsequent tests conducted after TC10 in the PCD cold-flow model showed that certain types of filter elements allow particle penetration. In particular, new Pall HR-160 and new Pall Hastelloy-X filter elements allowed significant particle penetration. The same types of elements allowed much less particle penetration after they had been seasoned for a period of time in the hot-gas filter.

Prior to TC09, no more than six elements of the type that allow particle penetration (either new Hastelloy X or new HR-160) were installed in any given run. The filter element layout used in TC09 included a total of 22 new elements of these types, while the layout used in TC10 included 32 new elements of these types. Because of the relatively low number of Hastelloy-X and HR-160 elements used prior to TC09, it is not surprising that the earlier test programs did not show any evidence of particle penetration of the type seen in TC09 and TC10.

The tests in the cold-flow model showed that the HR-160 and Hastelloy-X elements apparently undergo a conditioning effect in which the particle penetration is reduced over time as the residual dustcake is established, and particles partially plug the pores of the elements. This conditioning effect may explain why the outlet particle loading decreased from the initial value of 0.22 ppmw to below the lower limit of resolution (<0.1 ppmw).

4.4.1.3 Syngas Moisture Content

As in previous tests, measurements of the syngas moisture content were made in conjunction with the outlet particulate sampling runs. The water vapor content of the syngas was determined by collecting the condensate from the syngas in an ice-bath condenser and calculating the vapor concentration from the volume of gas sampled and the volume of condensate collected. The values determined for individual sample runs are included in Table 4.4-1. The data obtained in TC10 with oxygen-blown operation showed an average syngas moisture content of about 20 percent compared to only about 12 percent in the single measurement obtained with air-blown gasification. These results are very similar to the moisture measurements obtained in TC08 where the average moisture content was about 22 percent with oxygen-blown operation and about 9 percent with air-blown operation. Higher moisture content is expected in oxygen-blown operation due to the higher rate of steam addition required to cool the lower mixing zone.

The condensate samples that were collected during TC10 contained variable amounts of oils and tars. Liquid and/or solid globs of tar and/or oily films were present in all of the condensate samples that were obtained during the collection of the contaminated particulate samples. In the cases where the particulate loading was less than 0.1 ppmw, the condensate samples were almost clear except for a thin oily film on the water surface and on the walls of the sample bottles.

4.4.1.4 Real-Time Particle Monitoring

The PCME DustAlert 90 showed little or no response during most of TC10. The monitor would occasionally give an erratic signal, but there was no response whatsoever during much of the run. In the past, there has been some noise in the PCME signal even when the particle concentration was below the lower limit of detection (about 0.5 ppmw). However, most of TC10 was characterized by the complete absence of any PCME response (not even any noise in the signal). It was clear that the PCME was not operating normally, and the unusual behavior led us to suspect there was some sort of short-circuiting of the signal or some type of internal electrical problem with the instrument.

On the next-to-last day of testing, the PCME was tested by injecting g-ash into the PCD outlet piping ahead of the PCME. The PCME failed to respond, even at very high injection rates that had produced large PCME responses in the past. The failure of the PCME to respond to the injected dust and the complete absence of any response during much of the run confirmed that there was definitely a problem with the instrument. After consulting with the instrument supplier, it was decided that an electrical circuit board in the sensing unit had probably gone bad. After TC10, the PCME was removed from the PCD outlet piping, and the electrical sensing board was replaced. The repaired unit will be tested again in TC11.

4.4.2 Sampling of PCD Dustcakes

After TC10, measurements were made of the dustcake thickness, and bulk samples of the dustcake were collected. Dustcake thickness measurements were made on several individual filter elements of each type to determine whether the element type had any effect on the dustcake thickness. As shown in the table below, the cake seemed to be thinner on the iron aluminide elements than it was on either the HR-160 or Hastelloy-X elements.

Element Type	Range of Measured Dustcake Thickness, in.	Average Thickness, in.
Iron Aluminide	0.0053 to 0.0099	0.0071
HR-160	0.0127 to 0.0138	0.0134
Hastelloy X	0.0111 to 0.0137	0.0127

The differences in dustcake thickness are not completely understood, but they could be related to the cleanability of the filter elements. Flow tests have shown that dirty iron aluminide filters have less flow resistance than do dirty Hastelloy-X and dirty HR-160 filters. Because of this difference in flow resistance, it seems reasonable that the iron aluminide elements would be cleaned more effectively than the Hastelloy-X and HR-160 filter media. The more effective cleaning would naturally result in a thinner residual cake on the iron aluminide elements, which is consistent with the thickness measurements shown above.

The lower flow resistance of the dirty iron aluminide elements may be related to differences in the internal structure and pore size of the filter media. Since the iron aluminide has a smaller pore size and a more tortuous flow path, it tends to allow less penetration of particles into the filter media. The sintered-fiber construction of the HR-160 elements gives them a larger effective pore size than the iron aluminide elements, resulting in more particle penetration and more pore blockage. The Hastelloy-X filters are made from sintered powder like the iron aluminide but appear to be much more highly sintered, producing smooth rounded passages through the media. The more angular morphology of the iron aluminide sintered powder creates a more tortuous flow path than does the smooth cylindrical shape of the passages through the Hastelloy-X filters. These structural differences in the filter media apparently resulted in less particle penetration into the iron aluminide, which produced less blockage of the internal pores and more effective cleaning with the iron aluminide elements.

The dustcake was generally too thin to allow the collection of bulk samples from the different types of filter elements. However, separate bulk samples were collected from the top and bottom plenums. The physical properties and chemical composition of these samples are discussed in sections 4.4.3 and 4.4.4.

4.4.3 Physical Properties of In situ Samples and Dustcakes

The TC10 in situ particulate samples and dustcake samples were subjected to the standard suite of physical measurements, including true (skeletal) particle density, bulk density, uncompacted bulk porosity, specific-surface area, and particle-size analysis. The instruments and procedures used for making these measurements have been described in previous reports.

4.4.3.1 In situ Particulate Samples

Physical properties of the in situ particulate samples from TC10 are presented in detail in Table 4.4-2, and the following table compares the properties of the g-ash produced under air- and oxygen-blown conditions. These properties are also compared to those of the in situ samples from TC08, which was also done with PRB coal under both air- and oxygen-blown conditions.

	TC10 Air	TC10 Oxygen	TC08 Air	TC08 Oxygen
Bulk density, g/cc	0.29	0.27	0.26	0.25
Skeletal particle density, g/cc	2.27	2.25	2.39	2.35
Uncompacted bulk porosity, %	87.2	87.8	89.1	89.4
Specific-surface area, m^2/g	138	146	228	217
Mass-median diameter, μm	11.3	12.3	18.6	18.7

The above comparison suggests that the use of air- versus oxygen-blown gasification has essentially no effect on the physical properties of the g-ash. The g-ash produced with oxygen-blown gasification has essentially the same physical properties as the g-ash produced with air-blown gasification. This assertion is supported by the data from both TC10 and TC08.

The TC10 g-ash appears to differ from that produced in TC08 in several respects. The g-ash produced in TC10 obviously has a finer particle-size distribution with a mean particle size of about 11 to 12 μm, compared to about 19 μm for the TC08 g-ash. The TC10 g-ash has a much lower specific-surface area (about 140 m^2/g compared to 220 m^2/g for the TC08 g-ash). The TC10 g-ash also has slightly lower uncompacted bulk porosity (87 to 88 percent versus 89 percent for the TC08 g-ash). With all other factors being equal, the smaller mean particle size and lower porosity of the TC10 g-ash would be expected to give it more drag (flow resistance) than the TC08 g-ash. However, the lower specific-surface area would tend to give the TC10 g-ash less drag than the TC08 g-ash. As discussed later in sections 4.4.6 and 4.4.7, drag measurements on the TC10 and TC08 g-ash showed there was no appreciable difference, suggesting that the lower surface area apparently offsets the smaller particle size and lower porosity, resulting in no net effect on drag.

The physical properties of the TC10 in situ samples are compared to those from other past tests with PRB coal in the following table. Since it has already been determined that there is no appreciable effect of air- versus oxygen-blown gasification, the values given below for TC10 and TC08 are averages that include both the air- and oxygen-blown samples. Oxygen-blown gasification was not used in any of the tests prior to TC08, so those values are for air-blown gasification only.

	TC10	TC08	TC07D	TC06
Bulk density, g/cc	0.28	0.25	0.32	0.29
Skeletal particle density, g/cc	2.25	2.37	2.47	2.45
Uncompacted bulk porosity, %	87.6	89.3	86.9	88.3
Specific-surface area, m^2/g	145	223	170	222
Mass-median diameter, μm	12.2	18.6	16.9	15.3

The above comparison generally supports the same conclusions that were reached when TC10 was compared to TC08. The TC10 g-ash has a relatively small MMD and a relatively low surface area. In terms of uncompacted bulk porosity, however, the TC10 g-ash is not significantly different from the TC07D g-ash. In terms of the MMD, a representative value for PRB g-ash would probably be in the range of 15 to 19 μm, as compared to 12 μm for TC10. In terms of the specific-surface area, a representative value for PRB gasification ash would probably be in the range of 170 to 220 m^2/g, compared to 145 m^2/g for TC10. Therefore, it must be concluded that the TC10 g-ash is not representative of the g-ash that has been produced from PRB coal previously. The atypical characteristics of the TC10 g-ash could be related to the coal feed disruptions and unstable gasifier operations mentioned earlier, but there is insufficient data to establish a definite cause-and-effect relationship.

4.4.3.2 Residual Dustcake Samples

The physical properties of the residual dustcake samples from TC10 are compiled in Table 4.4-3 and the average properties of the TC10 dustcake are compared to those of the TC06 dustcake in the table below. No comparisons could be made with the TC07 and TC08 dustcakes, because the TC07 dustcake was biased by coke feed, and the TC08 dustcake was damaged by partial oxidation.

	TC10	TC06
Bulk density, g/cc	0.23	0.25
Skeletal particle density, g/cc	2.06	2.28
Uncompacted bulk porosity, %	88.8	89.0
Specific-surface area, m^2/g	92	260
Mass-median diameter, μm	4.5	9.3

This comparison shows that the TC10 residual dustcake has a relatively small particle size and low surface area compared to the TC06 residual dustcake. These differences are similar to those noted previously between the TC10 and TC08 in situ samples. The characteristics of both the in situ samples and dustcake samples suggest that the g-ash produced in TC10 had a relatively small mean particle size and a relatively low specific-surface area compared to PRB g-ash from previous runs.

4.4.4 Chemical Composition of In situ Samples and Dustcakes

The TC10 in situ particulate samples and dustcake samples were analyzed for carbon, hydrogen, sulfur, nitrogen, ash, and CO_2 content. For all of the samples, hydrogen and nitrogen were below about 0.5-wt percent and were ignored in the calculation of the bulk chemical composition. The $CaCO_3$ content was calculated assuming that all of the CO_2 originated from $CaCO_3$. CaS content was calculated assuming that all of the sulfur was present as CaS. Any remaining calcium was assumed to be free lime (CaO). All carbon not accounted for in $CaCO_3$ was assumed to be present as elemental (noncarbonate) carbon. The balance was assumed to be inerts (ash and sand). The justification for these assumptions is discussed in detail in previous reports and will not be duplicated here.

4.4.4.1 In situ Particulate Samples

The chemical composition of the TC10 in situ samples is presented in detail in Table 4.4-4. Despite the apparent difference in composition between the single air-blown sample and the average composition of the oxygen-blown samples, all of the concentrations of the components in the air-blown sample are within the range of concentrations found in the oxygen-blown samples. Therefore, it must be concluded that there is no statistically significant difference in chemical composition associated with the type of oxidant used (air or oxygen).

The table below compares the average composition of the TC10 in situ samples to the in situ sample compositions from previous runs on PRB coal.

	TC10	TC08	TC07D	TC06
$CaCO_3$, Wt %	3.7	4.3	9.1	8.7
CaS, Wt %	0.4	1.1	0.1	1.3
Free Lime (CaO), Wt %	7.3	8.9	20.3	19.0
Noncarbonate Carbon, Wt %	39.4	37.5	24.2	33.0
Inerts (Ash/Sand), Wt %	49.2	48.3	46.3	38.0

In terms of bulk composition, the g-ash produced in TC10 appears to be fairly similar to that produced in TC08, but significantly different from that produced in TC07D and TC06. The primary difference between the TC10/TC08 samples and the TC07D/TC06 samples is in the concentration of the calcium-based components ($CaCO_3$, CaS, and CaO) that are, of course, primarily determined by the addition of limestone. No limestone was added to the gasifier in TC10 or TC08; while limestone was added in TC07D and TC06. Because of the lower levels of sorbent-related compounds, the TC10 and TC08 samples contain a higher percentage of noncarbonate carbon and more inerts than do the TC07D and TC06 g-ash.

4.4.4.2 Dustcake Samples

The chemical compositions of the residual dustcake samples from TC10 are compiled in Table 4.4-5, and the average properties of the TC10 dustcake are compared to the TC06 dustcake in the table below. Again, no data are given for the TC07 and TC08 dustcakes, because the TC07 dustcake was biased by coke feed, and the TC08 dustcake was damaged by partial oxidation.

	TC10	TC06
$CaCO_3$, Wt %	3.1	13.3
CaS, Wt %	1.5	1.8
Free Lime (CaO), Wt %	5.4	10.6
Noncarbonate Carbon, Wt %	49.6	40.2
Inerts (Ash/Sand), Wt %	40.4	34.2

This comparison shows that the TC10 dustcake contains much lower levels of the sorbent-related calcium compounds, which is to be expected, since limestone was added in TC06 but not in TC10. Because of the lower levels of sorbent-related compounds, the TC10 dustcake contains more noncarbonate carbon and more inerts than does the TC06 dustcake.

As noted in previous reports, the dustcake samples show a higher level of calcium sulfide (CaS) than do the in situ samples. For TC10, the average CaS content of the in situ samples was only 0.4-wt percent, compared to 1.5-wt percent in the dustcake. For TC06, the same comparison was 1.3-wt percent versus 1.8-wt percent. As suggested in previous reports, these results confirm that the dustcake provides additional capture of H_2S.

4.4.5 Particle-Size Analysis of In situ Samples

Figure 4.4-2 shows the particle-size distributions of the TC10 in situ g-ash samples obtained during oxygen-blown gasification. The size distributions were measured using a Microtrac X-100 Particle-Size Analyzer. All of the measured size distributions were reasonably consistent in shape even though the mass-median diameters (MMDs) varied from 9 to 16 μm. As noted earlier, the particle-size data suggest that the TC10 g-ash is somewhat finer than the g-ashes that have been produced from PRB coal in previous runs.

Figure 4.4-3 compares the average particle-size distribution of the oxygen-blown TC10 runs with the particle-size distribution of the single air-blown run. There does not appear to be any significant effect of the oxidant type (air or oxygen) on the particle-size distribution. This result is consistent with the measurements of the other key physical properties, which also showed no significant difference between air- and oxygen-blown samples.

4.4.6 Laboratory Measurements of G-Ash Drag

As in previous tests, the drag of the TC10 g-ash was measured as a function of particle size using the RAPTOR system with various combinations of cyclones to adjust the particle-size distribution reaching the filter. These measurements were made on a sample taken from the PCD hopper. The physical properties and chemistry of the hopper sample were similar to those of the TC10 in situ samples. The measured drag, as a function of particle size, is shown in Figure 4.4-4. As shown in this graph, the TC10 results are in fairly good agreement with the previous drag measurements obtained on PRB g-ash samples taken since the new lower mixing zone (LMZ) was placed in service. The slight difference in slope that is shown in the graph is within the scatter of the data.

As noted in previous reports, recent results suggest that the addition of the new LMZ has caused a reduction in drag across all particle sizes. As first noted in the TC07 report, the reduction in drag does not seem to be explained by a decrease in specific-surface area. The average specific-surface area of the TC10 g-ash was about 140 m^2/g, which is slightly lower than the specific-surface area of the g-ash produced in previous PRB runs (TC08, TC07-D, TC06, GCT4, and GCT3). The specific-surface areas for these runs varied from about 170 to 220 m^2/g.

Previous results have suggested that drag increases with increasing surface area up to a surface area value on the order of 100 m^2/g or so. At surface areas much beyond 100 m^2/g, drag no longer increases with increasing surface area. This result suggests that the additional surface area beyond about 100 m^2/g is primarily contained in pores too small to influence drag. This theory would explain why basically the same drag characteristics were observed in TC07-D, TC08, and TC10. However, this theory cannot explain the reduction in drag observed when the new LMZ was placed in service between TC06 and TC07. In comparing TC06 and TC07-D, there was a definite reduction in the drag without any significant change in the surface area of the g-ash.

An interesting feature of the drag-versus-particle size curves is the different slopes obtained with PRB coal and with the Hiawatha bituminous coal (TC09). A steeper slope is obtained with the Hiawatha gasification ash, suggesting that the drag is more sensitive to changes in particle size. Previous measurements made with the Alabama bituminous coal in TC07-C indicated slightly less drag than the Hiawatha bituminous coal, but the results from both bituminous coals fell on parallel lines (even though TC07-C was conducted prior to the addition of the new LMZ). Compared to the PRB g-ash, both of the bituminous g-ash (Hiawatha and Alabama) seem to have drag characteristics that are more sensitive to changes in particle size. This difference may be important when considering process modifications that affect particle size (e.g., modification of the disengager or cyclone).

4.4.7 Analysis of PCD Pressure Drop

In this section, the contribution of the transient dustcake to PCD ΔP is examined by comparing dustcake drag values calculated from the PCD ΔP to dustcake drag values measured by RAPTOR. This comparison is valuable, because mismatches between these two methods of determining drag can indicate that other factors (e.g., tar deposition, failsafe plugging, element blinding) may be influencing the filter ΔP. These comparisons also provide confidence in the use of the laboratory drag measurements for more general purposes, such as in the sizing of new PCDs.

This analysis was done using the same procedures described in previous reports. For each in situ particulate sampling run, the transient PCD drag during the run was determined from the rate of ΔP rise (ΔP/Δt) during the run and the rate of g-ash accumulation in the transient cake. The latter was determined from the measured particulate loading and the syngas mass flow rate during the run. To allow direct comparison of this PCD drag value with the RAPTOR drag measurements, the PCD drag was adjusted to the RAPTOR conditions using the ratio of the syngas viscosity at process temperature to the viscosity of air at laboratory room temperature. The RAPTOR drag value for each particulate sampling run was taken from the plot of drag versus MMD shown previously in Figure 4.4-4 using the MMD values determined by Microtrac analysis of each in situ g-ash sample.

Table 4.4-6 summarizes the PCD transient drag calculations discussed above and compares the PCD transient drag values to the corresponding drag values measured by RAPTOR. Average values of PCD transient drag and RAPTOR drag are given below for TC10, TC08, and TC06.

	Drag, inWc/(lb/ft^2)/(ft/min)		
	TC10	TC08	TC06
Average From PCD ΔP/Δt	45	46	83
Average From RAPTOR Data	58	48	94
Percent Difference	25	4	12

The drag values given above are on the viscosity basis of air at 77°F. This comparison shows that the TC10 PCD performance calculations and the TC10 RAPTOR measurements agree within 25-percent difference. The agreement is not as good as that obtained in TC08 or TC06, which is probably not too surprising considering the variability of the PCD drag during TC10. As shown in Table 4.4-6, PCD drag varied from 19 to 72 inWc/(lb/ft^2)/(ft/min). The large degree of variation in PCD drag may be related to the problems with coal feed disruptions and unstable operation. These problems undoubtedly produced considerable variations in carbon conversion and other process parameters, which in turn could have affected the drag characteristics of the g-ash. The RAPTOR drag measurements show a lesser degree of variation – 38 to 76 inWc/(ft/min)/(lb/ft^2) – because they were made on two consistent hopper samples, which did not reflect all of the variations seen in the individual in situ sampling runs.

As shown in Figure 4.4-5, plotting the individual values of PCD drag and RAPTOR drag determined for each sampling run also shows good agreement between these two methods of determining drag. This plot shows that the RAPTOR drag values track the PCD transient drag values reasonably well. This result suggests that the flow resistance of the g-ash is high enough to fully account for the transient PCD ΔP. There is no evidence that tar deposition or any other anomalies affected the PCD ΔP.

Based on both the RAPTOR data and the PCD ΔP, there does not appear to be any fundamental difference in the flow resistance of the TC10 and TC08 g-ash. However, both the RAPTOR measurements and the PCD drag values show that the TC10, TC08, and TC07-D g-ash (i.e., all of the PRB g-ash produced since the new LMZ was placed in service) have less flow resistance than does the TC06 g-ash. Again, this result confirms that the addition of the new LMZ has resulted in a reduction in drag. The reduction cannot be explained in terms of a change in the specific-surface area of the g-ash. We can only speculate that the addition of the new LMZ has apparently produced a change in particle morphology that has reduced the flow resistance of the g-ash. Examination of the particles under the scanning electron microscope (SEM) has thus far failed to identify any definite morphological differences between the particles produced before and after the LMZ was placed in service.

4.4.8 Conclusions

Despite problems with coal feed disruptions and the associated fluctuations in process conditions, the particulate concentration entering the PCD during TC10 was not significantly different from that measured in TC08. The single PCD inlet sample that was obtained under air-blown conditions yielded a particulate loading that was in good agreement with that measured in the air-blown portion of TC08 (about 15,000 ppmw). As in previous tests, much higher loadings (ppmw) were obtained with oxygen-blown gasification due to the elimination of the nitrogen diluent from the syngas. Compared to previous runs on PRB coal, the TC10 g-ash had a relatively small MMD (e.g., 11-12 μm for TC10 versus 18-19 μm for TC08). The TC10 g-ash also had a relatively low specific-surface area (140 m^2/g compared to 170-220 m^2/g for the previous PRB runs). Despite these differences, the TC10 g-ash had drag characteristics that were similar to those of the previous PRB g-ash produced since the new LMZ was placed in service.

The problems with coal feed disruptions and unstable operations apparently led to the intermittent carryover of tars and oils, which caused contamination of four out of the nine outlet particulate samples collected during TC10. Disregarding these contaminated samples, the outlet particulate loading apparently dropped from an initial value of about 0.2 ppmw to a value that was at or below the lower limit of resolution (≤ 0.1 ppmw) within a few days. Inspection of the sampling filters showed a few particles larger than 10 μm.

Comparison of the TC10 in situ g-ash samples obtained with air- and oxygen-blown gasification showed that there was no significant difference in the physical properties or chemical composition of the g-ash produced in the two modes of operation. This result was consistent with the findings in TC08, which also showed no significant differences between the air- and oxygen-blown samples. The results from both TC10 and TC08 also showed that there was no significant effect of the oxidant type on the PCD drag or the drag measured in the laboratory as a function of particle size.

Comparison of the laboratory-measured drag and the drag values calculated from the PCD ΔP continue to show good agreement between the two methods of determining drag. Based on this good agreement, it seems feasible to use the laboratory drag measurements as a basis for troubleshooting PCD performance and for the sizing of a new PCD (assuming that a representative sample of the g-ash is available). Additional research is clearly needed, however, to develop methods for correlating the drag with other g-ash characteristics (e.g., surface area, pore-size distribution, and morphology).

During the post-TC10 PCD inspection, the dustcake was found to be thicker on the HR-160 and Hastelloy filter elements than it was on the iron aluminide elements. Analysis of the results suggests that the thickness of the dustcake may be related to the cleanability of the filter element. The HR-160 and Hastelloy elements are apparently cleaned less effectively than are the iron aluminide elements. Because of the relatively large pores and smooth flow passages, the HR-160 and Hastelloy elements apparently allow more particle penetration, resulting in more pore blockage and less effective cleaning. The iron aluminide has a smaller pore size and more tortuous flow path that tends to keep more particles on the filter surface, facilitating cleaning and resulting in thinner residual dustcakes.

Table 4.4-1

PCD Inlet and Outlet Particulate Measurements From TC10

Test Date	PCD Inlet					PCD Outlet				
	SRI Run No.	Start Time	End Time	Particle Loading, ppmw	Mass Rate, lb/hr	SRI Run No.	Start Time	End Time	H_2O Vapor, vol. %	Particle Loading, ppmw
Air-Blown										
11/19/02	1	09:45	10:00	14,600	340	1	09:30	13:18	11.5	0.22
Oxygen-Blown										
11/20/02	2	09:45	10:00	21,600	375	2	09:30	11:52	25.0	0.32 (1)
11/21/02	3	10:40	10:55	---- (2)	---- (2)	3	09:30	13:30	18.3	0.13
11/25/02	4	11:10	11:25	18,100	251	4	11:00	11:30	29.4	2.6 (1)
12/09/02	5	11:10	11:25	30,800	437	5	09:45	13:45	18.1	< 0.1
12/10/02	6	10:45	11:00	24,800	348	6	10:35	14:35	20.3	< 0.1
12/11/02	7	12:15	12:30	32,800	489	8 (3)	12:10	15:10	14.5	< 0.1
12/12/02	8	12:30	12:45	33,300	466	9	12:00	15:00	17.8	1.7 (4)
12/17/02	9	12:45	13:00	21,000	347	----	----	----	----	----
12/18/02	10	10:55	11:10	32,400	499	10	10:35	12:26	13.7	0.40 (4)
Average (Oxygen-Blown Only)				26,900	402	Average			19.6	< 0.1 (5)
Standard Deviation				6,200	86	Standard Deviation			5.3	--

1. Apparent particle loading artificially high due to contamination with light yellow liquid.
2. No reliable measurement of particle loading due to leaking valve in sampling system.
3. Outlet Run No. 7 discarded due to coal feed loss during sampling.
4. Apparent particle loading artificially high due to contamination with black tar.
5. Includes only non-contaminated runs (Run Nos. 3, 5, 6, and 8).

Table 4.4-2 Physical Properties of TC10 In situ Samples

Date	SRI Run No.	Bulk Density, g/cm^3	True Density, g/cm^3	Uncom-pacted Bulk Porosity, %	Specific Surface Area, m^2/g	Mass-Median Diameter, µm
Air-Blown						
11/19/02	1	0.29	2.27	87.2	138	11.3
Oxygen-Blown						
11/20/02	2	0.30	2.23	86.5	133	14.2
11/21/02	3 (1)	0.27	2.24	87.9	177	16.4
11/25/02	4	0.28	2.33	88.0	113	10.5
12/09/02	5	0.27	2.19	87.7	160	16.8
12/10/02	6	0.23	2.34	90.2	150	13.5
12/11/02	7	0.26	2.16	88.0	176	9.6
12/12/02	8	0.29	2.24	87.1	154	16.0
12/17/02	9	0.27	2.40	88.8	113	9.3
12/18/02	10	0.29	2.10	86.2	166	9.0
TC10 Average (Oxygen Only) (2)		0.27	2.25	87.8	146	12.3
TC08 Oxygen–Blown Average (3)		0.25	2.35	89.4	217	18.7
TC08 Air-Blown Average		0.26	2.39	89.1	228	18.6
TC07-D Average (Air Blown)		0.32	2.47	86.9	170	16.9
TC06 Average (Air Blown)		0.29	2.45	88.3	222	15.3

1. Sample may not be representative because extra mass was collected due to leaking valve.
2. Run No. 3 not included in average, because sample may not be representative.
3. TC09 not included in comparison, because it was done with a different type of coal.

Table 4.4-3

Physical Properties of TC10 Dustcake Samples

Date	Type of Sample	Plenum	Bulk Density, g/cm^3	True Density, g/cm^3	Uncom-pacted Bulk Porosity, %	Specific Surface Area, m^2/g	Mass-Median Diameter, µm
1/7/03	Bulk	Top	0.23	2.14	89.3	81	5.5
1/7/03	Bulk	Bottom	0.23	2.00	88.5	100	3.7
TC10 Weighted Average (1)			0.23	2.06	88.8	92	4.5
TC06 Residual Dustcake (2), (3)			0.25	2.28	89.0	260	9.3

1. Weighted by number of filter elements in each plenum (36 in top and 49 in bottom).
2. No data given for TC09, because it was done with a different type of coal.
3. No data given for TC07 and TC08, because TC07 dustcake was biased by coke feed, and TC08 dustcake was damaged by partial oxidation.

Table 4.4-4 Chemical Composition of TC10 In situ Samples

Date	SRI Run No.	$CaCO_3$, Wt %	CaS, Wt %	Free Lime (CaO), Wt %	Non-Carbonate Carbon, Wt %	Inerts (Ash/ Sand), Wt %
Air-Blown						
11/19/02	1	2.64	0.69	10.43	29.40	56.84
Oxygen-Blown						
11/20/02	2	3.64	0.27	9.58	38.15	48.36
11/21/02	3 (1)	3.66	0.51	8.22	39.72	47.89
11/25/02	4 (2)	0.34	0.13	13.04	28.04	58.44
12/09/02	5	3.80	0.40	7.95	40.21	47.64
12/10/02	6	3.73	0.38	7.75	34.41	53.73
12/11/02	7	4.02	0.47	5.67	49.04	40.80
12/12/02	8	3.55	0.45	5.95	38.39	51.66
12/17/02	9	3.18	0.31	9.29	30.22	56.99
12/18/02	10	3.66	0.81	4.73	45.37	45.44
TC10 Average (Oxygen Only) (3)		3.65	0.44	7.27	39.40	49.23
TC08 Oxygen–Blown Average (4)		4.20	0.36	7.33	49.85	38.27
TC08 Air-Blown Average		4.29	1.06	8.89	37.45	48.31
TC07-D Average (Air Blown)		9.05	0.10	20.33	24.19	46.33
TC06 Average (Air Blown)		8.74	1.27	18.97	33.01	38.01

1. Sample may not be representative because extra mass was collected due to leaking valve.
2. Suspected analytical problem with this sample.
3. Run Nos. 3 and 4 not included in average, because Run No. 3 may not be representative, and there is a suspected analytical problem with Run No. 4.
4. TC09 not included in comparison, because it was done with a different type of coal.

Table 4.4-5

Chemical Composition of TC10 Dustcake Samples

Date	Type of Sample	Plenum	$CaCO_3$, Wt %	CaS, Wt %	Free Lime (CaO), Wt %	Non-Carbonate Carbon, Wt %	Inerts (Ash/Sand), Wt %
1/7/03	Bulk	Top	3.09	1.70	5.26	46.53	43.42
1/7/03	Bulk	Bottom	3.11	1.34	5.49	51.93	38.13
TC10 Weighted Average (1)			3.10	1.49	5.39	49.64	40.37
TC06 Residual Dustcake (2), (3)			13.27	1.78	10.59	40.19	34.17

1. Weighted by number of filter elements in each plenum (36 in top and 49 in bottom).
2. No data given for TC09, because it was done with a different type of coal.
3. No data given for TC07 and TC08, because TC07 dustcake was biased by coke feed, and TC08 dustcake was damaged by partial oxidation.

Table 4.4-6

TC10 Transient Drag Determined From PCD ΔP and From RAPTOR

Run No.	$\Delta P/\Delta t$, inwc/min	$\Delta(AL)/\Delta t$, lb/min/ft^2	FV, ft/min	MMD, µm	Drag, inwc/(lb/ft^2)/(ft/min)		
					PCD	PCD@RT	RAPTOR
Air-Blown							
1	9.23	0.022	3.74	11.3	111	66	59
Oxygen-Blown							
2	10.05	0.025	3.42	14.2	120	72	46
4	3.38	0.016	2.55	10.5	81	49	64
5	3.67	0.029	2.57	16.8	50	31	38
6	1.73	0.023	2.4	13.5	32	19	49
7	5.12	0.032	2.58	9.6	62	38	71
8	3.59	0.031	2.51	16.0	47	28	41
9	5.14	0.023	3.01	9.3	75	46	74
10	9.12	0.033	3.20	9.0	88	54	76

Nomenclature:
$\Delta P/\Delta t$ = rate of pressure drop rise during particulate sampling run, inwc/min
$\Delta(AL)/\Delta t$ = rate of increase in areal loading during sampling run, lb/min/ft^2
FV = average PCD face velocity during particulate sampling run, ft/min
MMD = mass-median diameter of insitu particulate sample, µm
RT = room temperature, 77°F (25°C)
RAPTOR = resuspended ash permeability tester

Note:
1. Run No. 3 omitted from table, because extra mass was collected due to valve leak.

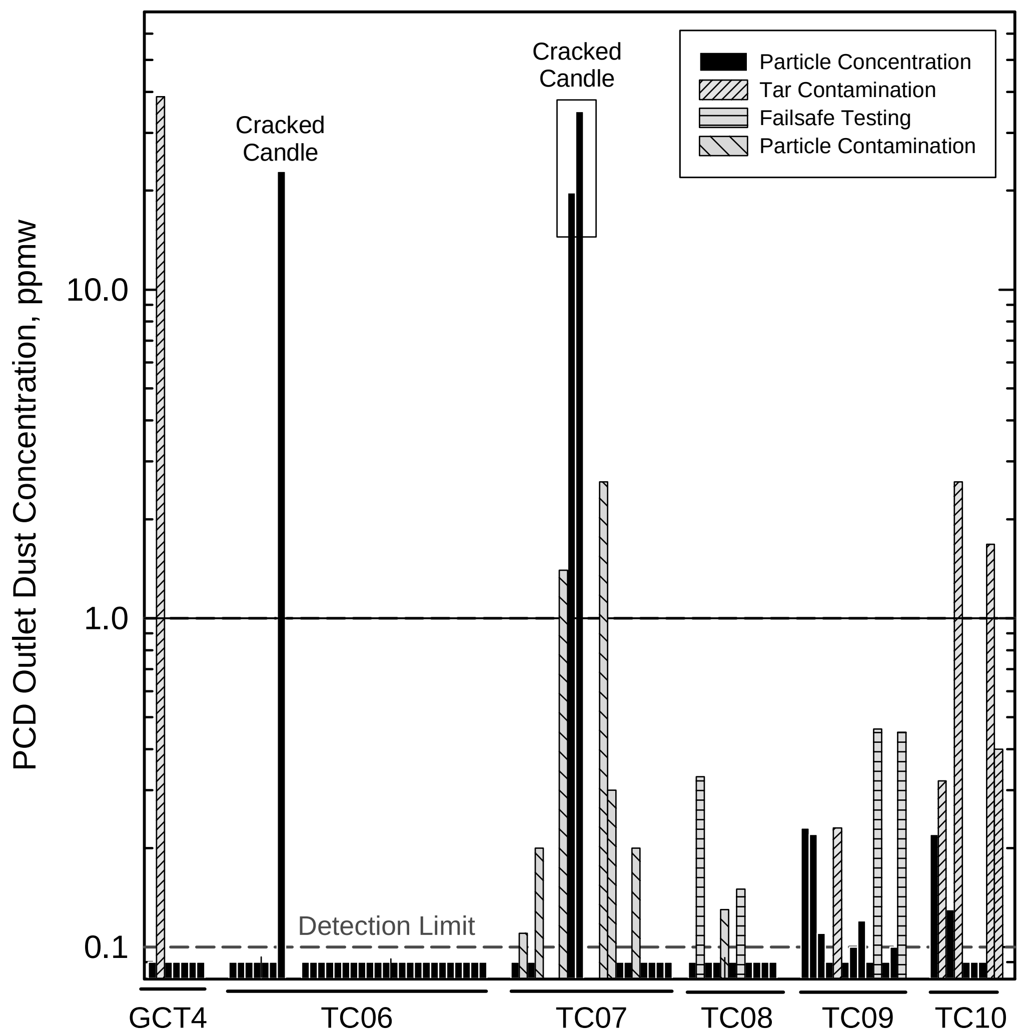

Figure 4.4-1 PCD Outlet Loadings Measured During TC10 and Previous Gasification Runs

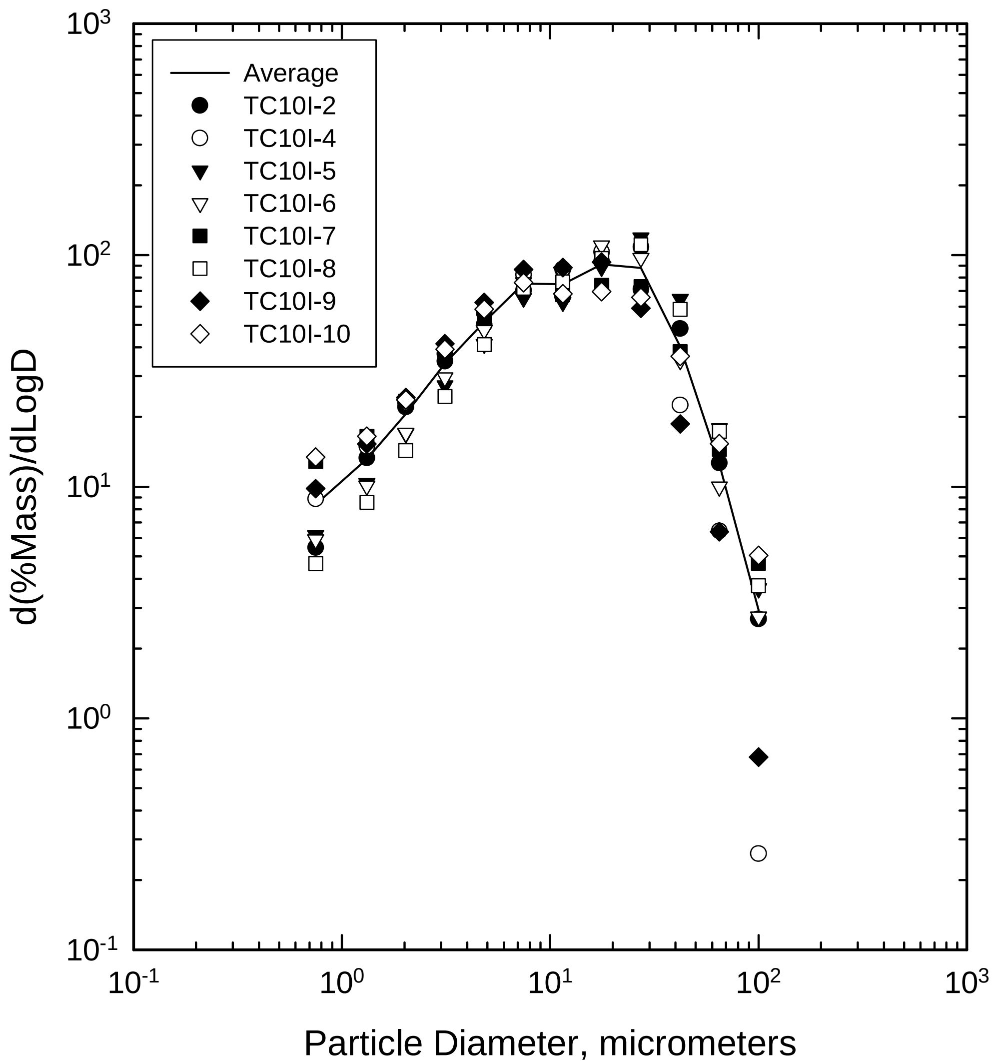

Figure 4.4-2 PCD Inlet Particle-Size Distributions Measured With Oxygen in TC10

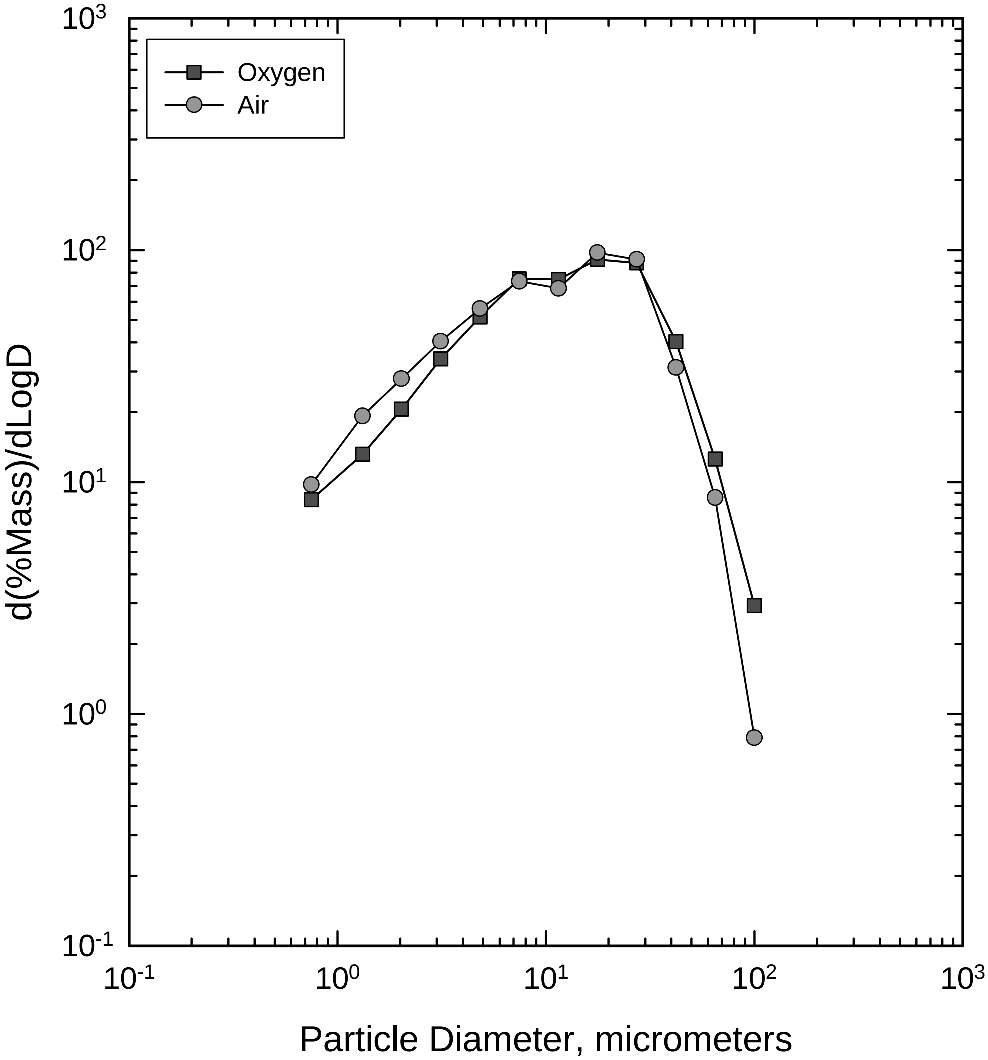

Figure 4.4-3 TC10 Air- and Oxygen-Blown PCD Inlet Particle-Size Distributions

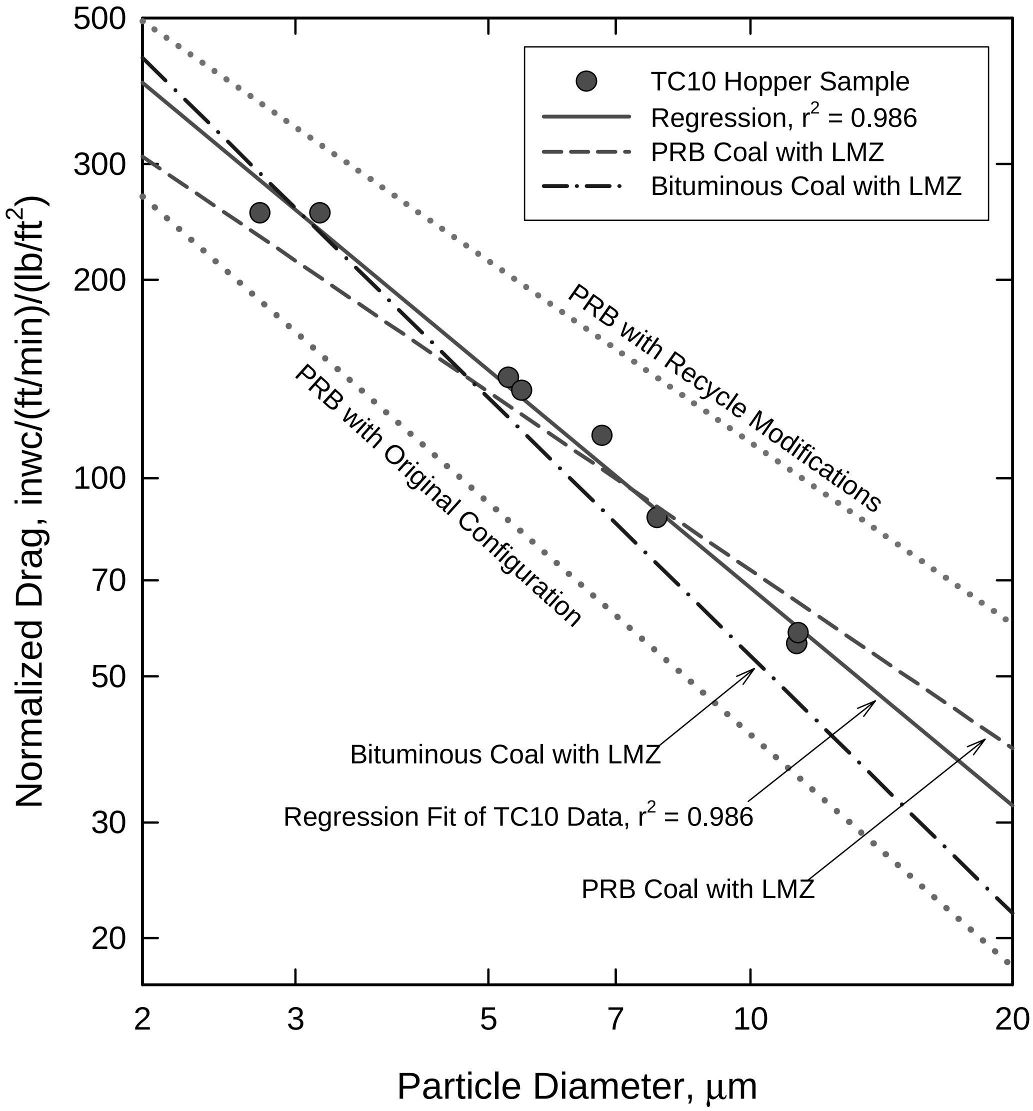

Figure 4.4-4 RAPTOR Measurements of Drag Versus Particle Size for TC10 and Previous Runs

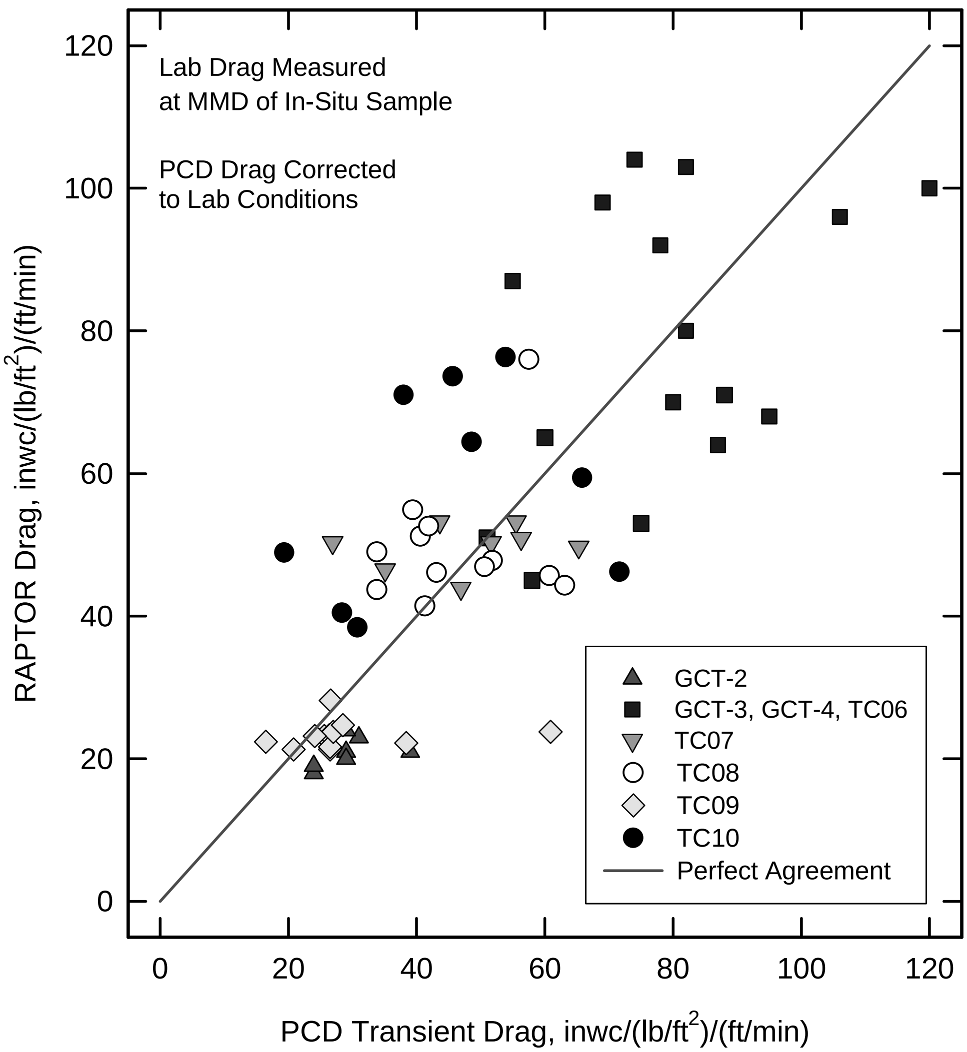

Figure 4.4-5 Comparison of Actual PCD Transient Drag With RAPTOR Measurements for All Previous Runs

4.5 FILTER MATERIAL TEST RESULTS

4.5.1 Mechanical Test Results

Property testing of filter elements continued during this test campaign. Pall PSS FEAL iron aluminide (Fe_3Al) and Pall Dynalloy HR160® elements were tested. Pall PSS FEAL elements were referred to simply as Fe_3Al elements in previous reports. A material description of the Pall PSS FEAL elements was provided in previous reports and will not be repeated here. Pall Dynalloy HR160® sintered metal fiber elements were constructed as follows:

Media formulation	D215 (1 micron blowback (surface-type) media)
Media material of construction	Haynes® Alloy HR160®. Nominal chemical composition of Haynes Alloy HR160® was 2%Fe, 37%Ni, 28%Cr, 29%Co, 0.5%Mn, 2.75%Si, and 0.05%C
Hardware material of construction	310SS

Overall dimensions of the elements were 60 mm outside diameter x 1,500 mm length which provided an overall filtration area of 2.9 ft^2. The elements were made in two sections welded to a solid metal (310SS) ring to give the overall element length of ~1,500 mm. A perforated metal cylinder at the inside surface and a coarse Hastelloy-X mesh between layers of sintered fiber HR160® filter media provided structural support. Design pressure was 35 psid at 850ºF and 25 psid at 1,200ºF. The nominal media porosity as reported by the manufacturer was 58 percent.

The elements tested and their operational histories are summarized in Table 4.5-1 and the test matrix used for all elements is shown in Table 4.5-2. Specimens required to conduct the testing were removed from the elements as shown on the cutting plans in Figures 4.5-1 and 4.5-2. Specimen configurations are shown in Figure 4.5-3 and 4.5-4 for FEAL and 4.5-5 for Dynalloy. For FEAL, the same specimen configurations and test methods were used as in previous test programs. Because of the perforated support cylinder on the inside of the Dynalloy elements, the hydrostatic burst test could not be used for the hoop tensile tests. Tensile tests in the hoop direction on Dynalloy elements were conducted using the same specimen configuration and test method as the axial test. To obtain specimens for these tests, rings were cut from the element, the rings were split axially, the HR160 filter media was removed from the perforated cylinder and laid flat, and the specimens were machined.

4.5.1.1 Pall PSS FEAL

Room temperature and 750°F axial tensile stress-strain responses for Pall PSS FEAL elements are shown in Figures 4.5-6 and 4.5-7. The axial and hoop tensile strengths and strain-to-failure are plotted versus hours in operation in Figures 4.5-8 and 4.5-9. All results are summarized in Tables 4.5-3 through 4.5-5. These results indicate no degradation in either the strength or ductility up to 2,073 hours in gasification operation at a nominal temperature of 700 to 1,000ºF with most operation between 700 and 800ºF. There was considerable scatter in the data, especially from element-to-element but sometimes within a single element. As normal, there was much more scatter in the strain-to-failure data.

Two FEAL elements were tested after cleaning at Southern Metal Processing (SMP). One was Element 39158 which was a virgin element sent through the cleaning process and the other was Element 27077 which was removed following TC07 with 1,413 hours in operation and then cleaned. Axial and hoop tensile strengths measured on these elements are compared with the strengths measured on other elements with similar operational history but not cleaned at SMP in Figures 4.5-10 and 4.5-11. The used elements shown in these two figures that were not cleaned at SMP were water washed at the PSDF. These results indicate no strength difference because of cleaning at SMP.

4.5.1.2 Pall Dynalloy HR160

Tensile stress-strain responses measured at room temperature and 750°F are shown in Figure 4.5-12. All results are summarized in Table 4.5-6. The average tensile strength was ~23 ksi at RT and ~18 ksi at 750ºF. While there was much variability in strain-to-failure, all of the stress-strain curves showed yielding and some nonlinear deformation before failure indicating that the material is nonbrittle.

4.5.2 Flow Test Results

Flow testing was conducted on several filter elements removed after TC10 and the measured pressure drop versus face velocity curves are shown in Figure 4.5-13. All flow tests were conducted using air at ambient temperature and pressure. The elements were not water washed nor chemical cleaned before testing, but loose g-ash was blown off the surface using compressed air. At a face velocity of 3 ft/min, the pressure drop measured was ~10 inH_2O on Pall PSS FEAL with no fuse, ~10 inH_2O on Pall Dynalloy HR160, ~14.5 inH_2O on Pall PSS FEAL with a fuse, and 13 – 16 inH_2O on Pall Hastelloy X.

Higher pressure drops have been measured on Pall Hastelloy-X elements after some other runs including TC06B and TC09 (see References 1 and 2) where the difference between Hastelloy-X elements and the others was more dramatic than seen here. After TC09, the pressure drops measured on Hastelloy-X elements ranged from 30 to 50 inH_2O. One of the Hastelloy-X elements with a higher measured pressure drop was examined using scanning electron microscopy (SEM) to determine if the increased flow resistance was because of particles in the pores or corrosion of the Hastelloy-X metal. An SEM image is shown in Figure 4.5-14. This image indicates that particles (sand and g-ash) from the process blocking the pores caused the increased flow resistance.

The pressure drop measured on two Pall PSS FEAL elements with no fuse installed in SWPC inverted filter holders was ~6.8 inH_2O at a face velocity of 3 ft/min. Elements were removed from the SWPC inverted filter holders and tested after one previous run, TC08, and these elements had lower pressure drops than any others after that run also.

4.5.3 References

1. Power Systems Development Facility, Technical Progress Report, Gasification Test Run TC06: July 4, 2001 – September 24, 2001; Under DOE Cooperative Agreement Number DE-FC21-90MC25140, August 2003.
2. Power Systems Development Facility, Technical Progress Report, Gasification Test Run TC09: September 3, 2002 – September 26, 2002: Under DOE Cooperative Agreement Number DE-FC21-90MC25140, ____ 2004.

Table 4.5-1

Operational History of Filter Elements Tested

Element Type	Element ID	Hours in Gasification Operation	Description
Pall PSS FEAL	39158	Virgin	Went through cleaning process at SMP
Pall PSS FEAL	27077	1413	Removed after TC07, Cleaned at SMP
Pall PSS FEAL	27073	1709	Removed after TC07D
Pall PSS FEAL	21080	1960	Removed after TC08
Pall PSS FEAL	27058	2073	Removed after TC08
Pall Dynalloy HR160	86	Virgin	

Table 4.5-2

Test Matrix for Filter Elements

Test	Orientation	Replications at	
		Room Temperature (RT)	750F
Tension	Axial	3	3
Tension	Hoop	3	3 (Dynalloy HR160 only)

Table 4.5-3

Room Temperature Hoop Tensile Test Results for Pall PSS FEAL

Element	Specimen Number	Hours in Operation	Maximum Hydrostatic Pressure (psig)	Ultimate Strength (psi)	Young's Modulus (msi)	Maximum Strain at O.D. (mils/in.)	Remarks
39158	Tn-Hoop-429	virgin	1140	15690	5.23	4.36	See Note 1
39158	Tn-Hoop-430	virgin	1190	15830	4.87	5.17	See Note 1
39158	Tn-Hoop-431	virgin	1060	14610	5.03	4.01	See Note 1
39158	Tn-Hoop-432	virgin	1120	16150	5.55	4.62	See Note 1
39158	Tn-Hoop-433	virgin	1150	15880	4.84	5.64	See Note 1
39158	Tn-Hoop-434	virgin	1150	16740	5.19	5.32	See Note 1
Average			1135	15817	5.12	4.85	
Standard Deviation			39	638	0.24	0.57	
Coefficient of Variation (COV)			3%	4%	5%	12%	
27077	Tn-Hoop-423	1413	1120	16050	5.75	3.94	See Note 1
27077	Tn-Hoop-424	1413	1130	15560	5.35	4.22	See Note 1
27077	Tn-Hoop-425	1413	1110	16170	5.37	4.55	See Note 1
27077	Tn-Hoop-426	1413	1120	16560	5.31	4.96	See Note 1
27077	Tn-Hoop-427	1413	1090	15360	5.13	4.30	See Note 1
27077	Tn-Hoop-428	1413	1040	15760	5.25	4.40	See Note 1
Average			1102	15910	5.36	4.40	
Standard Deviation			30	399	0.19	0.31	
Coefficient of Variation (COV)			3%	3%	4%	7%	
27073	Tn-Hoop-417	1709	1100	15610	5.27	4.48	
27073	Tn-Hoop-418	1709	910	13620	5.53	2.80	
27073	Tn-Hoop-419	1709	1080	14620	5.21	3.91	
27073	Tn-Hoop-420	1709	1130	15510	5.21	4.52	
27073	Tn-Hoop-421	1709	1130	15880	5.23	4.72	
27073	Tn-Hoop-422	1709	1290	17800	5.23	7.28	
Average			1107	15507	5.28	4.62	
Standard Deviation			111	1275	0.11	1.35	
Coefficient of Variation (COV)			10%	8%	2%	29%	
21080	Tn-Hoop-405	1960	1030	14290	4.90	5.34	
21080	Tn-Hoop-406	1960	1040	15450	5.51	5.32	
21080	Tn-Hoop-407	1960	970	14330	5.24	4.82	
21080	Tn-Hoop-408	1960	1020	14590	5.06	6.06	
21080	Tn-Hoop-409	1960	850	13340	5.15	4.08	
21080	Tn-Hoop-410	1960	840	13260	5.19	3.81	
Average			958	14210	5.18	4.91	
Standard Deviation			83	749	0.19	0.77	
Coefficient of Variation (COV)			9%	5%	4%	16%	
27058	Tn-Hoop-411	2073	1100	15670	5.18	4.95	
27058	Tn-Hoop-412	2073	1130	16310	5.53	5.35	
27058	Tn-Hoop-413	2073	1070	15460	5.18	4.76	
27058	Tn-Hoop-414	2073	1050	15240	5.25	4.30	
27058	Tn-Hoop-415	2073	1220	17300	5.47	5.07	
27058	Tn-Hoop-416	2073	1190	15030	4.86	4.60	
Average			1127	15835	5.25	4.84	
Standard Deviation			61	768	0.22	0.34	
Coefficient of Variation (COV)			5%	5%	4%	7%	

Notes:
1. Cleaned at Southern Metals Processing
2. All operation at SCS - PSDF in gasification mode. Nominal operating temperature was 700 - 800 °F.

Table 4.5-4

Room Temperature Axial Tensile Test Results for Pall PSS FEAL

Element	Specimen Number	Hours in Operation	0.05% Yield Strength (psi)	Ultimate Strength (psi)	Young's Modulus (msi)	Strain-to-Failure (mils/in.)	Remarks
39158	Tn-Ax-124	virgin	12.6	15.9	5.34	5.9	Note 2
39158	Tn-Ax-126	virgin	12.7	15.9	5.41	5.4	Note 2
39158	Tn-Ax-128	virgin	12.9	16.4	5.34	5.8	Note 2
		Average	12.7	16.1	5.36	5.7	
27077	Tn-Ax-118	1413	12.9	16.2	5.48	5.7	Note 2
27077	Tn-Ax-120	1413	13.0	16.2	5.40	5.7	Note 2
27077	Tn-Ax-122	1413	13.1	15.6	5.11	5.3	Note 2
		Average	13.0	16.0	5.33	5.5	
27073	Tn-Ax-112	1709	12.9	15.7	5.43	5.0	Note 3
27073	Tn-Ax-114	1709	13.1	16.6	5.59	6.2	Note 3
27073	Tn-Ax-116	1709	13.5	17.1	5.72	6.0	Note 3
		Average	13.2	16.5	5.58	5.7	
21080	Tn-Ax-100	1960	10.4	12.3	5.03	4.0	Note 3
21080	Tn-Ax-102	1960	10.7	12.9	5.04	4.6	Note 3
21080	Tn-Ax-104	1960	10.3	11.9	4.46	3.8	Note 3
		Average	10.5	12.4	4.84	4.1	
27058	Tn-Ax-106	2073	12.9	15.6	5.27	5.1	Note 3
27058	Tn-Ax-108	2073	12.7	14.2	5.41	3.8	Note 3
27058	Tn-Ax-110	2073	12.6	15.0	5.65	4.4	Note 3
		Average	12.7	14.9	5.44	4.4	

Notes:
1. All operation at SCS - PSDF in gasification mode. Nominal operating temperature was 700 - 800 °F.
2. Element cleaned at Southern Metals Processing before testing.
3. Rust on specimen edges after wire EDM.

Table 4.5-5

750ºF Axial Tensile Test Results for Pall PSS FEAL

Element	Specimen Number	Hours in Operation	0.05% Yield Strength (psi)	Ultimate Strength (psi)	Young's Modulus (msi)	Strain-to-Failure (mils/in.)	Remarks
39158	Tn-Ax-125	virgin	11.7	17.7	3.90	16.2	Note 2
39158	Tn-Ax-127	virgin	11.4	18.4	4.34	18.7	Note 2
39158	Tn-Ax-129	virgin	11.6	18.3	3.87	18.9	Note 2
		Average	11.6	18.1	4.04	17.9	
27077	Tn-Ax-119	1413	11.8	19.3	4.62	19.5	Note 2
27077	Tn-Ax-121	1413	11.9	18.9	4.41	20.8	Note 2
27077	Tn-Ax-123	1413	11.4	18.3	4.38	17.5	Note 2
		Average	11.7	18.8	4.47	19.3	
27073	Tn-Ax-113	1709	12.0	19.2	4.31	20.2	Note 3
27073	Tn-Ax-115	1709	11.4	19.1	5.00	19.0	Note 3
27073	Tn-Ax-117	1709	11.8	18.6	4.52	17.6	Note 3
		Average	11.7	19.0	4.61	18.9	
21080	Tn-Ax-101	1960	10.6	14.1	4.34	8.3	Note 3
21080	Tn-Ax-103	1960	11.1	15.3	4.33	10.4	Note 3
21080	Tn-Ax-105	1960	10.7	14.5	4.02	19.5	Note 3
		Average	10.8	14.6	4.23	12.7	
27058	Tn-Ax-107	2073		18.4			Notes 3,4
27058	Tn-Ax-109	2073	11.2	17.6	4.51	15.8	Note 3
27058	Tn-Ax-111	2073	12.6	18.3	4.13	15.4	Note 3
		Average	11.9	18.1	4.32	15.6	

Notes:
1. All operation at SCS - PSDF in gasification mode. Nominal operating temperature was 700 - 800 °F.
2. Element cleaned at Southern Metals Processing before testing.
3. Rust on specimen edges after wire EDM.
4. Flag broke during run. Strain measurements not obtained.

Table 4.5-6

Tensile Test Results for Pall Dynalloy HR160

Element	Specimen Number	Hours in Operation	Test Temperature (°F)	0.05% Yield Strength (psi)	Ultimate Strength (psi)	Young's Modulus (msi)	Strain-to-Failure (mils/in.)	Remarks
86	Tn-Ax-1	virgin	RT[1]	11.8	22.5	8.32	22.0	
86	Tn-Ax-3	virgin	RT	15.1	23.0	6.90	29.2	
86	Tn-Ax-5	virgin	RT	16.0	23.8	10.00	21.0	
			Average	14.3	23.1	8.4	24.1	
86	Tn-Hoop-1	virgin	RT	13.8	22.4	6.42	40.5	
86	Tn-Hoop-3	virgin	RT	15.0	23.8	7.53	42.7	
86	Tn-Hoop-5	virgin	RT	14.2	22.8	6.49	31.6	
			Average	14.3	23.0	6.8	38.3	
86	Tn-Ax-2	virgin	750	14.0	18.4	6.56	14.0	
86	Tn-Ax-4	virgin	750	13.4	18.4	6.64	23.3	
86	Tn-Ax-6	virgin	750	15.1	18.9	8.50	9.4	
			Average	14.2	18.6	7.2	15.6	
86	Tn-Hoop-2	virgin	750	12.9	18.7	7.88	25.8	
86	Tn-Hoop-4	virgin	750	12.3	17.7	7.38	21.2	
86	Tn-Hoop-6	virgin	750	10.8	15.6	9.40	16.8	
			Average	12.0	17.3	8.2	21.3	

Notes:
1. RT = Room Temperature
2. All operation at SCS - PSDF in gasification mode. Nominal operating temperature was 700 - 800 °F.

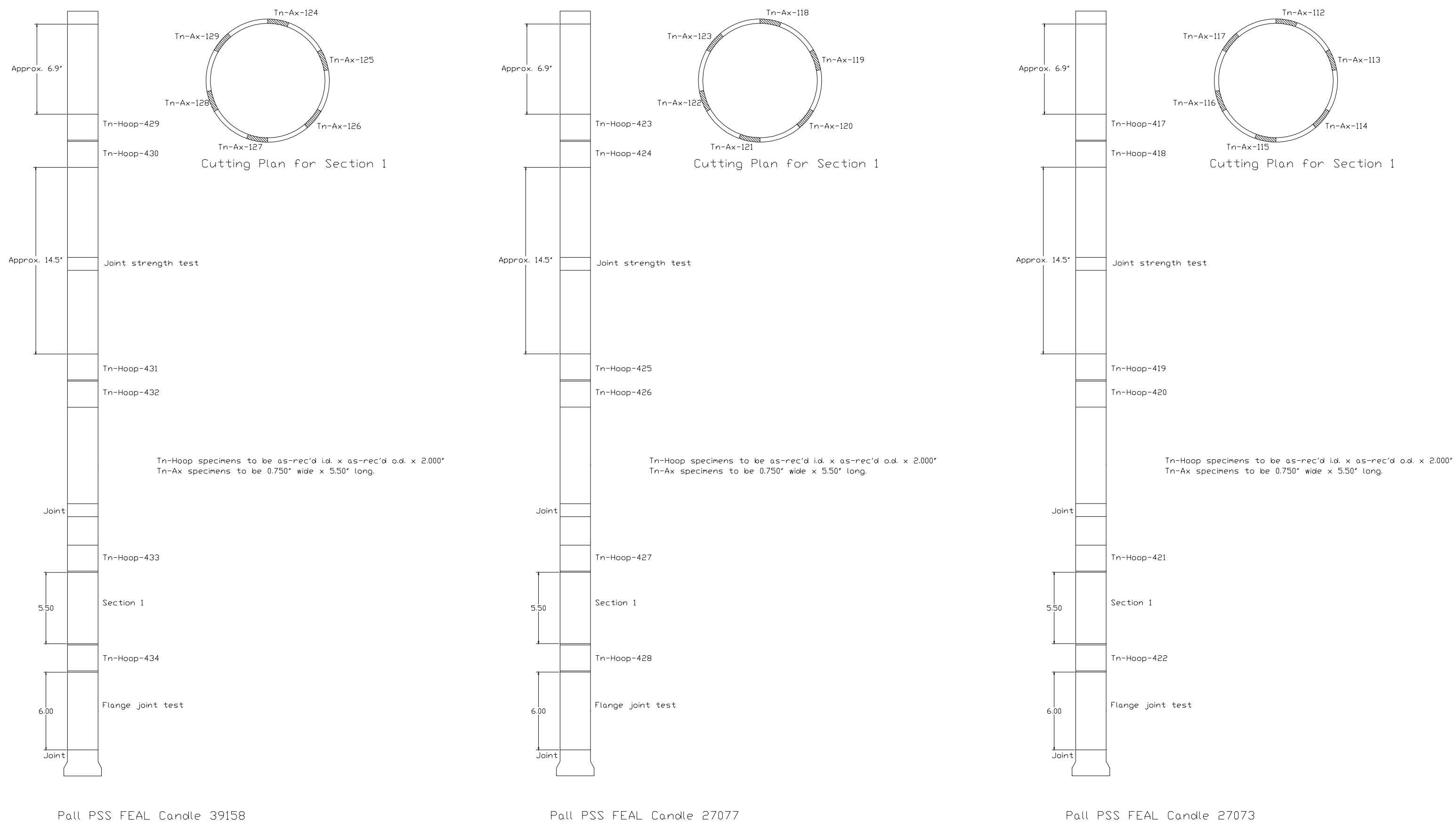

Figure 4.5-1 Cutting Plan for Pall PSS FEAL Filter Elements

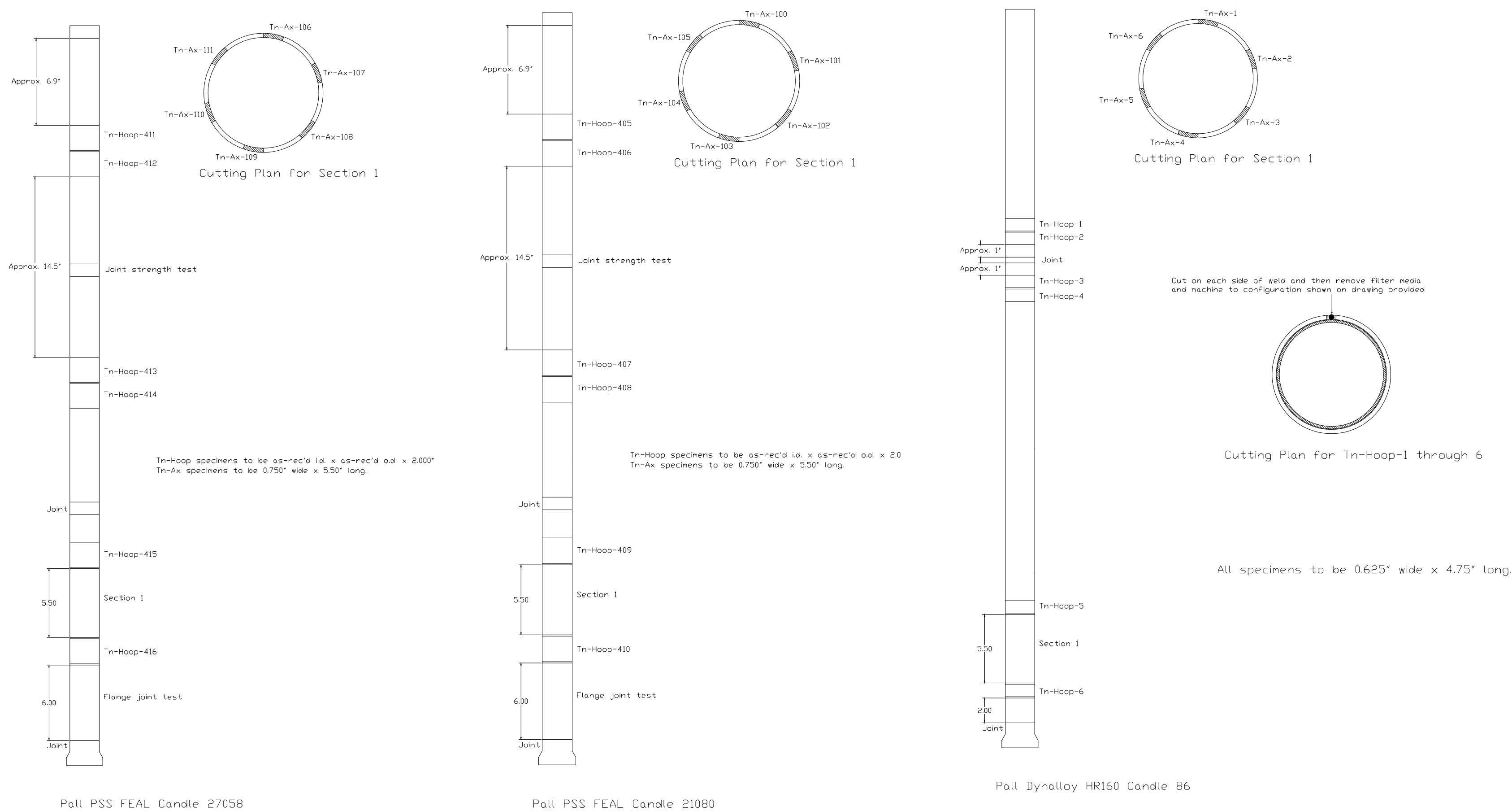

Figure 4.5-2 Cutting Plan for Pall PSS FEAL and Dynalloy HR160 Elements

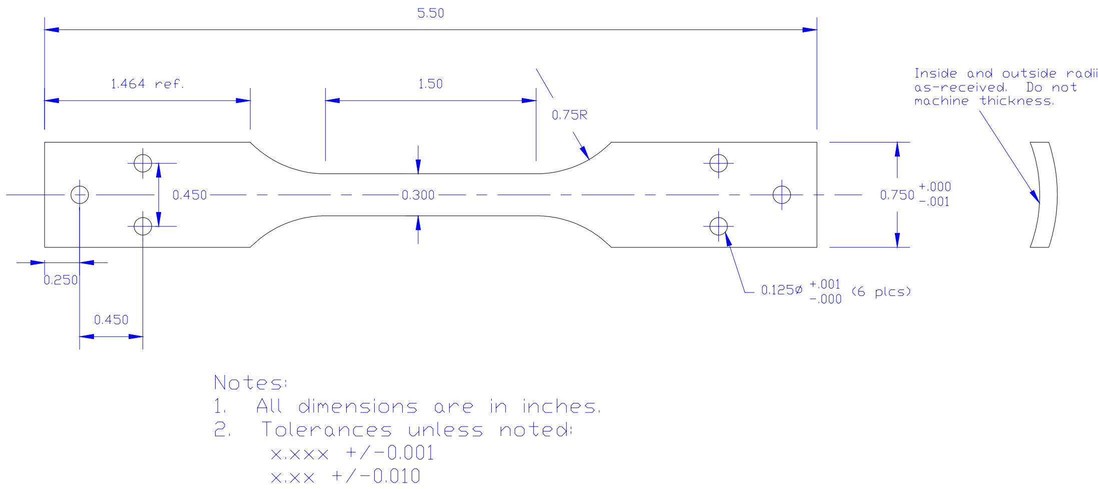

Figure 4.5-3 Axial Tensile Specimen Configuration for Pall PSS FEAL

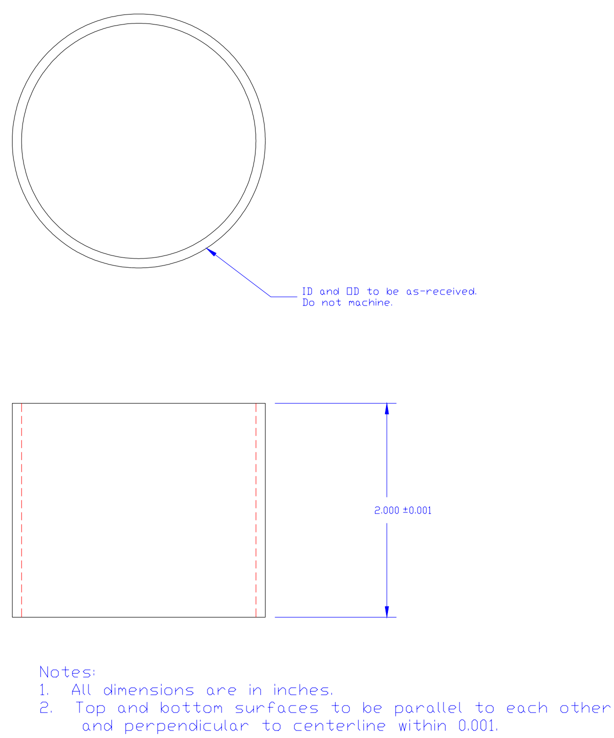

Figure 4.5-4 Hoop Tensile Specimen Configuration for Pall PSS FEAL

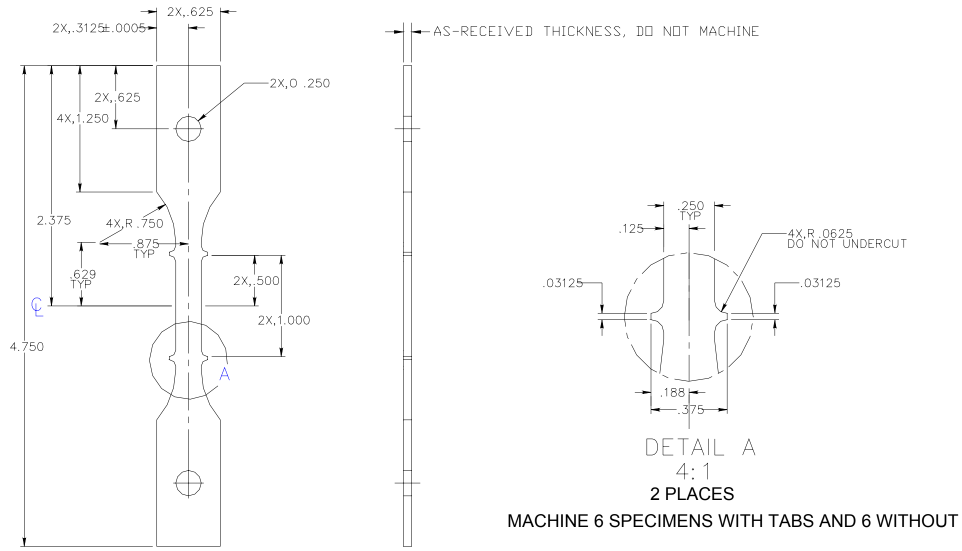

Figure 4.5-5 Axial and Hoop Tensile Specimen Configuration for Pall Dynalloy HR160

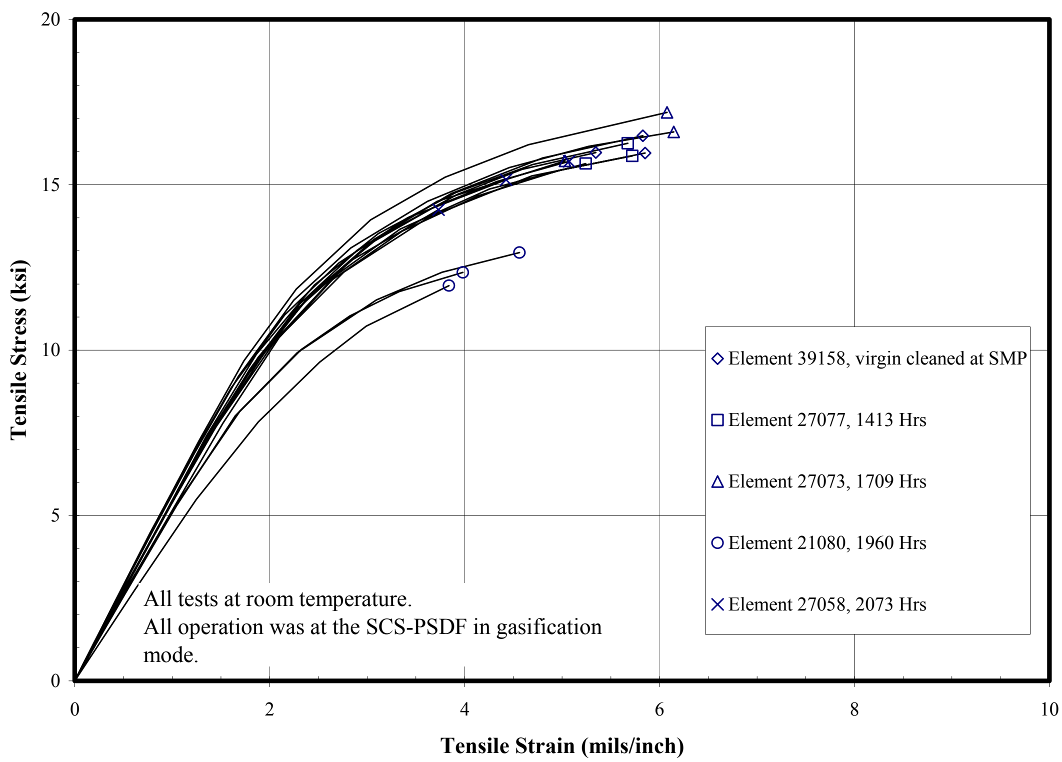

Figure 4.5-6 Axial Tensile Stress-Strain Responses at Room Temperature for Pall PSS FEAL

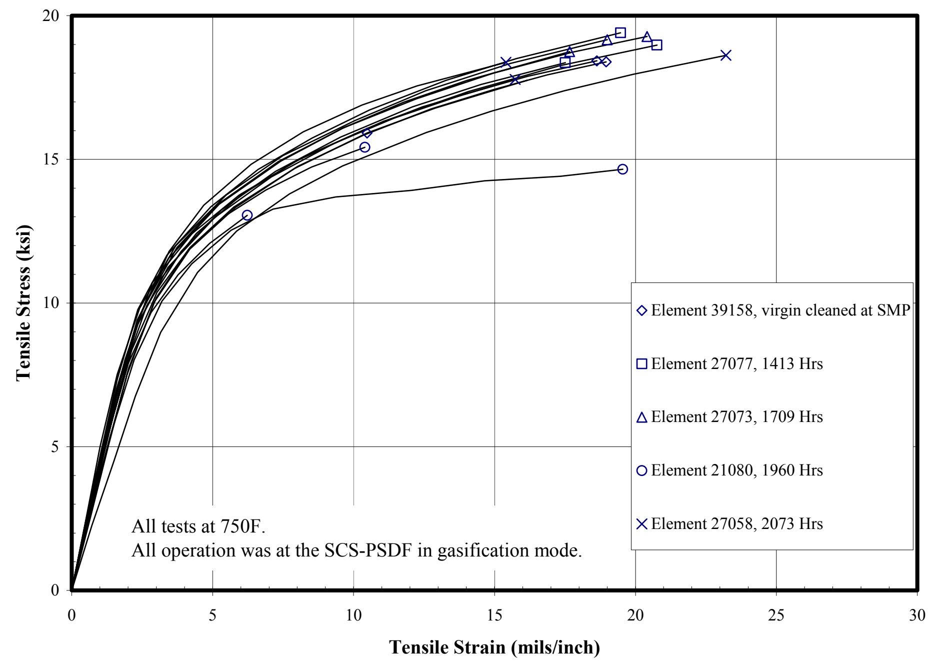

Figure 4.5-7 Axial Tensile Stress-Strain Responses at 750°F for Pall PSS FEAL

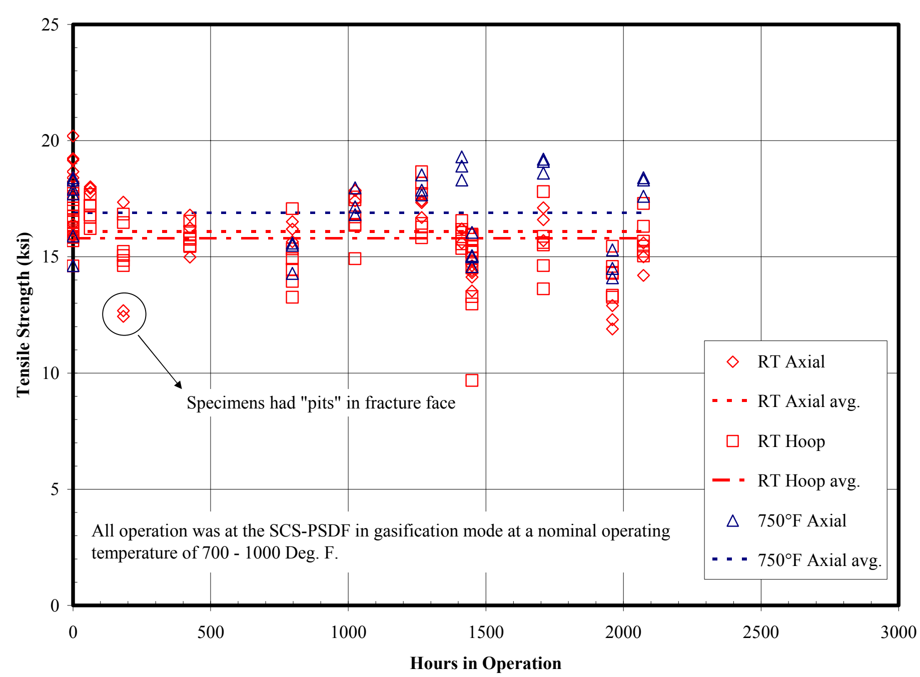

Figure 4.5-8 Tensile Strength Versus Hours of Gasification Operation for Pall PSS FEAL

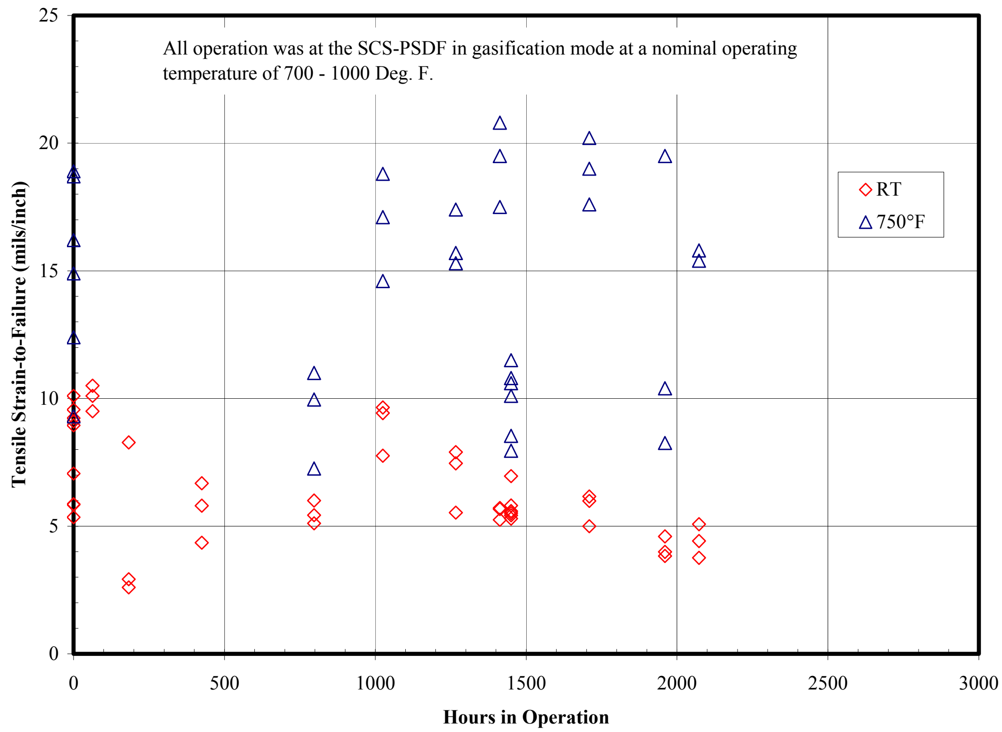

Figure 4.5-9 Tensile Strain-to-Failure Versus Hours of Gasification Operation for Pall PSS FEAL

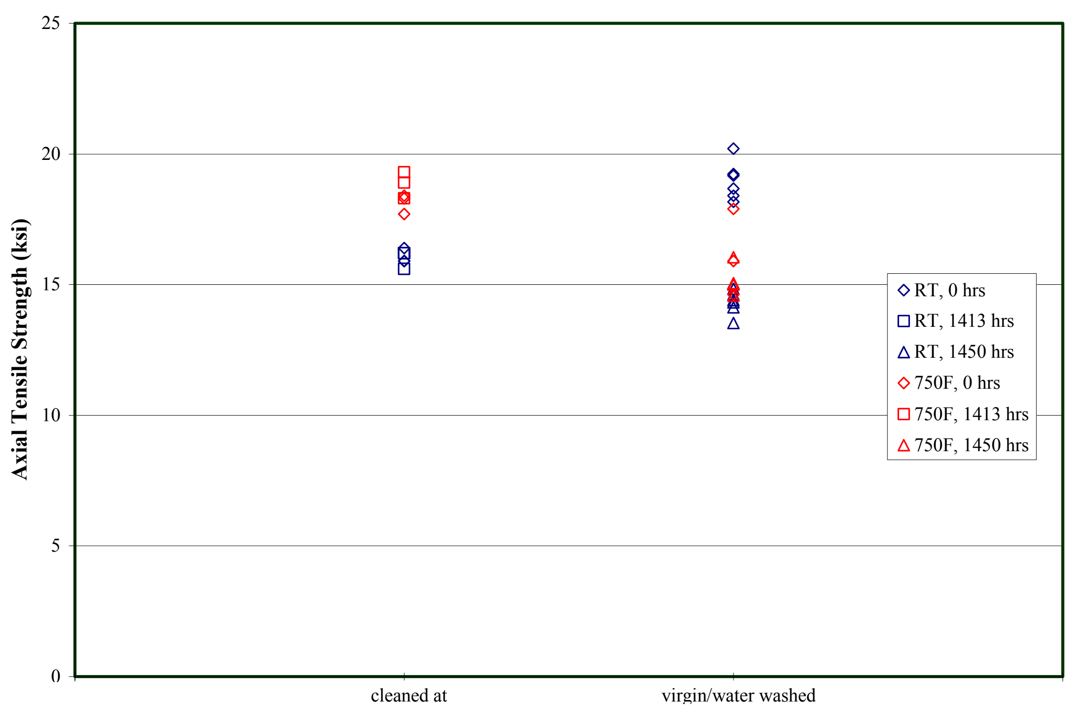

Figure 4.5-10 Axial Tensile Strength of Pall PSS FEAL

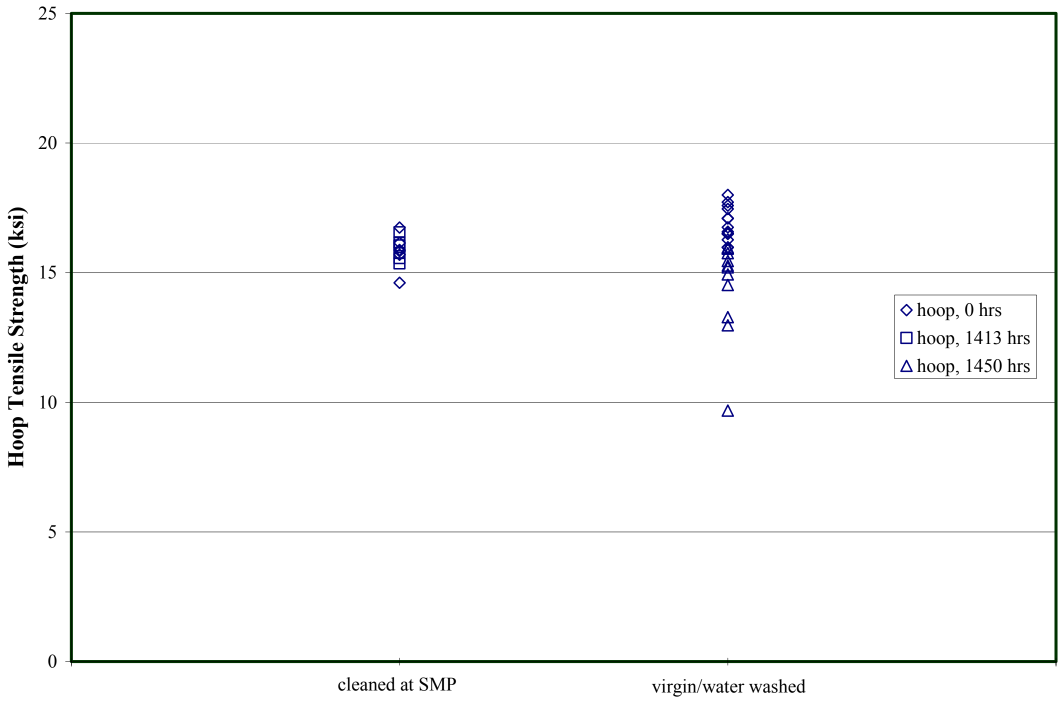

Figure 4.5-11 Hoop Tensile Strength of Pall PSS FEAL

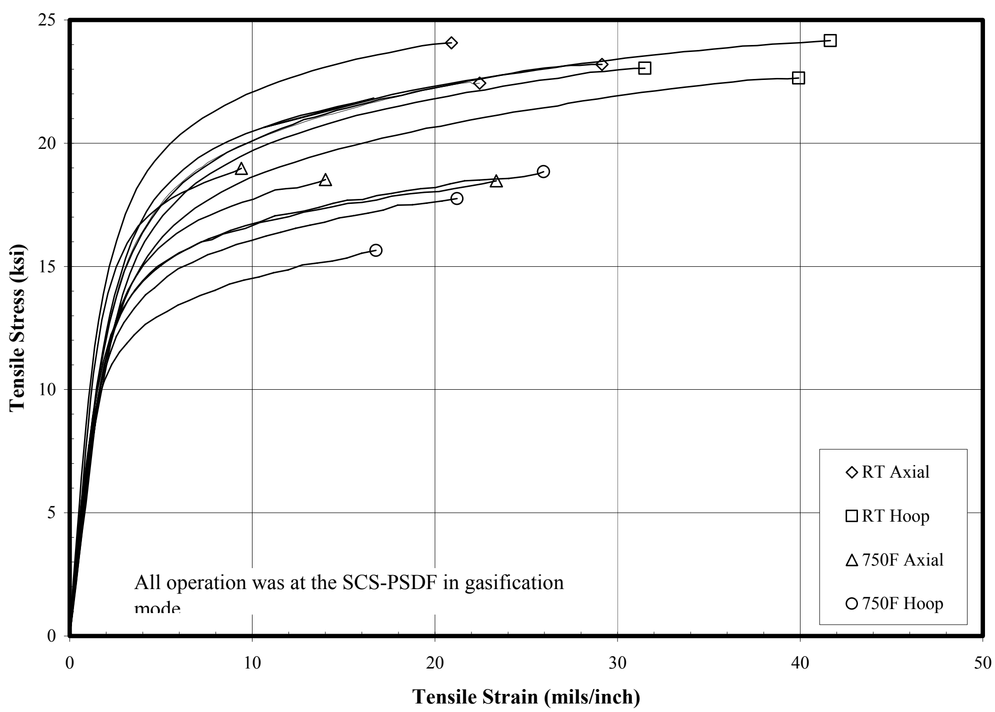

Figure 4.5-12 Axial and Hoop Tensile Stress-Strain Responses of Pall Dynalloy HR160

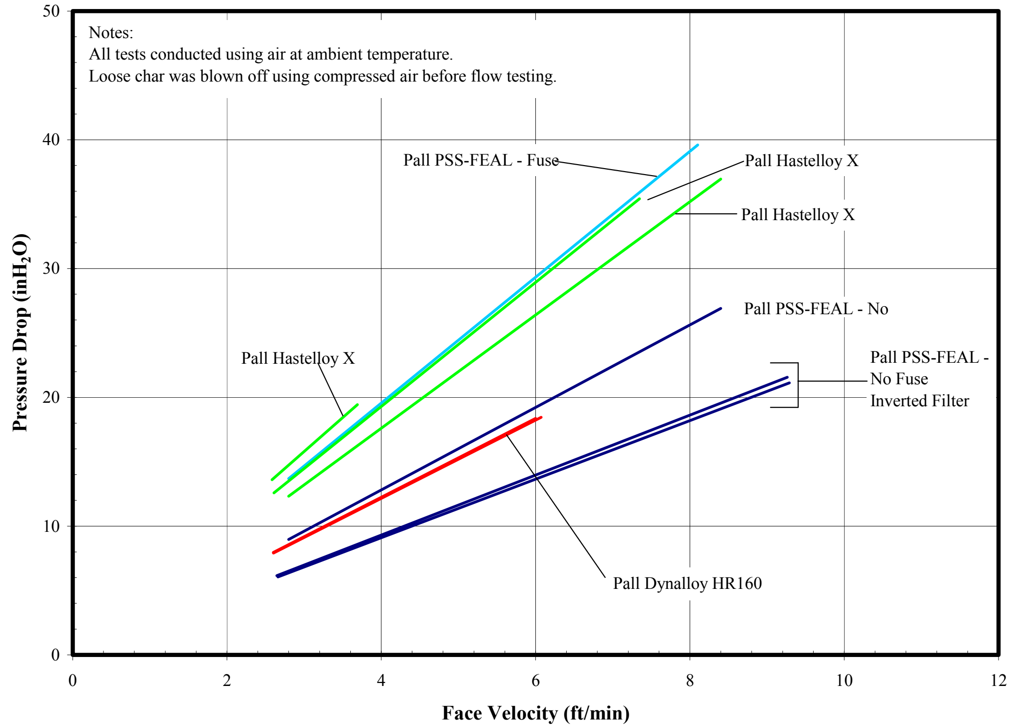

Figure 4.5-13 Pressure Drop Versus Flow Rate After TC10

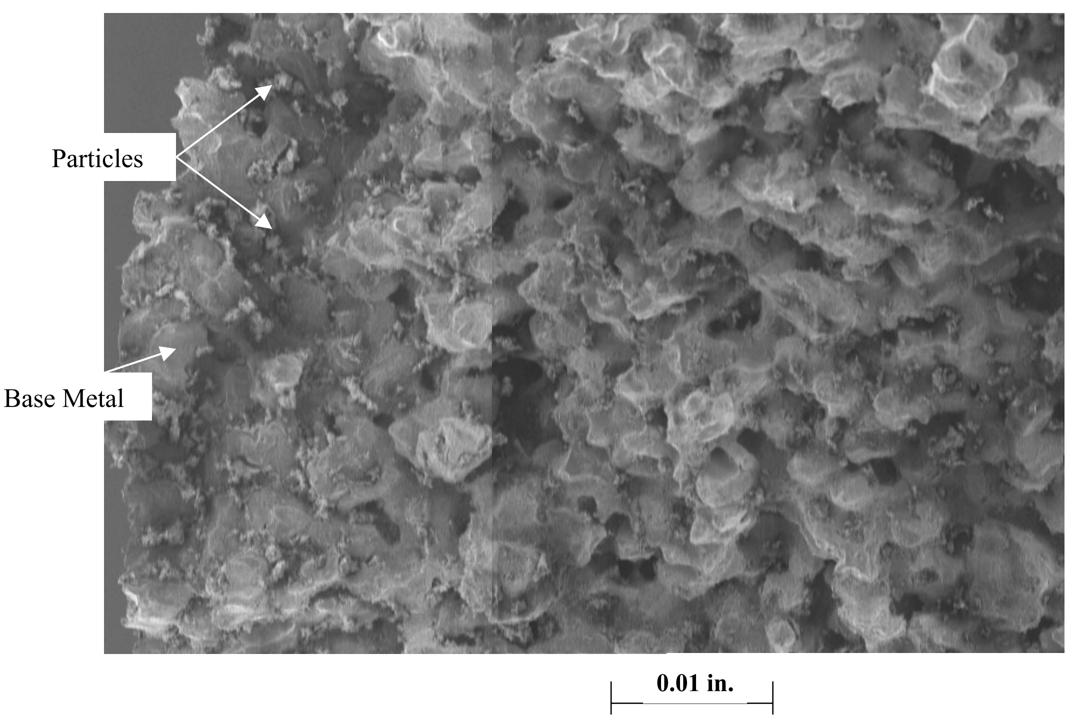

Figure 4.5-14 SEM Image of Pall Hastelloy-X Element With High Flow Resistance

TERMS

Listing of Abbreviations

AAS	Automated Analytical Solutions
ADEM	Alabama Department of Environmental Management
AFBC	Atmospheric Fluidized-Bed Combustor
APC	Alabama Power Company
APFBC	Advance Pressurized Fluidized-Bed Combustion
ASME	American Society of Mechanical Engineers
AW	Application Workstation
BET	Brunauer-Emmett-Teller (nitrogen-adsorption specific surface technique)
BFI	Browning-Ferris Industries
BFW	Boiler Feed Water
BMS	Burner Management System
BOC	BOC Gases
BOP	Balance-of-Plant
BPIR	Ball Pass Inner Race, Frequencies
BPOR	Ball Pass Outer Race, Frequencies
BSF	Ball Spin Frequency
CAD	Computer-Aided Design
CAPTOR	Compressed Ash Permeability Tester
CEM	Continuous Emissions Monitor
CFB	Circulating Fluidized Bed
CFR	Code of Federal Regulations
CHE	Combustor Heat Exchanger
COV	Coefficient of Variation (Standard Deviation/Average)
CPC	Combustion Power Company
CPR	Cardiopulmonary Resuscitation
CTE	Coefficient of Thermal Expansion
DC	Direct Current
DCS	Distributed Control System
DHL	DHL Analytical Laboratory, Inc.
DOE	U.S. Department of Energy
DSRP	Direct Sulfur Recovery Process
E & I	Electrical and Instrumentation
EDS or EDX	Energy-Dispersive X-Ray Spectroscopy
EERC	Energy and Environmental Research Center
EPRI	Electric Power Research Institute
ESCA	Electron Spectroscopy for Chemical Analysis
FCC	Fluidized Catalytic Cracker
FCP	Flow-Compacted Porosity
FFG	Flame Front Generator
FI	Flow Indicator
FIC	Flow Indicator Controller
FOAK	First-of-a-Kind
FTF	Fundamental Train Frequency

FW	Foster Wheeler
GBF	Granular Bed Filter
GC	Gas Chromatograph
GEESI	General Electric Environmental Services, Inc.
HHV	Higher Heating Valve
HP	High Pressure
HRSG	Heat Recovery Steam Generator
HTF	Heat Transfer Fluid
HTHP	High-Temperature, High-Pressure
I/O	Inputs/Outputs
ID	Inside Diameter
IF&P	Industrial Filter & Pump
IGV	Inlet Guide Vanes
IR	Infrared
KBR	Kellogg Brown & Root, Inc.
LAN	Local Area Network
LHV	Lower Heating Valve
LIMS	Laboratory Information Management System
LMZ	Lower Mixing Zone
LOC	Limiting Oxygen Concentration
LOI	Loss on Ignition
LPG	Liquefied Propane Gas
LSLL	Level Switch, Low Level
MAC	Main Air Compressor
MCC	Motor Control Center
MMD	Mass Median Diameter
MS	Microsoft Corporation
NDIR	Nondestructive Infrared
NETL	National Energy Technology Laboratory
NFPA	National Fire Protection Association
NO_X	Nitrogen Oxides
NPDES	National Pollutant Discharge Elimination System
NPS	Nominal Pipe Size
OD	Outside Diameter
ORNL	Oak Ridge National Laboratory
OSHA	Occupational Safety and Health Administration
OSI	OSI Software, Inc.
P&IDs	Piping and Instrumentation Diagrams
PC	Pulverized Coal
PCD	Particulate Control Device
PCME	Pollution Control & Measurement (Europe)
PDI	Pressure Differential Indicator
PDT	Pressure Differential Transmitter
PFBC	Pressurized Fluidized-Bed Combustion
PI	Plant Information
PLC	Programmable Logic Controller
PPE	Personal Protection Equipment

PRB	Powder River Basin
PSD	Particle-Size Distribution
PSDF	Power Systems Development Facility
ΔP or DP or dP	Pressure Drop or Differential Pressure
PT	Pressure Transmitter
RAPTOR	Resuspended Ash Permeability Tester
RFQ	Request for Quotation
RO	Restriction Orifice
RPM	Revolutions Per Minute
RSSE	Reactor Solid Separation Efficiency
RT	Room Temperature
RTI	Research Triangle Institute
SCS	Southern Company Services, Inc.
SEM	Scanning Electron Microscopy
SGC	Synthesis Gas Combustor
SGD	Safe Guard Device
SMD	Sauter Mean Diameter
SRI	Southern Research Institute
SUB	Start-up Burner
TCLP	Toxicity Characteristic Leaching Procedure
TR	Transport Reactor
TRDU	Transport Reactor Demonstration Unit
TRS	Total Reduced Sulfur
TSS	Total Suspended Solids
UBP	Uncompacted Bulk Porosity
UMZ	Upper Mixing Zone
UND	University of North Dakota
UPS	Uninterruptible Power Supply
UV	Ultraviolet
VFD	Variable Frequency Drive
VOCs	Volatile Organic Compounds
WGS	Water-Gas Shift
WPC	William's Patent Crusher
XRD	X-Ray Diffraction
XXS	Extra, Extra Strong

Listing of Units

acfm	actual cubic feet per minute
Btu	British thermal units
°C	degrees Celsius or centigrade
°F	degrees Fahrenheit
ft	feet
FPS	feet per second
gpm	gallons per minute
g/cm^3 or g/cc	grams per cubic centimeter
g	grams
GPa	gigapascals
hp	horsepower
hr	hour
in.	inches
inH_2O	conventional inch of water
inWg (or inWc)	inches, water gauge (inches, water column)
in.-lb	inch pounds
°K	degrees Kelvin
kg	kilograms
kJ	kilojoules
kPa	kilopascals
ksi	thousand pounds per square inch
m	meters
MB	megabytes
min	minute
mm	millimeters
MPa	megapascals
msi	million pounds per square inch
MW	megawatts
m/s	meters per second
MBtu	Million British thermal units
m^2/g	square meters per gram
μ or μm	microns or micrometers
dp_{50}	particle-size distribution at 50 percentile
ppm	parts per million
ppm (v)	parts per million (volume)
ppm (w)	parts per million (weight)
lb	pounds
pph	pounds per hour
psi	pounds per square inch
psia	pounds per square inch absolute
psid	pounds per square inch differential
psig	pounds per square inch gauge
ΔP	pressure drop
rpm	revolutions per minute
s or sec	seconds

scf	standard cubic feet
scfh	standard cubic feet per hour
scfm	standard cubic feet per minute
V	volts
W	watts